AD-A135 464 TIME-TEMPERATURE STUDIES OF HIGH TEMPERATURE 1/3
DETERIORATION PHENOMENA IN L..(U) FORD MOTOR CO
DEARBORN MICH RESEARCH STAFF S KORCEK ET AL. SEP 83
UNCLASSIFIED AFOSR-TR-83-0987 F49620-80-C-0061 F/G 11/8 NL

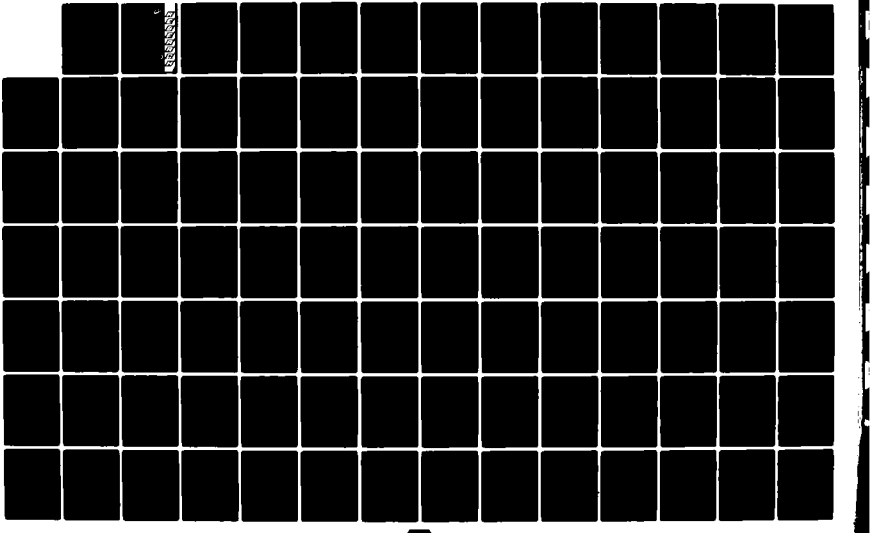

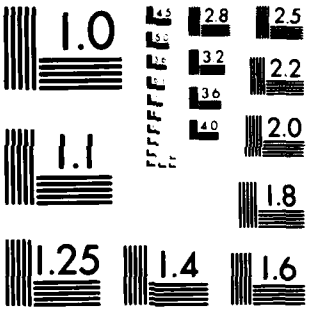

12

Ford

RESEARCH

CONTRACT F49620-80-C-0061

TIME-TEMPERATURE STUDIES OF HIGH TEMPERATURE DETERIORATION PHENOMENA IN LUBRICANT SYSTEMS: SYNTHETIC ESTER LUBRICANTS

Final Report to the Air Force Office of Scientific Research,
Directorate of Chemical and Atmospheric Sciences
for the period May 1, 1980 - April 30, 1983

by

S. Korcek, L. R. Mahoney, R. K. Jensen,
M. Zinbo, P. A. Willermet, and S. K. Kandah

Engineering and Research Staff

Research

Ford Motor Company

Dearborn, Michigan 48121

September 1983

UNCLASSIFIED

SECURITY CLASSIFICATION OF THIS PAGE (When Data Entered)

REPORT DOCUMENTATION PAGE		READ INSTRUCTIONS BEFORE COMPLETING FORM
1. REPORT NUMBER AFOSR-TR- 83-0987	2. GOVT ACCESSION NO. AD-A135464	3. RECIPIENT'S CATALOG NUMBER
4. TITLE (and Subtitle) Time-Temperature Studies of High Temperature Deterioration Phenomena in Lubricant Systems: Synthetic Ester Lubricants		5. TYPE OF REPORT & PERIOD COVERED Final May 1, 1980 - April 30, 1983 6. PERFORMING ORG. REPORT NUMBER
7. AUTHOR(s) S. Korcek, L. R. Mahoney, R. K. Jensen, M. Zinbo, P. A. Willermet, and S. K. Kandah		8. CONTRACT OR GRANT NUMBER(s) F49620-80-C-0061
9. PERFORMING ORGANIZATION NAME AND ADDRESS Ford Motor Company Dearborn, Michigan 48121		10. PROGRAM ELEMENT, PROJECT, TASK AREA & WORK UNIT NUMBERS 61102F 2303/A2
11. CONTROLLING OFFICE NAME AND ADDRESS Air Force Office of Scientific Research/NC Bolling Air Force Base, DC 20332		12. REPORT DATE September, 1983 13. NUMBER OF PAGES 212
14. MONITORING AGENCY NAME & ADDRESS(if different from Controlling Office)		15. SECURITY CLASS. (of this report) UNCLASSIFIED 15a. DECLASSIFICATION/DOWNGRADING SCHEDULE

16. DISTRIBUTION STATEMENT (of this Report)

Approved for public release: Distribution unlimited.

17. DISTRIBUTION STATEMENT (of the abstract entered in Block 20, if different from Report)

18. SUPPLEMENTARY NOTES

(alpha, delta) (alpha, gamma)

19. KEY WORDS (Continue on reverse side if necessary and identify by block number)

Autoxidation, Synthetic Ester Lubricants, Pentaerythrityl Tetraheptanoate, n-Hexadecane, Chemical Kinetics, Deterioration, Stirred Flow Reactor, Wear, Rate of Initiation, Antioxidants, Inhibition Mechanisms at Elevated Temperatures, Intramolecular Hydrogen Abstraction Reactions of Peroxy Radicals, Isomerization and Cyclization Reactions of Hydroperoxyalkyl Radicals

20. ABSTRACT (Continue on reverse side if necessary and identify by block number)

Kinetic and mechanistic investigations of the effects of oxygen pressure on liquid phase autoxidation reactions in model lubricants at elevated temperatures were carried out with n-hexadecane at 160 to 190°C and at oxygen pressures from 4 to 120 kPa. Results of these investigations showed that intramolecular α,γ and α,δ hydrogen abstraction reactions of peroxy radicals are highly reversible and that the intermediate hydroperoxyalkyl radicals formed from these abstractions, besides addition of oxygen and reverse intramolecular hydrogen abstracti

DD FORM 1 JAN 73 1473 EDITION OF 1 NOV 65 IS OBSOLETE

UNCLASSIFIED

SECURITY CLASSIFICATION OF THIS PAGE (When Data Entered)

alpha, gamma

(isomerization) reactions, undergo cyclization reactions leading to formation of cyclic ether products. A general reaction scheme for autoxidation of any system containing alkyl chains with carbon number greater than four is proposed. Absolute rate constants for formation, isomerization, and cyclization of hydroperoxyalkyl radicals have been determined for the first time for liquid-phase autoxidation and the corresponding Arrhenius parameters have been derived. Their values are in general agreement with those previously determined or estimated in gas phase combustion studies. Results of kinetic analysis of cleavage product formation are consistent with two modes of their formation in the entire range of oxygen pressures studied. The first mode involves decomposition of α,γ-hydroperoxyketone species and the second reactions of alkoxy radicals.

Determination of absolute rate constants required knowledge of the rate of initiation, R_i, at each experimental condition. Three approaches were used for that purpose: determination of R_i from the rate of formation of termination products, from the length of the inhibition period caused by addition of an antioxidant, and from the initial rate of antioxidant consumption. Correlation of results obtained indicates that stoichiometric factors, $\underline{n}$, for 2,6-di-tert-butyl-4-methylphenol, MPH, and 4,4'-methylene-bis(2,6-di-tert-butylphenol) at elevated temperatures are much lower than those determined at low temperatures (1.0-1.2 and 2.0-2.6 vs. 2 and 4, respectively) while $\underline{n}$ for N-phenyl-α-naphthylamine does not appear to change with temperature. In the case of MPH this was confirmed by the independent kinetic and mechanistic investigations.

Kinetic and mechanistic studies of inhibition reactions of MPH, and reactions of various MPH derived intermediates under autoxidation conditions at elevated temperatures revealed that the presence of hydroperoxides affects inhibition mechanisms. In the presence of excess hydroperoxides, conditions typical for our stirred flow reactor experiments, the most important reaction of MPH derived phenoxy radicals is that with alkylperoxy radicals leading to formation of the corresponding 4-alkylperoxy-2,5-cyclohexadienone, QOOR. At low hydroperoxide concentrations, conditions typical for inhibition in technological systems, the disproportionation reaction of phenoxy radicals leading to regeneration of MPH and formation of the corresponding quinonemethide also plays an important role. In both cases, however, QOOR is a major source of free radicals which effectively reduces $\underline{n}$ for MPH at elevated temperatures. In order to assess this reduction quantitatively, the decomposition reactions of a series of QOOR with R = $(CH_3)_3C$-, tetralyl-, and 1-,2-, and 5-$C_{16}H_{33}$- have been investigated in the presence of MPH. Kinetic analyses of the results yielded values of rate constants for radical and non-radical decomposition of QOOR which were used to estimate $\underline{n}$ for MPH as equal to 1.2 at 160°C.

A method for prediction of the effects of structure on the thermoxidative stability of synthetic ester lubricants, pentaerythrityl tetraalkanoates, in the presence of an antioxidant has been developed. Kinetic equations for the inhibited oxidation of these lubricants have been derived using the above proposed reaction scheme. Numerical solutions of these equations yielded the values of the relative inhibition periods as a function of antioxidant stoichiometric factor and relative reactivities of peroxy radicals in intra- and intermolecular hydrogen abstraction reactions with substrate and antioxidant. The inhibition periods calculated by this method have been found to be in excellent agreement

with the experimental values obtained for n-C_5 through n-C_8 pentaerythrityl tetraalkanoates containing 1 weight percent N-phenyl-α-naphthylamine at 232°C.

Laboratory studies of wear behavior were carried out with pentaerythrityl tetraheptanoate (PETH), n-hexadecane (HD), and a synthetic hydrocarbon (SHC) in the presence and absence of oxidation products using a Four-Ball Apparatus. In PETH, the presence of oxidation products increased wear while in SHC a reduction in wear was observed. With PETH, higher wear was observed on the rotating ball than on the three stationary balls above a critical test speed. With SHC, the direction of this wear asymmetry was reversed. With HD, wear kinetics and asymmetry were significantly affected by the type and distribution of oxidation products. Results with model oxidation products added into HD suggest that carboxylic acids and difunctional hydroperoxides are effective in reducing the stationary ball wear while monohydroperoxides do not appear to affect it over the range of conditions employed in these experiments.

A-1

TABLE OF CONTENTS

ATTACHMENT II

Wear Asymmetry - A comparison of the Wear Volumes of the Rotating and Stationary Balls in the Four-Ball Machine, by P. A. Willermet and S. K. Kandah, ASLE Transactions, 26, 2, 173 (1983).

ATTACHMENT III

Abstracts:

Autoxidation of n-Alkanes: Isomerization and Cyclization Reactions of Hydroperoxyalkyl Radicals, by S. Korcek, L. R. Mahoney, R. K. Jensen, and M. Zinbo, presented at 3rd International Symposium on Organic Free Radicals, Freiburg, West Germany, August 31-September 4, 1981, Abstracts, No. M3.

Rate of Initiation in the Autoxidation of n-Hexadecane at Elevated Temperatures, by S. Korcek, R. K. Jensen, L. R. Mahoney, and M. Zinbo, presented at Symposium on Free Radicals at the 65th CIC Conference, Toronto, Canada, May 30-June 2, 1982, Abstracts, No. OR5-6.

Liquid Phase Autoxidation of Organic Compounds at Elevated Temperatures, by S. Korcek, R. K. Jensen, L. R. Mahoney, and M. Zinbo, presented at Symposium on Inhibition of Liquid-Phase Autoxidation Reactions, ACS Meeting, Kansas City, September 12-17, 1982, Abstracts, No. ORGN 27.

Reactions of Alkylperoxycyclohexadienones during Autoxidation Inhibited by Hindered Phenols at Elevated Temperatures, by R. K. Jensen, S. Korcek, L. R. Mahoney, and M. Zinbo, presented at Symposium on Inhibition of Liquid Phase Autoxidation Reactions ACS Meeting, Kansas City, September 12-17, 1982, Abstracts, No. ORGN 28.

STATEMENT OF WORK

The contractor shall furnish scientific effort together with all related services, facilities, supplies and materials, needed to conduct the following research:

a. Determine the kinetics and mechanisms of the oxidative and thermal reactions of the model lubricant, n-hexadecane, and the synthetic ester lubricant, pentaerythrityl tetraheptanoate, in the presence and absence of antioxidant additives at temperatures from 160 to 200°C, at oxygen pressures from 5 to 20 kPa, and at reaction times from 20 to 10^3 seconds utilizing stirred flow and batch reactor techniques.

b. Investigate the effects of the reaction products obtained under conditions specified in "a" on the wear behavior in systems lubricated by the model hydrocarbon and synthetic ester lubricants.

INTRODUCTION

Basic information on lubricant deterioration and wear phenomena occurring in lubricant systems exposed to oxidative environments at high temperatures had not been available due to inherent limitations of conventional experimental techniques. Application of stirred flow reactor methods in our previous studies led to the elucidation of the kinetics and mechanisms of the autoxidation reactions of the synthetic ester lubricant, pentaerythrityl tetraheptanoate, at 180 to 200°C and of a model hydrocarbon lubricant, n-hexadecane, at 120 to 180°C, at an oxygen pressure of ~110 kPa, and to the discovery of increased wear phenomena caused by low concentrations of the hydroperoxide and dicarboxylic acid oxidation products of the ester.

The present research is an extension of that work to studies of the deterioration reactions and wear behavior of model hydrocarbon and synthetic ester lubricants at reduced oxygen pressures including atmospheric conditions. Since such oxygen pressure conditions exist in actual service applications of lubricants, the results derived from these studies will not only yield basic information on an important but unexplored area of free radical chemistry but will also provide a technical basis for improvements in practical lubrication systems operating under ambient oxygen pressures.

PREFACE

This is the final report on the work carried out during the period May 1, 1980 to April 30, 1983 under the Air Force Office of Scientific Research/Ford Motor Company Contract, F49620-80-C-0061, entitled "Time-Temperature Studies of High Temperature Deterioration Phenomena in Lubricant Systems: Synthetic Ester Lubricants".

Results of our investigations of the inhibited autoxidation of pentaerythrityl tetraheptanoate and other tetralkanoates are described in the paper entitled "Effects of Structure on the Thermoxidative Stability of Synthetic Ester Lubricants: Theory and Predictive Method Development". The paper was presented at the Symposium on Synthetic and Petroleum-Based Lubricants, at the 183rd ACS Meeting in Las Vegas, Nevada, and published in PREPRINTS of Division of Petroleum Chemistry (Attachment I).

Studies of wear behavior of pentaerythrityl tetraheptanoate and a synthetic hydrocarbon leading to discovery of wear asymmetry are described in the paper entitled "Wear Asymmetry - A Comparison of the Wear Volumes of the Rotating and Stationary Balls in the Four-Ball Machine". This paper was presented at the 37th ASLE Annual Meeting in Cincinnati, Ohio, and published in ASLE Transactions (Attachment II).

Abstracts of other presentations describing work performed under this contract are in Attachment III.

The unpublished research results are described in Parts I-VII of this report. Studies of effects of reduced oxygen pressures on product formation

in the liquid-phase autoxidation of n-hexadecane at 160 to 190°C are presented in Part I. A kinetic analysis based on the above studies resulting in determination of the absolute rate constants and Arrhenius parameters for formation, isomerization, and cyclization reactions of hydroperoxyalkyl radicals is in Part II. Determination of a basic kinetic parameter, rate of initiation, which is required for calculation of absolute rate constants for autoxidation reactions at elevated temperatures, is discussed in Part III. Investigations of inhibition mechanisms of 2,6-di-tert-butyl-4-methylphenol at elevated temperatures are presented in Part IV. These inhibition studies are extended into kinetic investigations of the contribution of major inhibitor reaction intermediates to the rate of initiation described in Part V. This work was presented at the Symposium on "Inhibition of Liquid Phase Autoxidation Reactions," at the 184th ACS Meeting in Kansas City, Missouri. A novel HPLC procedure used for analysis of autoxidation products throughout our studies is described in Part VI and is being printed the Journal of Chromatographic Science. A study of the effects of autoxidation products, formed in a model hydrocarbon lubricant at low and high oxygen pressures, on wear behavior is the subject of Part VII.

It is anticipated that following the completion of a limited number of additional experiments each Part will be prepared and submitted for publication in technical journals. The respective authors of these papers are indicated at the beginning of each Part.

SYMBOLS

The following symbols are used throughout this report to designate major substrates and antioxidants:

HD = n-Hexadecane

PETH = Pentaerythrityl tetraheptanoate

MPH = 2,6-Di-tert-butyl-4-methylphenol

PAN = N-Penyl-α-naphthylamine

BPH = 4,4'-Methylene-bis(2,6-di-tert-butylphenol)

PART I

EFFECTS OF OXYGEN PRESSURE ON LIQUID PHASE AUTOXIDATION of n-HEXADECANE AT 160 TO 190°C.

R. K. Jensen, S. Korcek, L. R. Mahoney and M. Zinbo

INTRODUCTION

Investigations of the liquid phase autoxidation of n-hexadecane with pure oxygen carried out in the stirred flow microreactor at 100 to 110 kPa and 120 to 180°C led to the discoveries of α,γ and α,δ intramolecular hydrogen abstraction reactions of alkylperoxy radicals[1] and the cleavage reaction of α,γ-hydroperoxyketones.[2] The occurrence of intramolecular hydrogen abstraction reactions explained the formation of difunctional oxidation products, namely α,γ and α,δ dihydroperoxides and hydroperoxy substituted ketones, which, together with monohydroperoxides, are the major primary oxidation products at these reaction conditions.[1] The cleavage reaction of α,γ-hydroperoxyketones was found to be one of the two independent processes of cleavage product formation.[2] It accounted for the formation of cleavage methyl ketones and 50-60% of alkanoic acids. The formation of remaining cleavage products was explained by a complex sequence of reactions which starts by β-scission and intramolecular hydrogen abstraction reactions of alkoxy radicals.

In the present study we describe the results of our investigations of the effects of oxygen pressure on kinetics and mechanisms of n-hexadecane autoxidation at elevated temperatures. The range of oxygen pressures studied was 4-120 kPa which includes atmospheric conditions.

EXPERIMENTAL

The reaction techniques, some of the analytical procedures and materials used in this study were described previously.[1,2,3]

Stirred Flow Microreactor. The stirred flow microreactor system used for the autoxidation of n-hexadecane was modified to allow the introduction of oxidation gas mixtures of oxygen and argon at different oxygen pressures. The flow rates of each gas were measured using mass flow meters (Matheson Models 8160-0452 and 8143).

Product Analysis. Primary C_{16} oxidation products were determined by GLC analyses of oxy fractions obtained from silica gel separation of sodium borohydride and triphenylphosphine reduced oxidates[1] using a packed Silar 10C column and a bonded-phase fused silica capillary column (DB-5; 60m x 0.317 mm ID). Typical chromatograms obtained with the packed Silar 10C column are shown in Figure 1.

C_{16} cyclic ethers, $-\overset{\frown O \frown}{CH(CH_2)_2CH}-$, were detected by the above technique only in the low oxygen pressure experiments. Their GLC peaks overlap those for C_{12}--C_{14} 2-alkanols (from methyl ketones) and C_{11} and C_{12} 1-alkanols (from 1-oxo and 1-oxyalkanes). Better separation of C_{16} cyclic ether products and 1- and 2-alkanols in $NaBH_4$ reduced samples was obtained using the capillary column. This analysis was performed using a Perkin-Elmer Sigma 3 gas chromatograph with a flame ionization detector, and an on-column injection system (J & W Scientific, Inc). A Perkin-Elmer Sigma 10 Data Station was used for recording and integration. One microliter samples were injected at room temperature using a timed, reduced inlet pressure technique.[4] The linear flow rate of hydrogen was 60 cm/s at 225 kPa, injection port temperature 75°C, and detector temperature

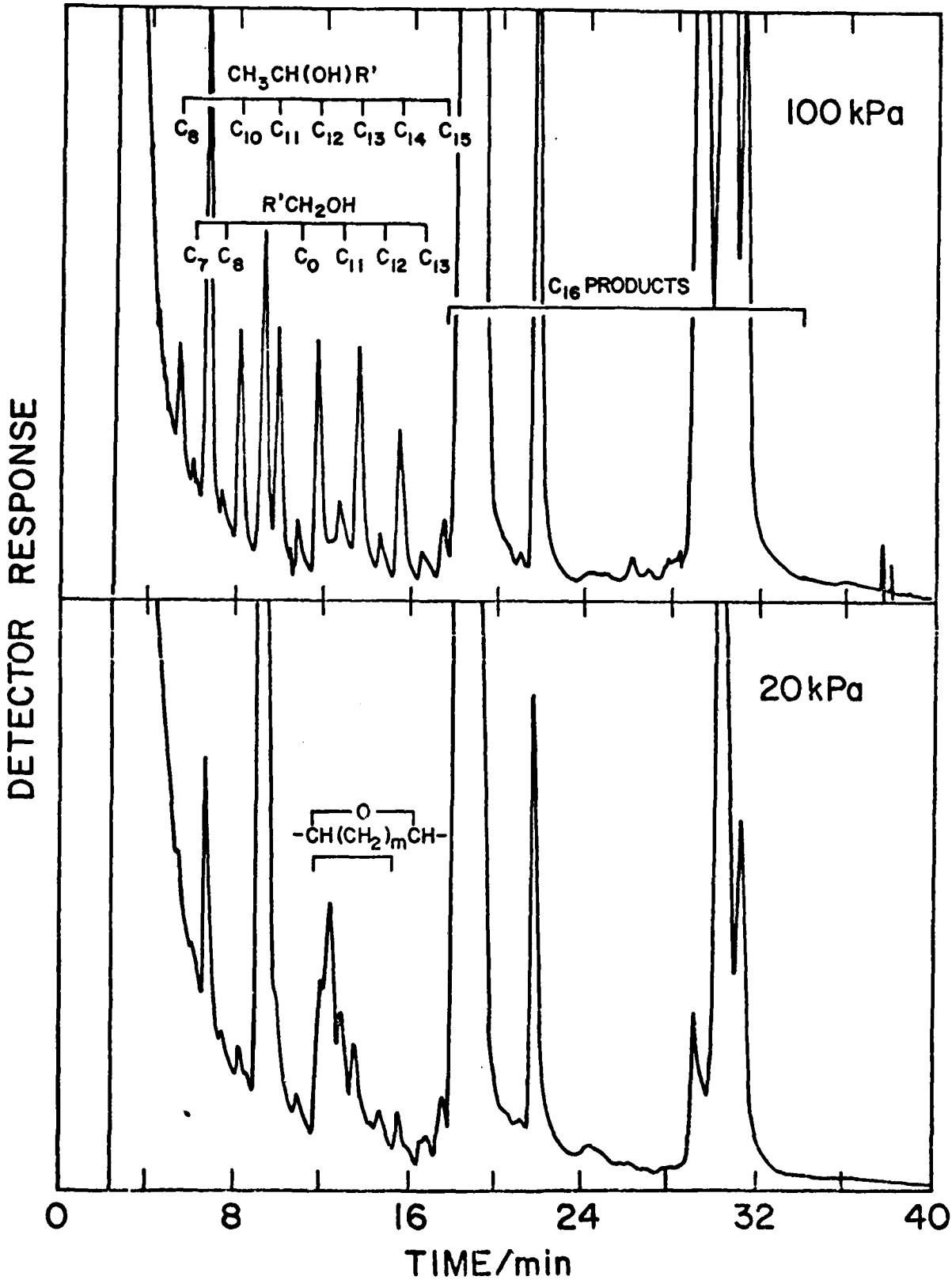

Figure 1 Chromatograms of oxy fractions from $NaBH_4$ reduced n-hexadecane oxidates (180°C, runs 149 and 225) obtained using a packed Silar 10C column.

185°C. The oven was programmed from 90 to 175°C with a post injection time of 15 minutes and heating rate of 2°C/min. Typical chromatograms obtained from this analysis are in Figure 2. The only peaks which interfere with determination of C_{16} cyclic ethers are those of 1-tetradecanol and 2-pentadecanol both of which are relatively minor. The sensitivity of this method is such that C_{16} cyclic ethers can also be determined in the high oxygen pressure samples (detection limit is 0.5 ng/mL). Identification of C_{16} cyclic ethers was accomplished by an ancillary gas chromatographic-CI mass spectrometric analysis and by gas chromatography of synthesized standards. A chromatogram of an oxidized n-hexadecane sample separated on silica gel to concentrate C_{16} cyclic ethers is in Figure 3. Peak assignments for C_{16} cyclic ethers are based on retention times of 2-methyl-5-undecyloxolane and 2-ethyl-5-decyloxolane which were synthesized by the method of Reynolds and Kenyon[5] from 2,5- and 3,6-hexadecanediols.[1]

Hexadecanal and 2--8-hexadecanones, [1--8-R'CO-], were determined by HPLC after derivatization using p-nitrobenzyloxyamine hydrochloride (PNBA).[6] An aliquot (0.2-0.5 mL) of a triphenylphosphine reduced oxidate mixed with 10-15 mg PNBA and 200 µL pyridine was heated at 60°C for 1 hour. The mixture was then transferred to a separatory funnel with CH_2Cl_2 and washed with dilute HCl. After washing, the CH_2Cl_2 layer was separated and evaporated. The derivatives obtained were dissolved in a known volume of CH_2Cl_2. HPLC was performed using a Radial-PAK C18, 10µ, 5 mm ID cartridge (Waters Assoc.), mobile phase of H_2O:CH_3OH:CH_2Cl_2:CH_3CN (7:8:25:60) at a flow rate of 0.6 mL/min, and detection at 280 nm.

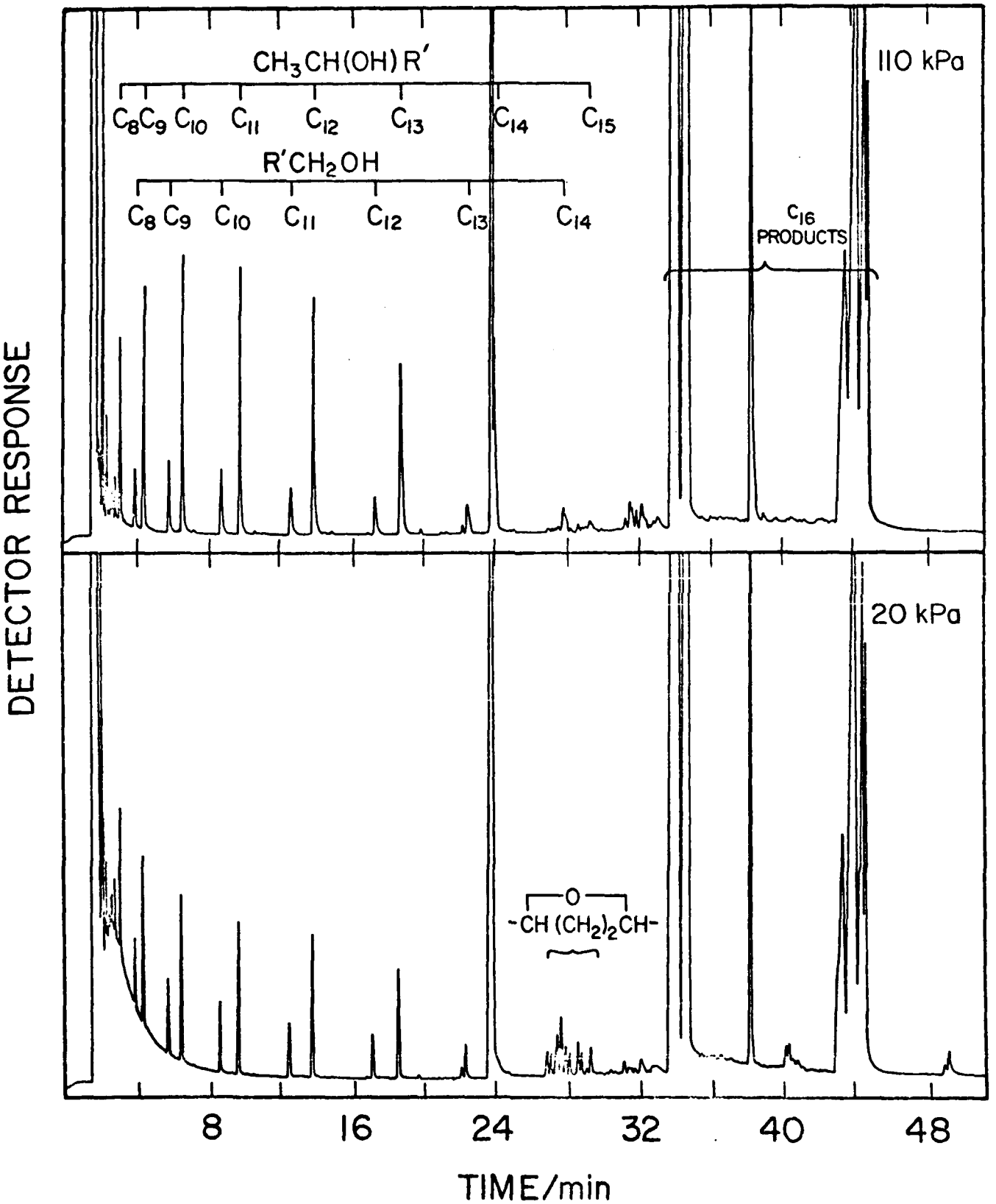

Figure 2 Chromatograms of oxy fractions from $NaBH_4$ reduced n-hexadecane oxidates (180°C, runs 151 and 260) obtained using a bonded phase fused silica capillary column.

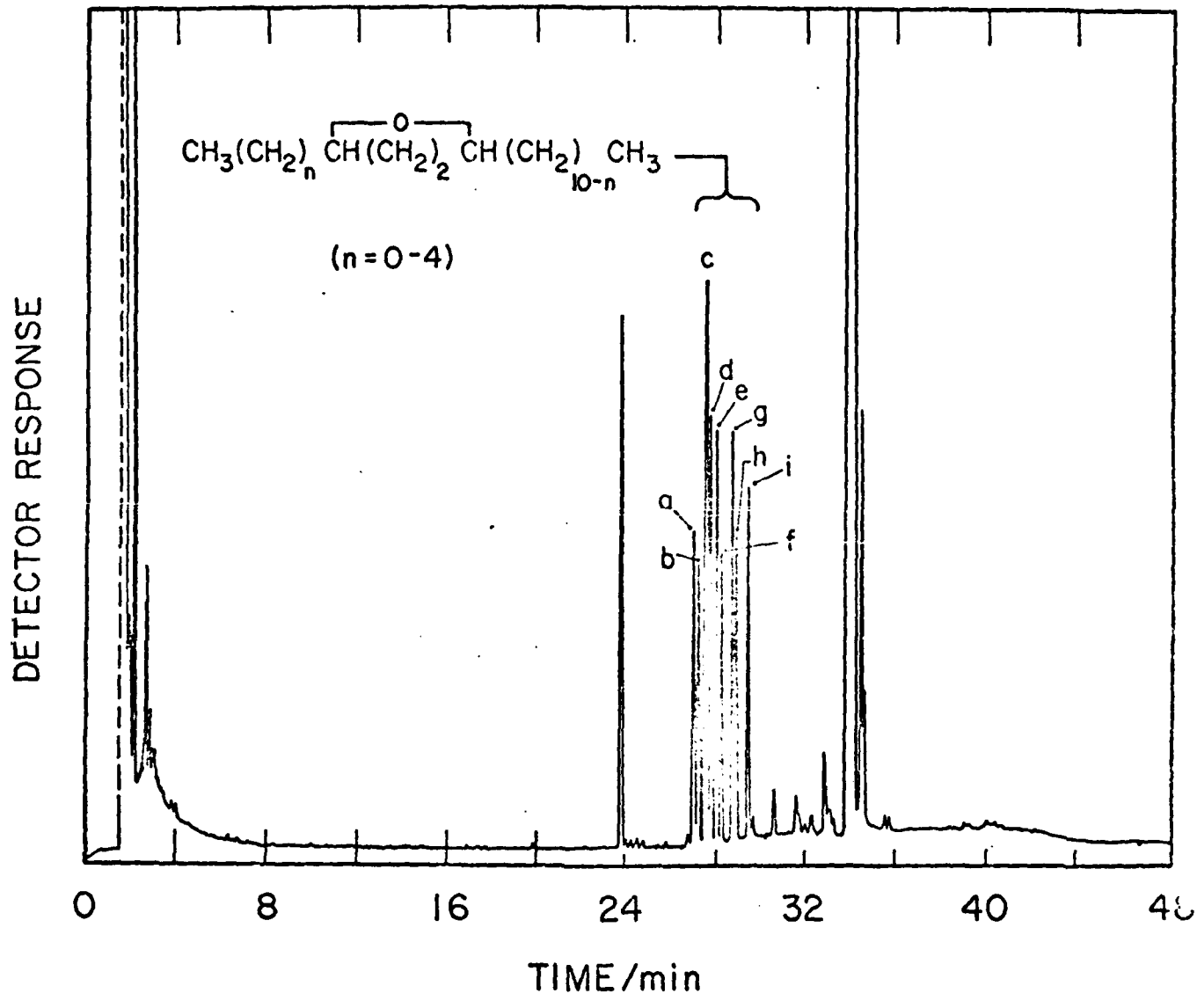

Figure 3 Chromatogram of an oxy fraction from $NaBH_4$ reduced n-hexadecane oxidate which has been concentrated in C_{16} dialkyloxolanes by silica gel chromatography. Peak assignments (cis and trans isomers) are: 2-methyl-5-undecyloxolane, h and i; 2-ethyl-5-decyloxolane, f and g; 2-propyl-5-nonyloxolane, c and e; 2-butyl-5-octyloxolane, b and d; 2-pentyl-5-heptyloxolane, a and c; and 2,5-di-hexyloxolane, a and c.

The carbon oxides were determined by a Fourier Transform Infrared method which also allowed estimation of other trace gaseous products.[7] Table I shows typical results obtained from this analysis.

RESULTS AND DISCUSSION

Oxidation Products. Results of analyses of samples obtained from the autoxidation of n-hexadecane in a stirred flow microreactor at 160 to 190°C and 4 to 120 kPa oxygen pressure are summarized in Tables II and III.

The C_{16} primary oxidation products include i) isomeric hexadecylhydroperoxides, ROOH, determined in sodium borohydride reduced oxidates (subscript A) as hexadecanols, $(ROH)_A$, ii) isomeric hexadecanedihydroperoxides, $R(OOH)_2$, and hydroperoxyhexadecanones, HOOR-O, determined together as hexadecanediols, $(R(OH)_2)_A$, and iii) isomeric C_{16} dialkyl oxolanes, $-\overset{\frown}{CH(CH_2)_2CH}-$. Termination products, isomeric hexadecanones, R'COR", were determined in triphenylphosphine reduced samples either directly or after derivatization.

The cleavage products include homologous series of i) alkanoic acids, R'COOH, determined after esterification, ii) methyl ketones, CH_3COR', determined as secondary alcohols, $(CH_3CH(OH)R')_A$, and iii) 1-oxo and/or 1-oxy alkanes (aldehydes, primary hydroperoxides, primary alcohols) determined as primary alcohols, $(R'CH_2OH)_A$, and H_2O_2, CO and CO_2.

Reaction Scheme. A reaction scheme which accounts for the results of n-hexadecane autoxidation at elevated temperatures obtained in this study and in our previous work[1,2] is in Figure 4.[8] According to this scheme, initiation of

Table I. Results from FTIR analysis of non-condensible gases (run 215).

Compound	ppm
Carbon Dioxide	25.0[a]
Carbon Monoxide	14.4
Formaldehyde	1
Ethylene	2
Ketene CH_2CO	0.5
Acetone	12
Methylethylketone	10
Butanal $CH_3(CH_2)_2CHO$	≈ 8
Pentanal $CH_3(CH_2)_3CHO$	≈ 0.5
Other Hydrocarbon as C_8	≈ 3

[a] Blank sample contained 1.1 ppm carbon dioxide

TABLE II. Analysis of C_{16} Products from the Autoxidation of n-Hexadecane in the Stirred Flow Microreactor[a]

Temp	P	τ	Run	[-OOH][b]	$[1\text{-ROH}]_A$	$[2\text{-ROH}]_A$	$[3\text{--}8\text{-ROH}]_A$	$[ROH]_A$	$[\alpha,\gamma\text{-R(OH)}_2]_A$	$[\alpha,\delta\text{-R(OH)}_2]_A$	[-CH(O)(CH$_2$)$_2$CH(O)-]	[4--8-R'COR"][c]	[1--8-R'COR"][c,d]
(°C)	(kPa)	(s)						(mM)					
160	4.66	340	245	3.50	0.08	0.52	2.49	3.09	0.11	0.39	0.046	0.018	
	4.60	664	244	12.23	0.26	1.80	9.63	11.69	0.32	1.17	0.15	0.16	
	8.96	337	249	4.49	0.09	0.59	2.61	3.29	0.12	0.47	0.035	0.024	
	8.81	653	248	16.92	0.34	2.16	10.54	13.04	0.40	1.60	0.13	0.20	
	15.95	338	250	5.48	0.13	0.68	3.13	3.94	0.31	0.63	0.032	0.027	
	15.86	655	251	21.83	0.53	3.03	13.57	17.13	1.01	2.66	0.13	0.25	
180	5.0	93	224	3.48	0.051	0.53	2.17	2.75	0.052	0.21		0.014	0.021
	5.0	178	223	10.8	0.17	1.78	7.32	9.27	0.12	0.68		0.105	0.115
	4.68	186	258	10.8	0.18	1.68	9.13	10.99	0.13	0.75	0.28	0.122	
	7.34	185	259	14.6	0.27	2.23	11.68	14.18	0.23	1.30	0.30	0.153	
	12.5	78	219	4.87	0.066	0.76	2.72	3.58	0.16	0.50		0.018	
	12.2	138	218	12.6	0.21	1.96	7.94	10.11	0.37	1.29		0.70	
	11.4	154	216	14.2	0.30	1.70	10.40	12.40	0.44	1.41	0.235	0.105	0.127
	12.1	181	217	19.1	0.40	2.33	12.62	15.35	0.41	1.75	0.279	0.136	
	11.3	198	215	20.5(7)[e,f]	0.43(2)[2]	2.67(7)[2]	15.44(7)[2]	18.54	0.34(5)[2]	1.87(14)[2]	0.39(4)[2]	0.219(9)[2]	0.274
	30.2	140	225	15.3(7)[f]	0.49	11.43		11.92	0.48	2.83	0.80	0.130	0.153
	19.25	167	260	21.5	0.51	2.56	13.87	16.94	0.94	2.63	0.231	0.239	
	33.7	200	153	46.4	1.07	5.39	21.4	27.86	2.51	5.05		0.586	
	56.6	197	152	54.1	1.38	6.44	25.0	32.82	3.30	5.92		0.732	
	110	78	150	9.3	0.24	1.06	3.84	5.14	1.00	0.957		0.046	0.077
	110	146	149	31.4	0.83	3.72	13.8	18.35	2.74	3.52		0.291	
	110	202	151	63.1	1.75(3)[2]	6.91(15)[2]	29.50(15)[2]	38.16	3.46(10)[2]	7.73(8)[2]	0.138(4)[2]	0.95	
190	4.99	69.3	262	5.14	0.09	0.72	4.56	5.37	0.070	0.32	0.171	0.045	
	7.71	68.7	265	6.59	0.14	0.98	5.64	6.76	0.15	0.57	0.191	0.056	
	10.20	69.6	266	8.28	0.16	1.04	6.18	7.38	0.14	0.69	0.197	0.070	
	15.45	69.2	263	10.59	0.22	1.40	7.04	8.66	0.25	1.13	0.202	0.072	
	20.36	68.9	267	13.00	0.31	1.65	8.95	10.91	0.41	1.49	0.211	0.109	
	117	66.2	264	32.78	0.97	4.09	16.23	21.29	2.63	3.91	0.118	0.239	

[a] Initial concentrations of n-hexadecane were 2.98, 2.91, and 2.86 M at 160, 180, and 190°C, respectively. All experiments were performed at total pressures of 110-130 kPa. [b] Determined by the iodometric titration, Ref. 1. [c] Determined in triphenylphosphine reduced samples. [d] 1-Hexadecanal. [e] The uncertainties of measured values are indicated in parentheses. The number of independent analyses are designated by the superscript.

TABLE III. Analysis of Cleavage Products from the Autoxidation of n-Hexadecane in the Stirred Flow Microreactor.[a]

Temp	P	τ	Run	[R'COOH][b]	[$CH_3CH(OH)R'$][c]	[$R'CH_2OH$][c]	[H_2O_2][d]	[CO][e]	[CO_2][e]
(°C)	(KPa)	(s)			(mM)				
160	4.66	340	245		0.086	0.046	0.06		
	4.60	664	244		0.428	0.233	0.17		
	8.96	337	249		0.135	0.057			
	8.81	653	248		0.784	0.337	0.46		
	15.95	338	250		0.232	0.081	0.14		
	15.86	655	251		1.45	0.57	0.79		
180	5.0	93	224	0.038	0.026		0.037		
	5.0	178	223	0.213	0.149	0.15	0.13		
	4.68	186	258		0.22	0.27			
	7.34	186	259		0.47	0.40			
	12.6	78	219	0.164	0.117	0.044	0.14		
	12.2	138	218	0.715	0.473	0.24	0.31		
	11.4	154	216	0.76(7)[2][f]	0.54	0.35	0.31	0.043	0.039
	12.1	181	217	1.30	0.85	0.55	0.49		
	11.3	198	215	1.14(2)[2]	0.84(8)[2]	0.65(6)[2]	0.39	0.083	0.042
	20.2	140	225	1.33	1.08	0.46	0.52		
	19.25	167	260		1.40	0.67	0.60		
	33.7	200	153	7.69	4.08	1.17		0.23	0.88
	56.6	197	152	9.69	5.37	1.44		0.25	1.23
	110	78	150	1.13	0.48		0.6	0.008	0.097
	110	148	149	6.18	2.97	0.72	2.5	0.075	0.65
	110	202	151	15.4	8.98(25)[2]	2.58(12)[2]	5.8	0.25	1.77
190	4.99	69.3	262		0.073	0.101			
	7.71	68.7	265		0.153	0.174	0.05		
	10.20	69.6	266		0.22	0.21	0.11		
	15.45	69.2	263		0.40	0.26	0.20		
	20.36	68.8	267		0.65	0.39	0.28		
	117	66.2	264		3.41	1.56	1.41		

[a] See [a] in Table II. [b] By potentiometric acid-base titration. See Ref. 2. [c] Calculated as in Ref. 2. [d] By iodometric titration. See Ref. 1. [e] By FTIR. [f] See [e] in Table II.

Reaction Scheme. A reaction scheme which accounts for the results of n-hexadecane autoxidation at elevated temperatures obtained in this study and in our previous work[1,2] is in Figure 4.[8] According to this scheme, initiation of autoxidation occurs via the homolytic decomposition of peroxidic products, reaction 1. This reaction ultimately leads to formation of alkyl radicals, R•, which react with oxygen to produce alkylperoxy radicals, RO_2•, reaction 2. Alkylperoxy radicals either undergo irreversible intermolecular hydrogen abstraction, reaction 3, producing monohydroperoxide products, ROOH, or reversible intramolecular α,γ (m=1) and α,δ (m=2) hydrogen abstraction, reactions 4, leading to α,γ and α,δ hydroperoxy substituted carbon radicals, HOOR•. These carbon radicals, depending on oxygen pressure, can either isomerize, reaction -4, or undergo intramolecular cyclization (α,δ only), reaction 10, to produce C_{16} cyclic ethers, $-\overset{\frown O \frown}{CH(CH_2)_2CH}-$, and hydroxyl radicals, or irreversibly react with oxygen to give hydroperoxy substituted peroxy radicals, $HOORO_2$•, reaction 2'. These hydroperoxyperoxy radicals, similarly as RO_2•, can undergo intermolecular hydrogen abstraction, reaction 3', to form dihydroperoxides, $R(OOH)_2$, and intramolecular abstraction of secondary hydrogen, similar to reaction 4, which leads to trifunctional oxidation products. In addition to reactions 2' and 4 $HOORO_2$• undergo an intramolecular abstraction reaction of tertiary hydrogen, reaction 4*, to form hydroperoxy substituted ketone products, HOOR=O, and hydroxyl radical. The α,γ-hydroperoxyketone products undergo molecular decomposition to methyl ketones, CH_3COR', and alkanoic acids, R'COOH, via reaction 7.

Formation of Primary C_{16} Products. Results of our present kinetic investi-

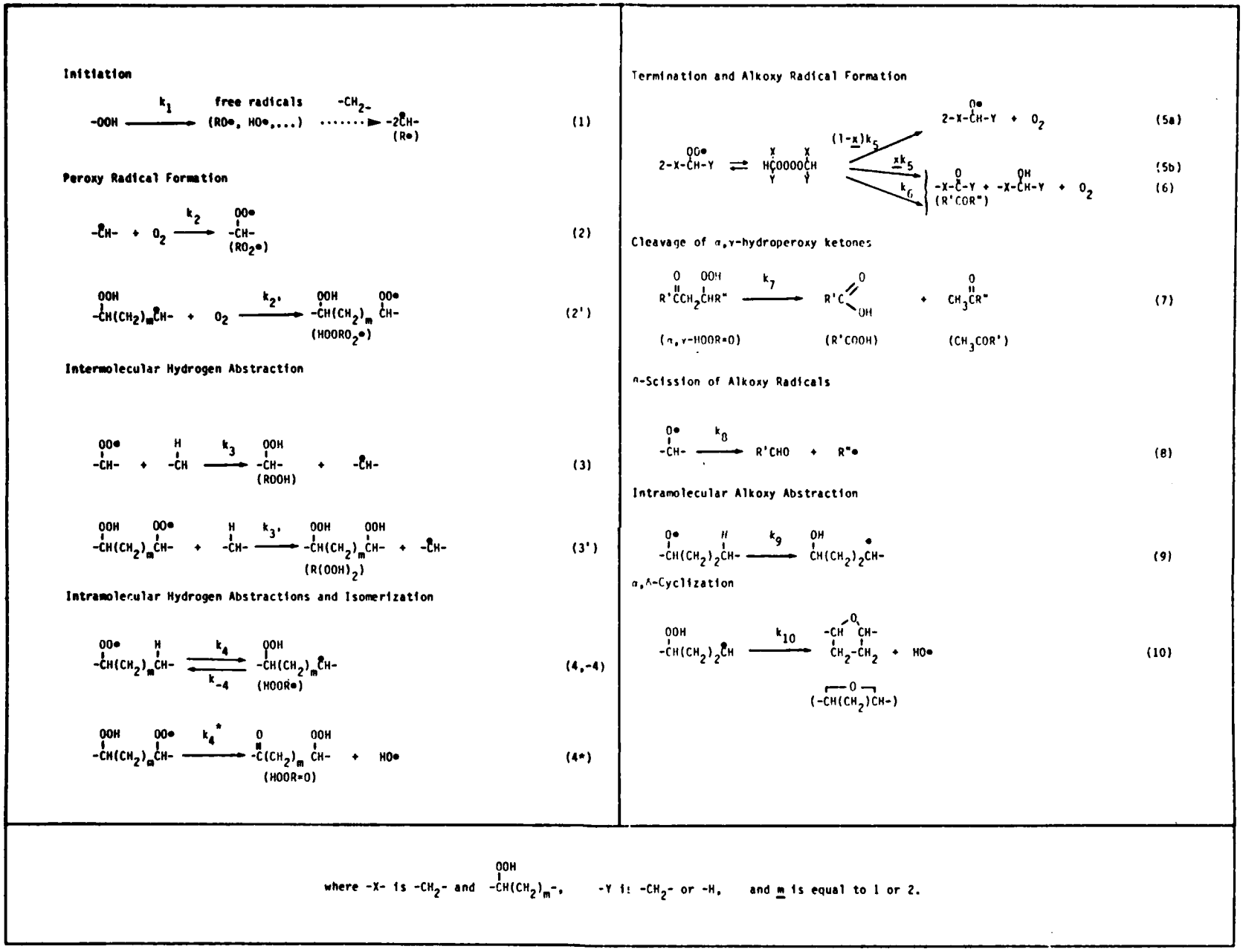

Figure 4 Reaction scheme for the autoxidation of n-hexadecane at elevated temperatures.

gations and those reported previously[1,2] show that the rates of formation of hydroperoxides at a given hydroperoxide concentration decrease i) with decreasing oxygen pressure (Figure 5) and ii) with increasing temperature (e.g. at [-OOH] of 10 m'l the rates at 160, 180, and 190°C and 5 kPa are equal to ca. 87, 46, and 36% of the corresponding 110 kPa values). These decreases are mostly due to the decreased rates of formation of difunctional hydroperoxide products which are more pronounced with those α,γ substituted (Figure 6). The rates of formation of monohydroperoxide products (Figure 7) are much less affected by reduced oxygen pressures. From all products analyzed, only the rates of formation of C_{16} dialkyloxolanes increase with decreasing oxygen pressure (Figure 8). Results obtained at 160 and 190°C are similar to those shown in Figures 5-8 for 180°C.

The above kinetic information suggests that concentration of $HOOR{O_2}^{\bullet}$ decreases with decreasing oxygen pressure more than that of $RO_2^{\bullet}$. Such preferential decrease must be due to the occurrence of reactions -4 and 10 which at lower oxygen pressures effectively compete for HOOR• with reaction 2'. No such competitive reactions, besides termination, consume R• which react with oxygen to give $RO_2^{\bullet}$ via reaction 2. Based on a kinetic analysis for the proposed scheme (Figure 4), the ratio of $[HOOR{O_2}^{\bullet}]$ amd $[RO_2^{\bullet}]$, ψ, is given by expression I

$$\psi = \frac{[\alpha,\gamma\text{-}HOOR{O_2}^{\bullet}] + [\alpha,\delta\text{-}HOOR{O_2}^{\bullet}]}{[RO_2^{\bullet}]}$$

$$= \frac{k_{4\text{-}\alpha,\gamma}}{k_3[RH] + k_{4^*\text{-}\alpha,\gamma}} \cdot \frac{1}{1 + \frac{k_{\text{-}4\text{-}\alpha,\gamma}}{k_2'[O_2]}} + \frac{k_{4\text{-}\alpha,\delta}}{k_3[RH] + k_{4^*\text{-}\alpha,\delta}} \cdot \frac{1}{1 + \frac{k_{\text{-}4\text{-}\alpha,\delta} + k_{10\text{-}\alpha,\delta}}{k_2'[O_2]}} \qquad (I)$$

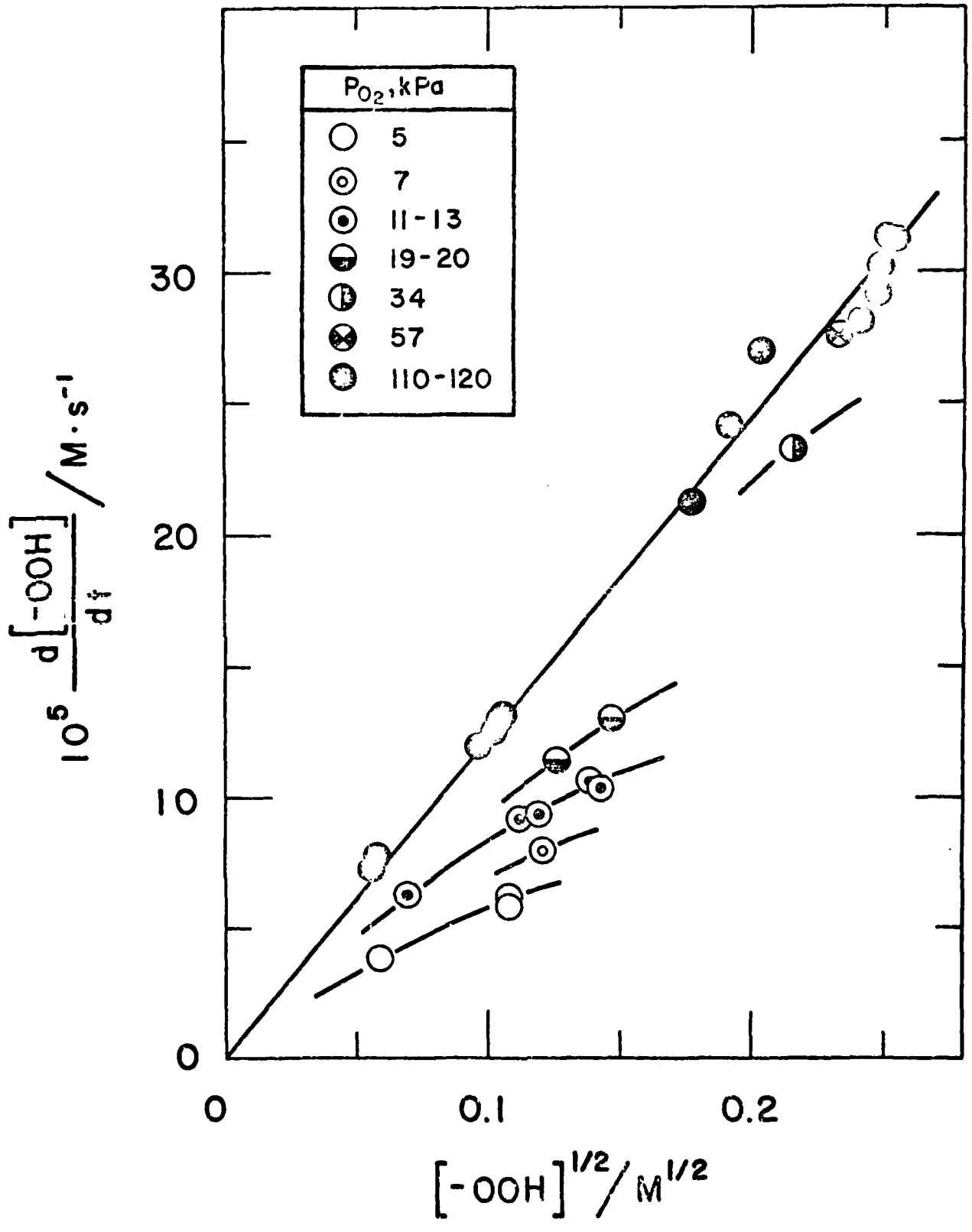

Figure 5 Rate of formation of hydroperoxides vs. $[-OOH]^{1/2}$ at 180°C and at different oxygen pressures.

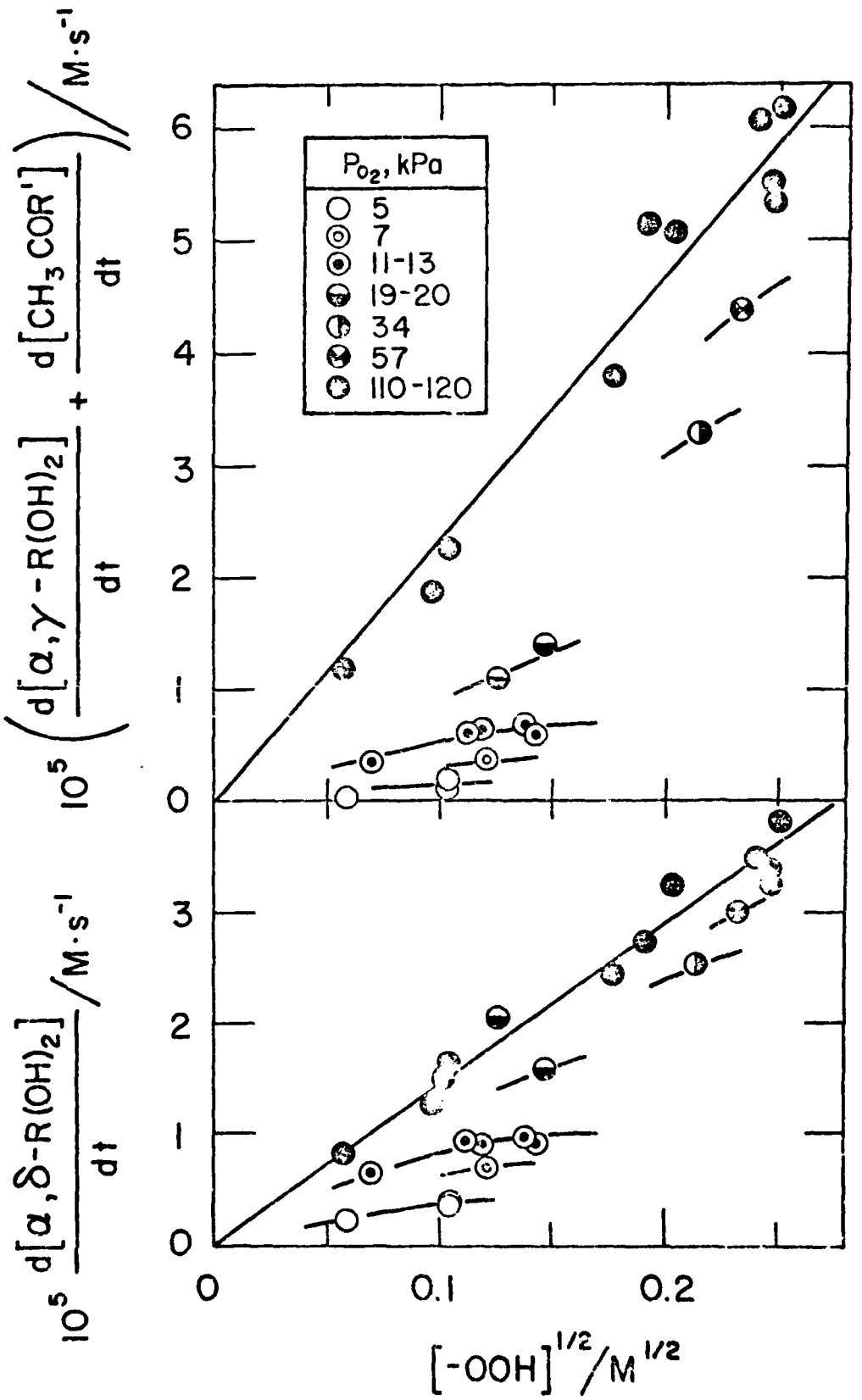

Figure 6 Rates of formation of difunctional products vs. $[\text{-OOH}]^{1/2}$ at 180°C and at different oxygen pressures.

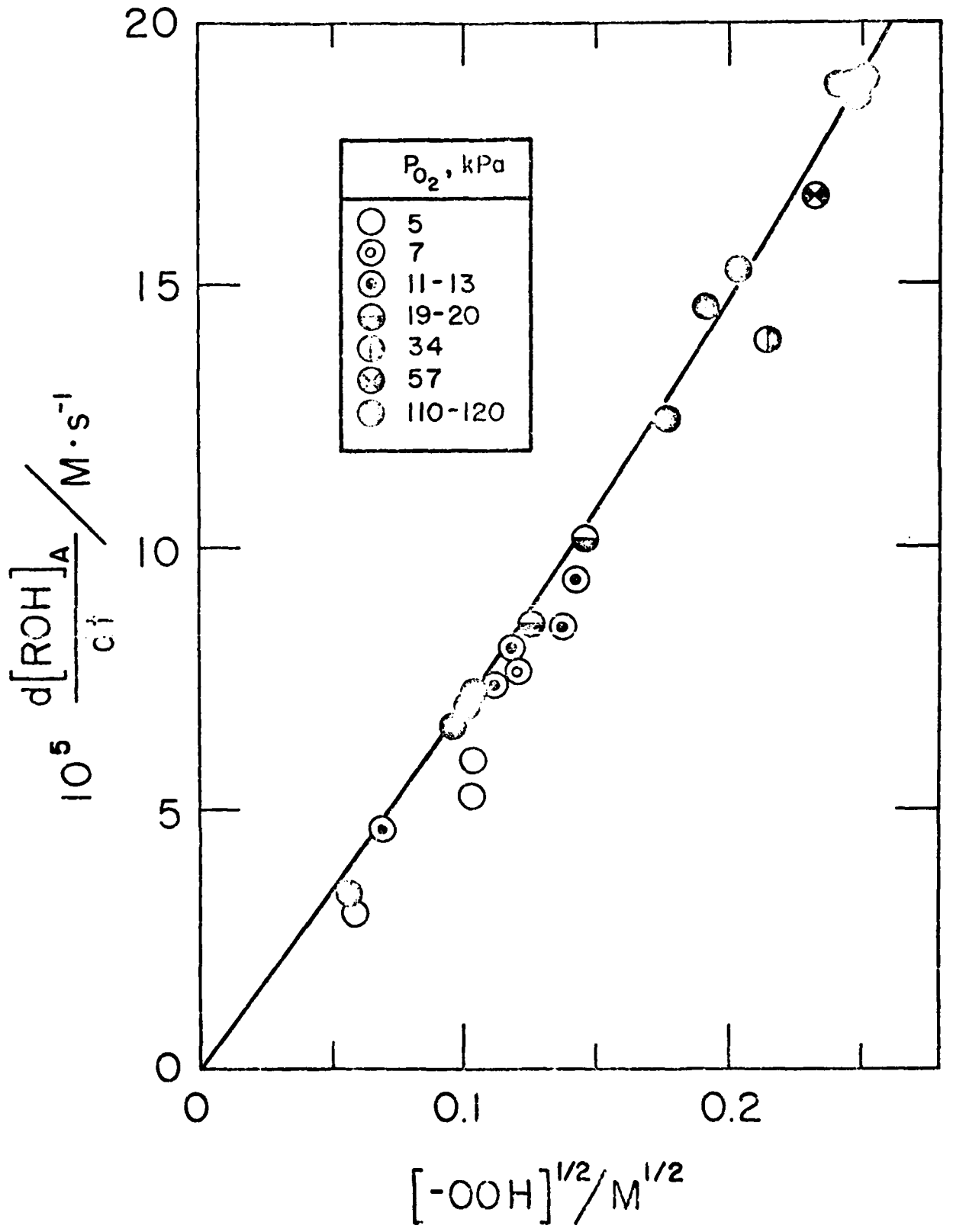

Figure 7 Rate of formation of monofunctional oxidation products vs. $[-OOH]^{1/2}$ at 180°C and different oxygen pressures.

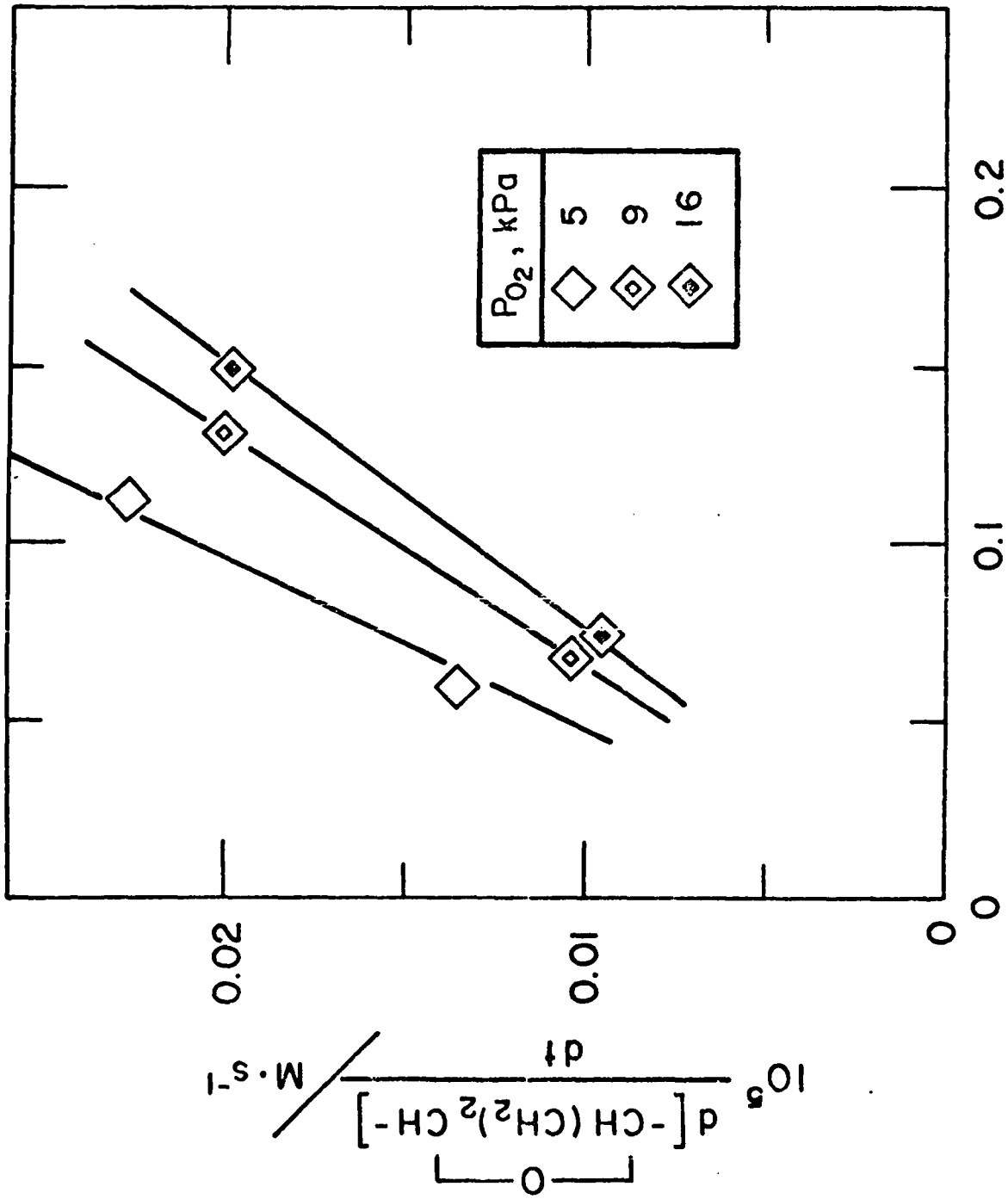

Figure 8 Rates of formation of dialkyloxolanes vs. $[-OOH]^{1/2}$ at 160° and at different oxygen pressures.

and the ratio of [α,δ-HOOR•] to [RO_2•], θ, by expression II:[8]

$$\theta = \frac{[\alpha,\delta\text{-HOOR}\bullet]}{[RO_2\bullet]} = \frac{k_{4-\alpha,\delta}}{k_{-4-\alpha,\delta} + k_{10-\alpha,\delta} + k_{2'-\alpha,\delta}[O_2]} \qquad (II)$$

At high oxygen pressures, when $k_2'[O_2] >> k_{-4} + k_{10}$, ψ approaches its maximum while θ approaches its minimum. At oxygen pressures within our experimental range (4-120 kPa) the values of ψ and θ will depend on the relative values of $k_2'[O_2]$ and $k_{-4} + k_{10}$. It is clear, however, that with decreasing oxygen pressure ψ will decrease while θ will increase. This is consistent with the decreased rate of formation of difunctional hydroperoxide products and increased rate of formation of C_{16} dialkyloxolanes at lower oxygen pressures, since these rates are proportional to [HOORO_2•] and [α,δ-HOOR•], respectively.

The concentration of RO_2• is given by expression III,

$$[RO_2\bullet] = \frac{(R_{RO_2\bullet})^{1/2}}{(2xk_5 + 2k_6)^{1/2}} \frac{1}{(1 + \psi)} \qquad (III)$$

where $R_{RO_2\bullet}$ is the rate of formation of RO_2•, which at high oxygen pressures is equal to the rate of initiation, R_i. Expression III suggests that [RO_2•] approaches its minimum when $k_2'[O_2] >> k_{-4} + k_{10}$, i.e., at high oxygen pressures. If $R_{RO_2\bullet}$ remains the same, [RO_2•] should increase with decreasing oxygen pressure. Under such conditions, the rate of formation of monofunctional hydroperoxide products should also increase with decreasing oxygen pressure since the rate is proportional to [RO_2•]. However, no such increase has been observed, instead, no change at 160°C and some decreases at 180 and 190°C

occurred. The lower the oxygen pressure, the lower [-OOH] at which decreases were observed. This finding suggests that at a given oxygen pressure there is a certain limiting [-OOH], i.e., limiting rate of initiation, at which the oxygen supply and concentration become insufficient to transform all R• to RO_2• and that under such conditions alkyl radicals also contribute to termination. In such case $R_{RO_2•}$ at low oxygen pressures must be lower than $R_{RO_2•}$ at high oxygen pressures and lower than R_i. This view is supported by results shown in Figure 9 where the rates of initiation, determined from the rates of formation of termination products,[10] $R_{t(RO_2•)}$, are plotted against [-OOH]. The lower values of $R_{t(RO_2•)}$ at lower oxygen pressures confirm reduced contribution of RO_2• and some contribution of R• to termination.

The increased concentration of R• may also be a contributing factor leading to the change of monohydroperoxide isomer distribution exhibited by decreased formation of primary 1-hexadecylhydroperoxide at low oxygen pressures (Figure 10). This indicates lower concentration of primary RO_2• at low oxygen pressures. It can be explained by the lower concentration of non-selective •OH radicals due to decreased rate of their formation from reaction 4* and/or by higher concentration of secondary R• and RO_2•. These higher concentrations would result from higher reactivity of primary versus secondary R• in radical transfer reaction with secondary hydrogens of RH. Consequently, the ratio of overall reactivity of primary versus secondary hydrogens in hydrogen abstraction reactions by mixture of free radicals present in the autoxidized n-hexadecane at high oxygen pressures is found to be 1:5 while at oxygen pressure of 5 kPa it is 1:14.

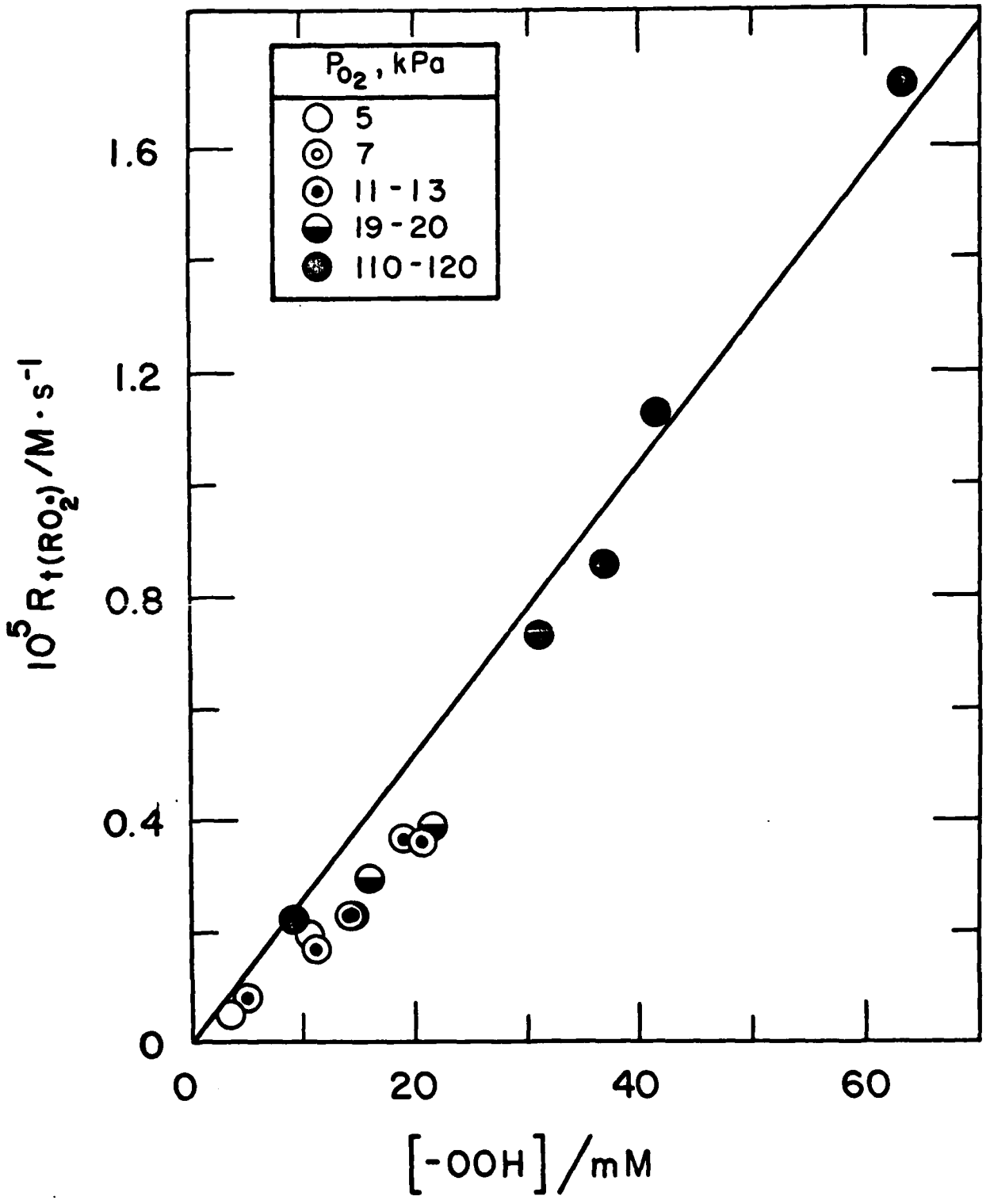

Figure 9 Rate of formation of peroxy radical termination products as function of [-OOH].

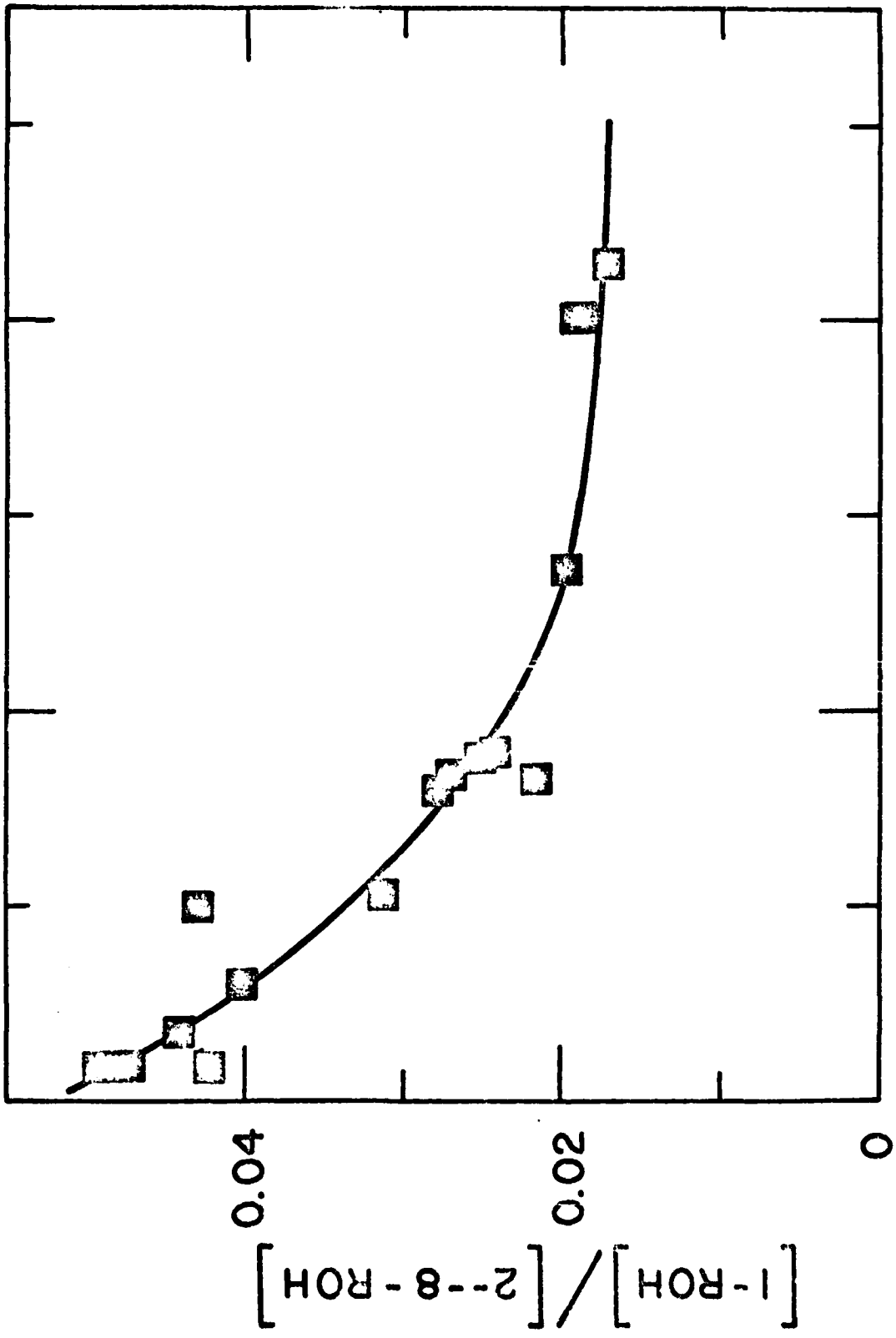

Figure 10 Ratio of rates of formation of primary and secondary monofunctional hydroperoxide products as function of oxygen pressure.

Formation of Cleavage Products. A reaction scheme which depicts formation of cleavage products is in Figure 11.[2] Methyl ketones, CH_3COR', and corresponding equimolar amounts of alkanoic acids, R'COOH, are formed from cleavage of α,γ-hydroperoxyketones, reaction 7. Excess alkanoic acids, $(R'COOH)_{exc}$,[11] and all other cleavage products originate from reactions of alkoxy radicals. Initial step in the latter sequence is β-scission of alkoxy radicals leading to the formation of an aldehyde and an alkyl radical, reaction 8, which is followed by an abstraction of aldehydic hydrogen, reaction 11, decarbonylation of intermediate acyl radicals, reaction 12, formation of alkanoic acids by reaction sequence 13a-13c, decarboxylation of alkanoic peracids, reaction 13d, and formation of lower molecular weight primary hydroperoxides, reaction 14. The formation of hydrogen peroxide could be explained by α,δ intramolecular abstraction reactions of alkoxy radicals, reaction 9a, followed by the series of reactions 9b leading to aldehydes, acids, H_2O_2, and ethylene.

The rates of formation of major cleavage products, CH_3COR' and R'COOH, at low oxygen pressures are significantly lower than those at high oxygen pressures and the same rate of initiation. The decreased rate of formation of CH_3COR' (Figure 12) reflects a decreased rate of formation of α,γ-hydroperoxyketones, while the decreased rate of formation of $(R'COOH)_{exc}$ (Figure 13) indicates the decreased rates of formation of alkoxy radicals and/or of their subsequent reactions. In the following sections the rates of formation of excess cleavage products ($(R'COOH)_{exc}$ and all other cleavage products except CH_3COR') are compared to the rate of formation of RO• in terms of kinetic chain length.

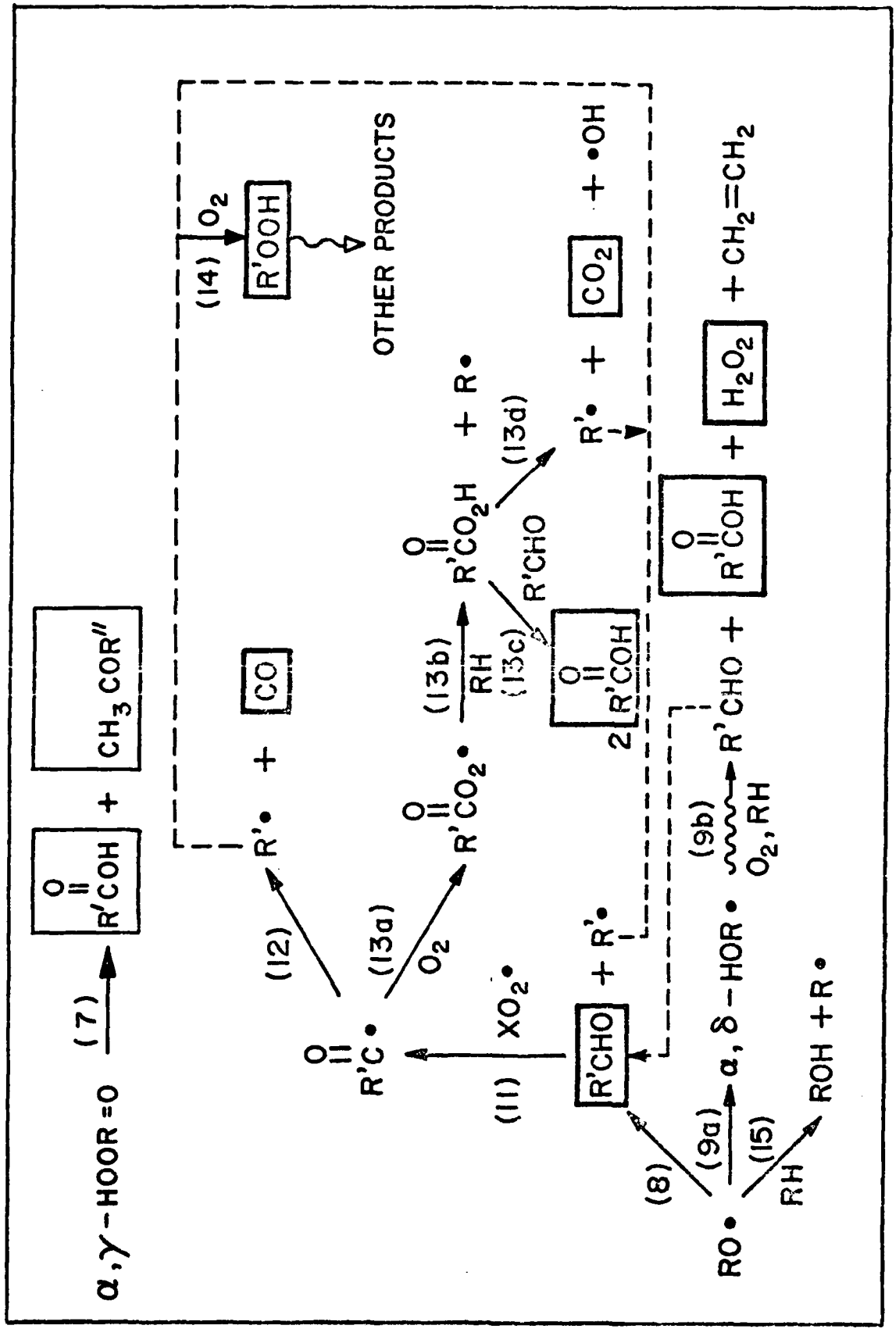

Figure 11 Reaction scheme for the formation of cleavage products in the autoxidation of n-hexadecane at elevated temperatures.

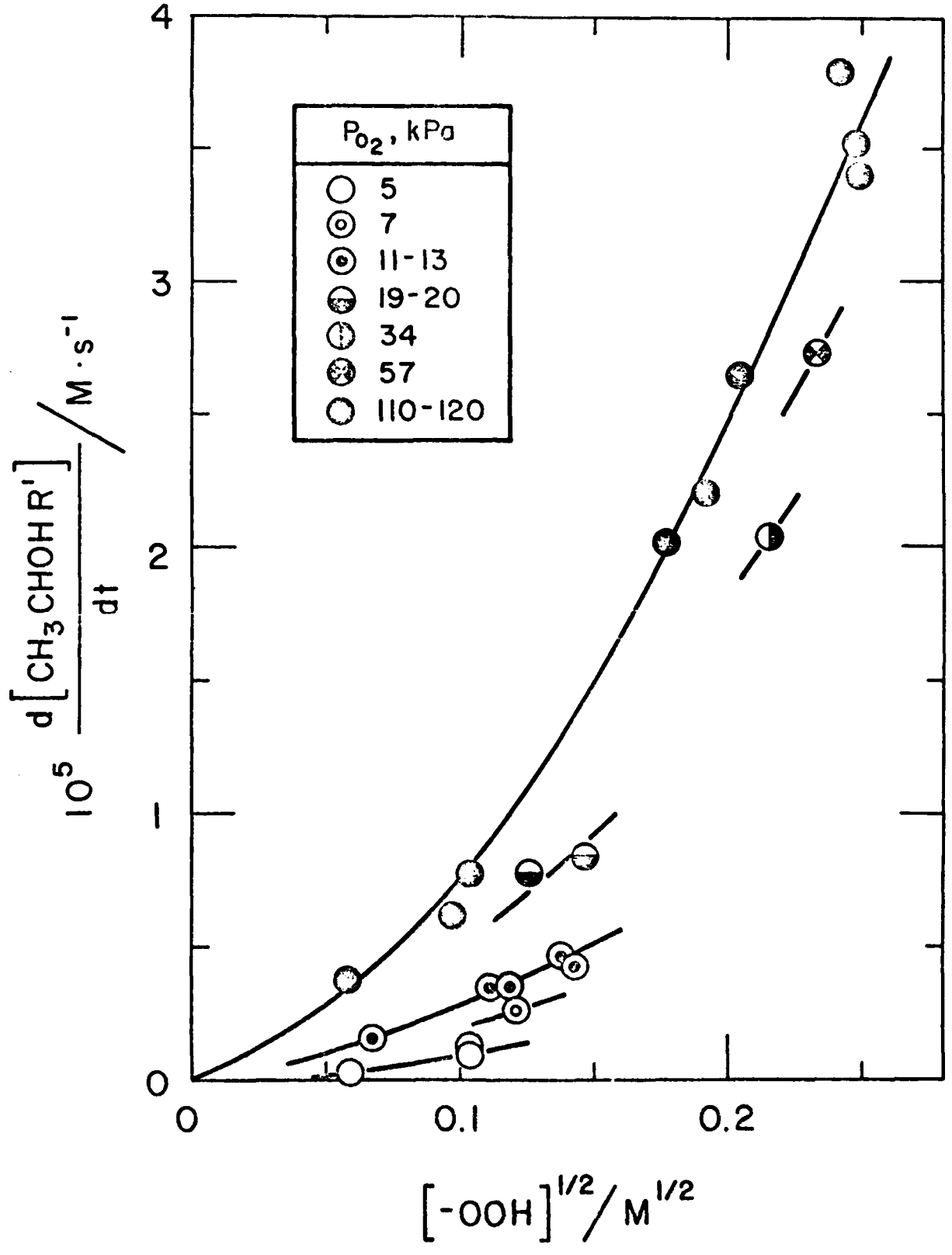

Figure 12 Rate of formation of cleavage methyl ketones vs. $[-OOH]^{1/2}$ at 180°C and different oxygen pressures.

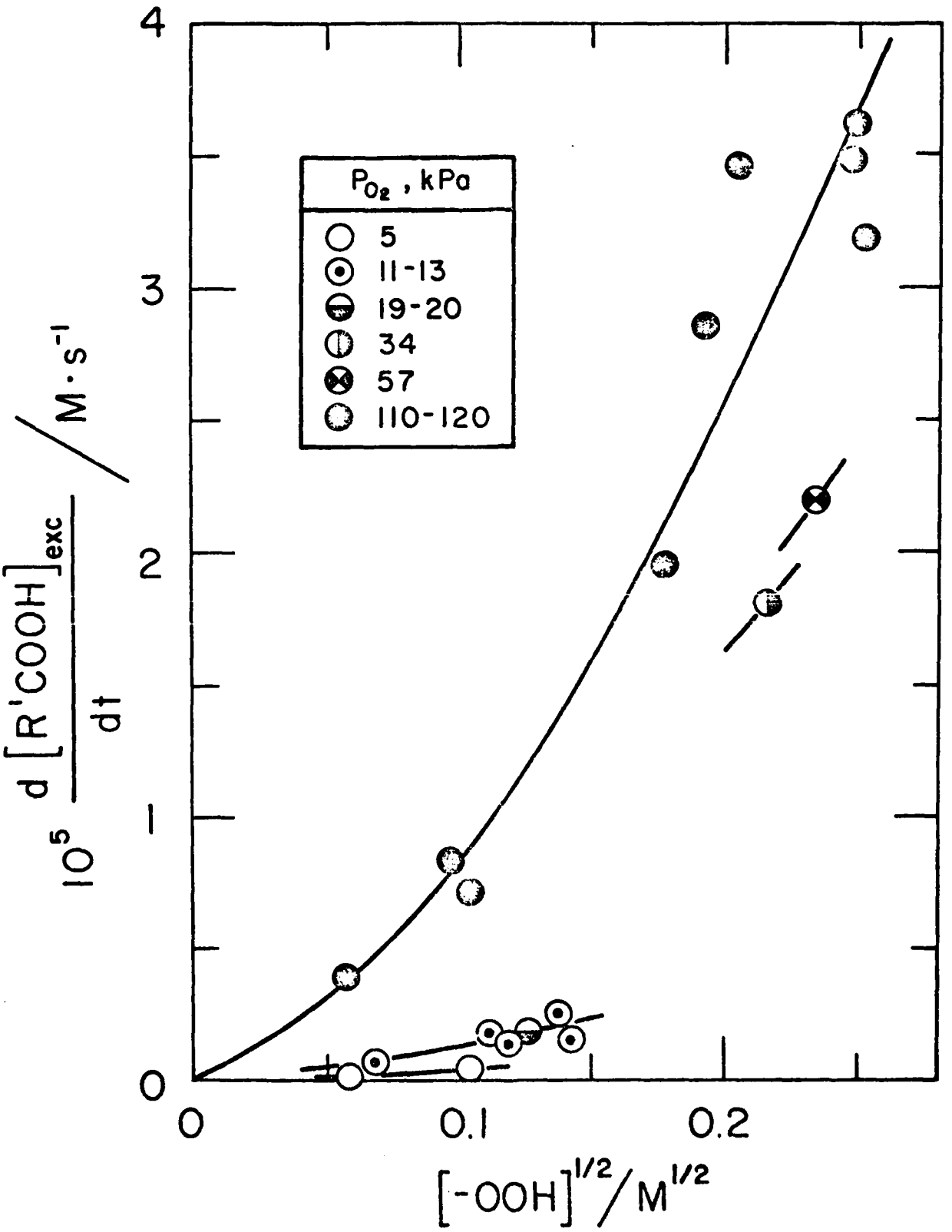

Figure 13 Rate of formation of excess alkanoic acids vs. $[-OOH]^{1/2}$ at 180°C and different oxygen pressures.

Kinetic Chain Length for Alkoxy Radical Formation. In an autoxidizing hydrocarbon alkoxy radicals are formed in the homolysis of hydroperoxide products, reaction 1, and via nonterminating decomposition of tetroxide, reaction 5a, [12,13] where (1 - x) is that fraction of alkoxy radicals which survive termination reaction and diffuse from the solvent cage.

The kinetic chain length for the formation of alkoxy radicals, $\nu_{RO\bullet}$, is then given by eq. IV:

$$\nu_{RO\bullet} = \frac{\left(\frac{d[RO\bullet]}{dt}\right)_1 + \left(\frac{d[RO\bullet]}{dt}\right)_{5a}}{R_t} \qquad (IV)$$

where R_t is the rate of termination which under steady state conditions is equal to the rate of initiation, R_i. It follows from the kinetic analysis that

$$\nu_{RO\bullet} = \frac{k_1[\text{-OOH}]}{R_i} + \frac{(1-x)k_5}{xk_5 + k_6} \qquad (V)$$

The maximum $\nu_{RO\bullet}$ can be calculated from eq. V assuming the initiation via reaction 1 and the termination via reaction 6 only. Under such conditions R_i is equal to $2k_1[\text{-OOH}]$ and x is equal to zero. Then,

$$(\nu_{RO\bullet})_{max} = 0.5 + \frac{k_5}{k_6} \qquad (VI)$$

Utilizing values of k_5/k_6 estimated from the data of Mill et al.[12] for the sec-butylperoxy system, $(\nu_{RO\bullet})_{max}$ is calculated to be 2.0 at 180°C.

The actual $\nu_{RO\bullet}$, however, must be smaller than $(\nu_{RO\bullet})_{max}$. At higher oxygen pressures this is mainly due to the contribution of reaction 13d to initiation and at low oxygen pressures due to the contribution of alkyl radicals to termination. Thus,

$$\nu_{RO\bullet} = 0.5 + \frac{k_5}{k_6} \frac{R_{t(RO_2\bullet)}}{R_i} - \nu_{CO_2} \qquad \text{(VII)}$$

where ν_{CO_2} is the kinetic chain length for the formation of CO_2 via reaction 13d.

Kinetic Chain Length for Cleavage Product Formation. The kinetic chain length for the formation of any reaction product or intermediate, X, in stirred flow reactor experiments can be calculated using expression VIII

$$\nu_X = \frac{[X]_\tau/\tau}{(R_i)_\tau} \qquad \text{(VIII)}$$

where $(R_i)_\tau$ is the instantaneous rate of radical formation at residence time, τ. The values of $(R_i)_\tau$ used in these calculations were at higher oxygen pressures (P_{O_2} > 50 kPa) determined from the rates of formation of termination products[10] and at lower oxygen presures calculated from the hydroperoxide concentration in the stirred flow reactor using k_1 $^{180°C}$ = 12 x 10^{-5} s^{-1}.[10]

Plots of ν_X for excess cleavage products versus oxygen pressure (Figures 14 and 15) show that yields of these products vary with oxygen pressure. This observation is in keeping with results from our earlier work[2] which showed that excess cleavage products are formed via a complex series of secondary reactions

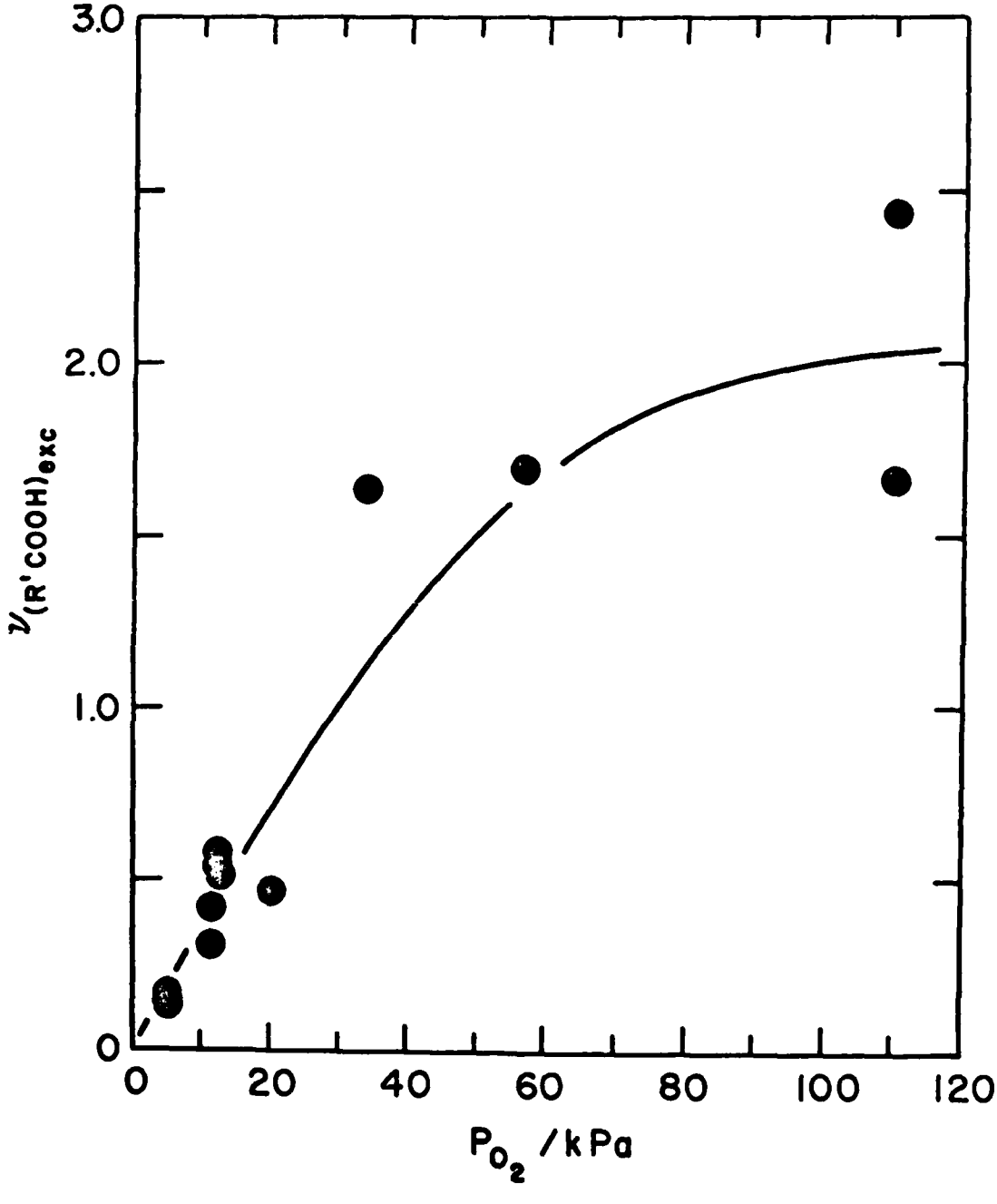

Figure 14 Kinetic chain lengths for the formation of excess alkanoic acids vs. oxygen pressure at 180°C.

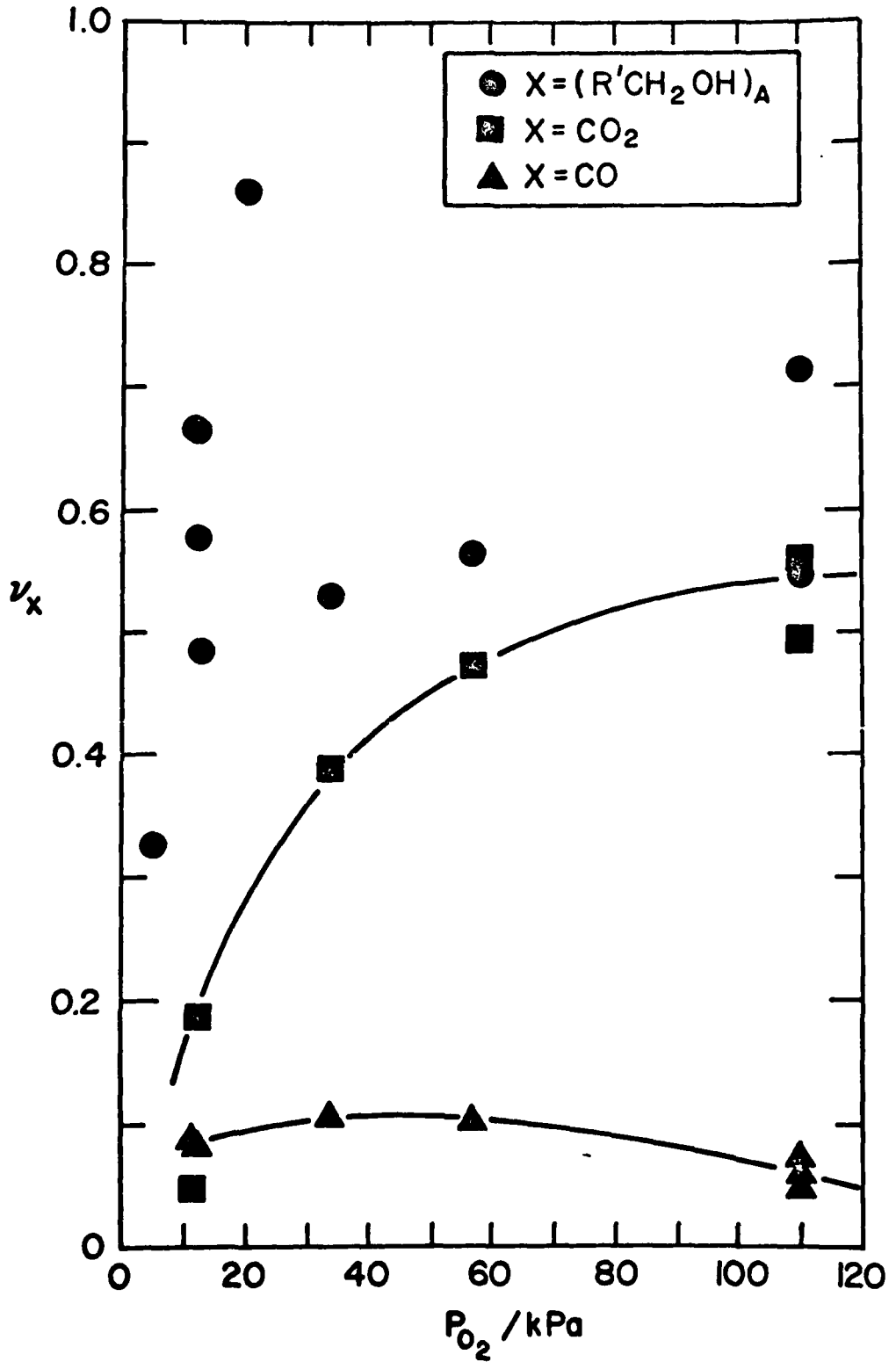

Figure 15 Kinetic chain lengths for the formation of 1-oxo and 1-oxy-alkanes, $(R'CH_2OH)_A$, CO_2, and CO vs. oxygen pressure at 180°C.

some of which involve oxygen addition as shown in Figure 11. The results obtained for ν_{CO} are consistent with the formation of CO via decarbonylation, reaction 12, which is in competition with oxygen addition, reaction 13a, and final formation of CO_2 and alkanoic acids.

If the excess cleavage products would be formed only via reaction sequence 8, 11, 12, and 13 and acids would originate only from oxidation of aldehydes, then the values of the sum $\nu_{(R'COOH)_{exc}} + \nu_{CO_2} + \nu_{CO}$ should be approximately equal to $\nu_{(R'CH_2OH)_A}$. The values of the sum, however, are found to be much larger than $\nu_{(R'CH_2OH)_A}$. That suggests, that there must be routes leading to formation of acids or aldehydes other than those via reactions 8 and 13, such as reaction sequence 9 or reactions involving cleavage alkyl radicals R'• or products of their conversions.

Although the kinetic chain length for the formation of the sum of excess cleavage products, ν_{ECP}, depends upon the subsequent reactions of alkoxy radicals, its value, based on the scheme in Figure 11, can not be greater than two times the value for alkoxy radicals, i.e.,

$$\nu_{ECP} = \nu_{(R'COOH)_{exc}} + \nu_{(R'CH_2OH)_A} + \nu_{CO} + \nu_{CO_2} \leq 2\nu_{RO\bullet} \qquad \text{(IX)}$$

The values of $2\nu_{RO\bullet}$ and ν_{ECP} obtained from eqs VII and IX using experimentally determined ν_X values for various cleavage products are plotted as functions of oxygen pressure in Figure 16. These plots indeed show that ν_{ECP} is approximately equal to or smaller than $2\nu_{RO\bullet}$ and thus support the idea that even at reduced oxygen pressure excess cleavage products originate from alkoxy radicals. These results also suggest that alkoxy radicals almost entirely undergo reactions 8 and 9, except at very low oxygen pressures.

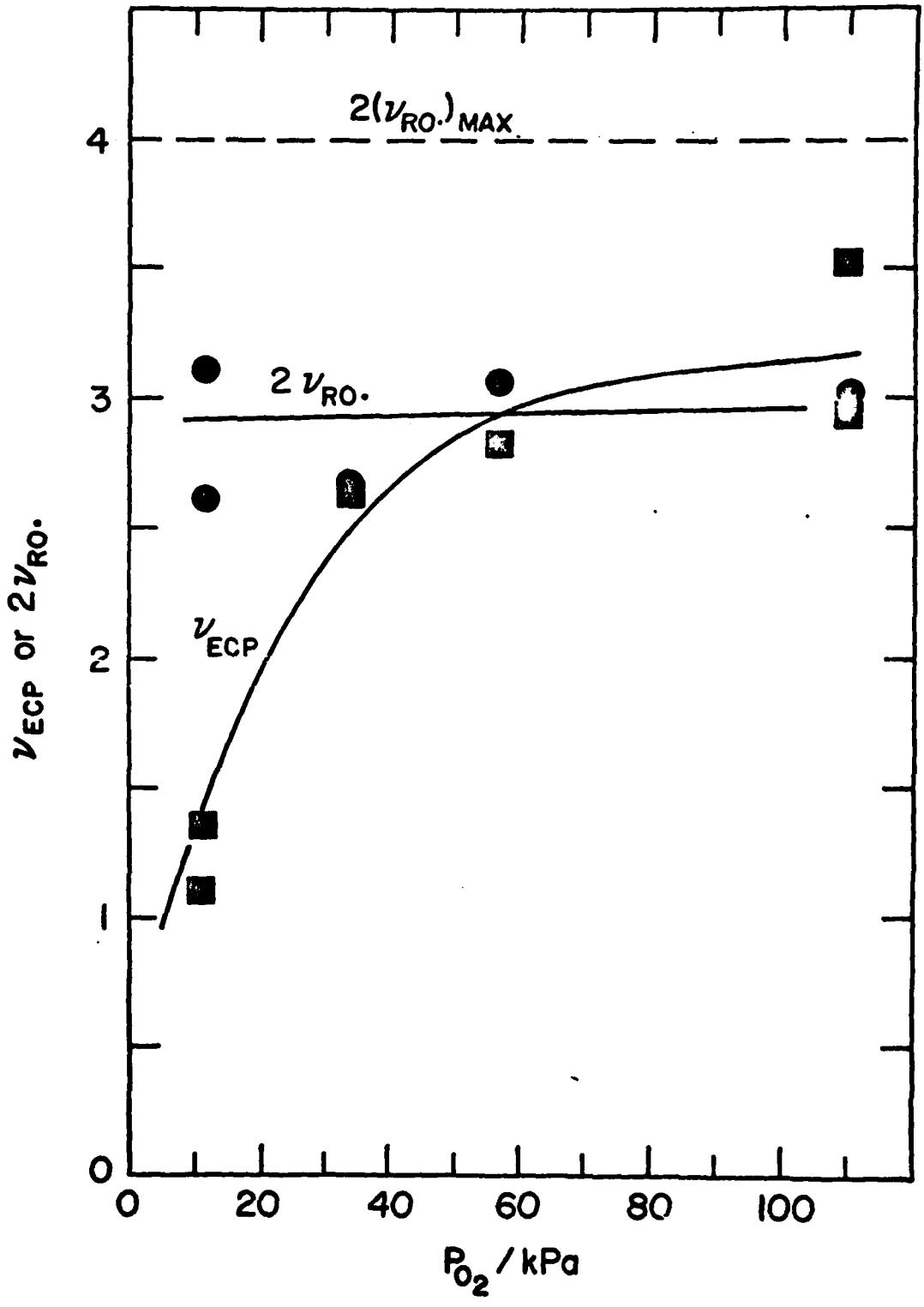

Figure 16 Kinetic chain lengths for the formation of alkoxy radicals and sum of the excess cleavage products vs. oxygen pressure at 180°C.

REFERENCES AND NOTES

(1) R. K. Jensen, S. Korcek, L. R. Mahoney, and M. Zinbo, J. Am. Chem. Soc. 101, 7574 (1979).

(2) R. K. Jensen, S. Korcek, L. R. Mahoney, and M. Zinbo, J. Am. Chem. Soc. 103, 1742 (1981).

(3) E. J. Hamilton, Jr., S. Korcek, L. R. Mahoney, and M. Zinbo, Int. J. Chem. Kinet. 12, 577 (1980).

(4) M. Zinbo, to be published.

(5) D. D. Reynolds and W. O. Kenyon, J. Am. Chem. Soc. 72, 1593 (1950).

(6) "HPLC Derivatization Procedures" in "Regis Chromatography Catalog", Regis Chemical Co., Morton Grove, IL, 1980; p. 76.

(7) P. D. Maker, H. Niki, C. N. Savage, and L. P. Breitenbach, in "ACS Symposium Series", 94, Am. Chem. Soc., Washington, D.C., 1979; p. 161.

(8) The reaction denotation system used throughout this work is consistent with that used in our previous publication.

(9) Derived using the steady-state approximation for each radical at sufficiently long kinetic chain length and assuming k_3 to be equal to $k_{3'}$ and terminations to occur via reactions 5b and 6 of $RO_2^{\bullet}$ and $HOORO_2^{\bullet}$.

(10) R. K. Jensen, S. Korcek, L. R. Mahoney, and M. Zinbo, Part III, of this report.

(11) The yield of excess alkanoic acids is equal to the difference of the yields of total alkanoic acids and acids formed by α,γ-cleavage reaction 7, i.e.,

$$[R'COOH_{exc}]_\tau = [R'COOH]_\tau - [CH_3COR']_\tau$$

(12) T. Mill, F. Mayo, H. Richardson, K. Irwin, and D. Allara, J. Am. Chem. Soc., 94, 6802 (1972).

(13) The alternate mechanism of peroxy radical termination proposed by Benson[30] also leads to the formation of alkoxy radical intermediates.

PART II

FORMATION, ISOMERIZATION, AND CYCLIZATION REACTIONS OF HYDROPEROXYALKYL RADICALS IN n-HEXADECANE AUTOXIDATION AT 160 TO 190°C

R. K. Jensen, S. Korcek, L. R. Mahoney, and M. Zinbo

INTRODUCTION

Our previous studies of kinetics and mechanisms of the liquid phase autoxidation of n-hexadecane at elevated temperatures (160-190°C) included investigations of the effects of oxygen pressure in the range of 4 to 120 kPa.[1] These investigations revealed that intermediate α,γ- and α,δ-hydroperoxyhexadecyl radicals, HOOR•, which are formed by intramolecular hydrogen abstraction reaction 4, besides the addition of oxygen, reaction 2', undergo isomerization reaction -4 and only in the case of α,δ isomers also cyclization reaction 10 (see Figure 1 or for a detailed scheme Figure 4 in Ref. 1).[2] Reactions -4 and 10 were previously documented by Benson.[3-6] The latter reaction is generally accepted as a source of cyclic ether products in the gas phase oxidation of n-alkanes of carbon number 4 or greater in the temperature region of 300 to 480°C.[7-14] In the liquid phase the formation of cyclic ethers was detected in the oxidation of n-dodecane by air at 200°C[15] and in the oxidation of substrates containing tertiary hydrogens, such as 2-methyl-hexadecane[16] and 2,4-dimethylpentane.[17]

Kinetic information obtained in our previous studies[1] is now used to derive, for the first time, the absolute rate constants and Arrhenius parameters for reactions 4,-4 and 10 involving formation, isomerization, and cyclization of secondary hydroperoxyalkyl radicals in the liquid phase.

EXPERIMENTAL SECTION

Measurement of Oxygen Solubility in n-Hexadecane. The method used was a modification of the standard Alsterberg procedure (ASTM D-888-81)[18] of measuring dissolved oxygen in water. The modifications involved using 40 mL of deoxygenated water, 1 mL of manganous sulfate solution, 10 mL of n-hexadecane sample

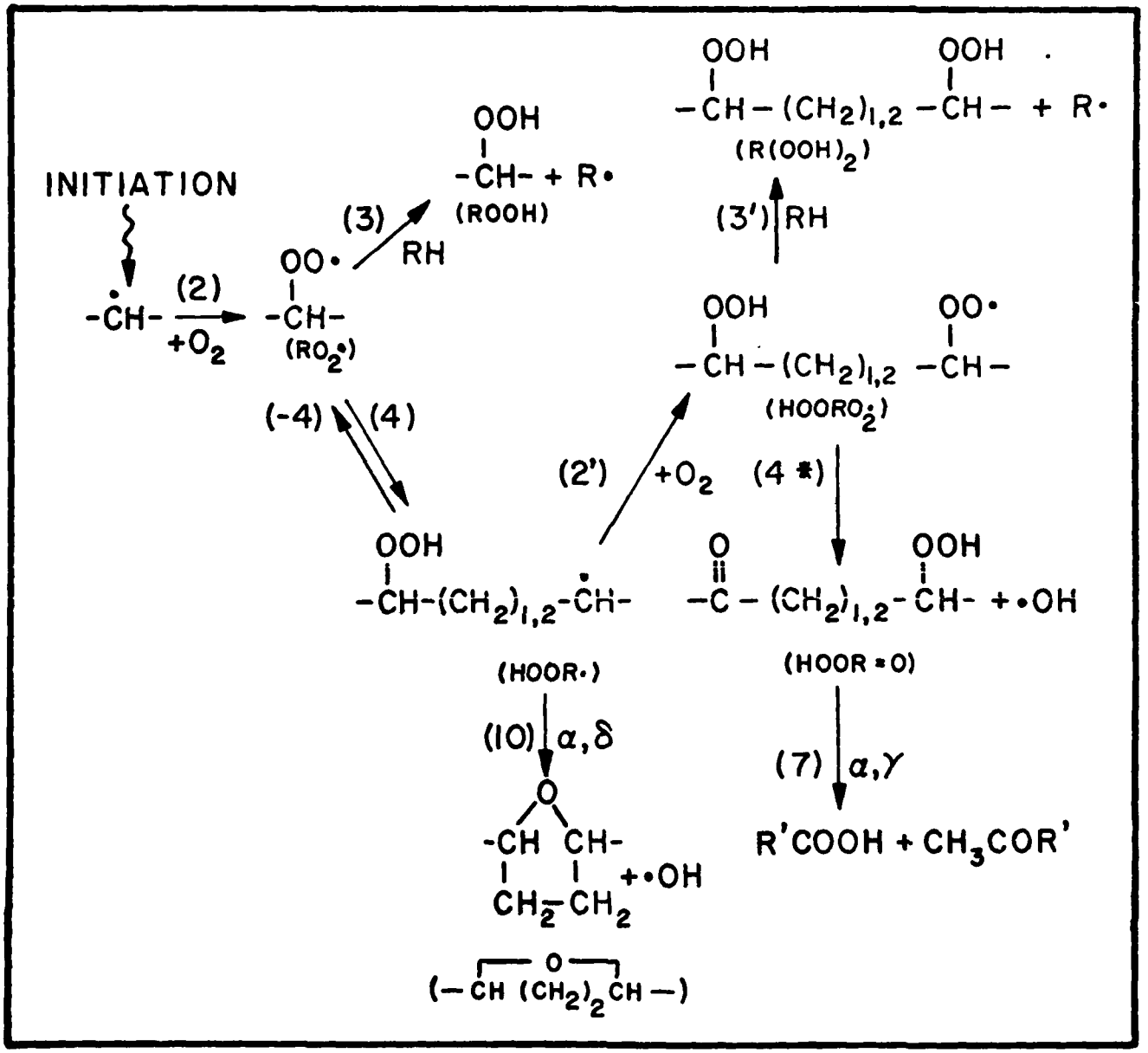

Figure 1 Simplified reaction scheme for the formation of primary oxidation products in the autoxidation of n-hexadecane at elevated temperatures.

and 1 mL of alkaline iodide-sodium azide solution along with vigorous mixing under an inert atmosphere to ensure complete reaction of oxygen dissolved in the n-hexadecane sample with reagents in the aqueous media. The total reaction mixture was titrated with 0.01 N sodium thiosulfate. In the higher temperature (>100°C) samples 1.8-3.6 mM MPH was added to the n-hexadecane to inhibit oxidation.

RESULTS AND DISCUSSION

Kinetic Analysis. A kinetic analysis for the proposed reaction scheme (see Figure 1 and for detailed scheme Figure 4 in Ref. 1) leads to the following expressions for the ratios of rates of product formation:[19]

$$\frac{\left(\frac{d[ROOH]}{dt}\right)_f}{\left(\frac{d[\alpha,\gamma\text{-R(OOH)}_2]}{dt}\right)_f + \left(\frac{d[\alpha,\gamma\text{-HOOR=O}]}{dt}\right)_f} = \frac{k_3[RH]}{k_3[RH] + k^*_{4-\alpha,\gamma}} \frac{[RO_2\bullet]}{[\alpha,\gamma\text{-HOORO}_2\bullet]}$$

$$= \frac{k_3[RH]}{k_{4-\alpha,\gamma}}\left(1 + \frac{k_{-4-\alpha,\gamma}}{k_{2'-\alpha,\gamma}[O_2]}\right) \qquad (I)$$

$$\frac{\left(\frac{d[ROOH]}{dt}\right)_f}{\left(\frac{d[\alpha,\delta\text{-R(OOH)}_2]}{dt}\right)_f + \left(\frac{d[\alpha,\delta\text{-HOOR=O}]}{dt}\right)_f} = \frac{k_3[RH]}{k_3[RH] + k^*_{4-\alpha,\delta}} \frac{[RO_2\bullet]}{[\alpha,\delta\text{-HOORO}_2\bullet]}$$

$$= \frac{k_3[RH]}{k_{4-\alpha,\delta}}\left(1 + \frac{k_{-4-\alpha,\delta} + k_{10-\alpha,\delta}}{k_{2'-\alpha,\delta}[O_2]}\right) \qquad (II)$$

$$\frac{\left(\frac{d[\overset{\overset{O}{\frown}}{-CH(CH_2)_2CH-}]}{dt}\right)_f}{\left(\frac{d[\alpha,\delta\text{-}R(OOH)_2]}{dt}\right)_f + \left(\frac{d[\alpha,\delta\text{-}HOOR{=}O]}{dt}\right)_f} = \frac{k_{10-\alpha,\delta}}{k_3[RH] + k^*_{4-\alpha,\delta}} \frac{[\alpha,\delta\text{-}HOOR\bullet]}{[\alpha,\delta\text{-}HOOR{O_2}\bullet]}$$

$$= \frac{k_{10-\alpha,\delta}}{k_{2'-\alpha,\delta}[O_2]} \qquad \text{(III)}$$

The ratios of rates can be obtained from the stirred flow reactor experiments as the ratios of the corresponding concentrations in the reactor[20] or as the ratios of the yields of corresponding products obtained from the $NaBH_4$ and Ph_3P reductions of oxidates.[21,23] Thus,

$$\frac{([ROH]_A)_\tau}{([\alpha,\gamma\text{-}R(OH)_2]_A)_\tau + ([CH_3CH(OH)R']_A)_\tau} = \frac{k_3[RH]}{k_{4-\alpha,\gamma}}\left(1 + \frac{k_{-4-\alpha,\gamma}}{k_{2'-\alpha,\gamma}[O_2]}\right) \qquad \text{(IV)}$$

$$\frac{([ROH]_A)_\tau}{([\alpha,\delta\text{-}R(OH)_2]_A)_\tau} = \frac{k_3[RH]}{k_{4-\alpha,\delta}}\left(1 + \frac{k_{-4-\alpha,\delta} + k_{10-\alpha,\delta}}{k_{2'-\alpha,\delta}[O_2]}\right) \qquad \text{(V)}$$

$$\frac{([\overset{\overset{O}{\frown}}{-CH(CH_2)_2CH-}]_A)_\tau}{([\alpha,\delta\text{-}R(OH)_2]_A)_\tau} = \frac{k_{10-\alpha,\delta}}{k_{2'-\alpha,\delta}[C_2]} \qquad \text{(VI)}$$

Eqs. IV-VI can be used in determination of rate constants from the ratios of product concentrations obtained from the stirred flow reactor experiments as a function of oxygen concentration.

Oxygen Concentration. Oxygen concentrations calculated using the method described by Prausnitz and Shair[25] and measured for n-hexadecane by Lin and Parcher[26] and for 2-methylhexadecane by Brown and Fish[16] differ significantly.

Therefore, oxygen concentration was independently determined at temperatures from 24 to 190°C (see Experimental Section). The results of these measurements are in Figure 2. Although there is considerable scatter in the data points, the results indicate essentially a linear decrease of oxygen concentration in n-hexadecane with temperature at constant oxygen pressure of 100 kPa. From the graph in Figure 2, Henry's constants for solubility of oxygen in n-hexadecane at 160, 180, and 190°C were 135, 146, and 154 MPa. These constants were used in determination of oxygen concentrations from partial pressure of oxygen using Henry's law.

Rate Constants. Plots of experimental data reported in Part I of this report and in our previous work[22,24] consistent with eqs. IV-VI are in Figures 3-7. The composite rate constants derived from the slopes and intercepts of these plots, $k_3[RH]/k_4$, $(k_{-4} + k_{10})/k_2'$, and k_{10}/k_2', are in Table I. The individual absolute rate constants calculated from the above composite rate constants are also in Table I. Values of k_4 were obtained from ratios $k_3[RH]/k_4$ using values of k_3 determined from rates of formation of monofunctional reaction products as described in Introduction to Part III of this report.[28] Values of k_{-4} and k_{10} were obtained assuming a diffusion controlled value of 10^9 $M^{-1}s^{-1}$ for k_2'. The absolute rate constants on per hydrogen basis were calculated using number of available active hydrogens in reactions 4-α,γ, 4-α,δ, -4-α,γ, and -4-α,δ equal 3.18, 2.94, 1, and 1, respectively.[29]

Arrhenius Parameters. Arrhenius plots for rate constants k_4/H, k_{-4}/H, and k_{10} are in Figures 8 and 9 and Arrhenius parameters derived from these plots are in Table II.

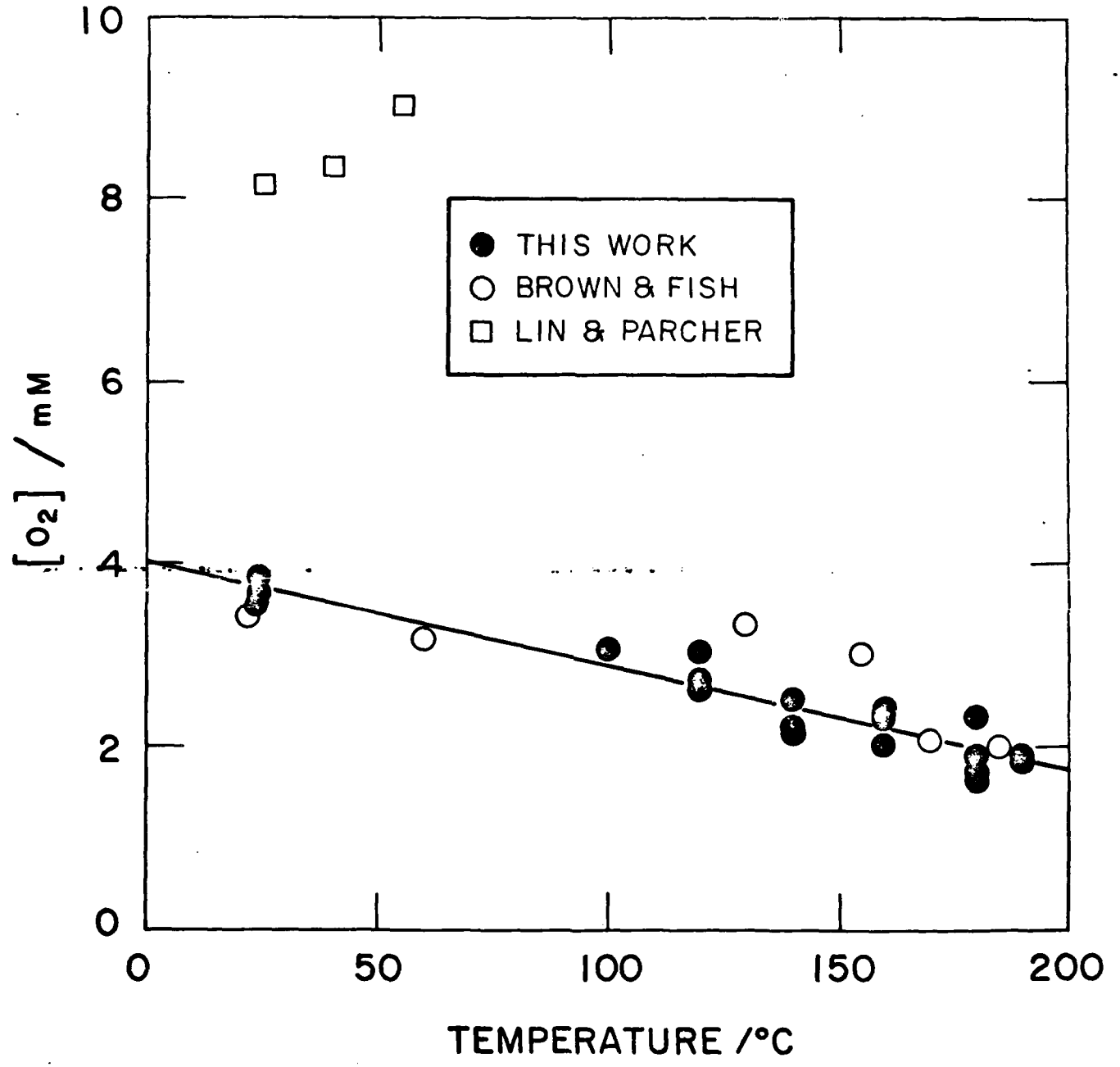

Figure 2 Concentration of dissolved oxygen vs. temperature for n-hexadecane (our data and Lin and Parcher's) and 2-methylhexadecane (Brown and Fish's data).

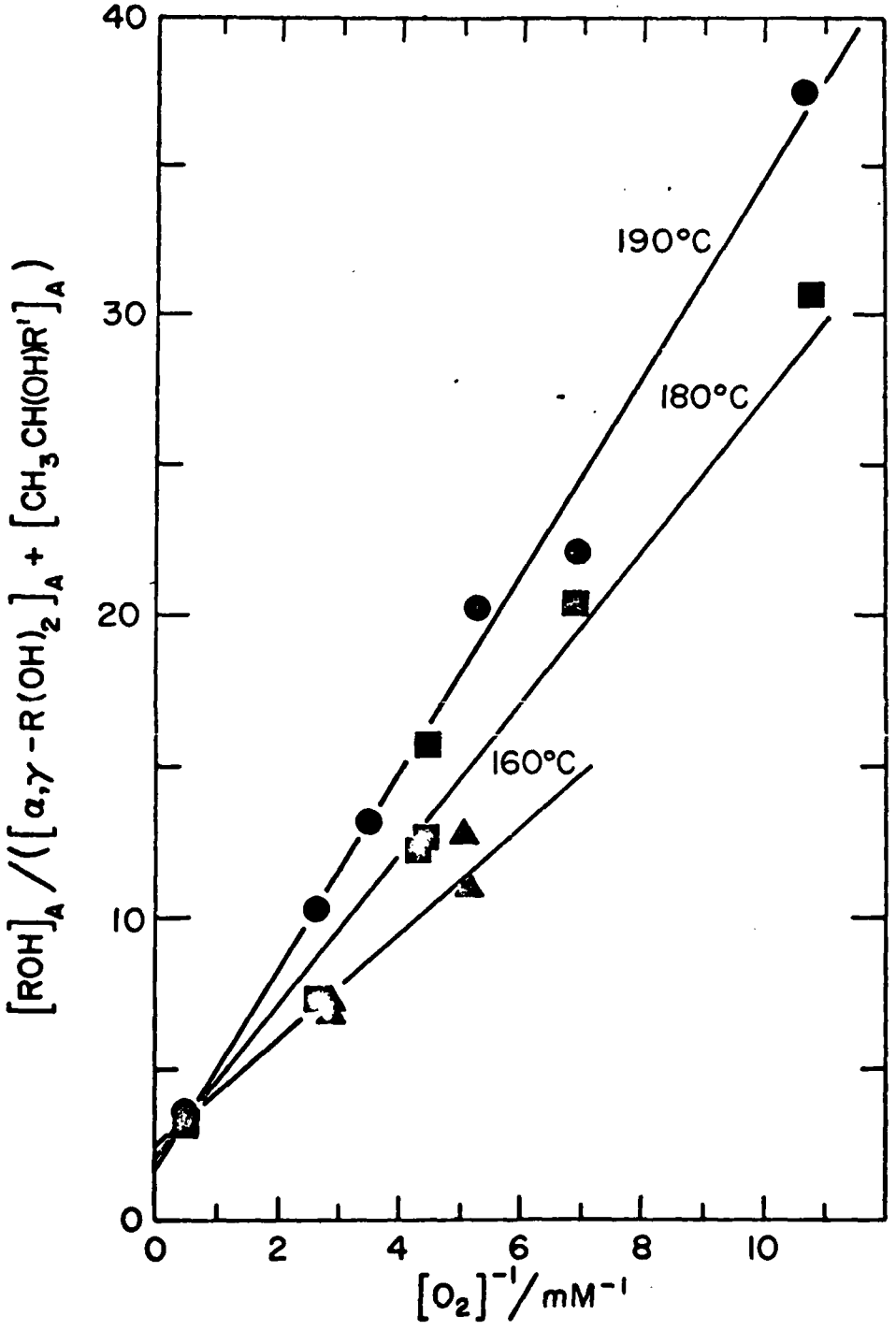

Figure 3 Ratio of rates of formation of monofunctional and α,γ-difunctional products vs. $[O_2]^{-1}$ (Eq. IV).

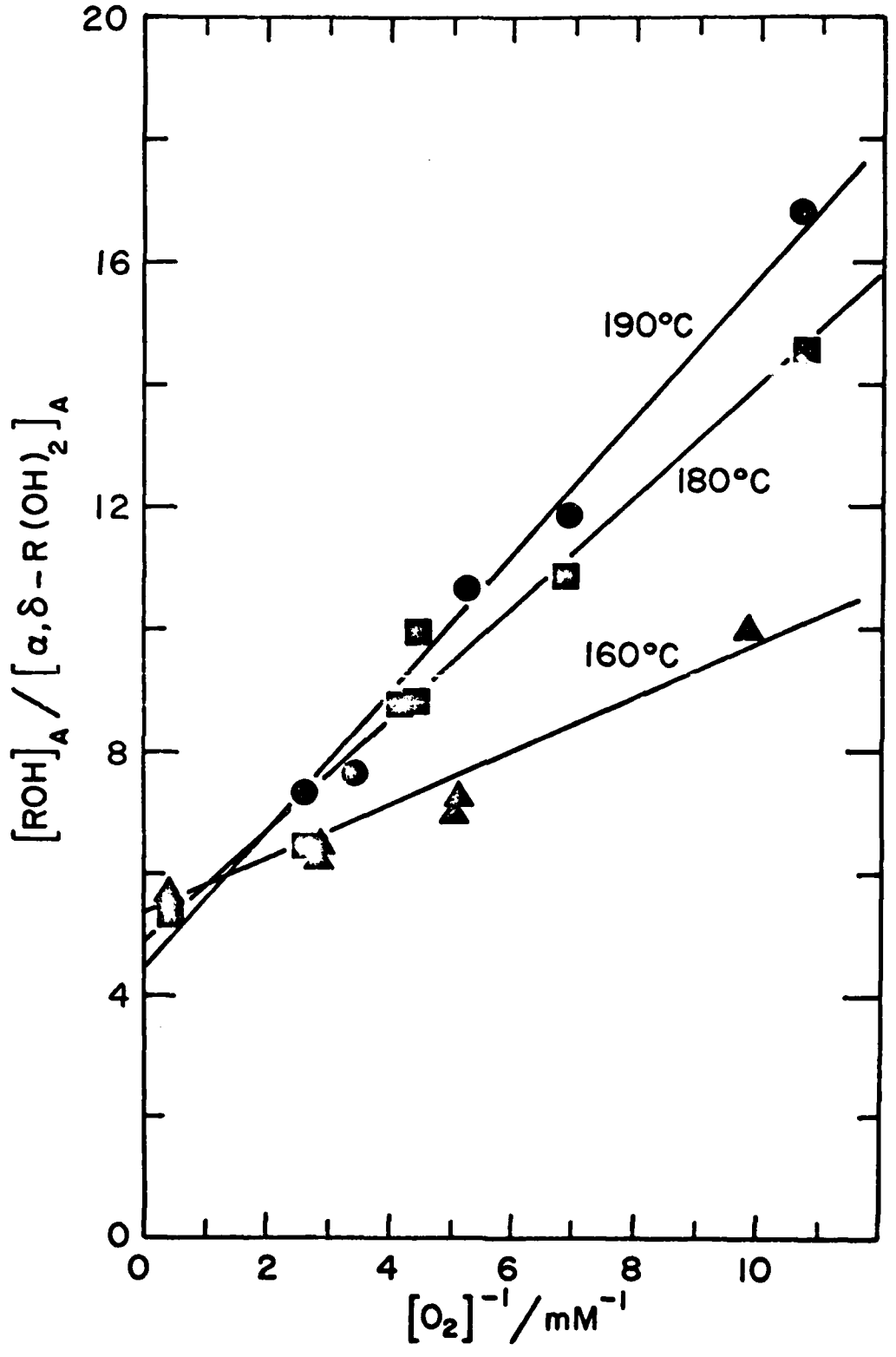

Figure 4 Ratio of rates of formation of monofunctional and α,δ-difunctional products vs. $[O_2]^{-1}$ (Eq. V).

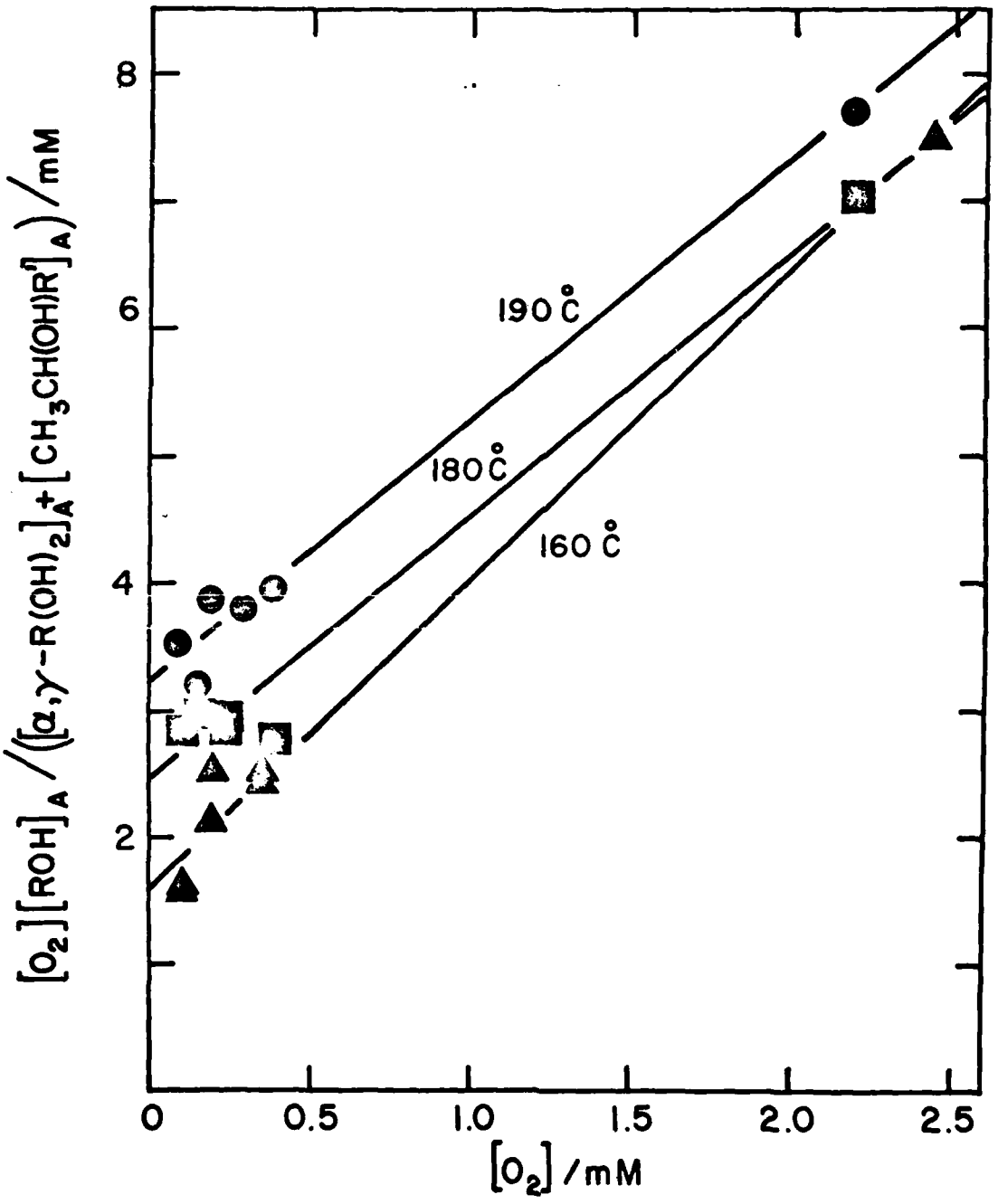

Figure 5 Ratio of rates of formation of monofunctional and α,γ-difunctional products times $[O_2]$ vs. $[O_2]$ (Eq. IV).

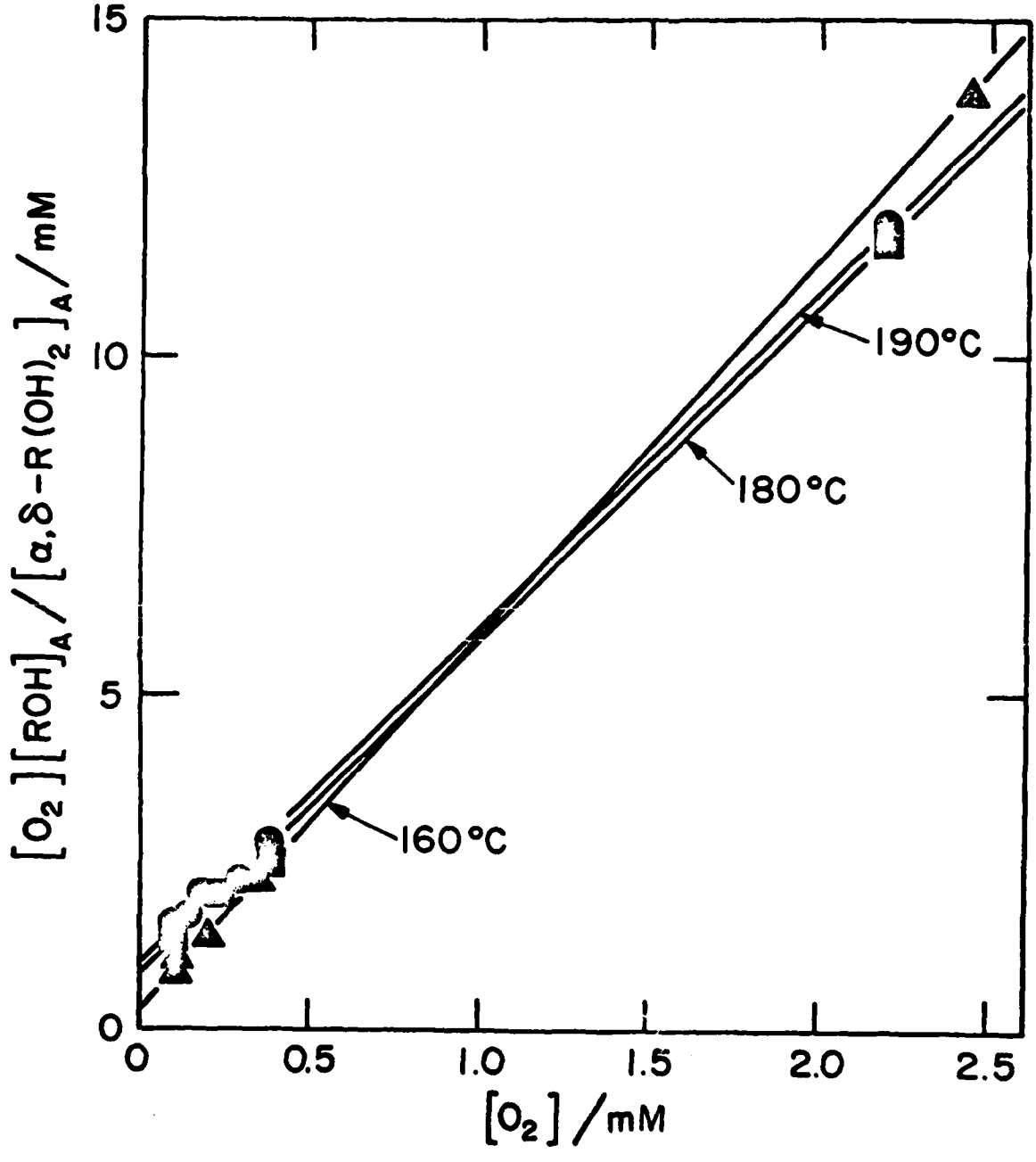

Figure 6 Ratio of rates of formation of monofunctional and α,δ-difunctional products times $[O_2]$ vs. $[O_2]$ (Eq. V).

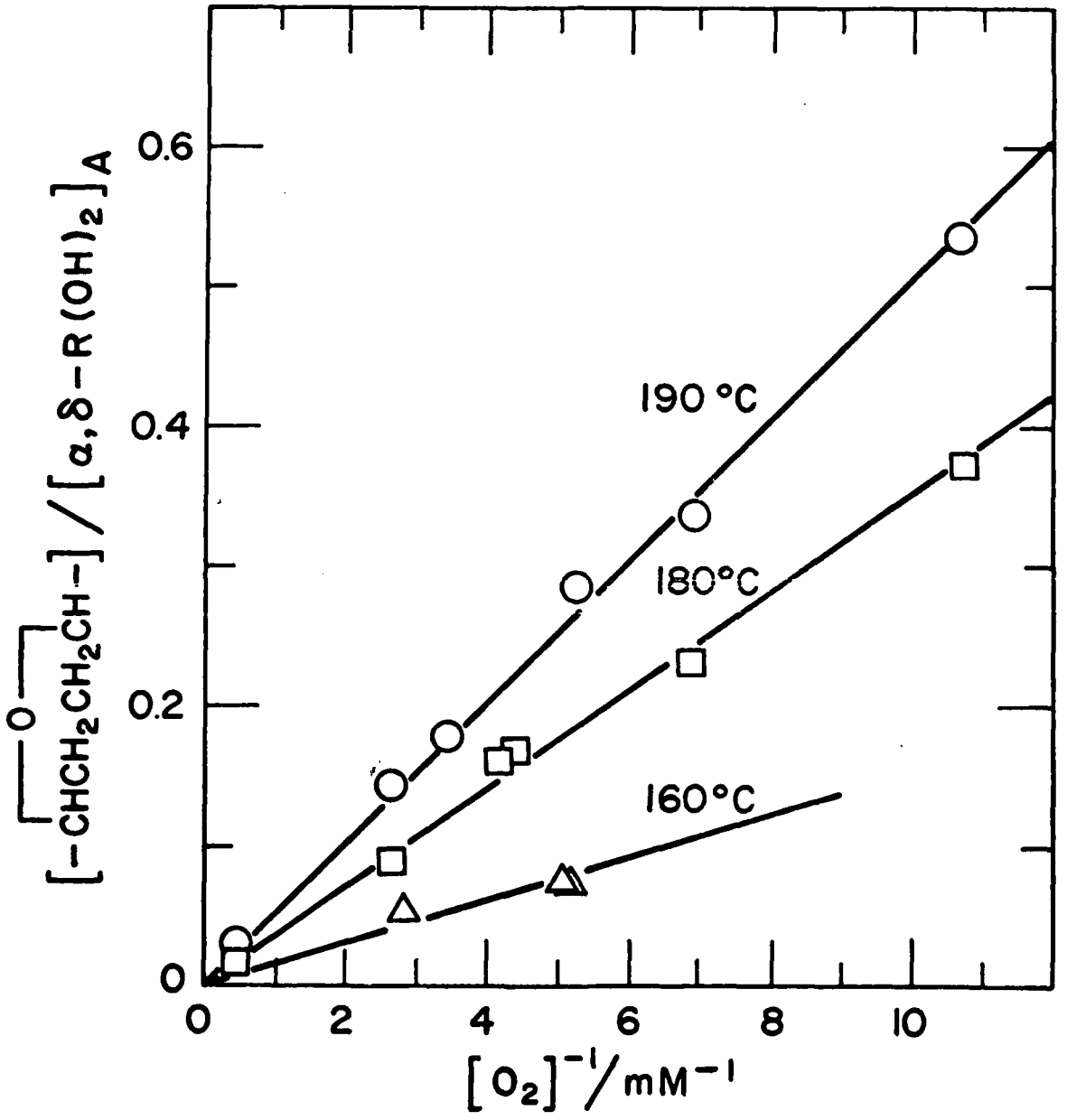

Figure 7 Ratio of rates of formation of 2,5-dialkyloxolanes and α,δ-difunctional products vs. $[O_2]^{-1}$ (Eq. VI).

Table I. Rate Constants

Rate Constant	Temperature, °C					
	160	180	190	160	180	190
	α,γ			α,δ		
$k_3[RH]/k_4$ [a,b]	2.30	1.98	1.84	5.41	4.96	4.42
$(k_3[RH]/k_4)(k_{-4} + k_{10})/k_2'(mM)$ [a]	1.82	2.56	3.27	0.44	0.87	1.13
$(k_{-4} + k_{10})/k_2'(mM)$	0.79	1.29	1.78	0.080	0.078	0.117
k_4/s^{-1}	123	295	488	52.4	118	203
$k_4/H(s^{-1})$	38.8	92.7	154	17.3	40.0	69.1
$k_{-4}/s^{-1} = k_{-4}/H(s^{-1})$	7.91×10^5	1.29×10^6	1.78×10^6	6.71×10^4	1.40×10^5	2.05×10^5
$k_{10}/k_2'(mM)$	-	-	-	0.015	0.035	0.051
k_{10}/s^{-1}	-	-	-	1.51×10^4	3.51×10^4	5.06×10^4

[a] Reference 27. [b] Values reported here differ from those reported in Reference 24 where they were obtained from measurements at oxygen pressure of 110-120 kPa.

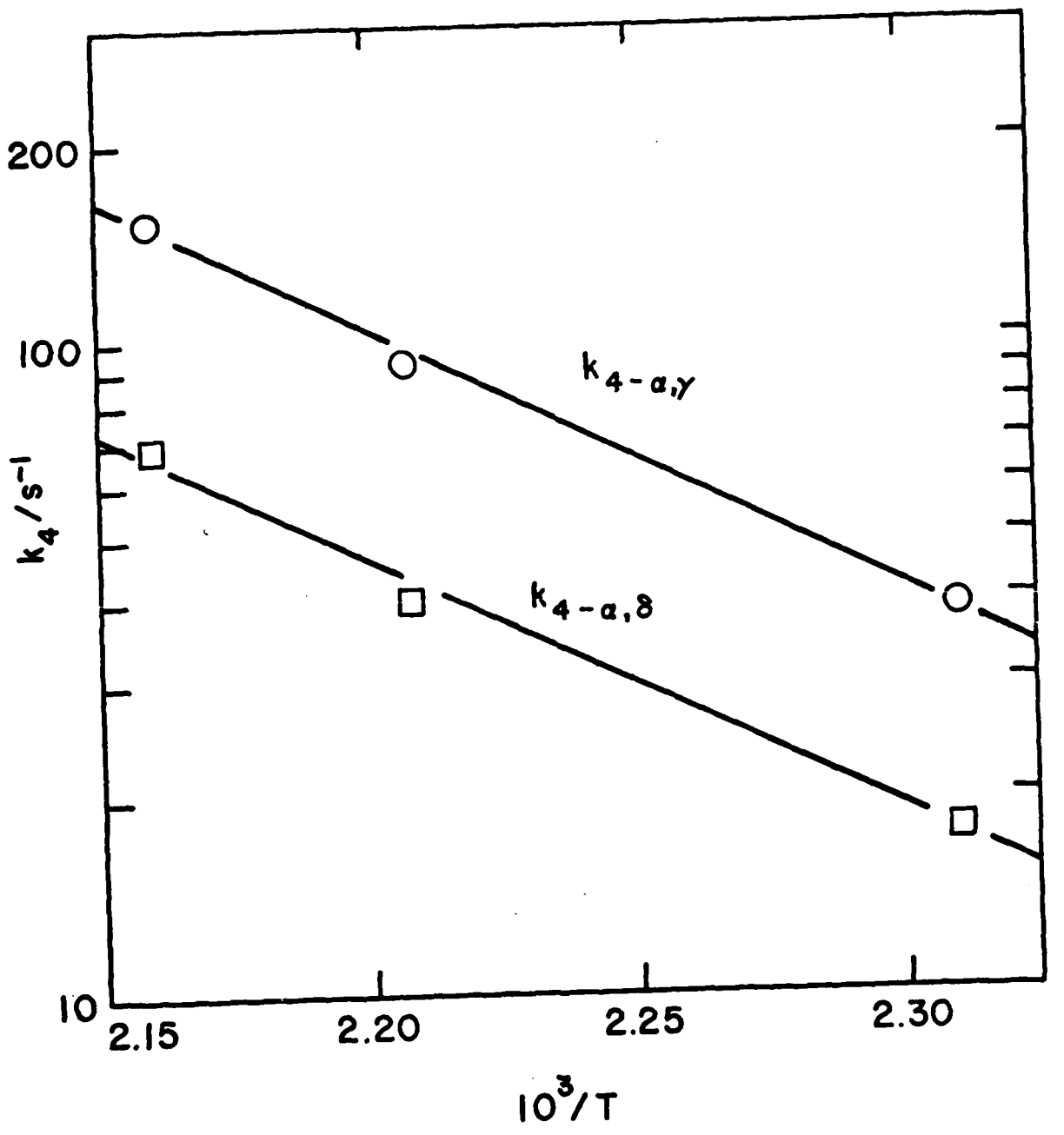

Figure 8 Arrhenius plots for $k_{4-\alpha,\gamma}$ and $k_{4-\alpha,\delta}$.

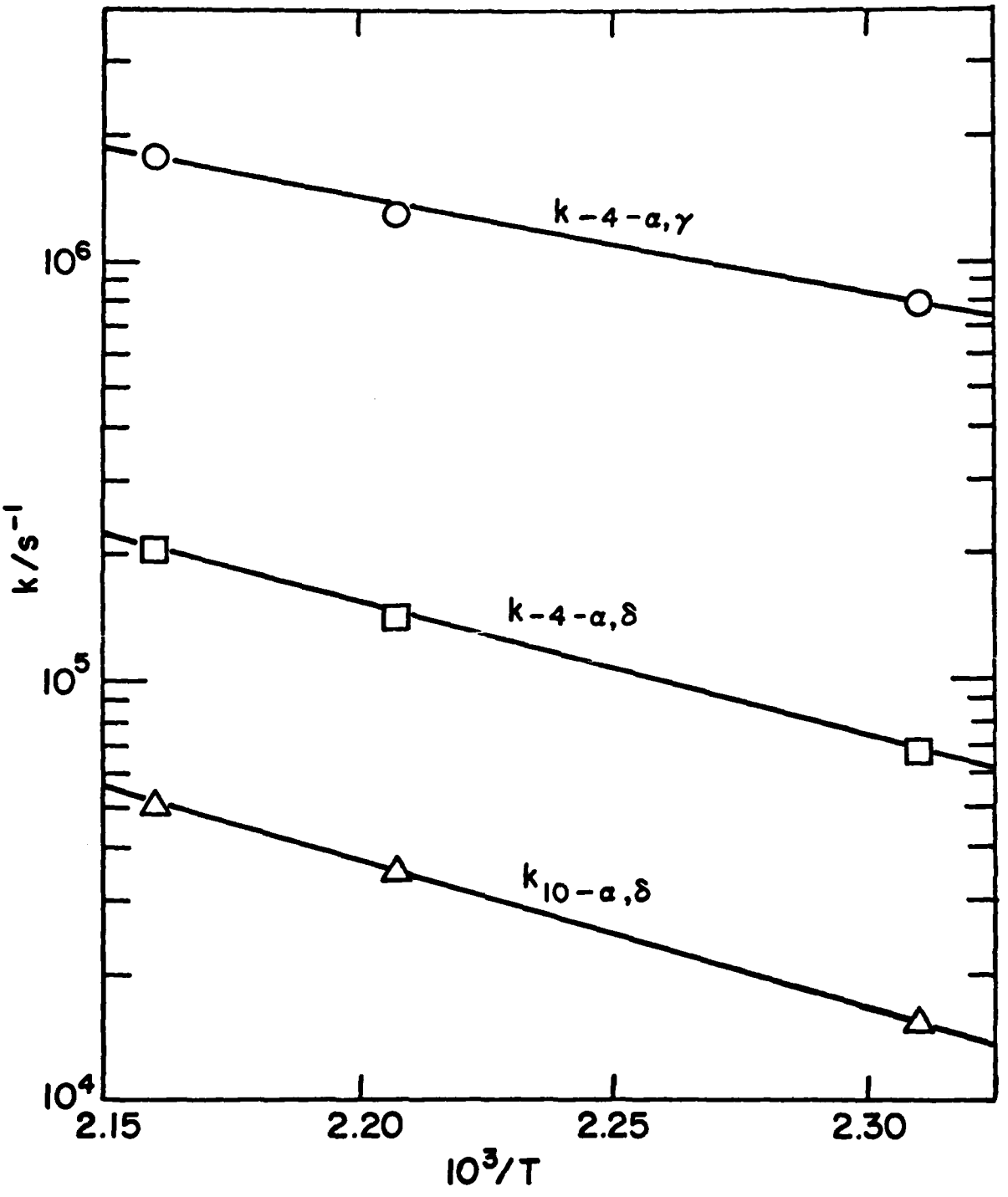

Figure 9 Arrhenius plots for $k_{-4-\alpha,\gamma}$, $k_{-4-\alpha,\delta}$, and $k_{10-\alpha,\delta}$.

Table II. Arrhenius Parameters

Rate constant	log A/H (s^{-1})	E_a/kcal mol^{-1}
$k_{4-\alpha,\gamma}/H$	10.7	18.0
$k_{4-\alpha,\delta}/H$	10.1	17.6
$k_{-4-\alpha,\gamma}/H$	11.2	10.5
$k_{-4-\alpha,\delta}/H$	12.3	14.7
$k_{10-\alpha,\delta}/H$	12.3	16.1

Discussion of Results. Values of absolute rate constants and Arrhenius parameters for reactions 4, -4, and 10 involving formation, isomerization and cyclization of secondary hydroperoxyalkyl radicals and abstractions of secondary hydrogens reported in this work represent the first experimentally determined values of these constants obtained in liquid phase. They originate from the treatment of series of heterogeneous data. Some data, such as those obtained at 180°C, resulted from exhaustive experiments at various reaction conditions using the most recent analytical techniques, while the others, such as the 190°C data, were the result of single experiments at each reaction condition. In the case of the 160°C data the values at high oxygen pressure resulted from our earlier work in which the analytical techniques used were not perfected yet. Due to time limitations and the time demanding complexity of these experiments they have not as yet been repeated. Therefore, the results reported here should be considered preliminary until the key experiments at 160° and 190°C can be verified.

Overall, the values of Arrhenius parameters reported here for α,γ hydrogen abstraction reaction 4 and -4 seem to be in general agreement with those estimated by Benson[5] for these types of reactions in gas phase. However, activation energies for intramolecular hydrogen abstraction by peroxy radicals, reactions 4, estimated by Benson to be equal to those reported for intermolecular hydrogen abstractions, are found to be greater by ca. 2 kcal/mol. Also, preexponential factors A are greater for reactions -4 than for 4. This gives negative values of ΔS_4^o and an equilibrium constant for reaction 4-α,γ, $K_{4-\alpha,\gamma}$, of 2.3×10^{-4} at 180°C which is ca. 7 times smaller than that estimated from Benson's data

($K_{4-\alpha,\gamma}$ = 1.7 x 10^{-3}). This can be attributed to the difference in $k_{4-\alpha,\gamma}$ (1 x 10^3 s^{-1} vs. our value of 0.9 x 10^2 s^{-1} at 180°C on per hydrogen basis) since values of $k_{-4-\alpha,\gamma}$ calculated from Benson's data and obtained in our work are in excellent agreement (1.2 x 10^6 s^{-1} vs. our value of 1.3 x 10^6 s^{-1} at 180°C on per hydrogen basis).

Relevant data were also reported by Baldwin et al.[13] for intramolecular abstraction of secondary hydrogen by 2-pentylperoxy (α,γ abstraction) and n-pentylperoxy (α,δ abstraction) radicals in gas phase. They obtained $k_{4-\alpha,\gamma}/H$ equal to 1.5 x 10^5 s^{-1} and $k_{4-\alpha,\delta}/H$ equal to 3.3 x 10^5 s^{-1} at 480°C. Our corresponding values, extrapolated to 480°C ($k_{4-\alpha,\gamma}/H$ = 2.8 x 10^5 s^{-1} and $k_{4-\alpha,\delta}/H$ = 1.0 x 10^5 s^{-1}) are in reasonable agreement with their data, however, our value for $k_{4-\alpha,\gamma}/H$ involving a six-membered ring transition state is greater than that for $k_{4-\alpha,\delta}/H$ involving a seven-membered ring.

The value of $k_{-4-\alpha,\gamma}$ calculated by Baldwin et al.[13] (6.3 x 10^5 s^{-1} at 480°C) is much smaller than our corresponding extrapolated value (1.4 x 10^8 s^{-1}). This difference seems to arise from the equilibrium constant, $K_{4-\alpha,\gamma}$, which Baldwin et al. used in calculation of $k_{-4-\alpha,\gamma}$ and assumed to be equal to 0.48 at 480°C. From Benson's data, $K_{4-\alpha,\gamma}$ at the same temperature should be equal to 0.06 and from our results it is equal to 0.004.

There is no relevant information in the literature on $k_{-4-\alpha,\delta}$. We would expect, however, that activation energies for reactions -4-α,γ and -4-α,δ should be similar, which is not what was observed. It should be pointed out again that our current values of Arrhenius parameters for reactions -4 are subject to veri-

fication since they are significantly affected by the accuracy of our results at 160°C which, as discussed above, need to be upgraded.

Fish[7,8] estimated activation energies for cyclization reactions of α,γ and α,δ-hydroperoxyalkyl radicals as 14 and 3 kcal/mol, respectively, assuming pre-exponential factor $A = 10^{11}$ s^{-1}. The value for α,δ cyclization seems to be underestimated. Mill[30] reported for α,γ cyclization of tertiary 2,4-dimethyl-2-hydroperoxy-4-pentyl radical $A = 3.2 \times 10^{11}$ and activation energy 14±2 kcal/mol. Our values for α,δ cyclization are A equal to 2×10^{12} s^{-1} and activation energy to 16 kcal/mol. The value of $k_{10-\alpha,\gamma}$ derived from Mill's data for 180°C (5.6×10^4 s^{-1}) is of the same order of magnitude as our $k_{10-\alpha,\delta}$ which is equal to 3.5×10^4 s^{-1}. As described in Part I of this report, we did not detect oxirane products in n-hexadecane autoxidation at our experimental conditions. Considering the sensitivity of our analytical procedures, it means that values of $k_{10-\alpha,\gamma}$ must be at least four times smaller than those obtained for $k_{10-\alpha,\delta}$.

REFERENCES AND NOTES

(1) R. K. Jensen, S. Korcek, L. R. Mahoney, and M. Zinbo, Part I of this report.

(2) The reaction denotation system used throughout this work is consistent with that used in our previous publications.

(3) S. W. Benson, J. Am. Chem. Soc. 87, 972(1965).

(4) S. W. Benson, Symp. on the Mechanisms of Pyrolysis, Oxidation and Burning of Organic Materials, NBS Spec. Publ. 357, 121(1972).

(5) S. W. Benson, Prog. Energy Combust. Sci. 7, 125 (1981).

(6) S. W. Benson, Oxidation Comm. 2, 169(1982).

(7) A. Fish, in "Organic Peroxides", D. Swern, Ed.; Wiley: New York, 1970; Vol. I, Chapter 3.

(8) A. Fish, in "Oxidation of Organic Compounds", R. F. Gould, Ed.; Advances in Chemistry Series; American Chemical Society: Washington, D.C., 1968; Vol. 76, p. 69.

(9) T. Berry, C. F. Cullis, M. Saeed, and D. L. Trimm, in "Oxidation of Organic Compounds", R. F. Gould, Ed.; Advances in Chemistry Series; American Chemical Society: Washington, D.C.; 1968; Vol. 76, p. 86.

(10) P. Barat, C. F. Cullis, and R. T. Pollard, in "13th Int. Combustion Symp."; The Combustion Institute: Pittsburgh, PA, 1977; p. 179.

(11) R. W. Walker, in "Reaction Kinetics", Specialist Periodical Report; The Chemical Society: London, 1975; Vol. I, p. 161.

(12) R. R. Baldwin, J. P. Bennet, and R. W. Walker, in "16th Int. Combustion Symp."; The Combustion Institute: Pittsburgh, PA, 1977; p. 1041.

(13) R. R. Baldwin, J. P. Bennett, and R. W. Walker, J. Chem. Soc., Faraday Trans. 1, 76, 1075(1980).

(14) R. R. Baldwin, M. W. M. Hisham, and R. W. Walker, J. Chem. Soc., Faraday Trans. 1, 78, 1615(1982).

(15) B. D. Boss and R. N. Hazlett, Can. J. Chem. 47, 4175(1969).

(16) D. M. Brown and A. Fish, Proc. R. Soc. London, Ser. A, 308, 547(1969).

(17) T. Hill and G. Montorsi, Int. J. Chem. Kinet. 5, 119(1973).

(18) "Standard Test Methods for Dissolved Oxygen in Water.", ASTM D888-81, in Annual Book of ASTM Standards, Part 31, 1982, p. 517.

(19) Derived using the steady-state approximation for each radical at sufficiently long kinetic chain length and assuming k_3 to be equal to $k_{3'}$ and terminations via reactions of $RO_2^{\bullet}$ and $HOORO_2^{\bullet}$.

(20) In the stirred flow reactor, the instantaneous rate of formation of any reaction product is given by the expression

$$\frac{d[X]}{dt} = \left(\frac{d[X]}{dt}\right)_f - \left(\frac{d[X]}{dt}\right)_c = \frac{[X]_\tau - [X]_0}{\tau}$$

where f designates formation and c consumption, $[X]_\tau$ is the concentration of the product in the reactor or in the effluent from the reactor under steady-state conditions at the residence time τ and $[X]_0$ is the concentration of this product in the entering fluid. If $[X]_0$ is equal to zero and X does not undergo significant further reactions leading to its consumption ($(d[X]/dt)_c \simeq 0$) then

$$\left(\frac{d[X]}{dt}\right)_f = \frac{[X]_\tau}{\tau}$$

and the ratio of rates of formation of any product is given by the ratio of their concentrations in the reactor.

(21) It was previously reported in Ref. 22 that at sufficiently long kinetic chain length

$$[ROOH] \simeq [ROH]_A$$

$$[R(OOH)_2] \simeq [R(OH)_2]_C$$

$$[HOOR{=}O] \simeq [R(OH)_2]_A - [R(OH)_2]_C$$

$$[R(OOH)_2] + [HOOR{=}O] \simeq [R(OH)_2]_A$$

$$[CH_3COR'] \simeq [CH_3CH(OH)R']_A$$

where the subscript letter in concentration terms designates the reducing agent used: A corresponds to $NaBH_4$ and C to Ph_3P.

(22) R. K. Jensen, S. Korcek, L. R. Mahoney, and M. Zinbo, J. Am. Chem. Soc. 101, 7574 (1979).

(23) $[CH_3CH(OH)R']_A$ represents that portion of α,γ-HOCR=O which was decomposed via reaction 7 to give CH_3COR'.[24]

(24) R. K. Jensen, S. Korcek, L. R. Mahoney, and M. Zinbo, J. Am. Chem. Soc. 103, 1742 (1981).

(25) J. M. Prausnitz and F. H. Shair, J. Am. Inst. Chem. Eng., 7, 682 (1961).

(26) P. J. Lin and J. F. Parcher, J. Chromatogr. Sci. 20, 33 (1982).

(27) Composite rate constants at 160 and 180°C were calculated from average values of slopes and intercepts obtained from Figures 3-6. At 190°C, however, these constants were calculated from values obtained from Figures 3 and 4 only since values from Figures 5 and 6 are strongly influenced by single data points available at high oxygen concentrations.

(28) R. K. Jensen, S. Korcek, L. R. Mahoney, and M. Zinbo, Unpublished Data. Values of k_3 used in calculation of k_4 from $k_3[RH]/k_4$ were 95, 201, and 312 at 160, 180, and 190°C, respectively. These values give the following Arrhenius parameters for $k_3/H(M^{-1}s^{-1})$: log A equal 8.4 and E equal 15.5 kcal/mole.

(29) Reference 24. Supplementary Material.

(30) T. Mill, 13th Int. Combustion Symp., The Combustion Institute, Pittsburgh, Pa., 1971, p. 237.

PART III

LIQUID PHASE AUTOXIDATION OF ORGANIC COMPOUNDS AT ELEVATED TEMPERATURES. 3. RATE OF RADICAL FORMATION IN DIPENTYLDECALINE AUTOXIDATION AT 100 AND 150°C

R. K. Jensen, S. Korcek, L. R. Mahoney, and M. Zinbo

INTRODUCTION

Mechanisms of n-hexadecane autoxidation at elevated temperatures have been established in our studies carried out using the stirred flow microreactor at 120 to 190°C and 4 to 120 kPa of oxygen pressure.[1,2,3] A reaction scheme which accounts for the formation of primary and cleavage oxidation products under the above conditions was previously described.[3] Kinetic analyses based on this scheme revealed i) that the reactivity ratios for intramolecular and intermolecular abstraction reactions of hexadecylperoxy radicals can be calculated from the ratios of yields of difunctional and monofunctional primary oxidation products[2] (Table I) and ii) that determination of absolute rate constants for these reactions and determination of the kinetic chain length require knowledge of the rate of radical formation, i.e., the rate of initiation, R_i.

The absolute rate constants for intermolecular abstraction reactions of peroxy radicals, k_3,

$$\text{-CH(OO}\bullet\text{)-} + \text{-CH(H)-} \xrightarrow{k_3} \text{-CH(OOH)-} + \text{-C}\bullet\text{H-} \qquad (3)$$

and intramolecular abstraction reactions k_4 and k_4^*,

$$\text{-CH(OO}\bullet\text{)(CH}_2\text{)}_m\text{CH(H)-} \underset{k_{-4}}{\overset{k_4}{\rightleftharpoons}} \text{-CH(OOH)(CH}_2\text{)}_m\text{C}\bullet\text{H-} \qquad (4,-4)$$

$$\text{-CH(OOH)(CH}_2\text{)}_m\text{CH(OO}\bullet\text{)-} \xrightarrow{k_4^*} \text{-C(=O)(CH}_2\text{)}_m\text{CH(OOH)-} + \bullet\text{OH} \qquad (4^*)$$

(where m is equal to 1 for α,γ and 2 for β,δ abstractions) can be obtained from the

Table I

RATIOS OF RATE CONSTANTS FOR INTRA- AND INTERMOLECULAR ABSTRACTION REACTIONS OF HEXADECYLPEROXY RADICALS

Ratio	Hydrogen Abstraction	Temperature, °C 120	160	180
$\frac{k_4}{k_3[RH]}$	α,γ	0.21	0.29	0.29
	α,δ	0.19	0.21	0.24
$\frac{k_4^*}{k_3[RH]}$	α,γ	3.5	4.6	4.0
	α,δ	1.1	1.3	1.1
$\frac{(k_4/H)}{(k_3/H)}\Big/ M$	α,γ	5.8	7.6	7.5
	α,δ	5.6	5.9	6.7
$\frac{(k_4^*/H)}{(k_3/H)}\Big/ M$	α,γ	300	380	330
	α,δ	100	110	90

J. Am. Chem. Soc., 103, 1742 (1981)

reactivity ratios in Table I if at least one of the rate constants in these ratios is independently determined. For this purpose, k_3 can be obtained from the rate of formation of monohydroperoxides, ROOH, using eq. I when peroxy radical termination rate constants k_5 and k_6 and R_i are known. In eq. I, [RH] is concentration of n-hexadecane and ϕ a complex rate constant which can be calculated from the reactivity ratios since it is a function of only these ratios (eq. II).

$$\frac{d[ROOH]}{dt} = \frac{k_3}{(2k_6 + 2xk_5)^{1/2}} [RH] \phi R_i^{1/2} \qquad (I)$$

$$\phi = f\left(\frac{k_{4-\alpha,\gamma}}{k_3[RH]} , \frac{k_{4-\alpha,\delta}}{k_3[RH]} , \frac{k^*_{4-\alpha,\gamma}}{k_3[RH]} , \frac{k^*_{4-\alpha,\gamma}}{k_3[RH]} \right) \qquad (II)$$

Rate of Initiation. In low temperature studies of kinetics of liquid phase hydrocarbon oxidation the rate of initiation, R_i, is maintained at known and constant value by the addition of initiators which thermally or photochemically decompose with known rates of radical production.[4] In contrast, the autoxidation of hydrocarbons at elevated temperatures is very strongly autocatalytic. The main source of free radicals under these conditions is homolytic decomposition of hydroperoxides, reaction 1.

$$-OOH \xrightarrow{k_1} \begin{pmatrix} \text{free radicals} \\ RO\bullet,\ HO\bullet,\ldots \end{pmatrix} \xrightarrow{-CH_2-} 2 - \overset{\bullet}{C}H - \qquad (1)$$

Since hydroperoxides are the primary oxidation products, the rate of radical production will vary with extent of autoxidation. To avoid the problem of variable rate of radical formation at elevated temperatures, our kinetic investigations have been conducted in the stirred flow reactor. In this reactor, under steady-state conditions, concentrations of all reactants, including hydroperoxides, are constant throughout the entire reaction volume and do not change with time. Thus, in this system, autoxidation studies are carried out at the constant rate of radical formation, $(R_i)_\tau$, which is given by eq. III. Under

$$(R_i)_\tau = 2k_1 [\text{-OOH}]_\tau \qquad \text{(III)}$$

steady-state conditions, the rate of radical formation must be identically equal to the rate of radical termination, $(R_t)_\tau$ and therefore determinations of $(R_i)_\tau$ can be based upon determinations of $(R_t)_\tau$.

Two general methods of determination of $(R_i)_\tau$ have been used in this study. The first method is based on determination of $(R_t)_\tau$ from the rate of of formation of termination products, the second, the inhibitor method, is based either on measurement of inhibition periods caused by the addition of a known amount of antioxidant or on determination of the initial rate of antioxidant consumption.

Termination Reactions. At sufficiently high partial pressures of oxygen (P_{O_2} > 75 kPa) the rates of formation of primary oxidation products in the n-hexadecane autoxidation are independent of oxygen pressure. This indicates that under these conditions all free radicals terminate via reactions 5b and 6.

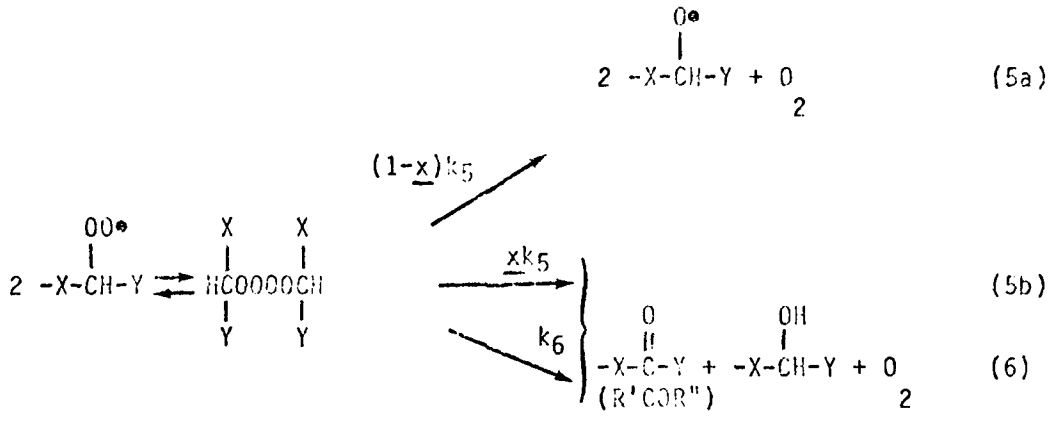

$$2\ \text{-X-CH-Y} \rightleftharpoons \text{HCOOOOCH} \quad (\text{X, Y})$$

$$\xrightarrow{(1-x)k_5} 2\ \text{-X-CH-Y} + O_2 \qquad (5a)$$

$$\xrightarrow{xk_5} \text{cage} \qquad (5b)$$

$$\xrightarrow{k_6} \text{-X-C(=O)-Y} + \text{(R'COR")} + \text{-X-CH(OH)-Y} + O_2 \qquad (6)$$

It is widely accepted that the first step in bimolecular termination reactions of peroxy radicals involves the reversible formation of dialkyltetroxide intermediates.[4,5] The nature of subsequent reactions of these dialkyltetroxides is strongly influenced by the structure of alkyl groups and temperature. In the temperature range of 25 to 75°C the primary and secondary tetroxides decompose to yield alcohol, carbonyl compound, and oxygen in equimolar amounts presumably via the Russell cyclic termination mechanism, reaction 6.[6] At temperatures over 100°C decomposition of tetroxides to alkoxy radicals and oxygen, reaction 5, becomes increasingly important.[7] Some of these alkoxy radicals recombine in the cage, reaction 5b, contribute to termination, and give the same products as Russell's cyclic mechanism.

An alternative mechanism for primary and secondary peroxy radical termination via Criegee zwitterion was recently proposed by Benson and Nangia.[8] This mechanism also leads to the formation of one molecule of ketone per two peroxy radicals terminated.

RESULTS AND DISCUSSION

Rate of Initiation from Rate of Formation of Termination Products. Based on the described termination mechanisms, the rate of initiation in n-hexadecane autoxidation must be equal to twice the rate of formation of hexadecanones, R'COR", provided that there are no alternative modes of their formation and that contribution of cleavage-derived peroxy radicals to termination is negligible. Thus, in the stirred flow reactor the rate of initiation is given by eq. IV

$$(R_{i(t)})_\tau = 2 \frac{[R'COR"]_\tau}{\tau} \qquad (IV)$$

where τ is the residence time. The analytical procedures used in this work did not allow determination of all R'COR" isomers formed from termination of hexadecylperoxy and hydroperoxyhexadecylperoxy radicals, $RO_2^\bullet$ + $HOORO_2^\bullet$, but only 4--8-R'COR" which originate from the corresponding 4--8-$RO_2^\bullet$. It can be shown by kinetic analyses, however, that $[R'COR"]_\tau$ can be estimated from $[4--8\text{-}R'COR"]_\tau$ using eq. V

$$[R'COR"]_\tau = [4--8\text{-}R'COR"]_\tau \frac{[ROOH]_\tau + [R(OOH)_2]_\tau}{[4--8\text{-}ROOH]_\tau} \qquad (V)$$

where $[ROOH]_\tau$ and $[4--8\text{-}ROOH]_\tau$ are the concentrations of hexadecylhydroperoxides and 4--8 substituted hexadecylhydroperoxides and $[R(OOH)_2]_\tau$ is the concentration

of all hexadecyldihydroperoxides. Eq. V was derived assuming that the values of k_3, k_{5b}, and k_6 for a subgroup 4--8-RO_2• are the same as overall average values of the corresponding rate constants for all isomeric hexadecylperoxy and hydroperoxyhexadecylperoxy radicals. Substituting $[R'COR"]_\tau$ expressed by eq. V into eq. IV yields eq. VI

$$(R_{i(t)})_\tau = 2 \frac{[4\text{--}8\text{-}R'COR"]_\tau}{\tau} \frac{[ROOH]_\tau + [R(OOH)_2]_\tau}{[4\text{--}8\text{-}ROOH]_\tau} \qquad \text{(VI)}$$

which can be used for determination of rate of initiation in the stirred flow reactor under any reaction conditions since the concentrations of all products needed for this calculation can be obtained from product analyses described previously.[1]

Combining eqs. III and VI gives eq. VII

$$\frac{[4\text{--}8\text{-}R'COR"]_\tau}{\tau} \frac{[ROOH]_\tau + [R(OOH)_2]_\tau}{[4\text{--}8\text{-}ROH]_\tau} = k_1[\text{-OOH}]_\tau \qquad \text{(VII)}$$

Eq.VII relates rate of formation of termination products to rate of initiation and allows determination of k_1 which then can be used for determination of the rate of initiation at any concentration of hydroperoxides from eq. III.

Plots consistent with eq. VII based on previously reported experimental data[1] and values of k_1 derived from these plots are in Figure 1. The plot of 160°C data gives good straight-line correlation, however, the plot of 180°C data

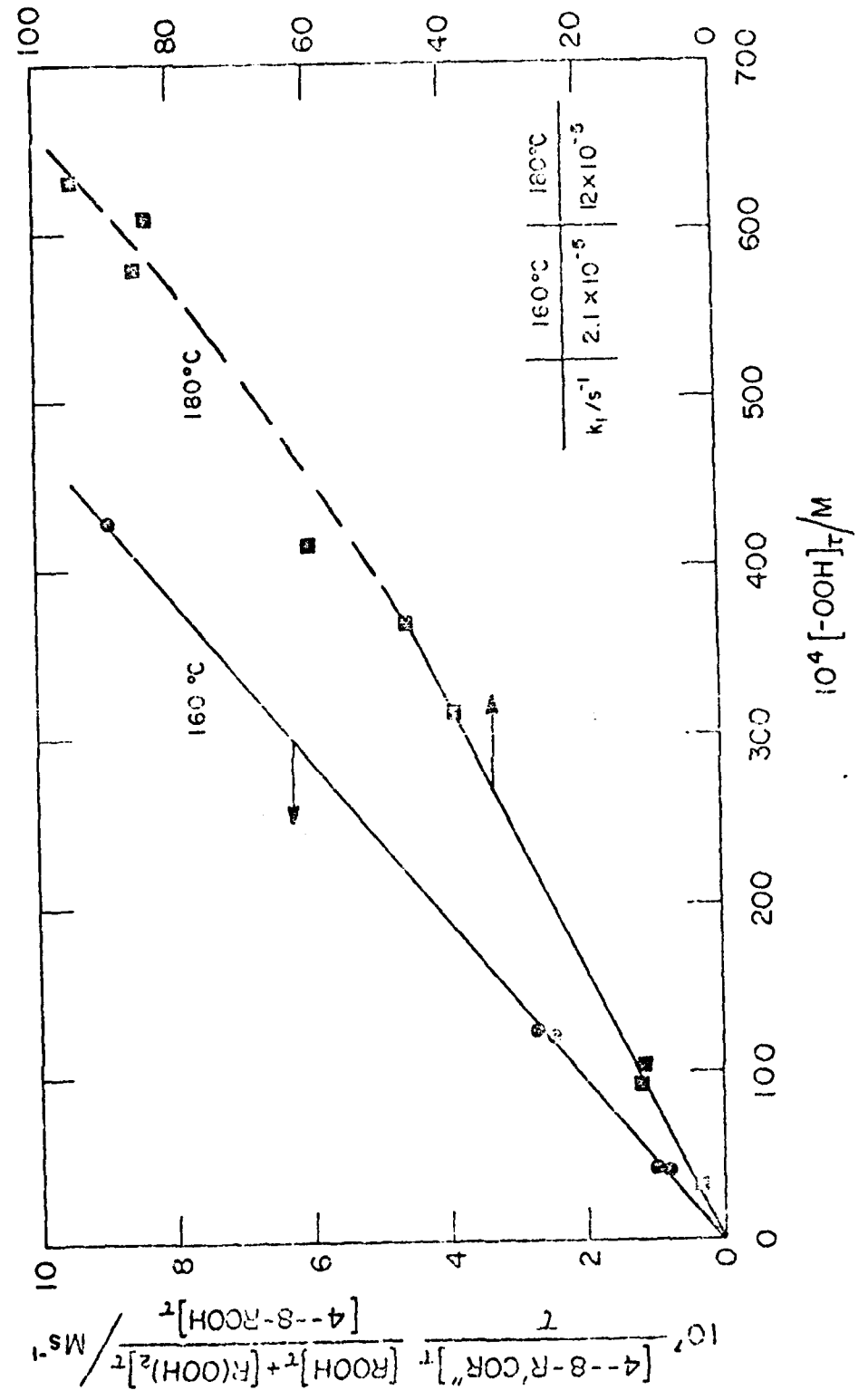

Figure 1. Plots of experimental data for HD autoxidation consistent with eq. VII.

deviates from linearity at higher concentrations of hydroperoxides.

The above deviation from linearity suggests the occurrence of other ketone producing reactions under such conditions. In fact, this should be anticipated from the results of other studies.[9,10] Ketones may be produced from α-attack of peroxy radicals on hydroperoxides,[9] reaction 11, or from direct molecular decomposition of hydroperoxides to yield ketone and water, reaction 12.

$$RO_2^{\bullet} + R'CH(OOH)R'' \longrightarrow ROOH + R'COR'' + {}^{\bullet}OH \qquad (11)$$

$$R'CH(OOH)R'' \longrightarrow R'COR'' + H_2O \qquad (12)$$

Based on results of Brown and Fish,[11] however, no detectable amounts of C_{12} ketones were formed on decomposition in an inert atmosphere of hydroperoxides from autoxidation of 2-methylhexadecane at 159°C.

Another reaction which could lead to production of ketones is direct reaction of oxygen with alkoxy radicals, reaction 13.[12] If this reaction

$$R'\overset{\bullet}{C}H(O)R'' + O_2 \longrightarrow R'COR'' + HO_2^{\bullet} \qquad (13)$$

was important in the formation of ketones, their rate of formation would approach first order in oxygen concentration. In our studies of n-hexadecane autoxidation at reduced oxygen pressures,[3] it was observed that the rate of ketone formation decreases with partial pressure of oxygen only when the pressure is lower than ca. 60 kPa. At such low pressures, however, alkyl radicals will

also participate in termination reactions and the reduced yields of ketones should be anticipated. Accordingly, it has been concluded that the reaction of oxygen with alkoxy radicals is not an important reaction in our system.

Due to the possibility of overestimating yields of R'COR" from termination reactions, the values of $(R_{i(t)})_\tau$ and k_1 obtained from eq. VII must be considered to be the maximum values possible.

Rate of Initiation by Inhibitor Method. In application of the inhibitor method it has been assumed that the rate of initiation in a stirred flow reactor is the same as that in a batch reactor as long as the hydroperoxide concentrations in both reactors are the same. Based on this assumption, the values of k_1 derived from batch reactor experiments must be applicable in calculation of the rate of initiation in the stirred flow reactor (eq. III). The validity of the above assumption is supported by the results of product analyses of samples of n-hexadecane autoxidized to the same final hydroperoxide concentration in both stirred flow reactor and batch reactor experiments. These results show that type and distribution of primary hydroperoxide products formed in both reactors are very similar. This suggests that initiation processes and the over-all rate constant for decomposition of these hydroperoxides, k_1, under such conditions should be essentially the same.

The inhibitor method for determination of the rate of initiation is based on measurements of inhibition time or rate of antioxidant consumption in batch reactor autoxidation experiments inhibited by an antioxidant.

Upon the addition of an efficient antioxidant, AH, to an oxidizing

substrate the bimolecular termination reactions of peroxy radicals, reactions 5b and 6, are replaced by reactions of peroxy radicals with AH and its reactive intermediates, INT, reaction 14,

$$n\ RO_2^{\bullet} + \left\{ \begin{matrix} AH \\ INT \end{matrix} \right\} \longrightarrow \text{INACTIVE PRODUCTS} \qquad (14)$$

where n is the stoichiometric factor of antioxidant AH which is equal to the total number of peroxy radicals consumed by a molecule of AH and corresponding INT. Due to the high rates of these reactions the steady-state concentration of peroxy radicals is dramatically decreased and chain oxidation reactions are strongly inhibited. This inhibition continues until the antioxidant and its reactive intermediates are completely consumed. If the rate of radical formation during inhibition, $R_{i(inh)}$, is constant, then inhibition time, t_{inh}, can be used for determination of $R_{i(inh)}$ since under steady-state conditions

$$R_{i(inh)}\ t_{inh} = n\ [AH]_o \qquad (VIII)$$

and

$$R_{i(inh)} = \frac{n[AH]_o}{t_{inh}} \qquad (IX)$$

Determination of the rate of initiation from the rate of antioxidant consumption during inhibition requires knowledge of the inhibition mechanisms for the antioxidants used.

We have utilized in our studies the following antioxidants:

2,6-di-tert-butyl-4-methylphenol (MPH),

4,4'-methylene-bis(2,6-di-tert-butylphenol) (BPH), and

N-phenyl-α-naphthylamine (PAN).

The inhibition mechanism of MPH at low temperatures is accurately described by reactions P1 and P2 (Scheme I).[4] In this sequence, the rate controlling step for MPH consumption is reaction P1 and therefore instantaneous rate of initiation at the time of AH addition is proportional to the instantaneous rate of antioxidant consumption (eq. X).

$$R_{i(AH)} = n - \left(\frac{d[AH]}{dt}\right)_0 \qquad (X)$$

Based on this mechanism, n for MPH at low temperatures is equal to 2.

The inhibition mechanism of PAN at low temperatures and in the presence of hydroperoxides is similar to that for MPH:[13,14] PAN reacts with $RO_2^{\bullet}$ to produce an aminyl radical which in turn reacts with another $RO_2^{\bullet}$ to give inactive products. Thus, eq. X is also applicable for determination of $R_{i(AH)}$ from the rate of decay of PAN. The n in this case is also equal to 2.

The inhibition mechanism of BPH at low temperatures is more complex than that for MPH or PAN due to the presence of two phenolic groups in each molecule of BPH (Scheme II).[15] Rate controlling steps for BPH consumption in this case are reactions BP1 and BP3. Based on the number of phenolic hydrogens in BPH and Q(OOR)H, k_{BP1} must be equal to $2k_{BP3}$ if the reactivities of all phenolic hydrogens are the same. It can be shown from kinetic analyses[16] that for the

SCHEME I
INHIBITION MECHANISM OF MPH AT LOW TEMPERATURES

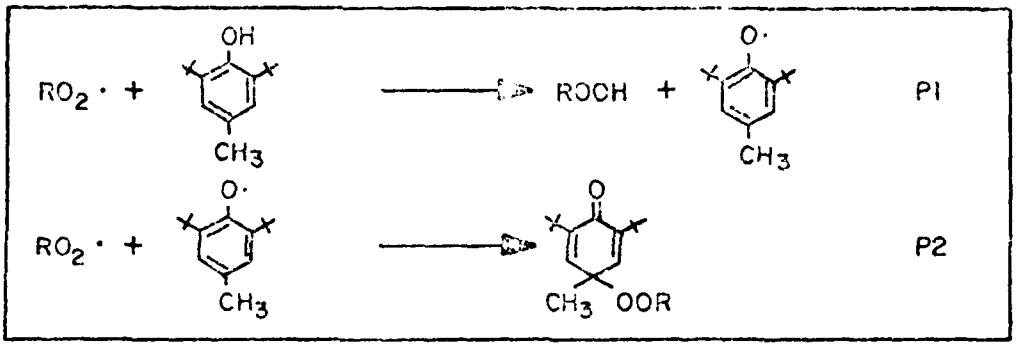

SCHEME II
INHIBITION MECHANISM OF BPH AT LOW TEMPERATURES

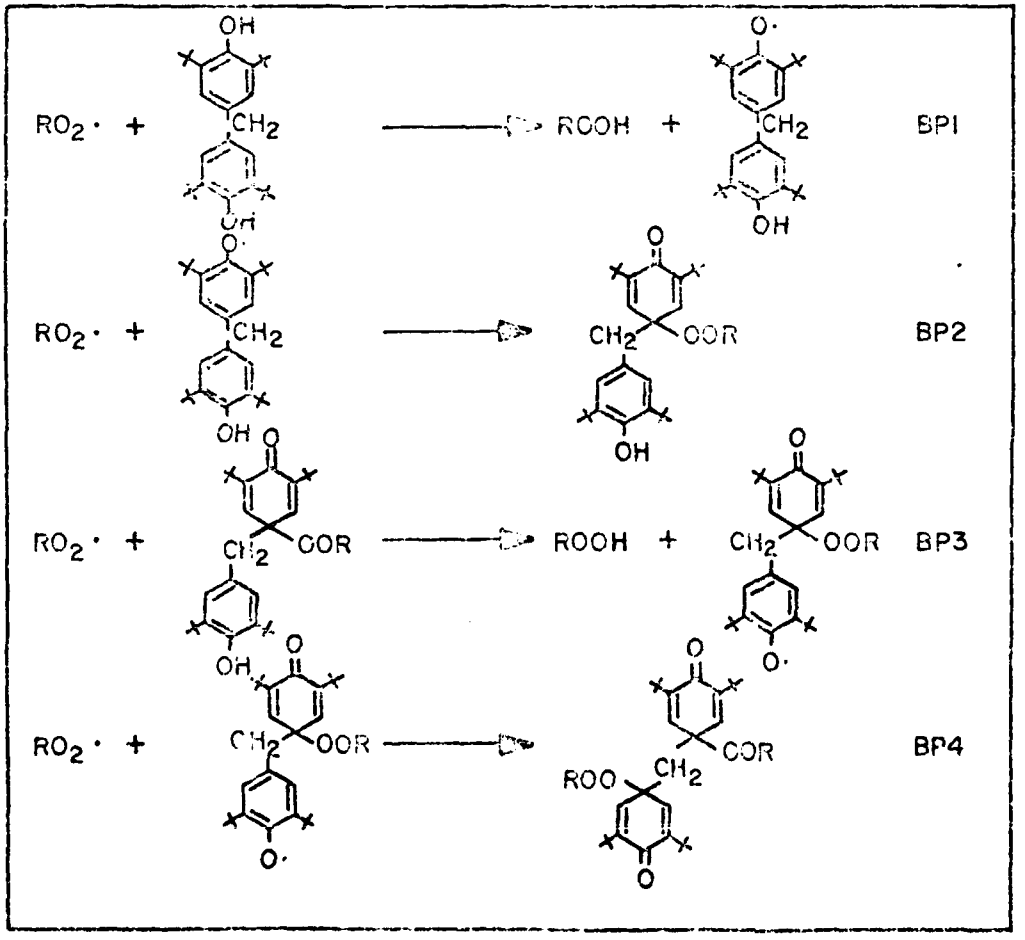

sequence of consecutive competitive reactions 21 - 24 BPH decay is expressed by eq. XI. Based on this mechanism the n-value for BPH is equal to 4.

$$1 - \left(\frac{[BPH]_o}{[BPH]_t} \right)^{0.5} = \frac{R_i(\quad)}{n[\quad]_o} t = \alpha t \qquad (XI)$$

If initiation occurs only via homolytic decomposition of hydroperoxides, combining eqs. IX, X, and XI with eq. III yields eqs. XII-XIV

$$\frac{n}{2} \frac{[AH]_o}{t_{inh}} = k_1[\text{-OOH}]_{av} \qquad (AH=TPH, BPH, PAH) \qquad (XII)$$

$$\frac{n}{2} \frac{-d[AH]}{dt}_o = k_1[\text{-OOH}]_o \qquad (AH=BPH,PAH) \qquad (XIII)$$

$$\frac{n}{2} \frac{-d[\quad]}{dt}_o = k_1[\text{-OOH}]_o \qquad (XIV)$$

which can be used for determination of k_1 using the inhibitor method. In these equations $[\text{-OOH}]_{av}$ is the average concentration of hydroperoxides during the inhibition period and $[\text{-OOH}]_o$ is their concentration at the time of antioxidant addition. When the antioxidant mechanisms are described by reaction sequences P1-P2 or BP1-BP4, concentation of hydroperoxides should not change during inhibition time and $[\text{-OOH}]_{av}$ should be equal to $[\text{-OOH}]_o$ since decomposition of one molecule of hydroperoxide produces two peroxy radicals which react with antioxidant with formation of another molecule of hydroperoxide per two peroxy radicals trapped. Thus, there should not be any change in hydroperoxide concentration during inhibition.

In order to obtain k_1 from eqs. XII-XIV, the stoichiometric factors of antioxidants, n, must be known and the values of $[AH]_o/t_{inh}$, $(-d[AH]/dt)_o$, and $\alpha[BPH]_o$ must be determined as a function of $[-OOH]_o$. For that purpose a series of batch reactor experiments was run in which n-hexadecane, HD, was preoxidized to desired levels of $[-OOH]_o$ and at that point varying amounts of an antioxidant were added. Samples of the reaction mixture were then withdrawn as a function of time and analyzed for $[-OOH]_t$ and $[AH]_t$. Typical results obtained from these inhibited autoxidation experiments with MPH are shown in Figure 2. Results obtained with BPH in the form consistent with eq. XI are in Figure 3. Values of t_{inh}, $(-d[AH]/dt])_o$ and α were obtained from these plots graphically.

Stoichiometric Factors of Antioxidants. The n-values for MPH, BPH, and PAH have been previously determined at low temperatures. They have been found to be in agreement with the mechanisms described above (Table II).[17,18] There is, however, no information on n-values nor on mechanisms of inhibition for these antioxidants at the elevated temperatures used in this work (160 and 130°C). Based on limited data available in the literature for temperatures up to 140°C,[19-20] it should be expected that QOOR, Q(OOR)H, and $Q(OOR)_2$ products formed during the inhibition with MPH and BPH would under our conditions decompose and contribute to formation of free radicals. This would then lead to n-values lower than those obtained at low temperatures.

In order to estimate the n-values for MPH and BPH, the results obtained by the inhibition method (eqs. XII-XIV) employing selected integral n-values have been compared to those obtained from the termination product method (Figures

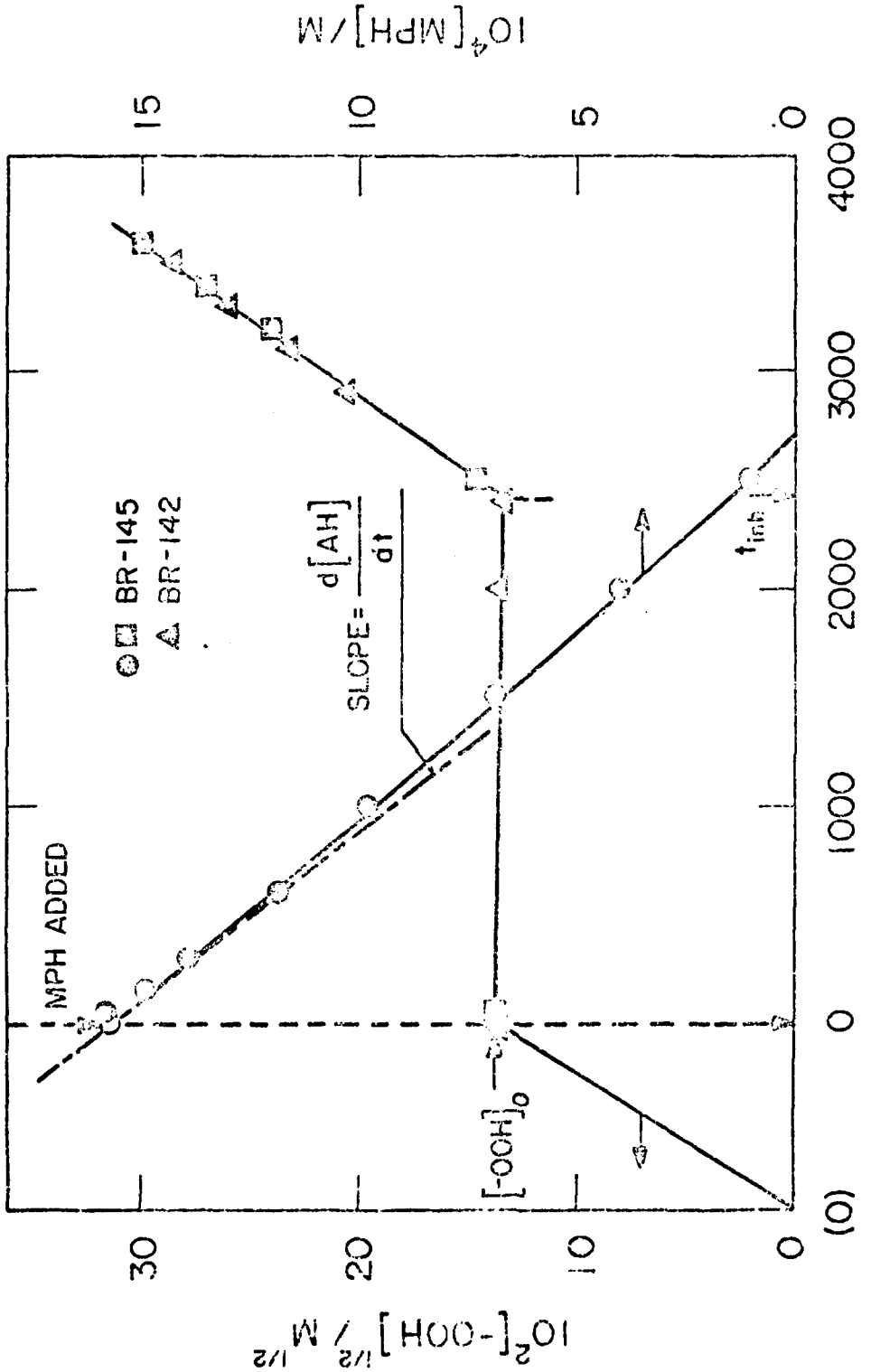

Figure 2 MPH inhibited autoxidation of HD at 100°C: Determination of the initial rate of antioxidant consumption and inhibition period.

BR-142 - $[-OOH]_o$ = 18.6 mM, $[MPH]_o$ = 1.50 mM
BR-145 - $[-OOH]_o$ = 19.0 mM, $[MPH]_o$ = 1.50 mM

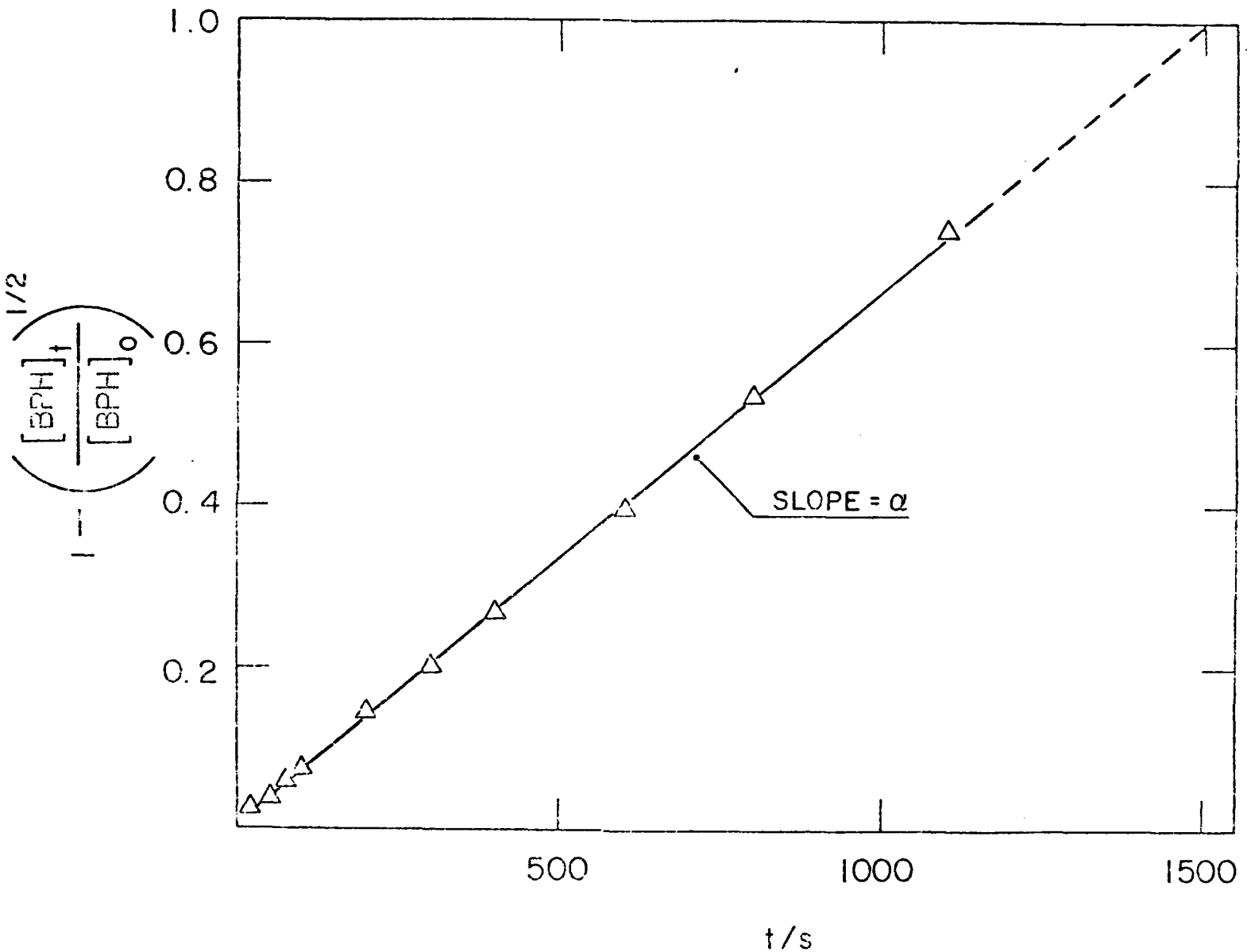

Figure 3 BPH consumption (in the form consistent with eq. XI) during inhibited autoxidation of HD at 180°C. $[\text{-OOH}]_0$ = 22.7 mM, $[BPH]_0$ = 3.80 mM.

Table II

STOICHIOMETRIC FACTORS OF ANTIOXIDANTS

	n	n_{max}		n_{min}	
AH	60°C	160°C	180°C	160°C	180°C
MPH	2[a]	1.2[c]	-	1.0[c]	-
BPH	4[a]	-	2.7[d]; 2.1[e]	-	2.0[d]
PAN	2[b]	2.6[c]	2.7[d]	(2.0)[f]	(2.0)[f]

[a]Ref. 17; [b]Ref. 13; [c]From Fig. 4; [d]From Fig. 5; [e]From Fig. 6; .

[f]Reference value

4-6). This comparison suggests more complex inhibition mechanisms for MPH and BPH than those described by reactions P1-P2 and BP1-BP4.

If k_1 values (slopes in Figures 4-6) obtained from the termination product method are the maximum values (see above), then n-values corresponding to these k_1 (slopes) must be the maximum stoichiometric factors, n_{max}, for a given antioxidant. From plots in Figures 4-6, n_{max} for MPH at 160°C is equal to ca. 1.2 and for BPH at 180°C to 2.0-2.6 (Table II). Similar comparisons for PAN, based on single data points in Figures 4 and 5 give n_{max} for PAN equal to ca. 2.7. This value theoretically should not be greater than 2.0 unless some of PAN inhibition intermediates or products possess inhibiting activity at elevated temperatures. If this is not the case, then k_1 obtained from the termination product method is overestimated and slopes of the lines for PAN in Figures 4 and 5 (single points only!) define the minimum value of k_1. The n-values of MPH and BPH corresponding to this minimum k_1 (slope for PAN) are then minimum stoichiometric factors, n_{min}. From plots in Figures 4 and 5 n_{min} for MPH at 160°C is equal to 1.0 and for BPH at 180°C to 2.0 (Table II). Thus, the actual value of the stoichiometric factor must be somewhere between n_{max} and n_{min}, i.e., for MPH at 160°C between 1.0 and 1.2 and for BPH at 180°C between 2.0 and 2.6.

In order to clarify inhibition mechanisms and positively determine n-values for hindered phenols used in this study at elevated temperatures, we have elected to further investigate MPH since the most extensive mechanistic information at low temperatures is available for this antioxidant. Results of these investigations with MPH obtained to date are discussed in Part IV of this report.

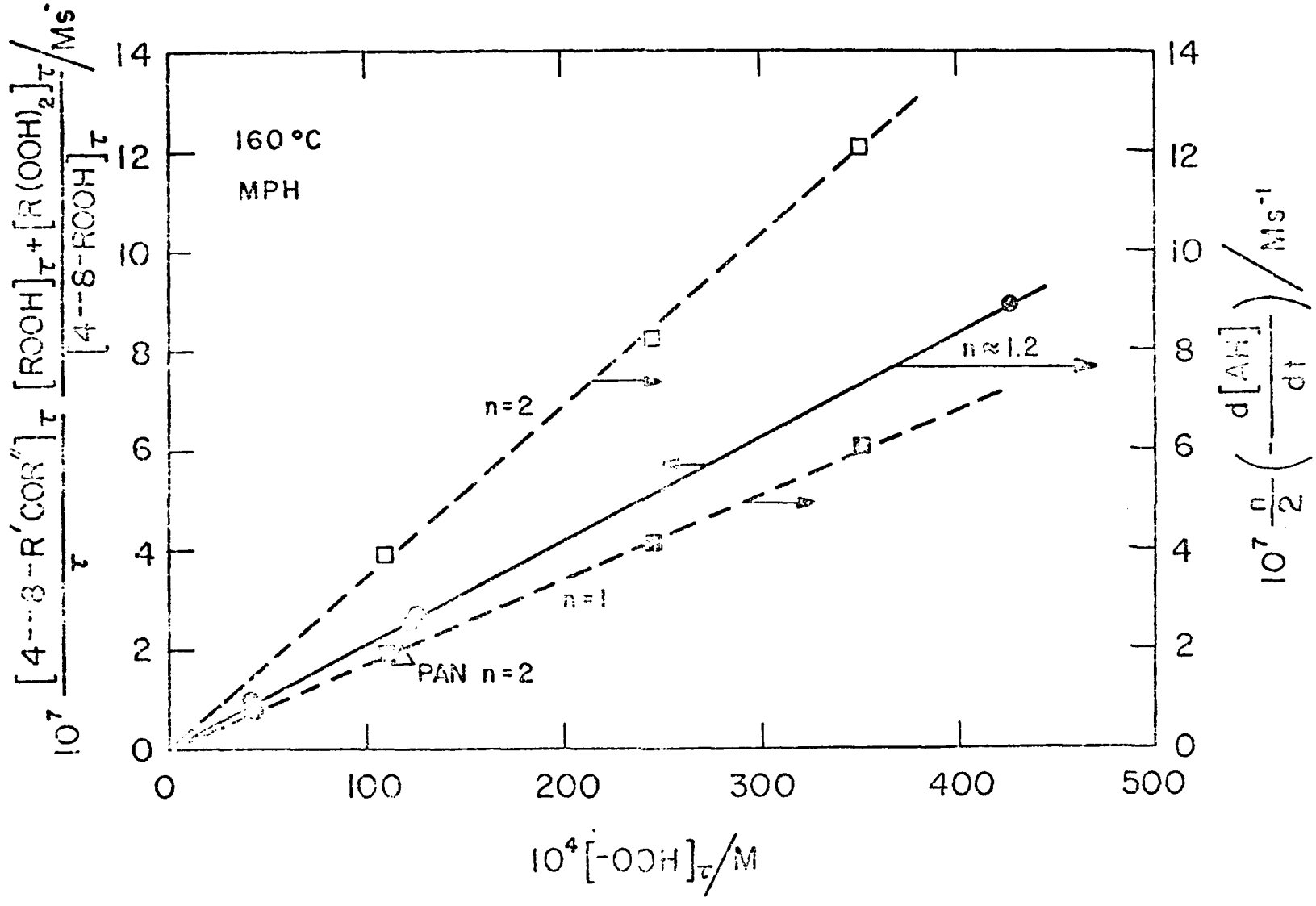

Figure 4. Estimation of n for MPH at 160°C from measurements of initial rates of MPH consumption in HD autoxidation (eq. XII).

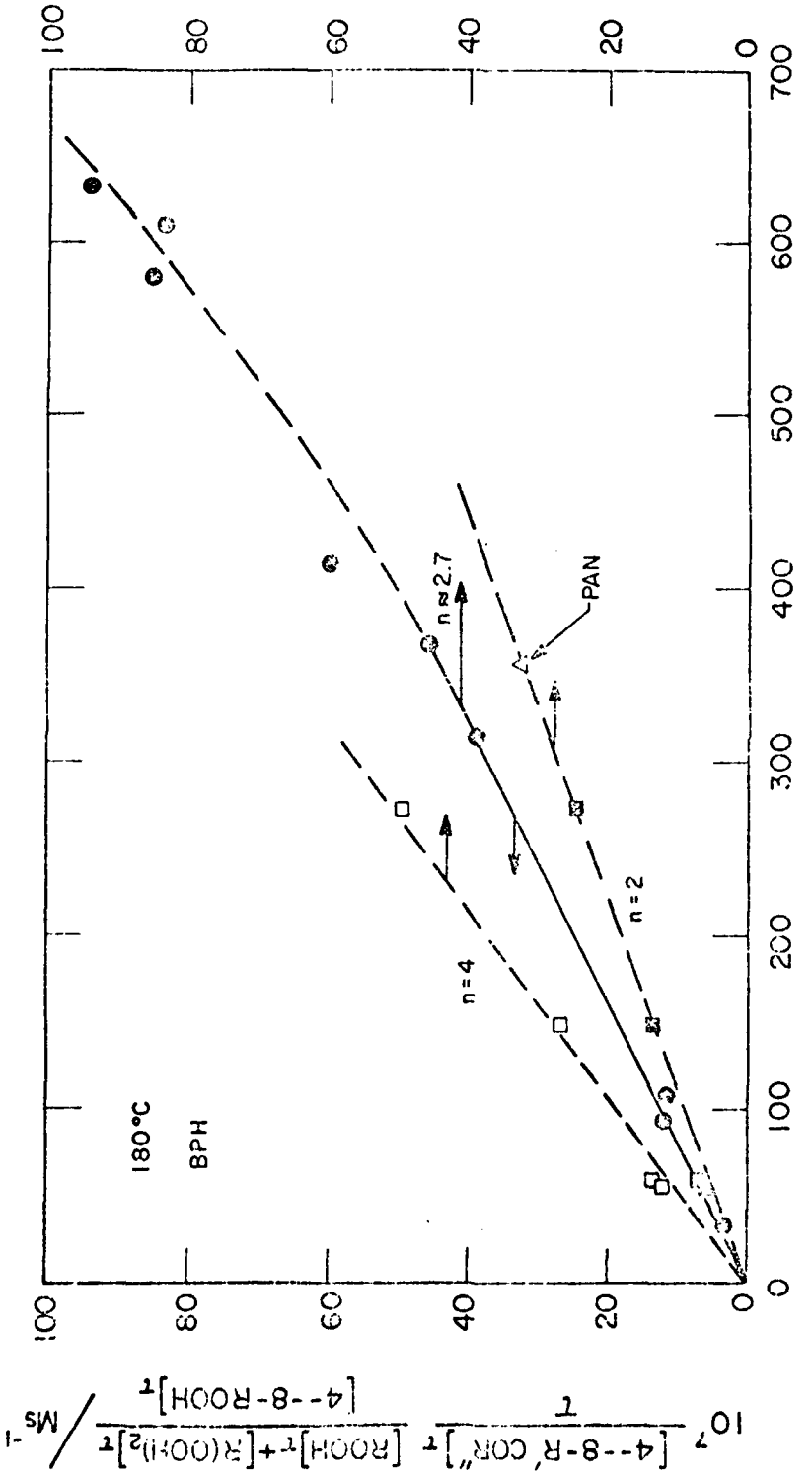

Figure 5. Estimation of $\bar{n}$ for BPH at 180°C from measurements of inhibition time in HD autoxidation (eq. XIII).

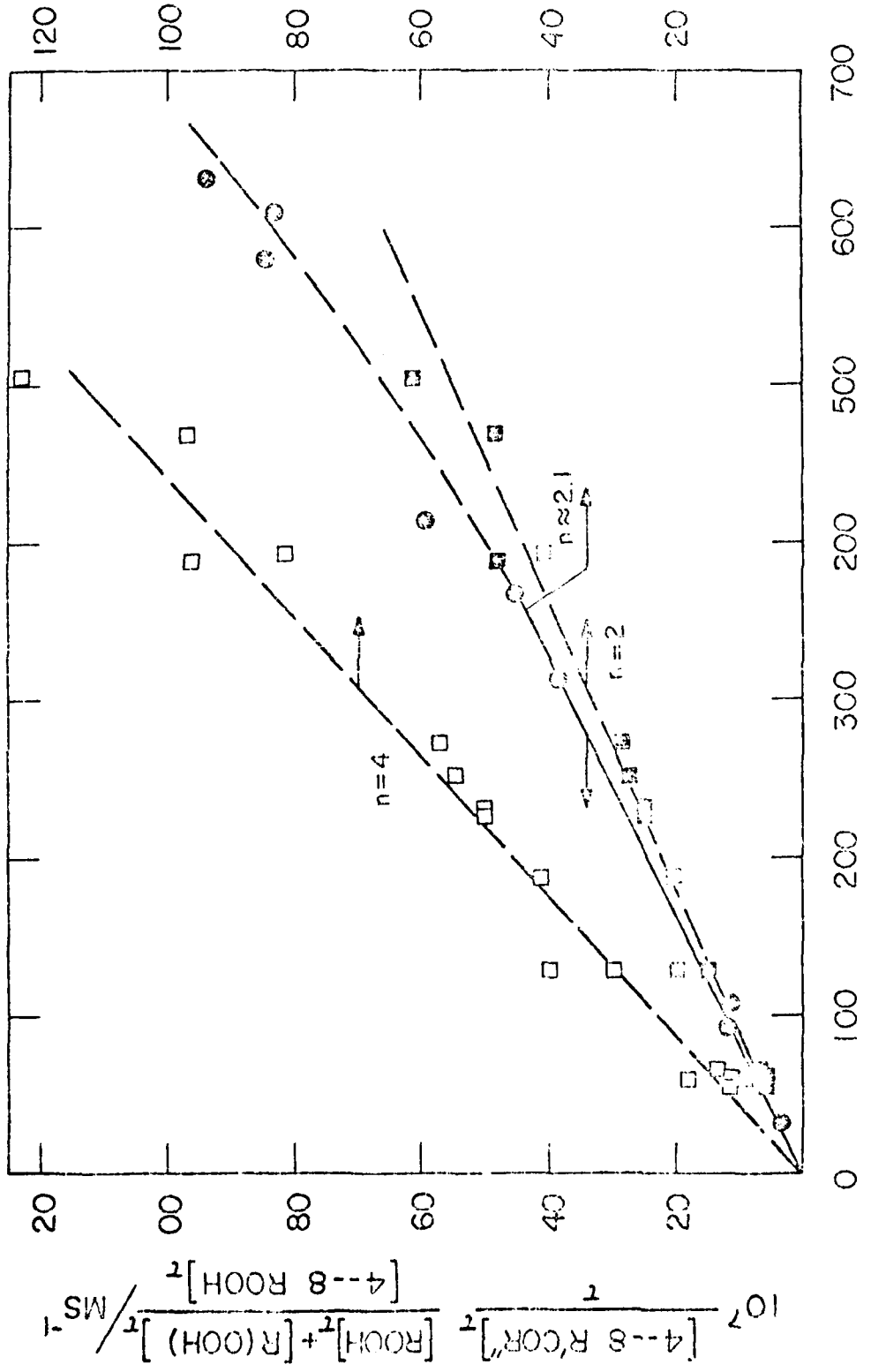

Figure 6. Estimation of n for BPH at 180°C from BPH consumption during inhibited HD autoxidation (eq. XIV).

Preliminary results obtained with PAN described above suggest that the inhibition mechanism of PAN is not adversely affected by elevated temperatures and that the use of PAN for determination of R_I and R_i is promising and warrants further investigations.

REFERENCES

(1) R. K. Jensen, S. Korcek, L. R. Mahoney, and M. Zinbo, J. Am. Chem. Soc. 101, 7574 (1979).

(2) R. K. Jensen, S. Korcek, L. R. Mahoney, and M. Zinbo, J. Am. Chem. Soc. 103, 1742 (1981).

(3) R. K. Jensen, S. Korcek, and M. Zinbo, Part I of this report.

(4) Cf. J. A. Howard in "Free Radicals", Vol. II., J. K. Kochi, Ed., Wiley, New York, 1973, Chapter 12.

(5) P. D. Bartlett and G. Guaraldi, J. Am. Chem. Soc. 89, 4799 (1967).

(6) G. A. Russell, J. Am. Chem. Soc. 79, 3871 (1957).

(7) T. Mill, F. Mayo, H. Richardson, K. Irwin, and D. Allara, J. Am. Chem. Soc. 94, 6802 (1972).

(8) S. W. Benson and P. S. Nangia, Acc. Chem. Res. 12, 223 (1979).

(9) D. G. Hendry, C. W. Gould, D. Schuetzle, M. G. Syz, and F. R. Mayo, J. Org. Chem. 41, 1 (1976).

(10) R. D. Doss and R. N. Hazlett, Ind. Eng. Chem. Prod. Res. Dev. 14, 135 (1975).

(11) D. M. Brown and A. Fish, Proc. Roy. Soc. A. 308, 547 (1969).

(12) J. R. Barker, S. W. Benson, G. D. Mendenhall, and D. M. Golden, U.S. NTIS, PB Rep. 1977, PB-274539.

(13) I. T. Brownlie and K. U. Ingold, Can. J. Chem. 44, 861 (1966).

(14) R. F. Bridger, "Antioxidant Reactions of Diarylaminyl Radicals," Abstracts, 184th National Meeting of the American Chemical Society, Kansas City, Mo., September 1982, No. ORGN 26.

(15) L. R. Mahoney, S. Korcek, P. A. Willermet, F. J. Hamilton, Jr., P. K. Jensen, M. Zinbo, S. K. Kandah, J. M. Norbeck, and L. A. Scheich, "Time-Temperature Studies of High Temperature Deterioration Phenomena in Lubricant Systems: Synthetic Ester Lubricants," Final Report to AFOSR, Contract #F44620-76-C-0097, October 1, 1979.

(16) S. W. Benson, Foundations of Chemical Kinetics, McGraw-Hill, New York, 1960.

(17) L. R. Mahoney, S. Korcek, S. Hoffman, and P. A. Willermet, Ind. Eng. Chem. Prod. Res. Dev. 17, 250 (1978).

(18) Cf. J. Pospisil, Pure Appl. Chem. 36, 207 (1973).

(19) J. Kovarova-Lerchova and J. Pospisil, Europ. Polymer J. 13, 975 (1977).

(20) V. A. Roginskii, V. Z. Dubinskii, I. A. Shlyapnikova, and V. B. Miller, Europ. Polymer J. 13, 1043 (1977).

PART IV

INHIBITION OF THE AUTOXIDATION OF n-HEXADECANE BY 2,6-DI-TERT-BUTYL-4-METHYLPHENOL AT ELEVATED TEMPERATURES

R. K. Jensen, S. Korcek, L. R. Mahoney, and M. Zinbo

INTRODUCTION

Kinetic and mechanistic information on inhibition of autoxidation by MPH in the temperature range of 160 to 180°C is not available. Based on extensive low temperature information on reactions of phenoxy radicals,[1] on the limited literature data on inhibition products at temperatures 120 to 140°C,[2-5] and on the results of our present studies, the inhibition mechanisms of MPH at elevated temperatures may be represented by the sequence of reactions shown in Scheme I. From this scheme it is obvious that the stoichiometric factor for MPH will depend on the relative rates of reactions of $PO^{\cdot}$ and on the fate and relative rates of reactions of intermediate species QOOR, QOOH, QH, etc. In this study we investigate reactions of MPH and selected MPH intermediates and products during the inhibited autoxidation of HD at 160 and 180°C and attempt to elucidate the inhibition mechanism of MPH at these temperatures.

EXPERIMENTAL SECTION

The reaction techniques, some of the analytical procedures and materials used in this study were described previously.[6,7,8]

Hydroperoxide Preparation. Hexadecylhydroperoxides used in the preparation of the corresponding QOOR were synthesized by alkylation of hydrogen peroxide with hexadecylmethanesulfonates using the method of Wawzonek, Klimstra and Kallio.[9] In order to prepare a 1--8-hexadecylhydroperoxide mixture, n-hexadecane was autoxidized under low oxygen pressure to enhance the formation of 1--8-hexadecylhydroperoxides, and a mixture of these hydroperoxides was then

AD-A135 464 TIME-TEMPERATURE STUDIES OF HIGH TEMPERATURE DETERIORATION PHENOMENA IN L..(U) FORD MOTOR CO DEARBORN MICH RESEARCH STAFF S KORCEK ET AL. SEP 83 2/3

UNCLASSIFIED AFOSR-TR-83-0987 F49620-80-C-0061 F/G 11/8 NL

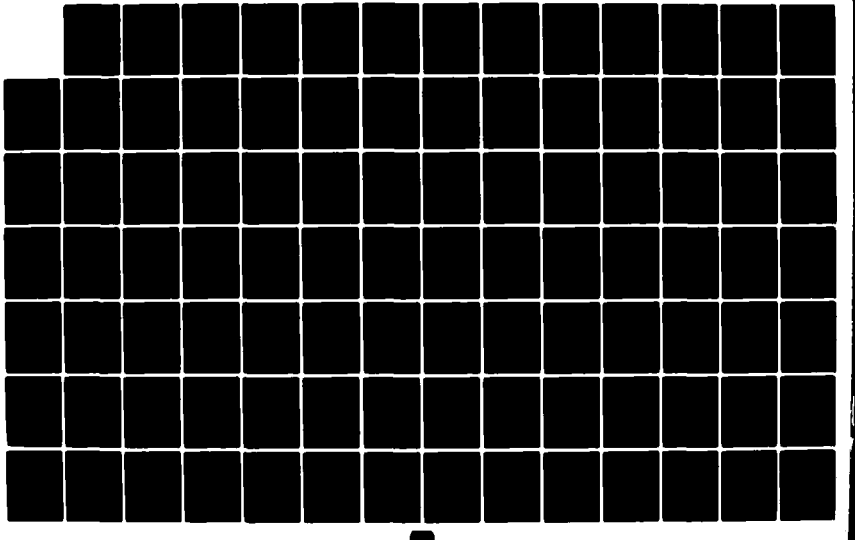

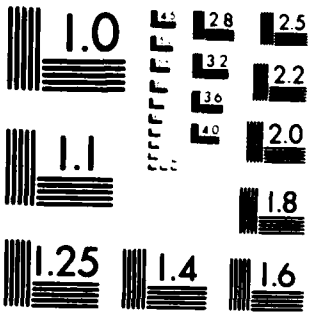

SCHEME I

INHIBITION MECHANISM OF MPH AT INCREASED TEMPERATURES

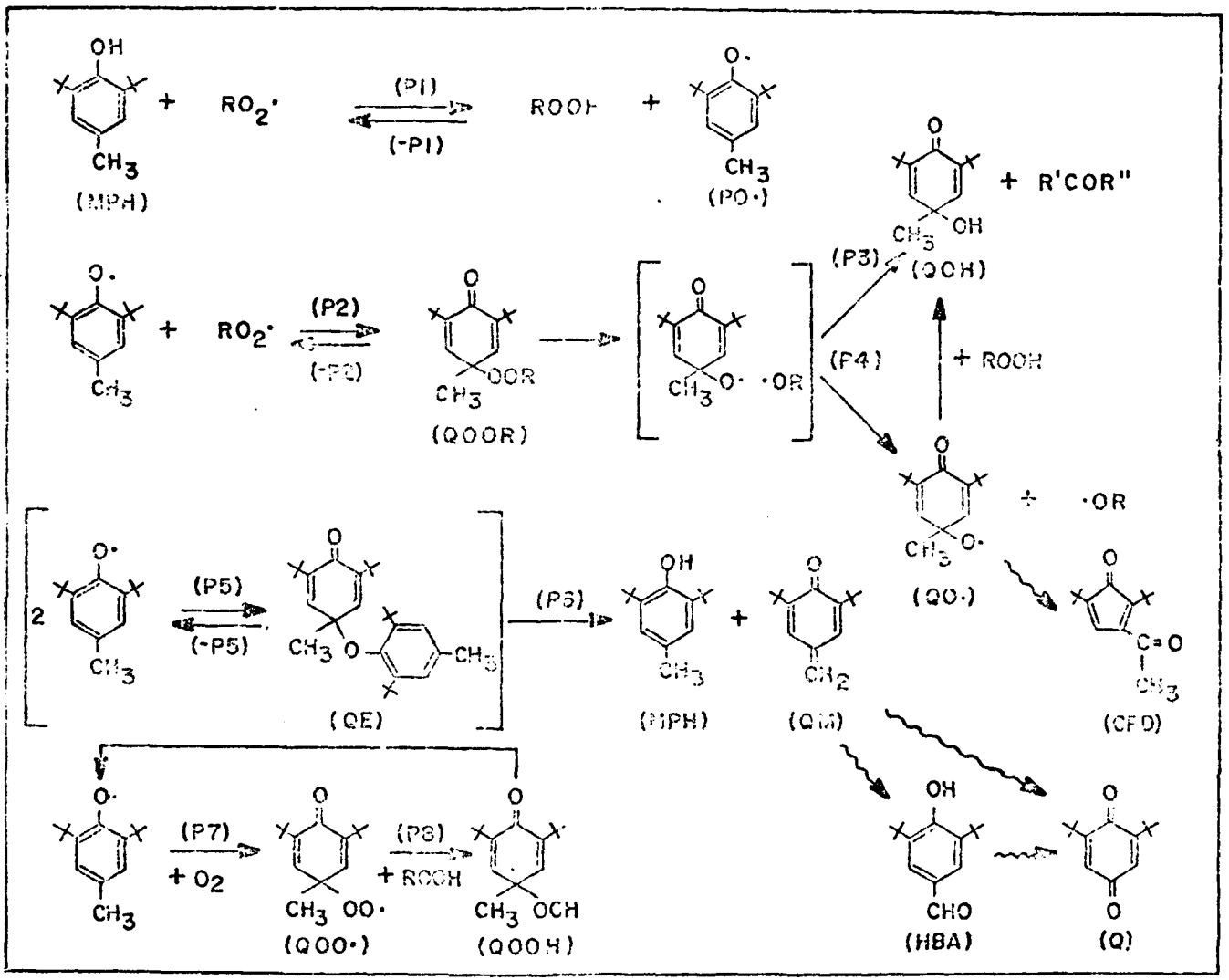

separated on silica gel. A portion (50 mL) of autoxidized n-hexadecane was placed on a 2.5 x 25 cm silica gel column and eluted with 550 mL of hexane, 500 mL methylene chloride and 100 mL methanol. The 1--5-hexadecylhydroperoxides were eluted with the first 450 mL of methylene chloride. This hydroperoxide concentrate was then used for the preparation of QOOR(R=1--8-$C_{16}H_{33}$).

QOOR Synthesis. QOOR compounds with R being t-butyl and n-,2-,5-, and 1--8-hexadecyl were prepared from the reaction between MPH and hydroperoxides. The synthesis of 4-(5-hexadecylperoxy)-4-methyl-2,6-di-t-butyl-2,5-cyclohexadienone, QOOR(R=5-$C_{16}H_{33}$), will be described as a representative of the general procedure used in synthesizing these compounds. A sample of 5-hexadecylhydroperoxide (~0.25 mmol) and 57.6 mg (0.20 mmol) MPH were dissolved in 6 mL of methanol. Over a 45 min. period, 2 mL of a 0.25 M solution of ceric ammonium nitrate in methanol was added dropwise with stirring. The resulting mixture was stirred for an additional 15 min., transferred to a separatory funnel with hexane and washed with acetonitrile and then water. With QOOR(R=t-butyl) the acetonitrile washing step was eliminated. Separation and evaporation of the hexane layer gave the desired product plus some of the 2-isomer.

HPLC Analyses. Several HPLC analytical procedures were developed in order to separate different components in the reaction mixtures. All of these analytical procedures involve reverse phase HPLC using Radial-Pak C_{18}, 8 mm ID cartridges (5 and 10μ), a flow rate of 1 mL/min, and UV detection at 254, 280 and 340 nm depending on the compounds being analyzed. Sample injection volume

was 5 ul. Four different mobile phases were used isocratically in the HPLC separations, which have been designated solvent systems S_1 through S_4

The first three of these solvent systems were used for the analysis of HPH and its reaction products and elution volumes for these compounds are given in Table 1. Solvent system S_1, H_2O:CH_3OH:CH_2Cl_2:CH_3CN (5:5:30:60) was initially used as the sole solvent system to analyze all of the components. Most of the major components were separated adequately with this system but in the region of QOH, HBA, and U2 the separation needed to be improved. For this reason solvent system S_2, H_2O:CH_3OH:CH_2Cl_2:CH_3CN (7:8:25:60), was developed to differentiate the more polar products and quantify all of the known products except QOOR($R=C_{16}H_{33}$). Quantitation of HPH and Q, which are not separated on the chromatogram, are possible by a dual UV detection at both 254 and 280 nm since these compounds absorb very differently at these wavelengths. The ratio of absorbance at 254 nm to that at 280 nm is 0.16 for HPH and 14.3 for Q which allows calculation of the concentration of each component based on the measured peak areas at the two wavelengths. Solvent system S_3, CH_3OH:CH_2Cl_2:CH_3CN (10:30:60), was used for QOOR($R=C_{16}H_{33}$) analysis.

A fourth solvent system, S_4, H_2O:CH_2Cl_2:CH_3CN (5:10:85), was applied for HPLC analysis of PAN and its main reaction product using a dual UV detection at 280 and 310 nm. Elution volumes under these conditions were 4.1 mL for PAN and 4.5 mL for its major product.

HPLC Standards. Samples of QE, QH, QOOH, OOH, and CPD used in this study were synthesized in our laboratory. QE was synthesized by DDQ oxidation of HPH

Table 1

HPLC ELUTION VOLUMES, V_E, FOR STANDARD COMPOUNDS

Compound	Designation	V_E(mL) S_1	S_2	S_3
Unknown	U1		3.4	3.2
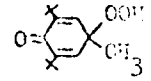	QOOH		3.6	
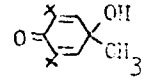	QOH	3.74	3.66	
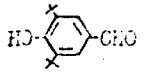	HBA	3.74	3.88	
Unknown	U2		3.88	3.45
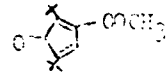	CPD	4.0	4.25	
Unknown	U3	4.3	4.6	3.84
Unknown	U4	4.4	4.8	3.84
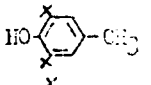	MPH	4.54	5.0	3.9
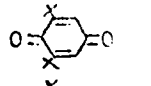	Q	4.54	5.0	
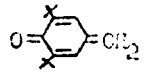	QM	5.0	5.45	
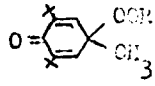	QOOR(R=tetralyl)	5.9	7.4	
	QOOR(R=t-butyl)		7.2	4.65
	QOOR(R=$C_{16}H_{33}$-)	22-24	~45	11.5-12

S_1 = H_2O:CH_3OH:CH_2Cl_2:CH_3CN(5:5:30:60)
S_2 = H_2O:CH_3OH:CH_2Cl_2:CH_3CN(7:8:25:60)
S_3 = CH_3OH:CH_2Cl_2:CH_3CN(10:30:60)

according to the method of Becker.[10] As anticipated, QK gave equal amounts of MPH and QH when in solution. QOOH was synthesized by oxidation of MPH under basic conditions.[11] QOH was prepared by reduction of QOOH with triphenylphosphine. CPD was synthesized photochemically in the solid state from QOOR(R=butyl).[12]

RESULTS AND DISCUSSION

MPH Inhibition Products. Complexity of inhibition reactions of MPH resulting in the multitude of products present at very low concentrations makes identification and determination of compounds formed during the inhibition process very difficult. In this work, an attempt has been made to solve this problem by application of HPLC methods for direct analysis of products obtained from the MPH inhibited autoxidation of HD in the presence and absence of hydroperoxides.

MPH Inhibited Autoxidation of Preoxidized HD. MPH decay and product formation during initial stages of inhibition of HD autoxidation at various hydroperoxide levels at 100°C are shown in Figures 1-6. The products which were analyzed included QOOR, QK, Q, QOH + QOOH, CPD, U1, U2 + HBA (U2 absorbs stronger at 254 nm while HBA at 280 nm), and U3 + U4 (U3 absorbs stronger at 254 nm while U4 at 280 nm), where U1-U4 are unidentified components.

Formation of QOOR was previously established in low temperature studies of inhibited autoxidation of tetralin[13] and formation of HBA was detected during inhibited oxidation of a lubricating oil.[14] QOOH was found to be a product of photooxidative transformation of MPH,[15] CPD of photochemical transformation of

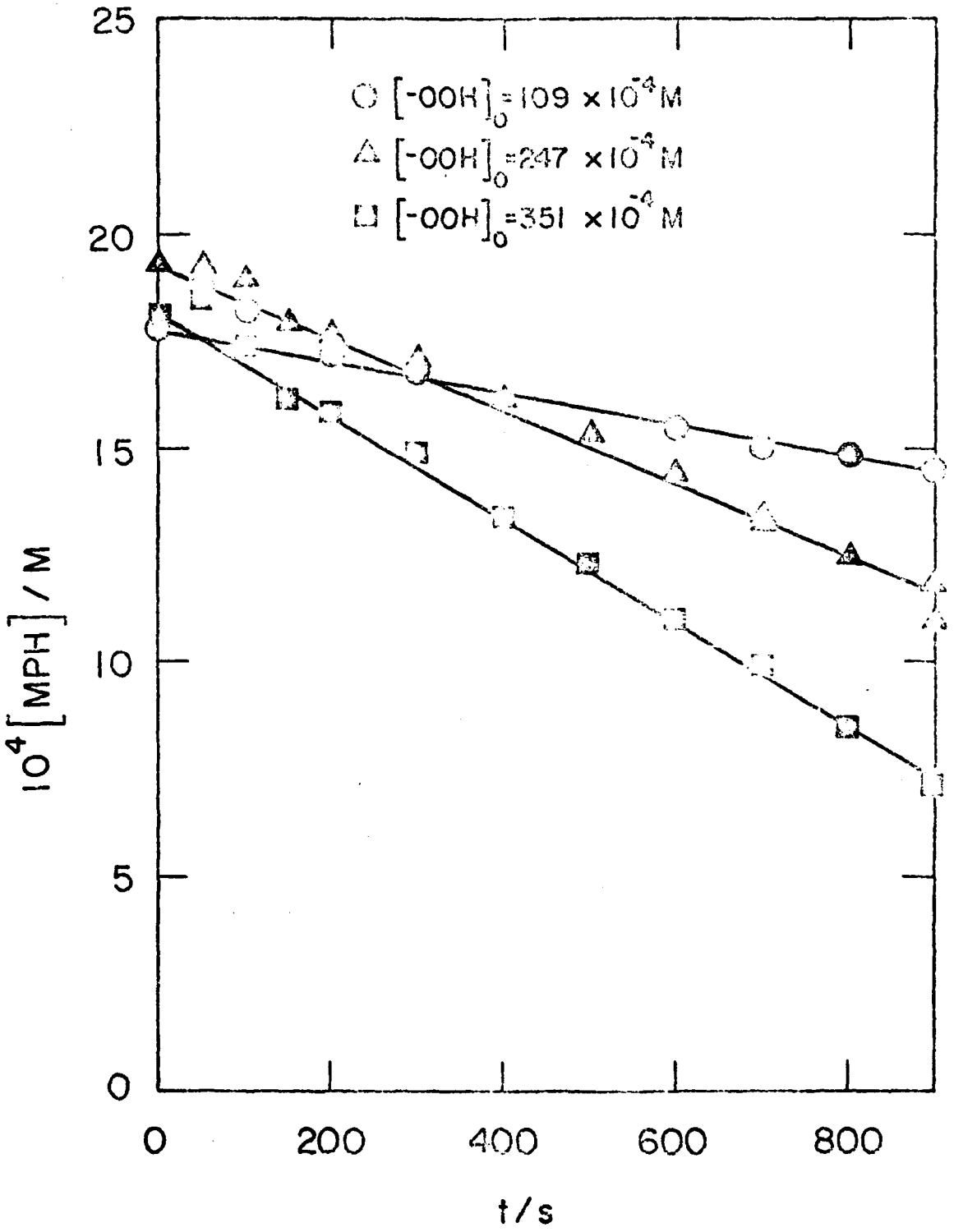

Figure 1. MPH decay during inhibited autoxidation of preoxidized HD at 160°C.

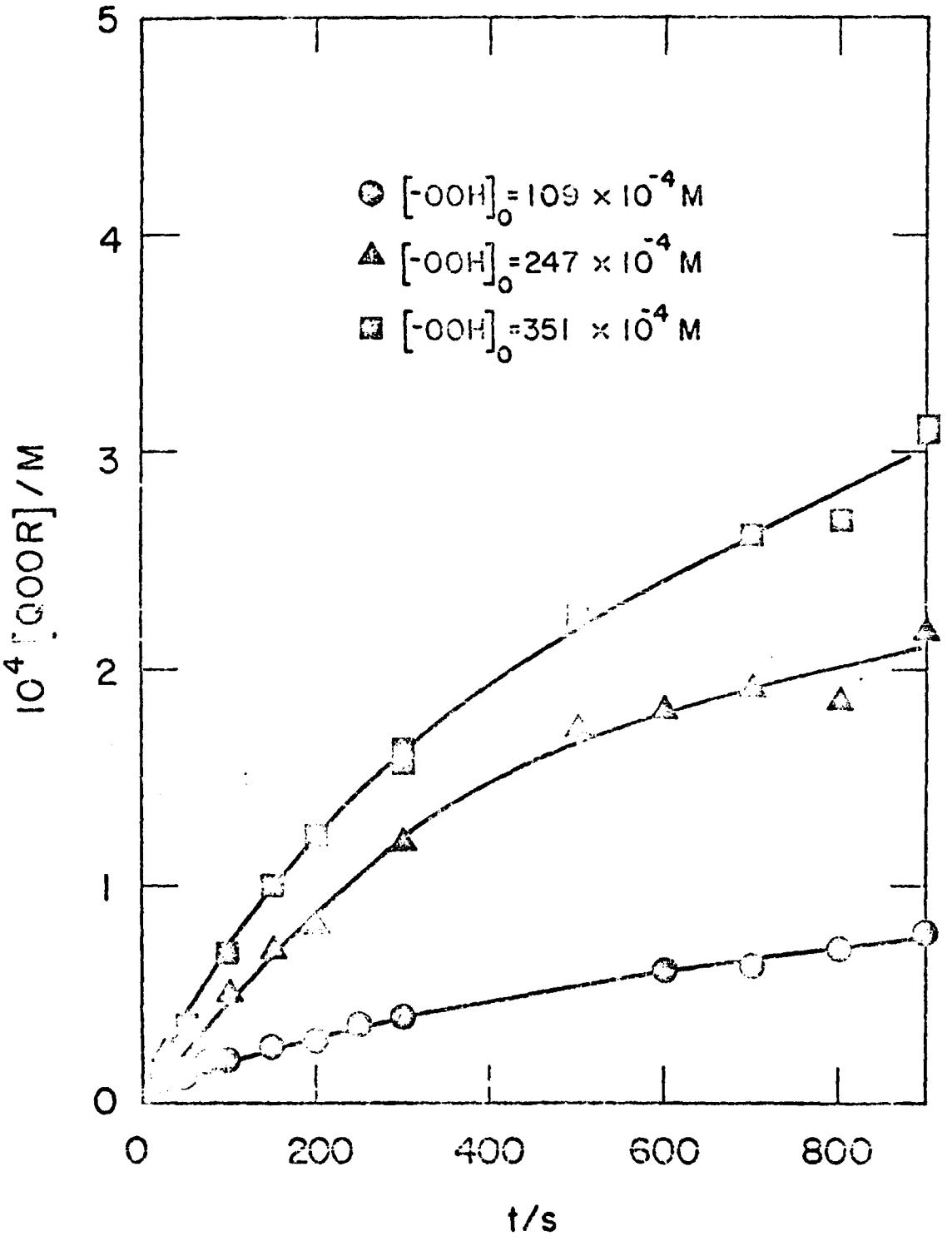

Figure 2. Formation of QOOR during MPH inhibited autoxidation of preoxidized HD at 160°C.

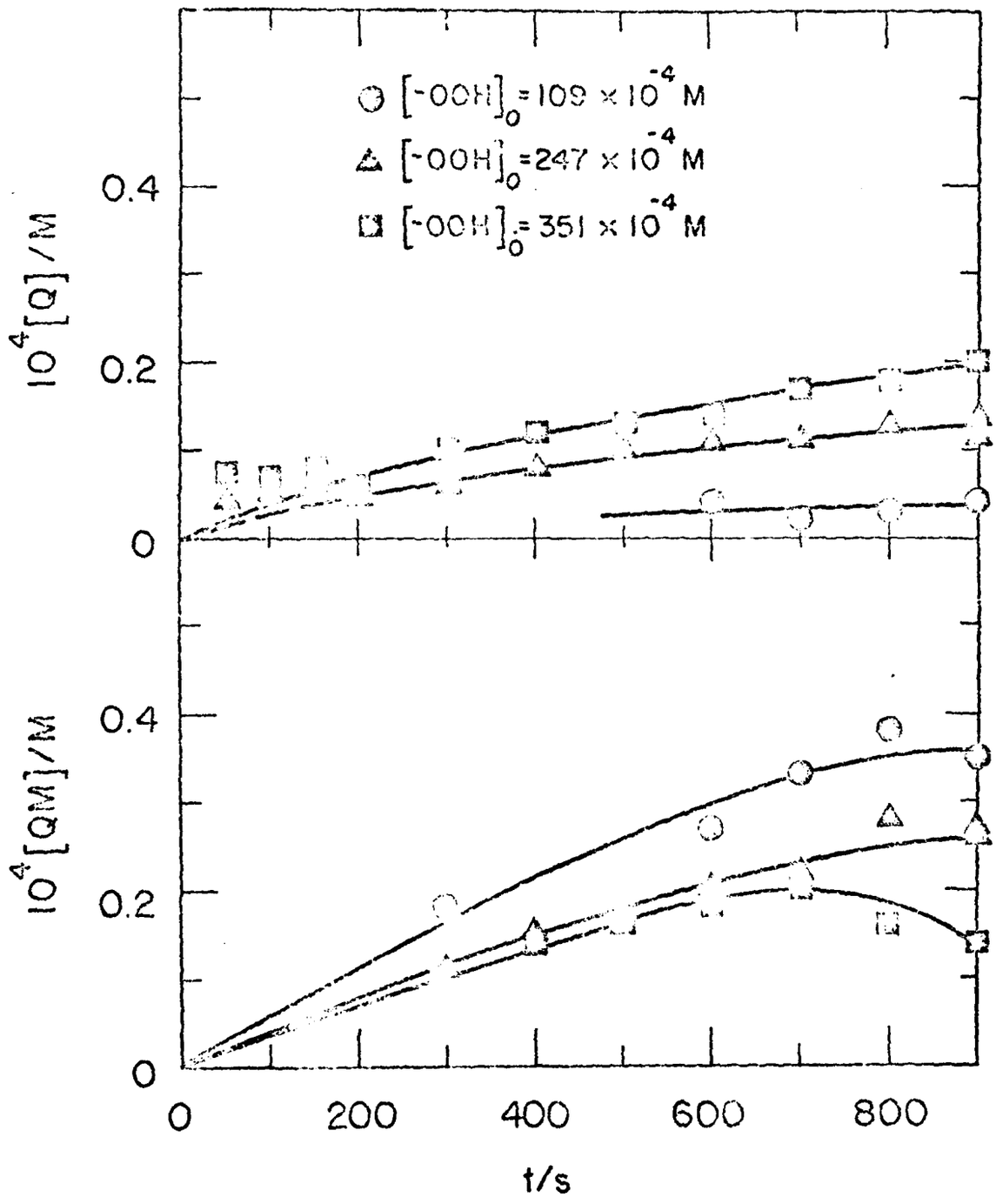

Figure 3. Formation of Q and QM during MPH inhibited autoxidation of preoxidized HD at 160°C.

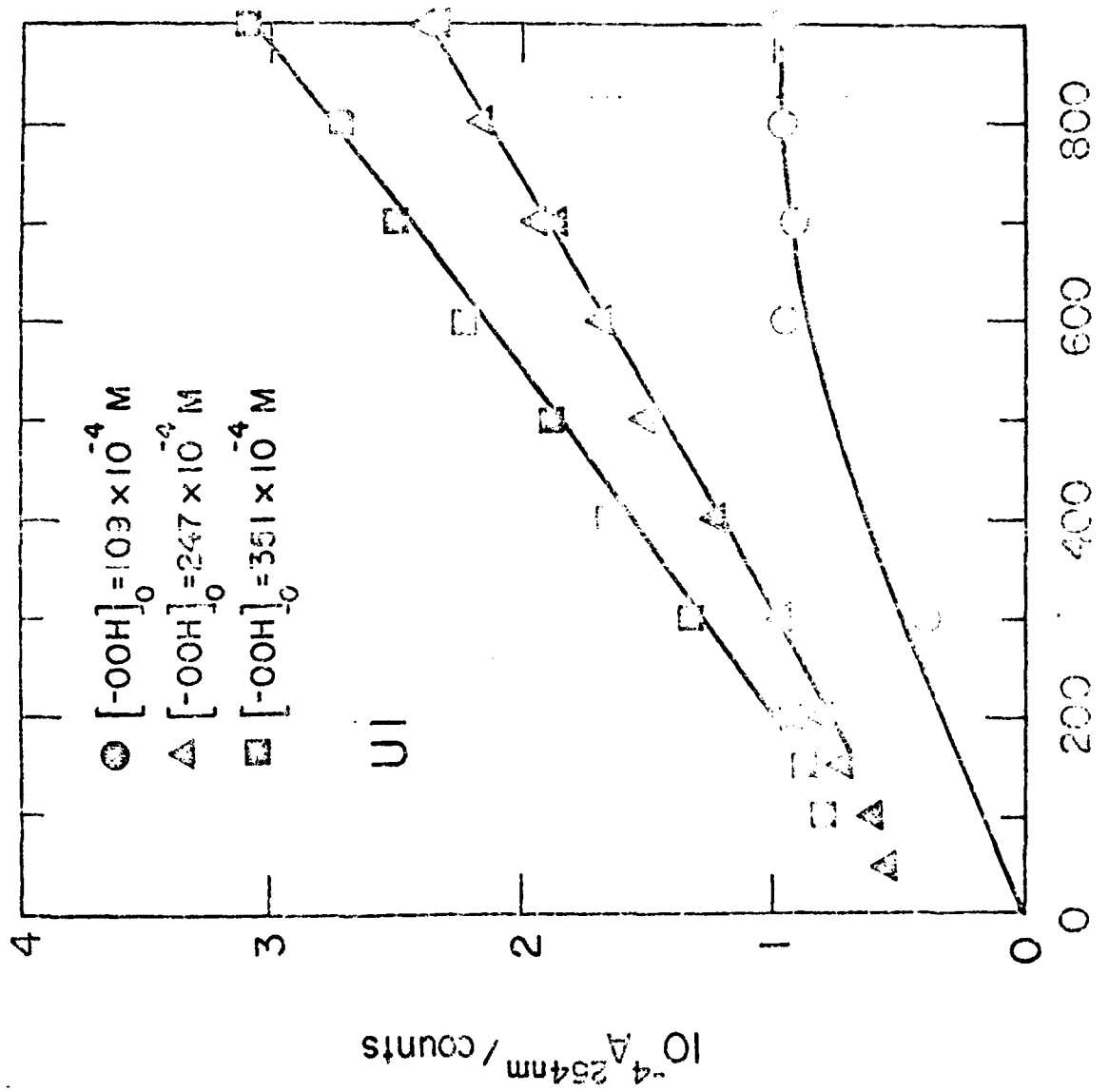

Figure 4. Formation of UI during MPH inhibited autoxidation of preoxidized HD at 160°C.

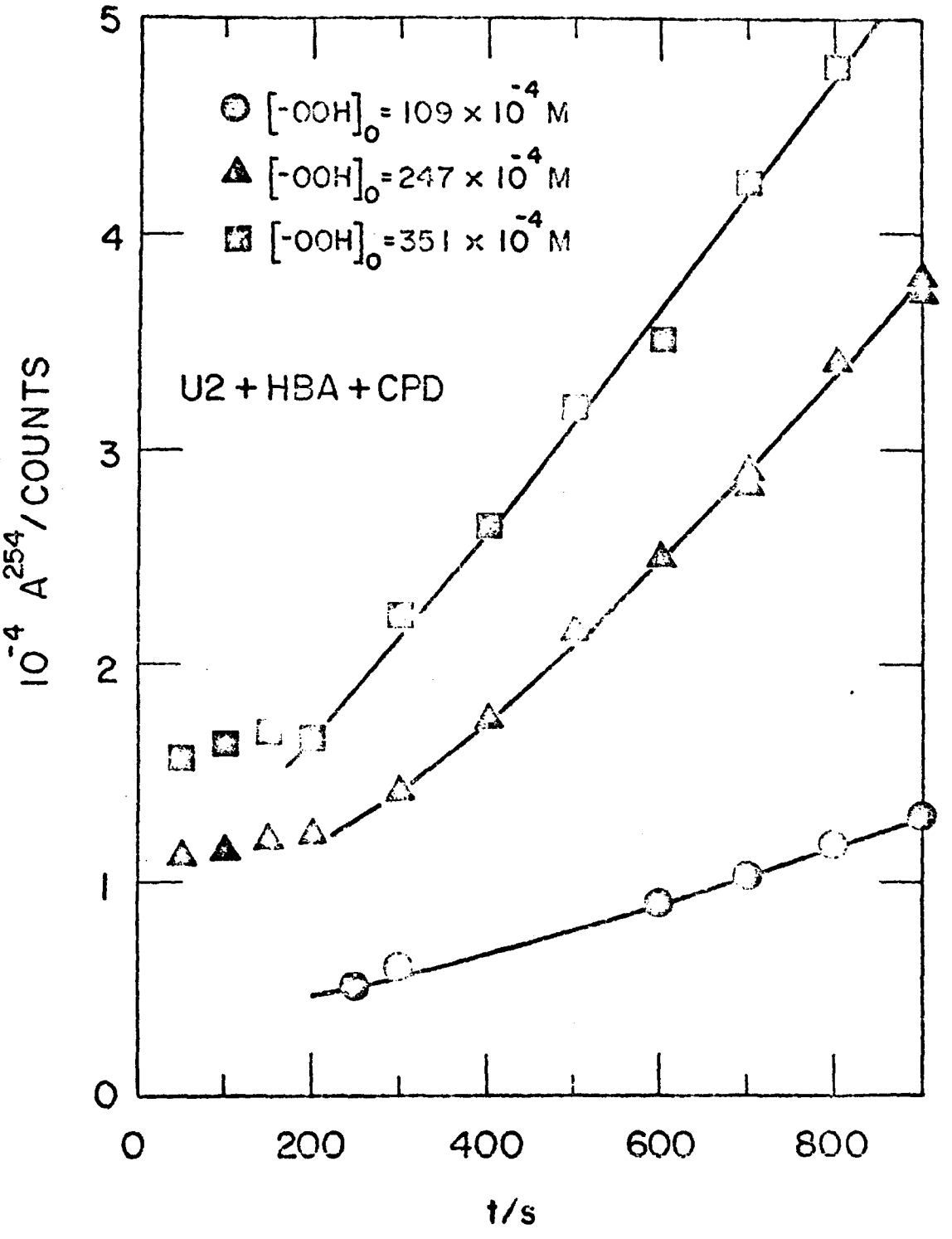

Figure 5. Formation of U2 + HBA + CPD during MPH inhibited autoxidation of preoxidized HD at 160°C.

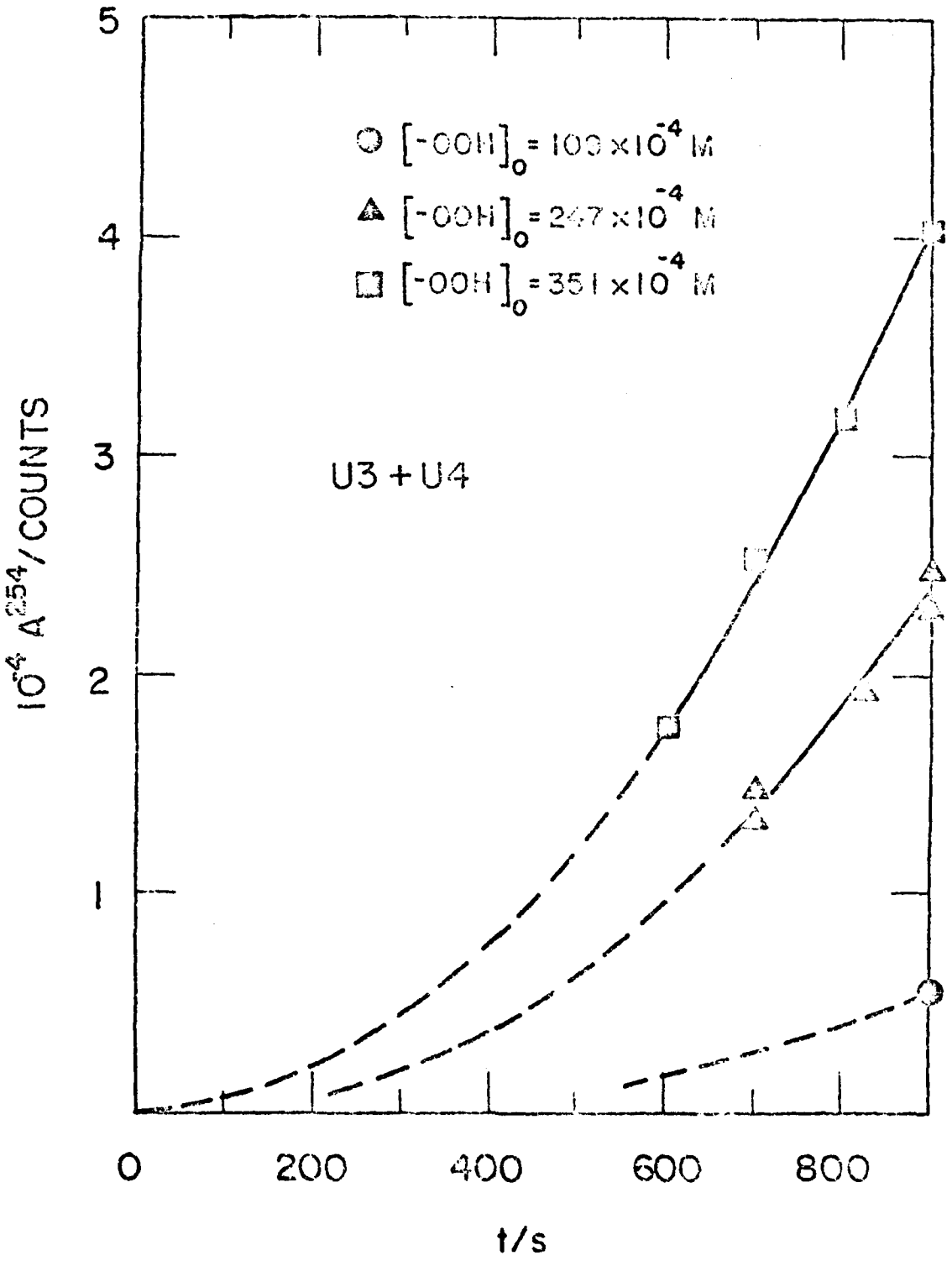

Figure 6. Formation of U3 + U4 during MPH inhibited autoxidation of pre-oxidized HD at 160°C.

QOOR,[12] Q of thermal decomposition of 4-tert-butyl substituted analog of QOOR(R=tert-butyl),[5] and QOH of thermal transformation of QOOH.[16]

No 3,5,3'5'-tetra-tert-butylstilbenequinone, SQ, has been detected under our reaction conditions. SQ has been found as a major product in MPH inhibited autoxidation of a transformer oil at 120°C[17] and in reaction of MPH with tert-butoxy radicals at 122°C.[18] The source of SQ has been reported to be dimerization of QM[19] which only occurs at higher QM concentrations. In the above studies,[17,18] initial MPH concentrations and subsequently QM concentrations were at least one to two orders of magnitude higher and the concentrations of hydroperoxides, which might participate in alternative reactions with QM, were much lower than those in this study.

Plots in Figure 7, where amounts of MPH reacted, $[MPH]_0-[MPH]_t$, and yields of QOOR, $[QOOR]_t$, are compared, reveal that QOOR, produced via reactions P1 and P2, is a major intermediate which undergoes further fast decomposition reactions. Due to these reactions the relative yields of QOOR (% of MPH converted) decrease with time (Table 2). The nature of QOOR decomposition reactions remains unknown since total yields of all other identified components, including those which could originate from QOOR decomposition (QOH, CPD, HBA, Q), are low and do not account for the difference between $([MPH]_0-[MPH]_t)$ and $[QOOR]_t$ mainly at higher MPH conversions (Table 2). These results suggest that some of the major products were not analyzed or recovered or that they are included in unidentified components. It is difficult to assess which of the unidentified components originate from decomposition of QOOR and which are formed via alternative reactions of $PO^{\bullet}$, reactions P6 and P7. It seems, however, that U3 + U4 originate from

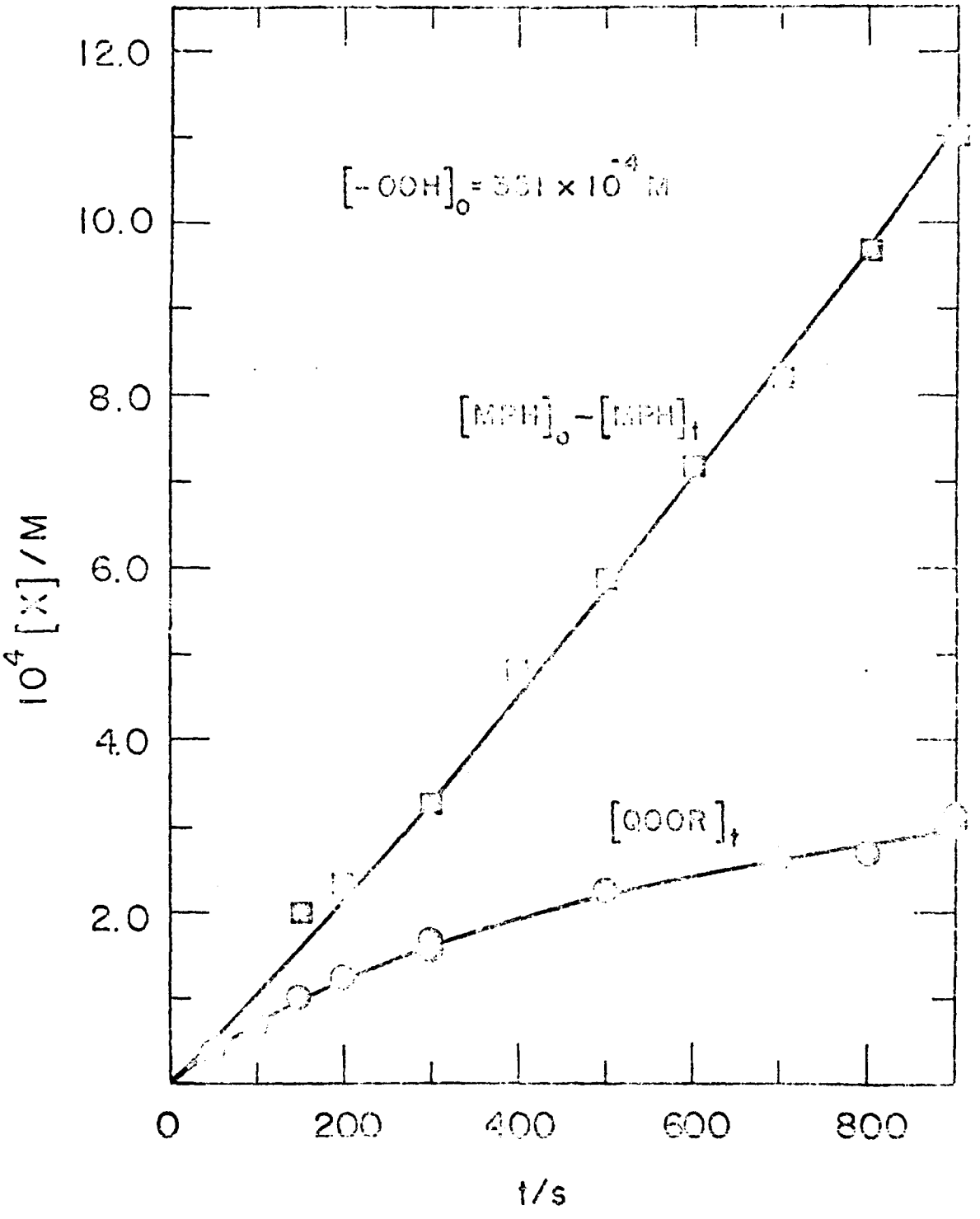

Figure 7. Formation of QOOR and consumption of MPH during MPH inhibited autoxidation of preoxidized HD at 160°C.

Table 2

RELATIVE YIELDS OF MPH INHIBITION PRODUCTS (% of MPH) AT 160°C

RUN	BR-177				BR-179				BR-178			
$[-OOH]_o$/M	109×10^{-4}				247×10^{-4}				351×10^{-4}			
$[MPH]_o$/M	17.8×10^{-4}				19.2×10^{-4}				18.1×10^{-4}			
t_{inh}/s	4600				2325				1500			
t/s	100	300	500	900	100	300	600	900	100	300	600	900
QOOR	59	40	26	23	62	48	37	28	58	45		28
QM		18	12	10		4	4	3			3	1
Q			2	1	6	2	2	2	6	3	3	2
QOH + QOOH								4				
HBA		<2	<2	<2				<1				<1
CPD				<9								

QOOR since the rate of formation of U3 + U4 increases with [QOOR] (Figure 4). A similar trend is observed with group U2 + HBA + CPD where component U2 is prevailing under these conditions (Figure 5).

From all products analyzed, only yields of QM decrease with increasing $[-OOH]_o$ at the same $[-OH]_o$ (Figure 3). This indicates that reaction P6 becomes more important at lower hydroperoxide concentrations when the concentration of peroxy radicals decreases. In addition, QM exhibits increased rate of decay at highest $[-OOH]_o$ even though QM concentrations are lowest in this case. This suggests that QM might be consumed by reactions with hydroperoxides or peroxy radicals.

Formation of QOOH, which would be indicative of reaction P7, was not positively identified, since under our analytical conditions QOOH is eluted together with QOH. It was previously reported,[16] however, that QOOH decomposes much faster than QOOR and therefore QOOH concentration would not be a measure of extent of reaction P7 anyway.

MPH Inhibited Autoxidation of Pure HD. Inhibition experiments with pure HD carried out at 180°C showed (Figure 8) that during the first half of inhibition time QM is formed in increased yields corresponding to about 15% of MPH consumed and that during the second half it undergoes further reactions. These reactions probably involve hydroperoxides which in this time span are formed at increased rates as indicated by the increased rate of MPH decay. QOOR, in these experiments at 180°C, was detected only in trace amounts. It seems to decompose as soon as it is formed. Formation of U3 + U4 again can be related to the

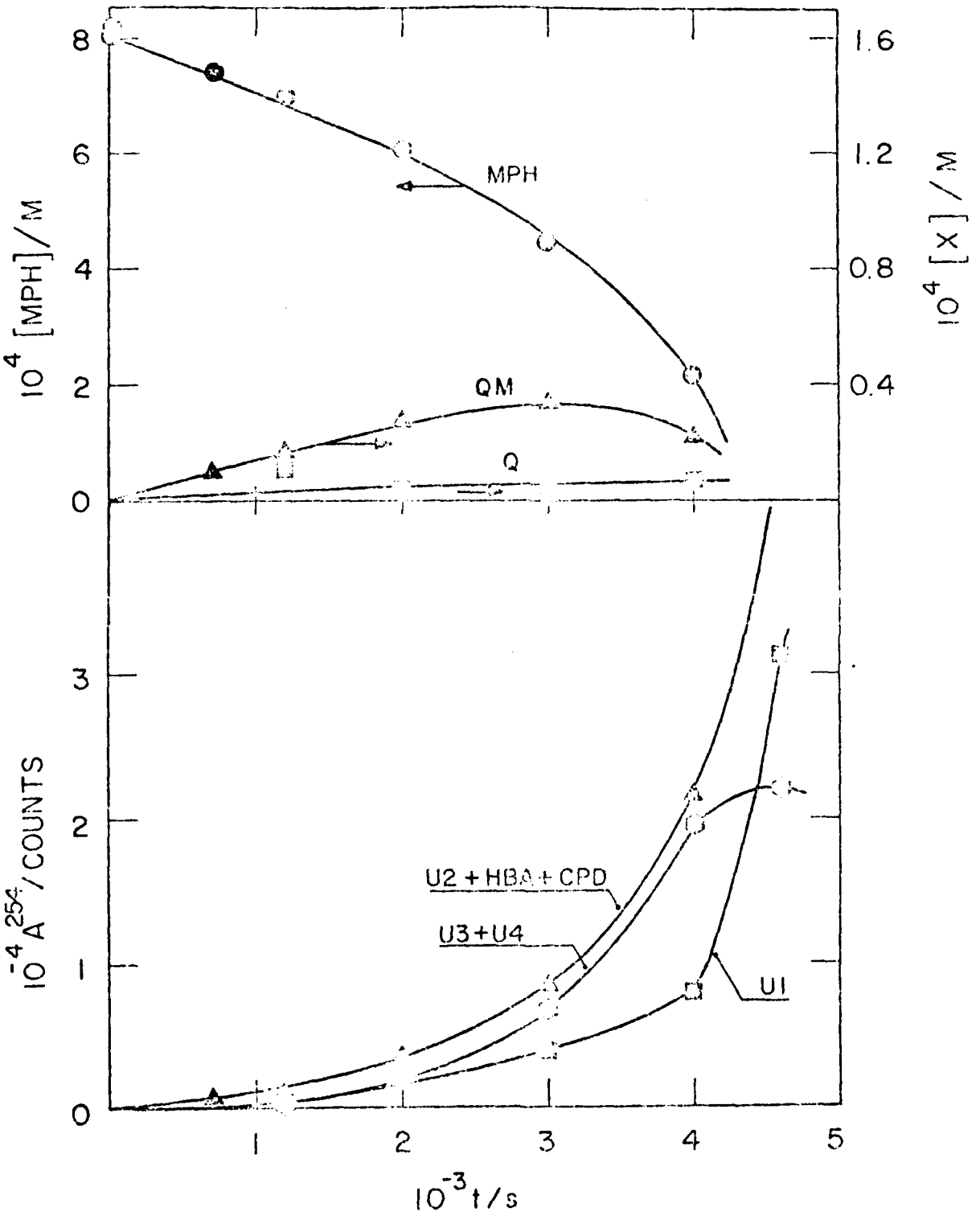

Figure 8. Decay of MPH and formation of MPH derived products during MPH inhibited autoxidation of pure HD at 100°C.

decomposition of QOOR since it coincides with increased formation of hydroperoxides and increased consumption of MPH and it ceases at the end of inhibition time when all POO· are consumed.

Reactions of MPH Products. Better assessment of relative importance of various POO· reactions requires studies of reaction behavior of QOOR, QH, and QOOH under autoxidation conditions. For this purpose, these compounds were added into autoxidizing HD at 100°C and formation of products under these conditions was compared to that from thermal decomposition under Ar. The list of experiments carried out with these compounds is in Table 3.

Reactions of QE and QH. The phenoxy dimer, QE, has been shown to decompose with formation of QH and MPH via disproportionation of phenoxy radicals.[19,20] The decomposition has been predicted to be irreversible at elevated temperatures.[20] Thus, in our experiments, QE has been used as a source of QH.

When QE was added in pure HD under Ar (Table 3, run 157) its fast formation of MPH and QH and no appreciable decay of these products with time (during 600 s) were observed. Under autoxidation conditions in the presence of hydroperoxides (run 156; Figure 9), however, QH decayed very fast and MPH decayed at the same rate as if it had been added separately. The QH decay appears to be an overall result of fast QH interactions with hydroperoxides and of slower QH formation from MPH derived POO·. At the end of induction time, when all MPH is consumed, also all QH is converted. A main product of this QH conversion appears to be unidentified component U3 (prevailing in U3 + U4 under these

Table 3

AUTOXIDATION AND THERMAL DECOMPOSITION EXPERIMENTS WITH ADDED [illegible] INHIBITION PRODUCTS IN n-HEXADECANE AT 160°C

Compound Added, A	Run #	$10^4[A]_o$/M	$10^4[\text{-OOH}]_o$/M	Notes
QE	156	22.21	≈424	
QE	157	8.52	0	Under Ar
Q	153	39.14	≈424	
QOOH	163	38.87	≈ 30	
QOOH	164	36.50	0	Under Ar
QOOH	165	43.09	≈360	
QOOR(R=t-butyl)	159	30.0	≈ 1	
QOOR(R=t-butyl)	160	32.6	0	Under Ar
QOOR(R=t-butyl)	161	26.8	≈ 30	
CPD	158	9.05	0	Under Ar

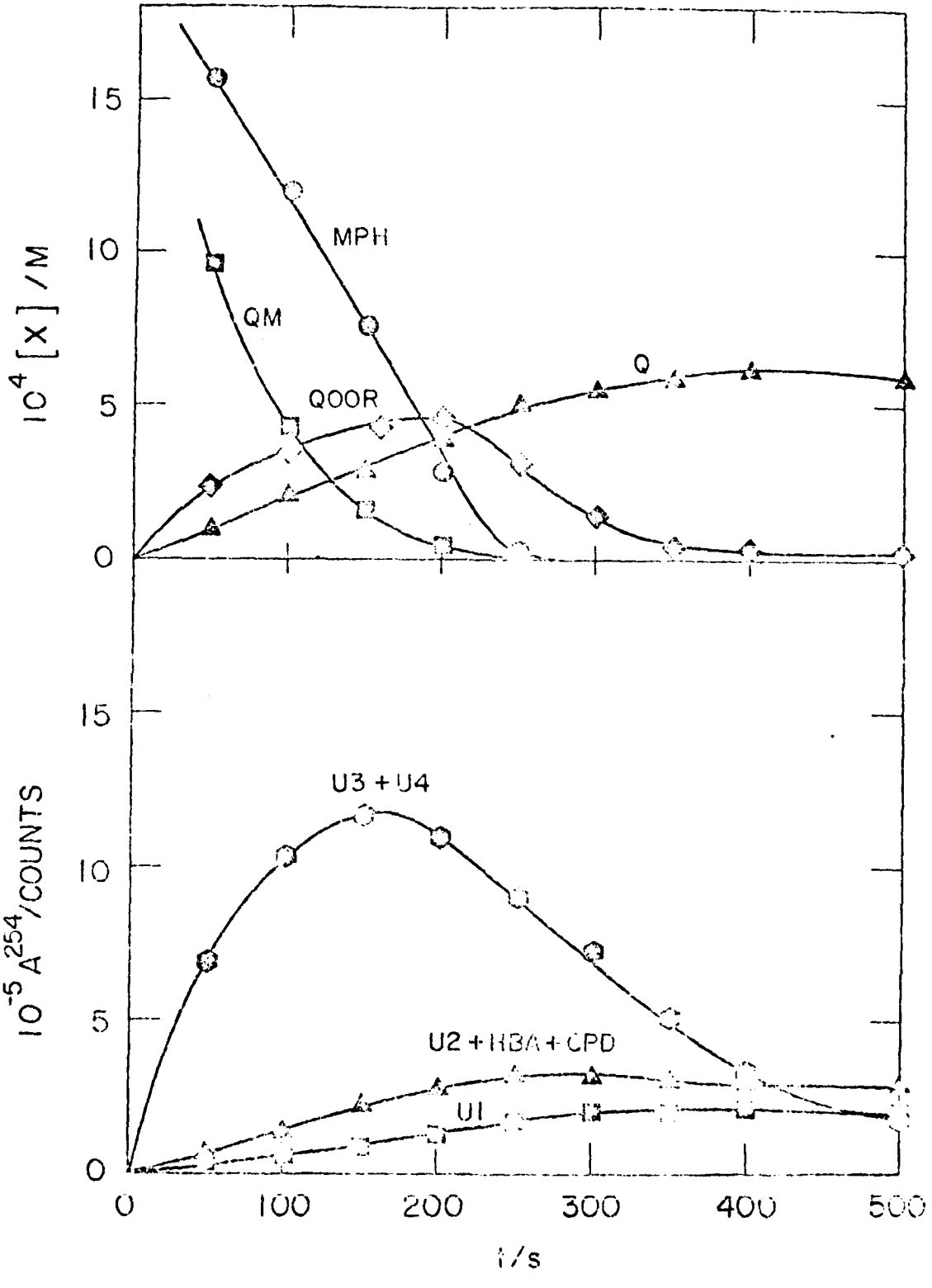

Figure 9. Decay of MPH and formation of products resulting from addition of QE into preoxidized HD at 150°C (run 156).

conditions) which is unstable or undergoes further reactions. This product was also found to be unstable during attempted separation on silica gel. Further investigations are needed to identify U3.

From plots in Figure 9, formation of Q appears to be more a result of decomposition of QOOR (formed from MPH derived $PO_2^{\cdot}$) than a product of reactions of U3 + U4 or QH since it continues to be formed when all QH is consumed and stops being formed when U3 + U4 is still present. This is misleading, however, because U3, which is a major component in U3 + U4 in early stages of the experiment, is a lesser component at the time when formation of Q diminishes. In addition, Q also undergoes further reactions as exhibited by retarded autoxidation observed after inhibition time (Figure 10) which could be attributed to Q (see below). In such case, Q still could be formed when its concentration appears to be constant. Thus, based on these results, Q could originate from QH via U3. This is also supported by an observation that about ten times less of Q is formed during inhibition with MPH where amounts of QOOR produced are comparable to those in the QE added experiment but very little QH and U3 + U4 are formed.

The group of products U2 + HBA + CPD (in this experiment CPD is a minor component which could not be separated from U2 + HBA) and U1 seem to be final products of QE conversions. In reality, however, in early stages of reaction HBA is a major component which later decays while total yields of U2 + HBA + CPD remain the same due to increased formation of U2.

Despite much higher concentrations of QH in the experiments with QE than

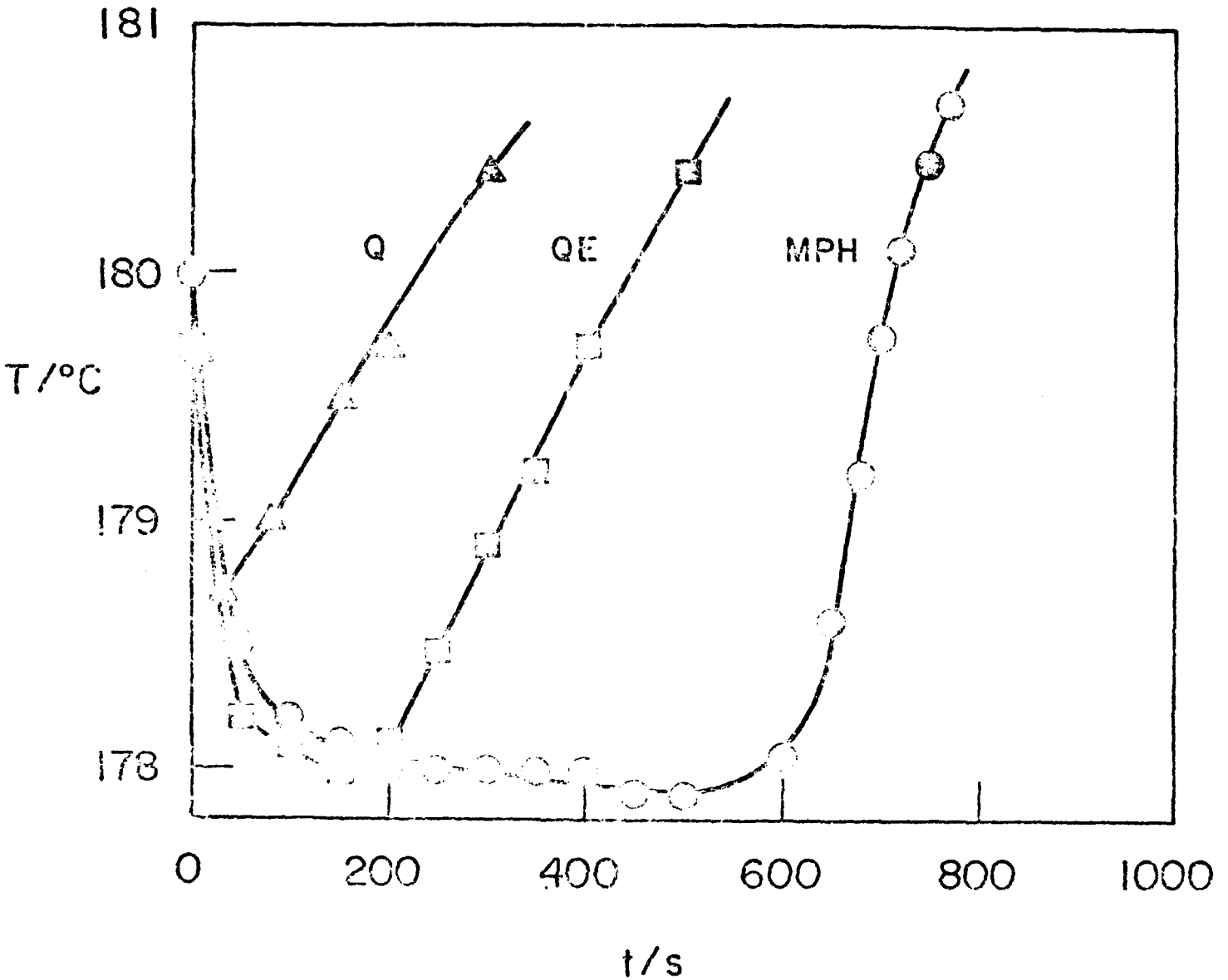

Figure 10. Inhibition and retardation of autoxidation of preoxidized HD upon addition of Q, QE, and MPH at 180°C (runs 153, 156, and 152; $[MPH]_0 = 65.3 \times 10^{-6}$ M).

with MPH, no SQ has been detected under these conditions suggesting that dimerization of QM is slower than other reactions.

Reactions of Q. The retarding ability of Q mentioned above was confirmed in a separate autoxidation experiment with Q added (Figure 10). This behavior contrasts with that of Q in autoxidizing tetralin at 120°C where it was reported that Q does not affect oxygen absorption.[4]

Reactions of QOOH. In the same study as above,[4] QOOH was reported to have retarding activity which was attributed to MPH, one of the two QOOH thermal decomposition products (MPH and QOH).

In our experiments (Table 3, runs 163-165), the fast decomposition of QOOH (Figure 11) and formation of MPH (Figure 12) was also observed, however, only minor amounts of QOH, which is stable under conditions of this experiment, were detected. Instead, formation of substantial amounts of QM (Figure 13) were observed. Decomposition of QOOH was accelerated and formation of MPH and QM was significantly affected by the presence of excess hydroperoxides. In the absence of hydroperoxides (or at their low concentrations), MPH was formed in the amount corresponding to half of QOOH decomposed, while in the presence of excess hydroperoxides in the amount corresponding to only one sixth of that (based on the inhibition period corresponding to a complete decay of MPH). A very similar trend was exhibited by QM which, however, as in experiments with QE, underwent further reactions, the extent of which was again dependent on the presence of hydroperoxides. Yields of QM were highest when QOOH was decomposed under Ar and negligible when excess hydroperoxides were present. Correspondingly, highest

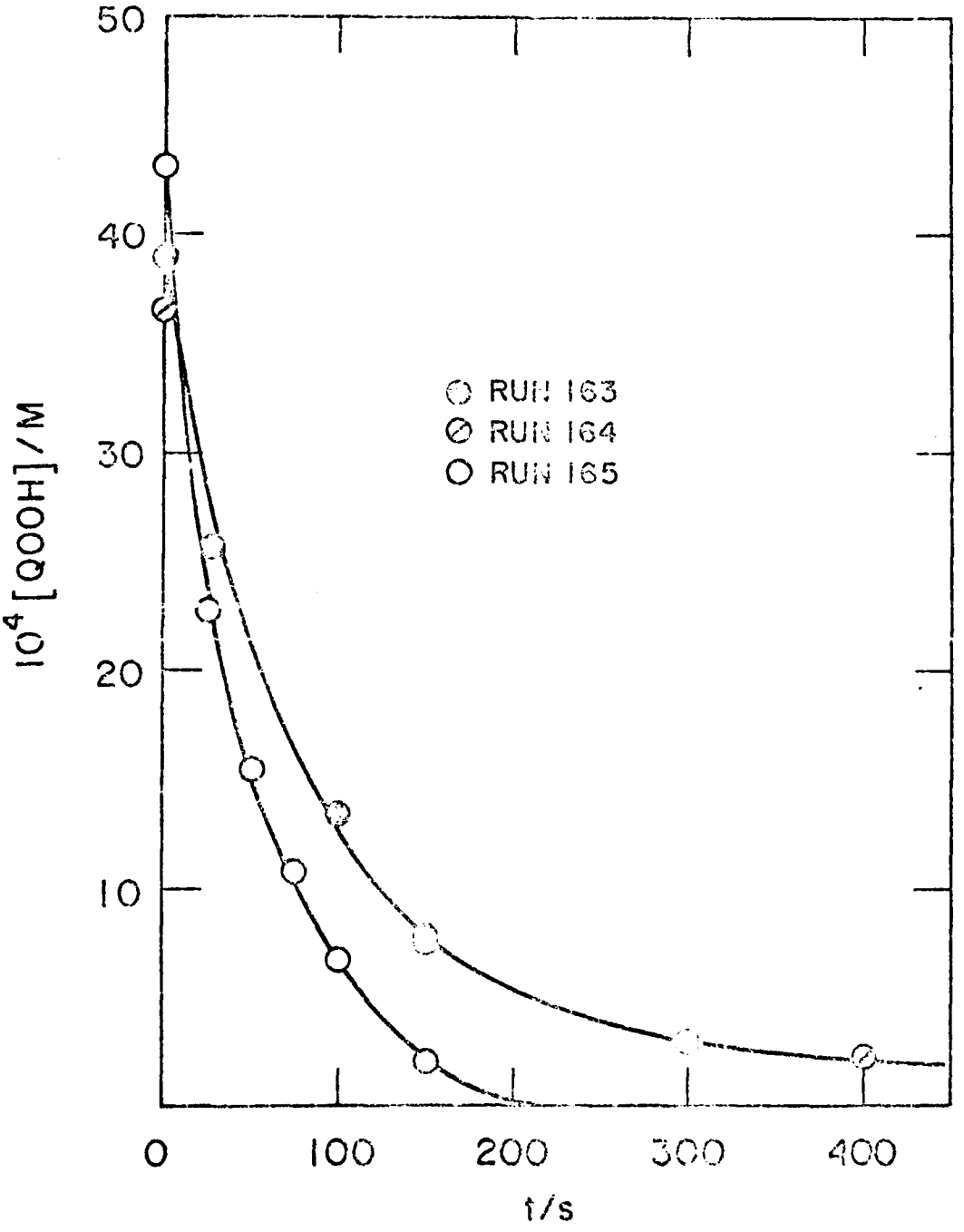

Figure 11. Decay of QOOH upon addition into HD at 180°C.

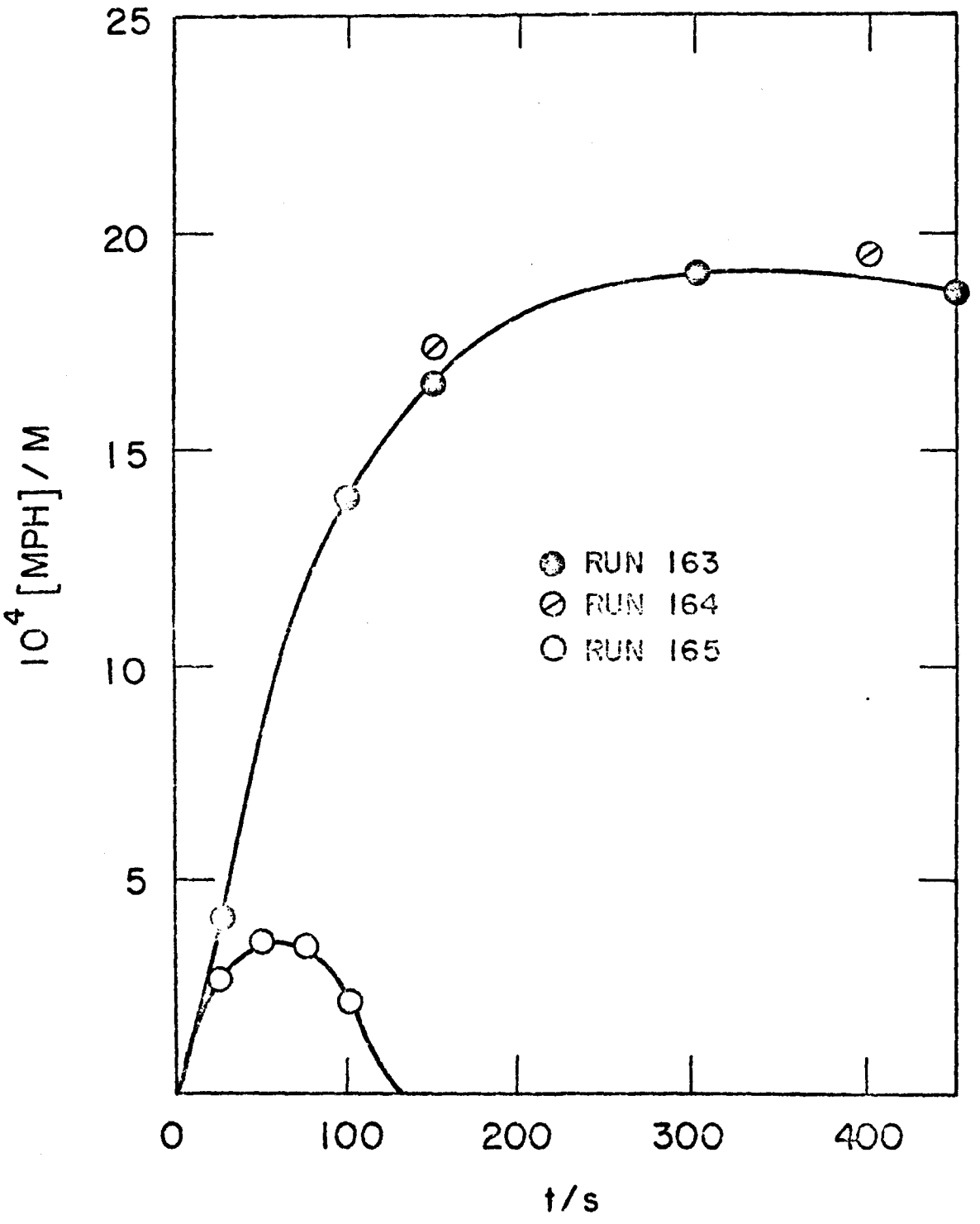

Figure 12. Formation of MPH upon addition of QOOH into HD at 180°C.

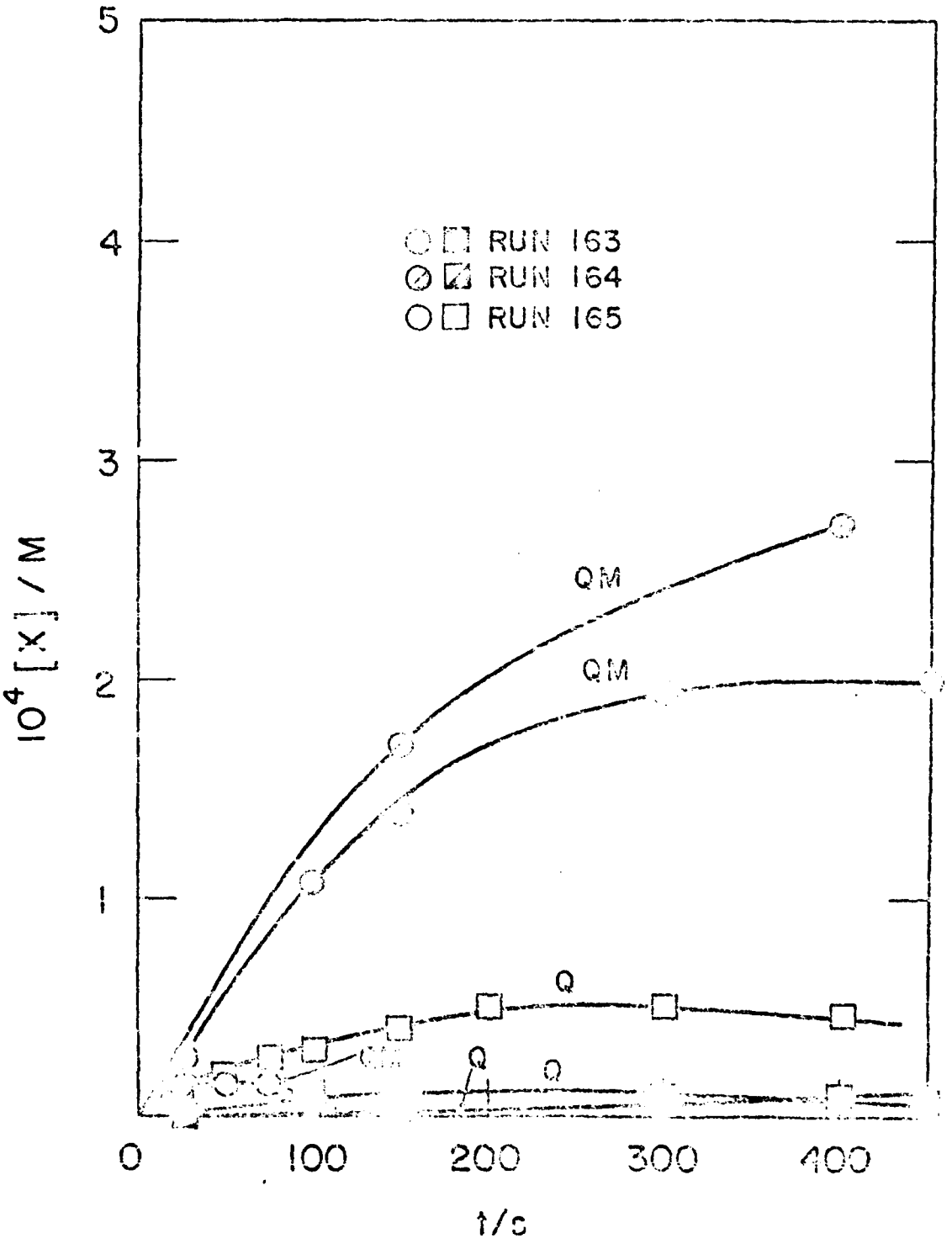

Figure 13. Formation of QM and Q upon addition of QOOH into HD at 180°C.

yields of U3 + U4 (Figure 14) and Q (Figure 13) were observed in preoxidized EE. In comparison to QE experiments, however, significantly increased yields of U3 + HBA + CPD and U1 (Figure 14) were observed upon addition of QOOH in the presence of excess hydroperoxides. This suggests that these products do not originate from QH but from other interactions specific for these conditions. These interactions could include fast decomposition of QOOR which, for that reason, was detected only in trace amounts. The decomposition of QOOR would also support increased formation of CPD and QOH (Figure 15) under these conditions.

Based on results obtained, it is likely that QOOH decomposes with formation of PO• and •OOH. When oxygen, hydroperoxides, and RO_2• are absent PO• undergoes disproportionation reactions leading to QH and MPH, reaction P6, while in the presence of hydroperoxides under autoxidation conditions PO• in addition to reaction P6 reacts with RO_2• to form QOOR, reaction P2. Due to the occurrence of reaction P2 reaction P6 is suppressed and so is the formation of MPH and QH.

Reactions of QOOR(R=tert-butyl). Results obtained with QOOR(tBu) showed that this compound undergoes fast decomposition (Figure 16) which is faster than that of QOOH but it does not produce any appreciable amounts of QH and MPH as it did in the case of QOOH. In the absence of hydroperoxides this decomposition leads to formation of QR and an unknown component, U5. These results could be explained by the presence of two modes of decompositon: one leading to PO• and $tBuO_2$• and the other to QO• and tBuO•. Abstraction of hydrogen from RH by $tBuO_2$• and tBuO• produces R• which reacts with PO• to form QR. Recombination of $tBuO_2$• with PO• leads to original QOOR(tBu) and combination of tBuO• with PO• to QOR(tBu). Thus, component U5 probably is QOR(tBu). This assignment seems to be

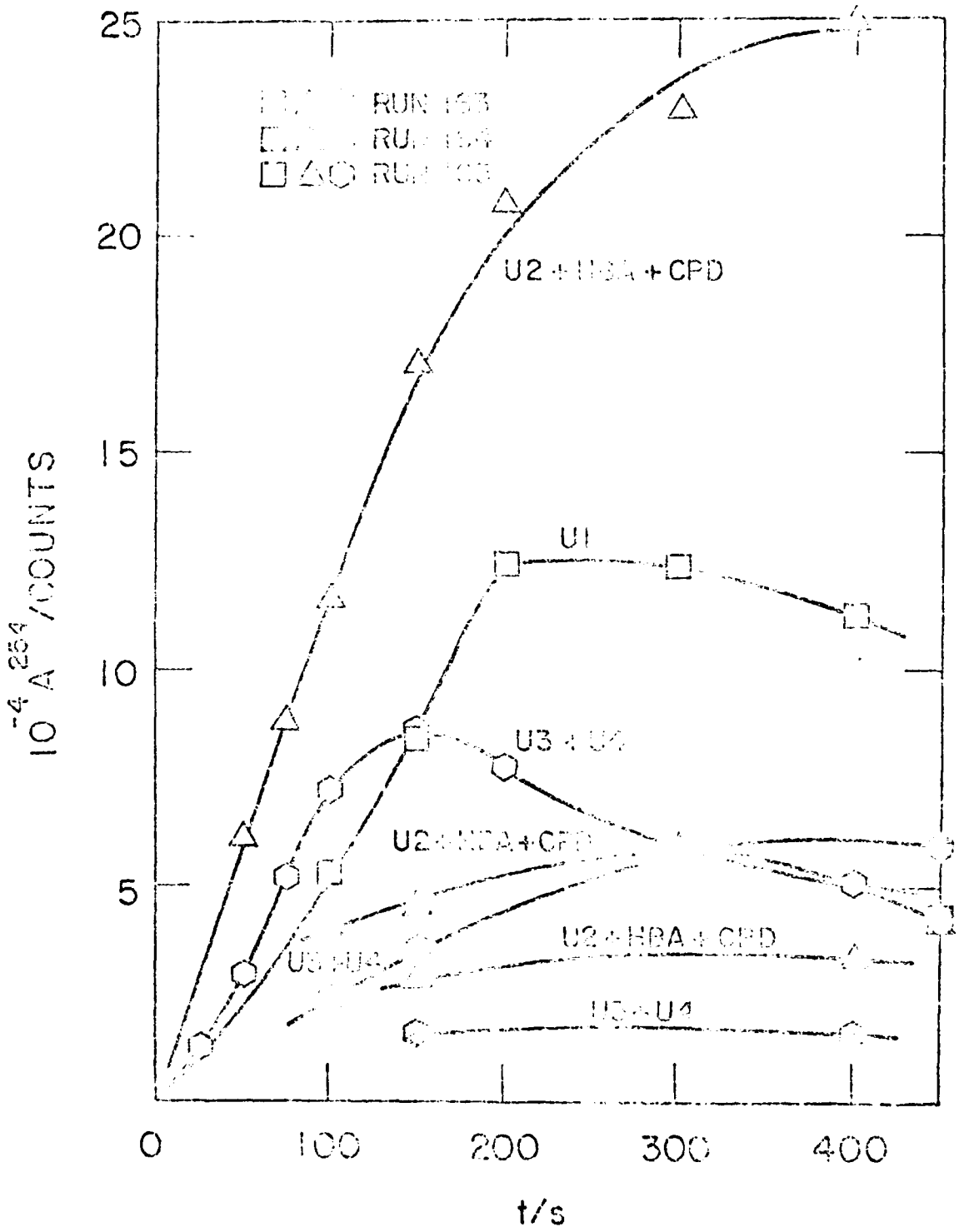

Figure 14. Formation of unidentified products upon addition of COOH into HD at 100°C.

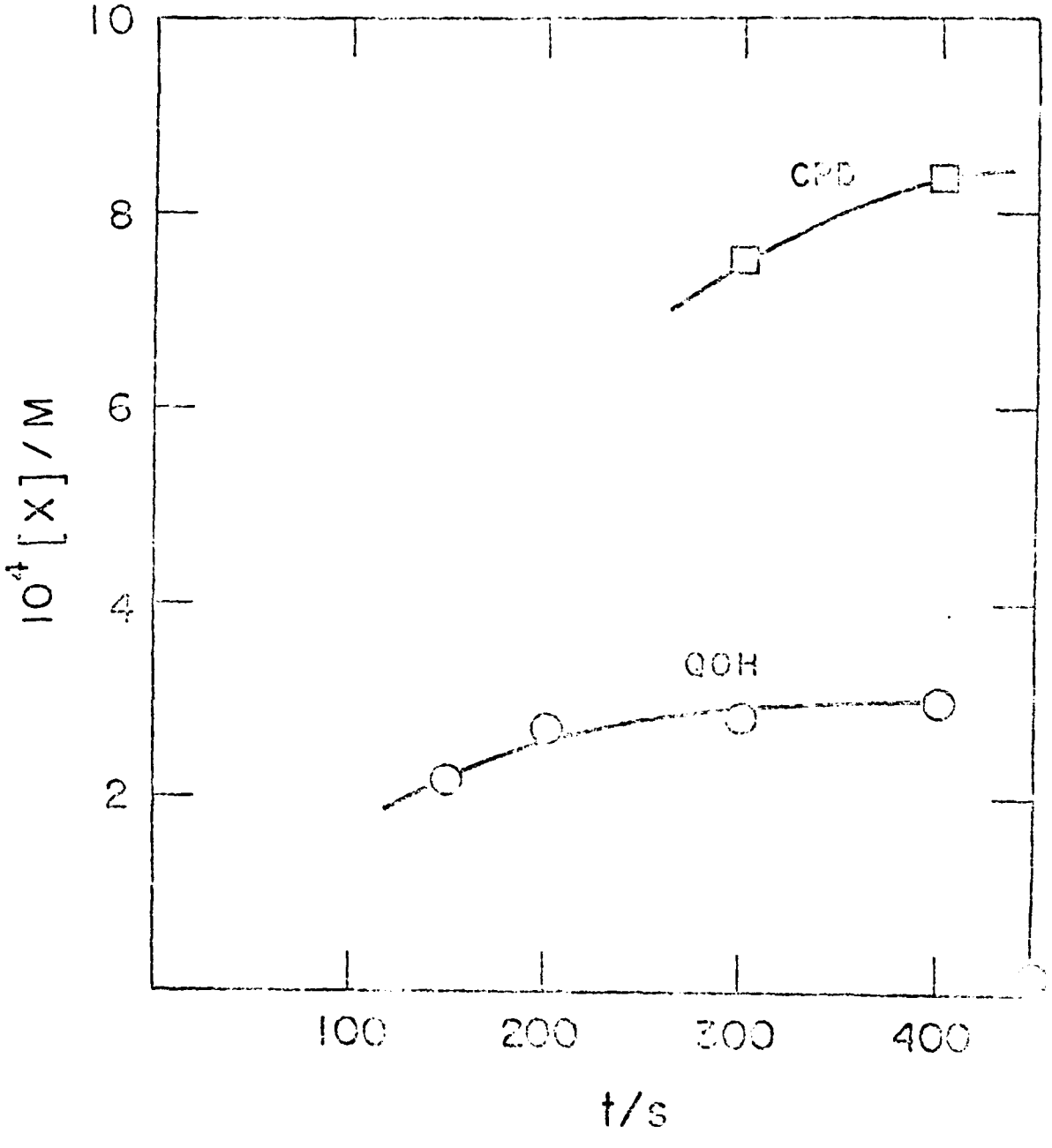

Figure 15. Formation of QOH and CPD upon addition of QOOH into preoxidized DD at 180°C (run 165).

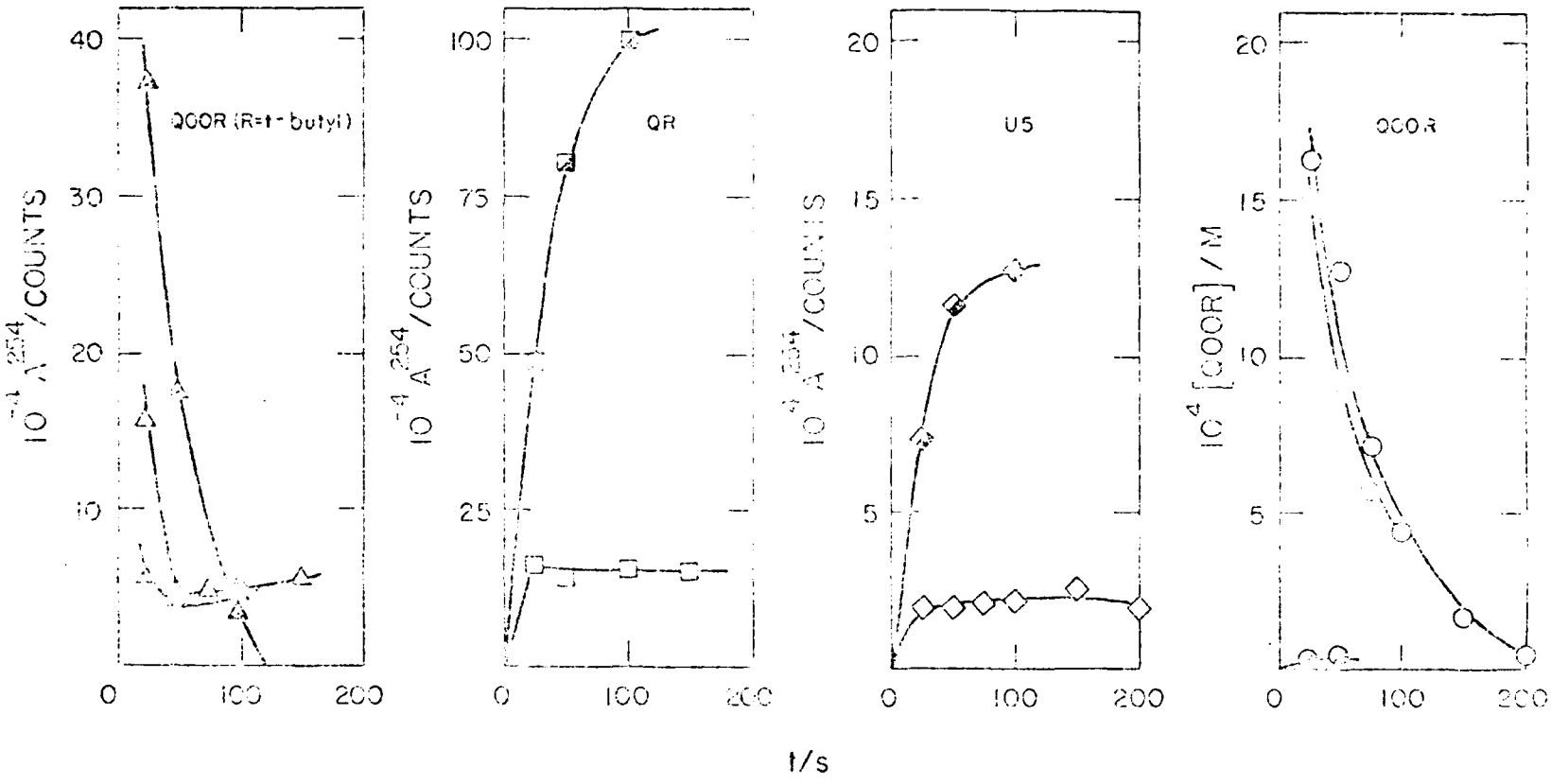

Figure 16. QOOR(tBu) and QOOR decomposition and QR and U5 formation upon addition of QOOR(tBu) into HD at 139°C (open, half-filled and filled points are for runs 159, 160, and 161, respectively).

In agreement with [illegible] function of [illegible] compounds. In the presence of hydroperoxides, preferential abstraction of [illegible] hydroxyl groups and abstraction of hydrogen from RH by the [illegible] leads to increased concentrations of hexahydroperoxy radicals and subsequently to formation of [illegible] (Figure 16) which under these conditions may undergo decomposition to produce OH and HO + HDA + CPD (Figure 17). Formation of HO + [illegible] in presence of added HP is indicative of formation of some Q which could rapidly undergo further conversions without it being detected.

Reactions of QOOH under Conditions of Limited Autoxidation. In order to further investigate reactions of QOOH intermediates in various alkyl substituents, a series of these compounds has been synthesized and their effects on product formation and on rate of initiation have been studied. A list of experiments performed is in Table 4. Results of the investigation are given in our kinetic studies described in Part I of this report.

Mechanistic Implications of Product Studies. A list of our studies of product formation during RH inhibited autoxidation [illegible] of the structures QOOH, and QOOR(HO) on inhibition as described above suggest that in the absence of hydroperoxides the principal mode of QOOH consumption is reaction (7) leading to QO'R and that reaction (8) competes with it only at high hydroperoxide concentrations or in non-preoxidized RH. Assessment of relative importance of these two processes under the [illegible] conditions requires further studies. In the presence of hydroperoxides, reactions of QOOH are key processes which must be understood for determination of stoichiometric factor of HPH at elevated temperatures (cf. Part I of this report).

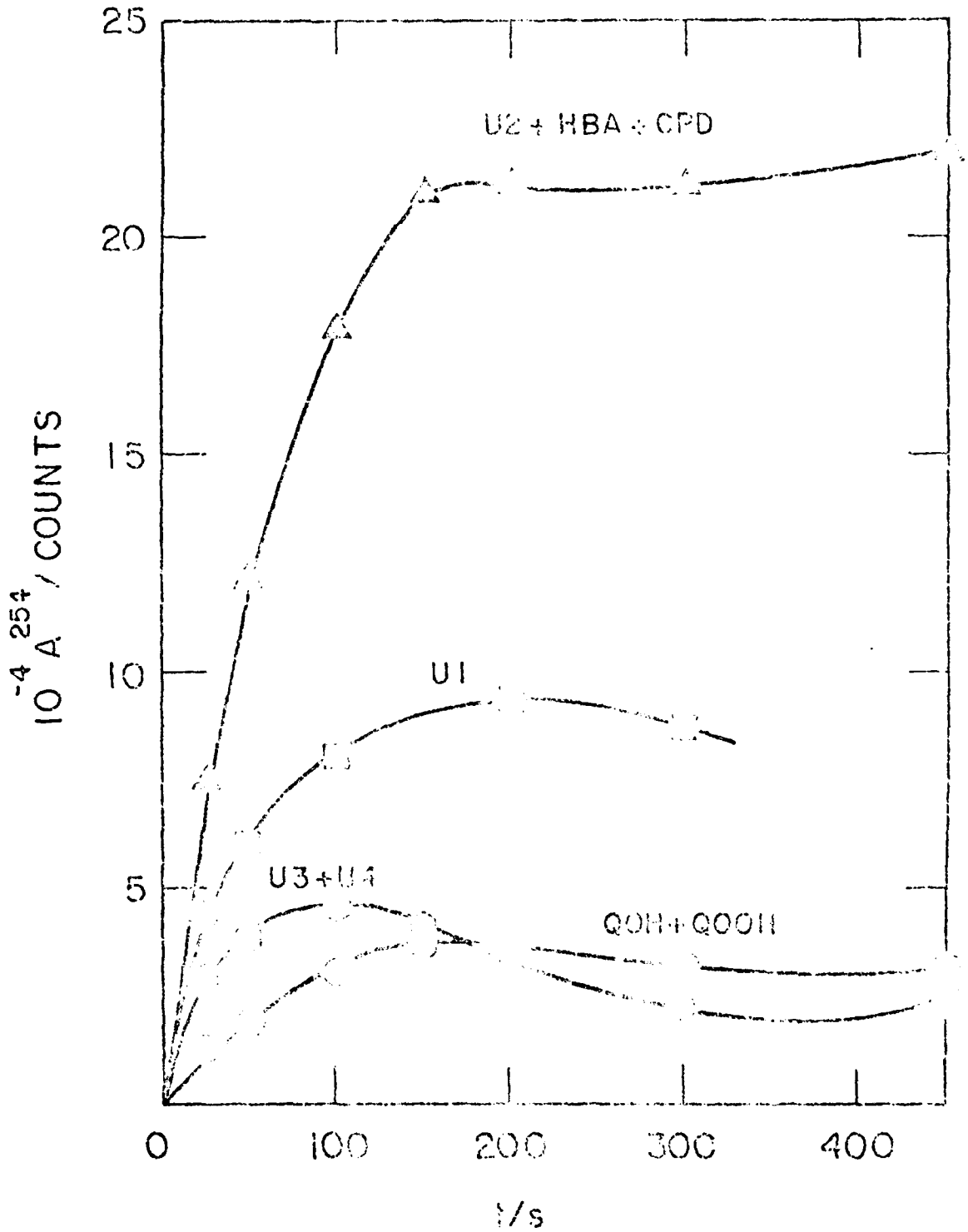

Figure 17. Product formation upon addition of QOOH(tBu) into preoxidized HD at 150°C (run 161).

Table 4

n-HEXADECANE AUTOXIDATION EXPERIMENTS
WITH VARIOUS QOOR COMPOUNDS
ADDED AT 100°C

QOOR Added (R=)	Run #	$10^4[MPH]_o/M$	$10^4[QOOR]_o/M$	$10^4[-OOH]_o/M$
t-butyl-	175	19.64	18.66	108
tetralyl-	144			178
tetralyl-	168	17.50	16.18	108
1-$C_{16}H_{33}$-	169	18.15	~4.6	112
1-$C_{16}H_{33}$-	170	16.27	~8.3	113
2-$C_{16}H_{33}$-	171	18.83	~13.5	107
5-$C_{16}H_{33}$-	176	16.32	~7.1	109
1--8-$C_{16}H_{33}$-	173	~18	~3.9	~1
1--6-$C_{16}H_{33}$-	174	~18	~16.0	~1
1--9-$C_{16}H_{33}$-	172	18.80	~15.5	111
1--8-$C_{16}H_{33}$-	180	21.24	~17.4	241

REFERENCES

(1) Cf. J. Pospisil, Pure Appl. Chem. 54, 2[illegible] (2[illegible]).

(2) J. Kostrova-Kerchova and J. Pospisil, Europ. Polymer J. 13, 975 (1977).

(3) V. A. Reginskii, V. Z. Bulinskii, I. A. Shlyapnikova, and V. B. Miller, Europ. Polymer J. 13, 1013 (1977).

(4) I. Buben and J. Pospisil, Collect. Czech. Chem. Commun. 40, 977 (1975).

(5) I. Buben and J. Pospisil, J. Polymer Sci., Symposium No. 57, 201 (1976).

(6) R. E. Jensen, S. Korcek, L. R. Mahoney, and M. Zinbo, J. Am. Chem. Soc. 101, 7574 (1979).

(7) E. J. Hamilton, Jr., S. Korcek, L. R. Mahoney, and M. Zinbo, Int. J. Chem. Kinet. 12, 577 (1980).

(8) R. E. Jensen, S. Korcek, L. R. Mahoney, and M. Zinbo, J. Am. Chem. Soc. 103, 1742 (1981).

(9) S. Mayzonek, P. D. Klimstra, and R. F. Dallio, J. Org. Chem. 28, 621 (1963).

(10) H. D. Becker, J. Org. Chem. 30, 982 (1965).

(11) M. S. Kharasch and B. S. Joshi, J. Org. Chem. 22, 1435 (1957).

(12) J. Kerchova, L. Matolak, S. Kotcachova, J. Vilem, and J. Pospisil, J. Polymer Sci. Symposium No. 57, 229 (1976).

(13) E. C. Horswill and K. U. Ingold, Can. J. Chem. 44, 263 (1966).

(14) J. T. Wesson and W. H. Smith, Ind. Eng. Chem. 4, 197 (1952).

(15) L. Reich and J. Pospisil, Makromol. Chem. 39, 189 (1977).

(16) I. Buben and J. Pospisil, J. Polymer Sci., Symposium No. 57, 255 (1976).

(17) C. D. Cook, J. Org. Chem. 19, 261 (1954).

(18) K. U. Ingold, Can. J. Chem. 41, 2807 (1963).

(19) R. P. Bauer and G. H. Coppinger, Tetrahedron 19, 1991 (1963).

(20) L. R. Mahoney and M. A. DaRooge, J. Am. Chem. Soc. 96, 5029 (1974).

PART V

REACTIONS OF ALKYLPEROXYCYCLOHEXADIENYL RADICALS [illegible] INHIBITED BY HINDERED PHENOLS AT ELEVATED TEMPERATURES

R. K. Jensen, S. Korcek, L. R. Mahoney, and M. Zinbo

Presented at the Symposium on "Inhibition of Liquid Phase Autoxidation Reactions" organized in the memory of Lee Mahoney by the Division of Organic Chemistry and Division of Petroleum Chemistry, 184th National Meeting of the American Chemical Society, Kansas City, Mo., September 12-17, 1982.

Determination of the absolute rate constants for autoxidation reactions at elevated temperatures requires accurate determination of the rate of initiation as a funciton of hydroperoxide concentration. One method of measuring the rate of initiation is the inhibitor method which is commonly used at low temperatures. In this method, the rate of initiation can be derived from either measuring the initial rate of inhibitor consumption or by measuring the inhibition period providing that the mechanism of radical termination with the antioxidant is known. 2,6-Di-t-butyl-4-methylphenol, DBPH, which is commonly used for this purpose at low temperatures, functions by the mechanism shown in Figure 1. In this case each molecule of antioxidant terminates two radicals and the final product is a peroxycyclohexadienone, QOOP. At elevated temperatures peroxycyclohexadienones are unstable and their decomposition lead to formation of free radicals.

When DBPH is added into an autoxidizing substrate at higher temperatures (Figure 2) it still inhibits the autoxidation reactions as measured by the hydroperoxide concentration which remains constant until the DBPH is completely consumed and only then the autoxidation resumes. The concentration of QOOR during the inhibition period increases but the yields of QOOR are lower than the consumption of DBPH (Figure 3). The shape of the curve for accumulation of QOOR in the system seems to be consistent with QOOR formation from DBPH and its first order decomposition. Also, the increasing rate of DBPH consumption could be due to formation of radicals from QOOR decomposition.

Concentrations of DBPH and QOOR shown in Figure 3 were measured by reversed-

INHIBITION MECHANISM OF MPH AT LOW TEMPERATURES

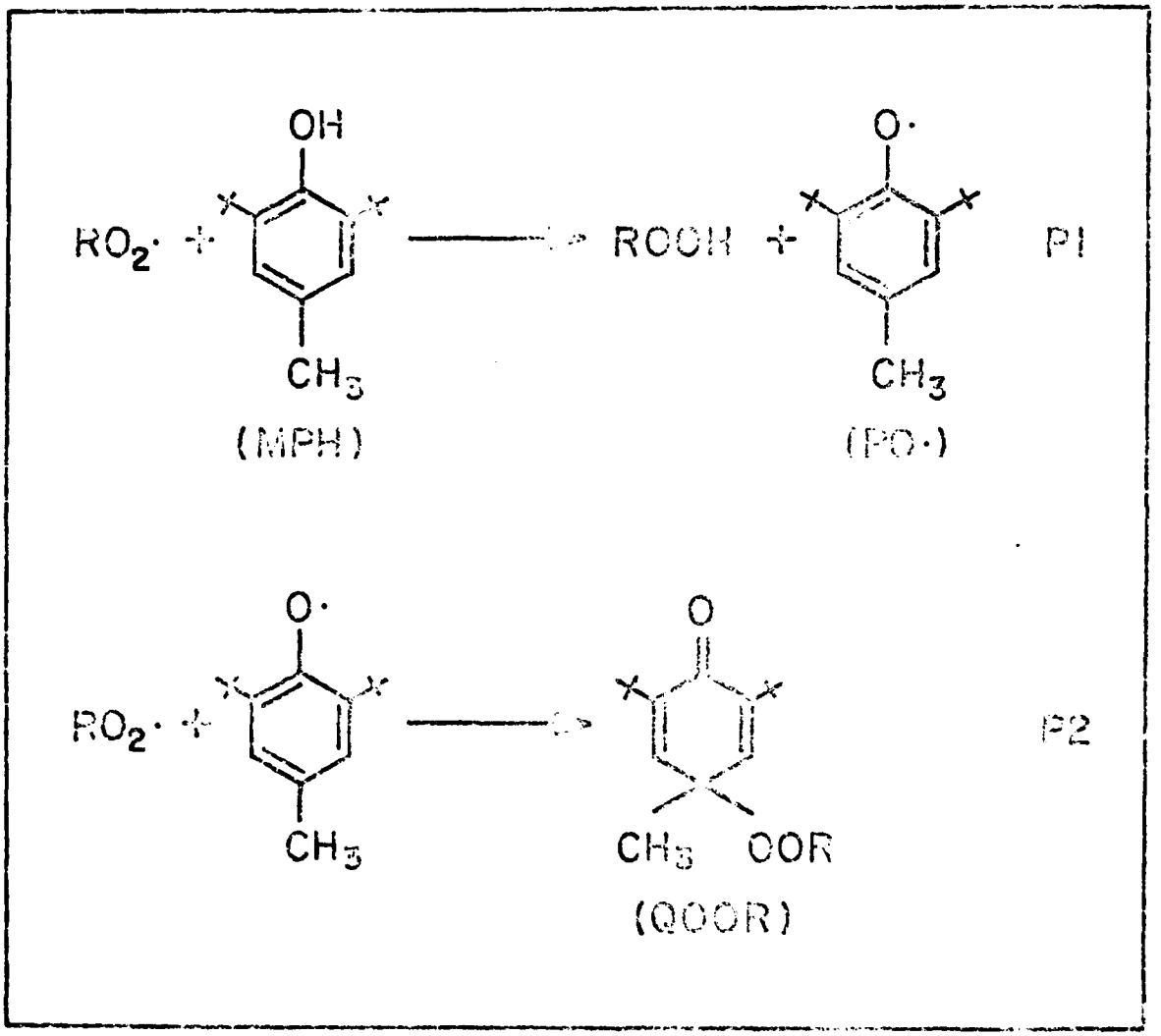

Figure 1 Inhibition mechanism of MPH at low temperatures.

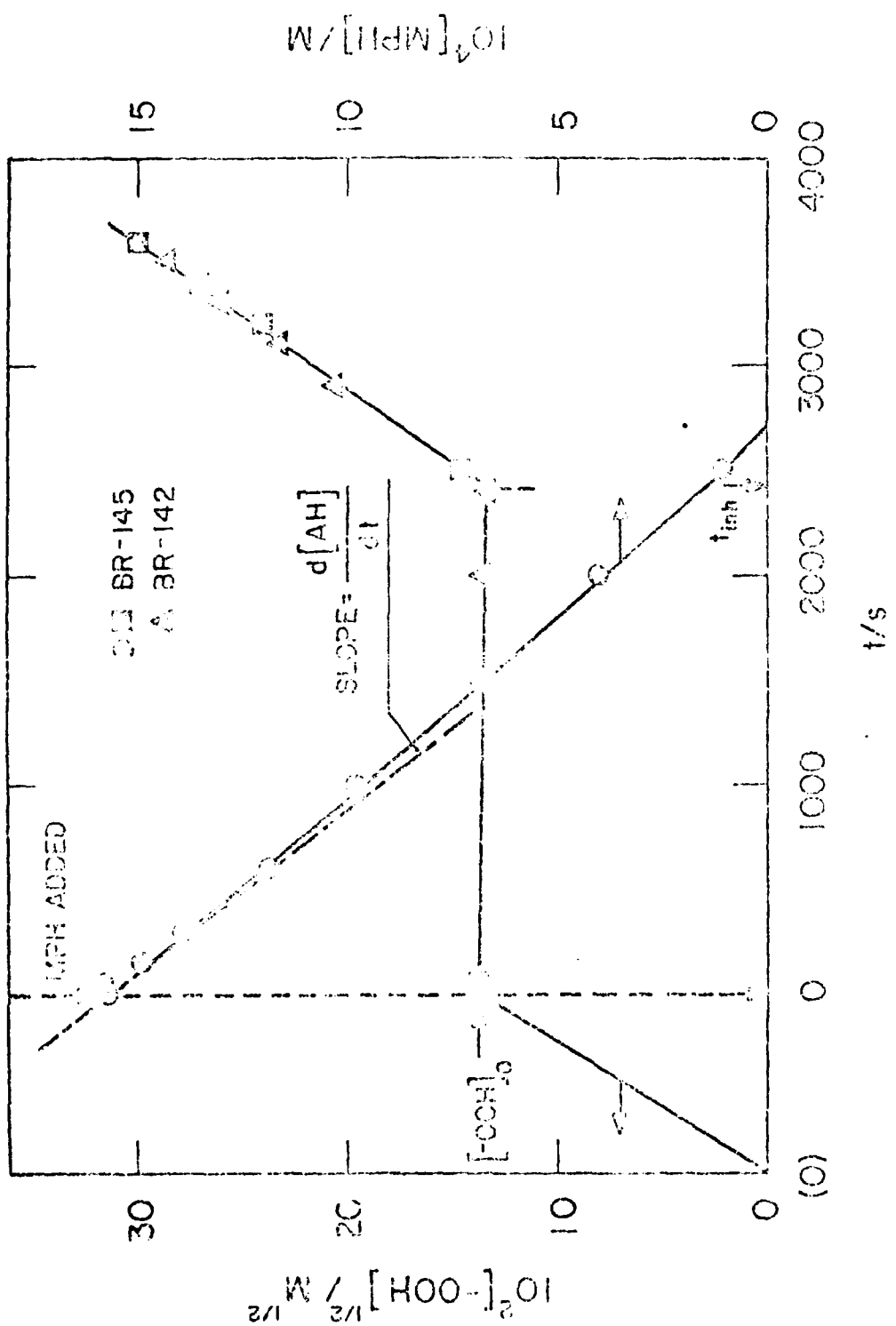

Figure 2 MPH inhibited autoxidation of HD at 150°C: determination of the initial rate of antioxidant consumption and inhibition period.

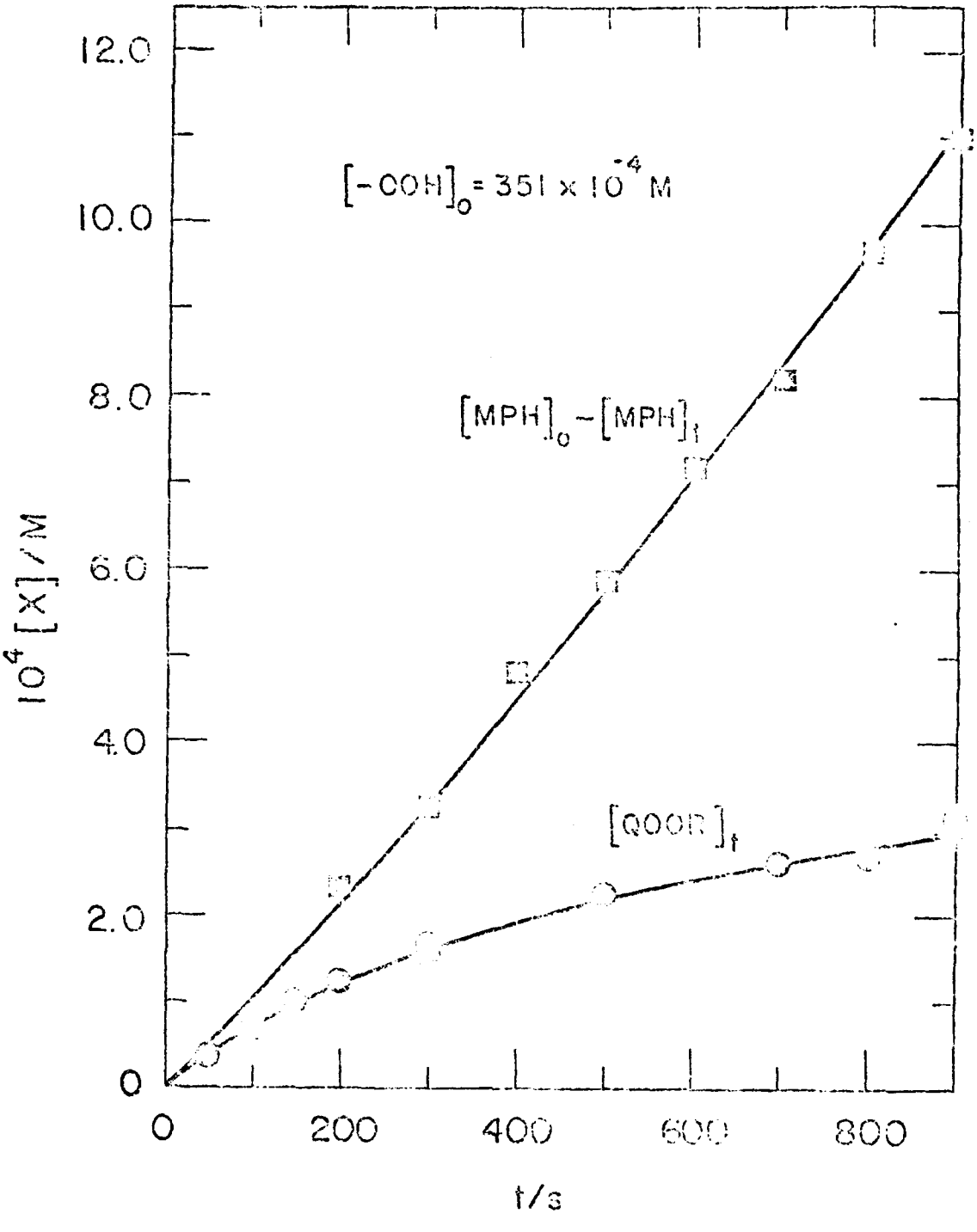

Figure 3 Formation of QOOR and consumption of MPH during MPH inhibited autoxidation of preoxidized n-hexadecane at 130°C.

phase HPLC. This analysis showed that besides QOOH at least ten other inhibition products are being formed under our conditions (Figure 4). From these products we have identified six, which along with QOOR account for only about 60% of MPH reacted. Even with this incomplete product recovery the information obtained combined with the data from the literature allows that a reaction scheme for the mechanism of inhibition by MPH at increased temperatures can be proposed (Figure 5). The first two reactions are the same as those for low temperatures, however, reaction 2 is reversible as we will see later. Reactions 3 and 4 are the molecular and radical decomposition reactions of QOOR which in the latter case effectively reduce the number of radicals terminated. Two other reactions which could be important mainly at low peroxy radical and higher phenoxy radical concentrations are bimolecular reaction of phenoxy radicals and reaction of phenoxy radicals with oxygen. In the case of bimolecular reaction a molecule of MPH is regenerated and the net effect is no reduction in the number of peroxy radicals terminated. Reaction with oxygen would, however, lower the number of radicals terminated. In order to assess the importance of each of these reactions we obtained or synthesized the identified intermediates and products of MPH inhibition and conducted a series of experiments to study their behavior in our reaction system under oxidative and thermal degradation conditions.

We have found that under our conditions QOH and CPO are stable and do not affect the inhibition. Q, as was reported previously,[1] slightly retards oxidation but only a small fraction is reacted at the end of the inhibition periods.

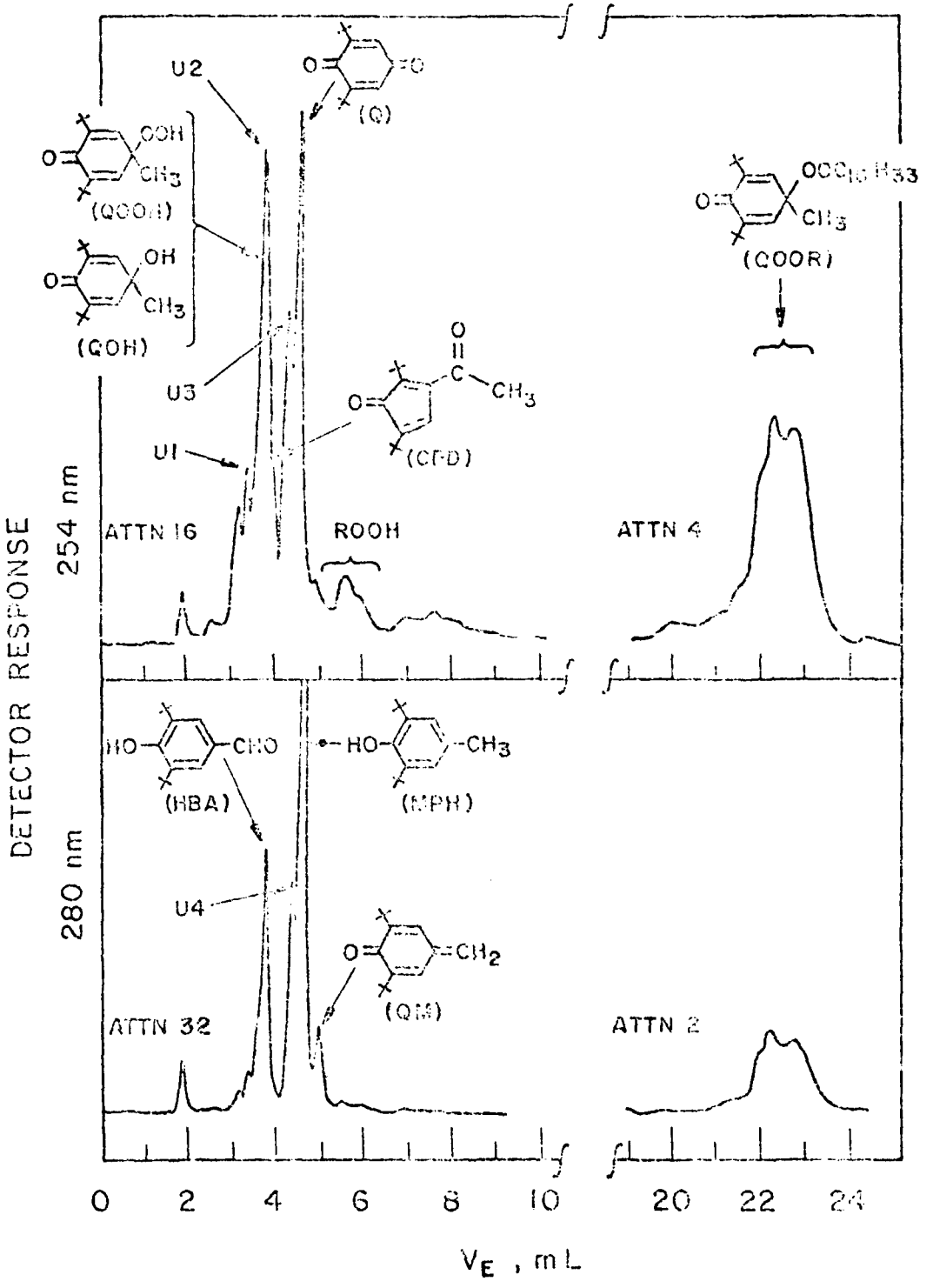

Figure 4. HPLC separation of sample from BPH inhibited autoxidation of peroxidized n-hexadecane at 150°C.

INHIBITION MECHANISM OF MPH AT INCREASED TEMPERATURES

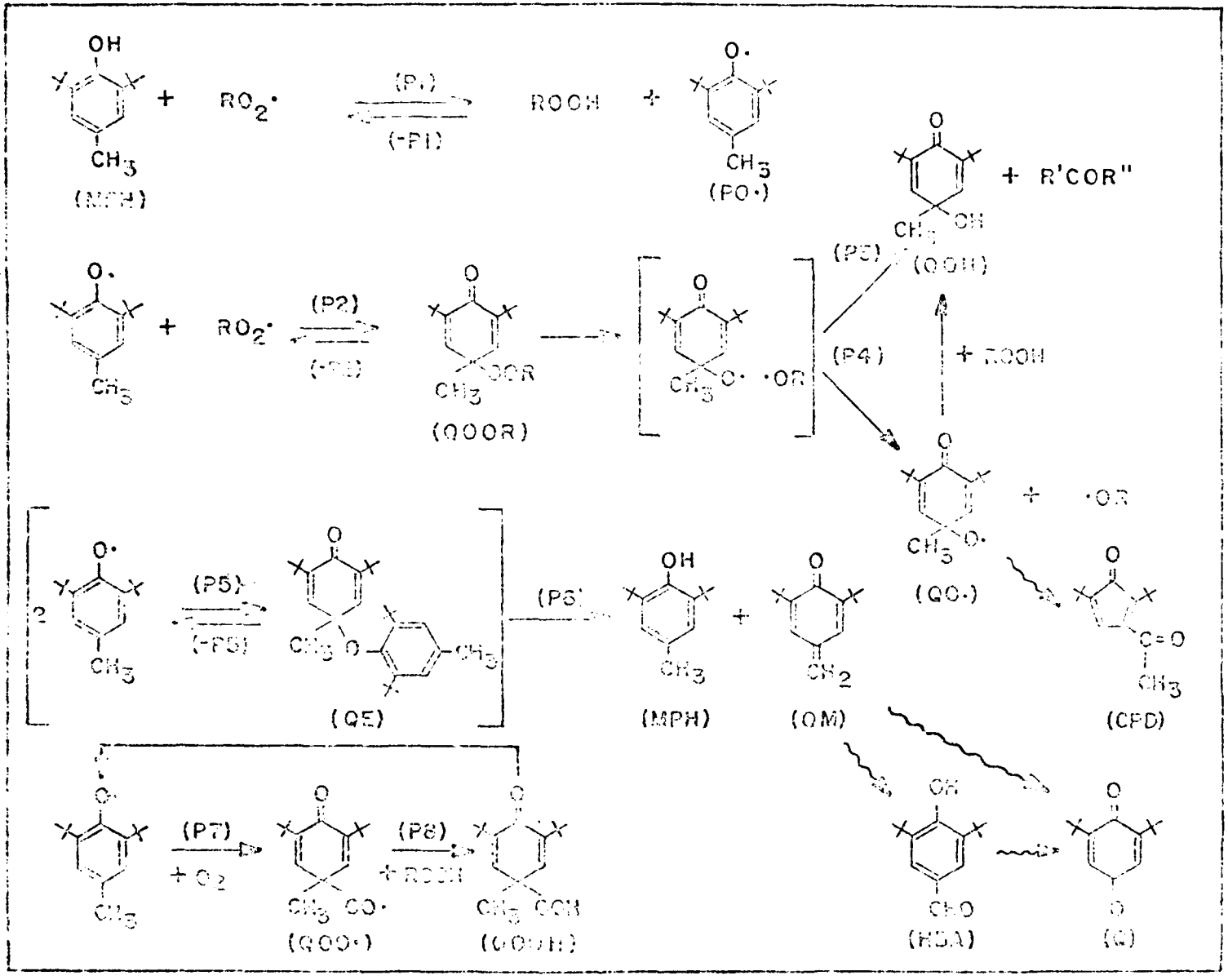

Figure 5. Inhibition mechanism of MPH.

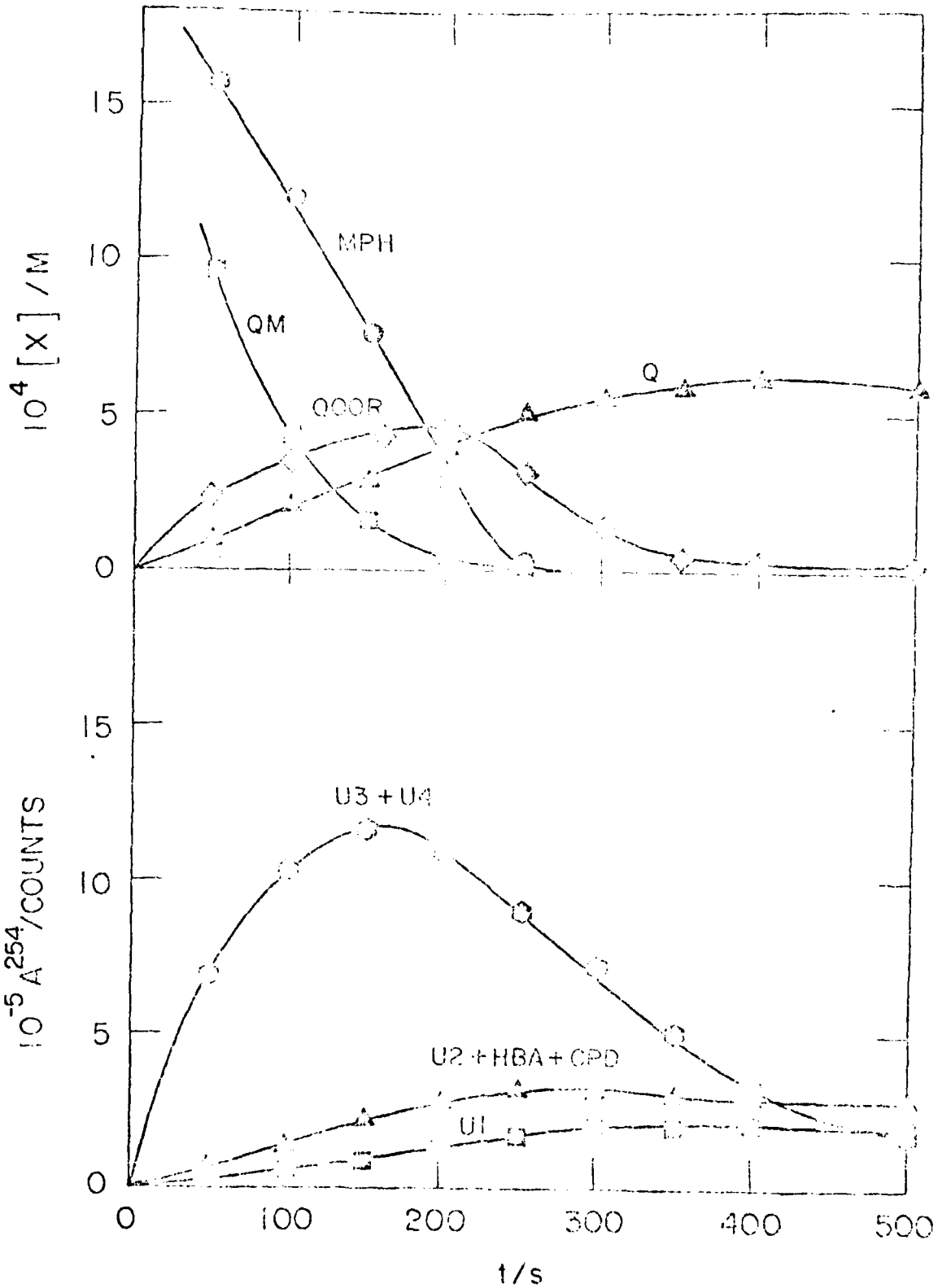

Figure 6 Decay of MPH and formation of prod[illegible]s resulting from addition of [illegible] into preoxygenated n-hexad[illegible]ane at 1[illegible]C (run 1[illegible]).

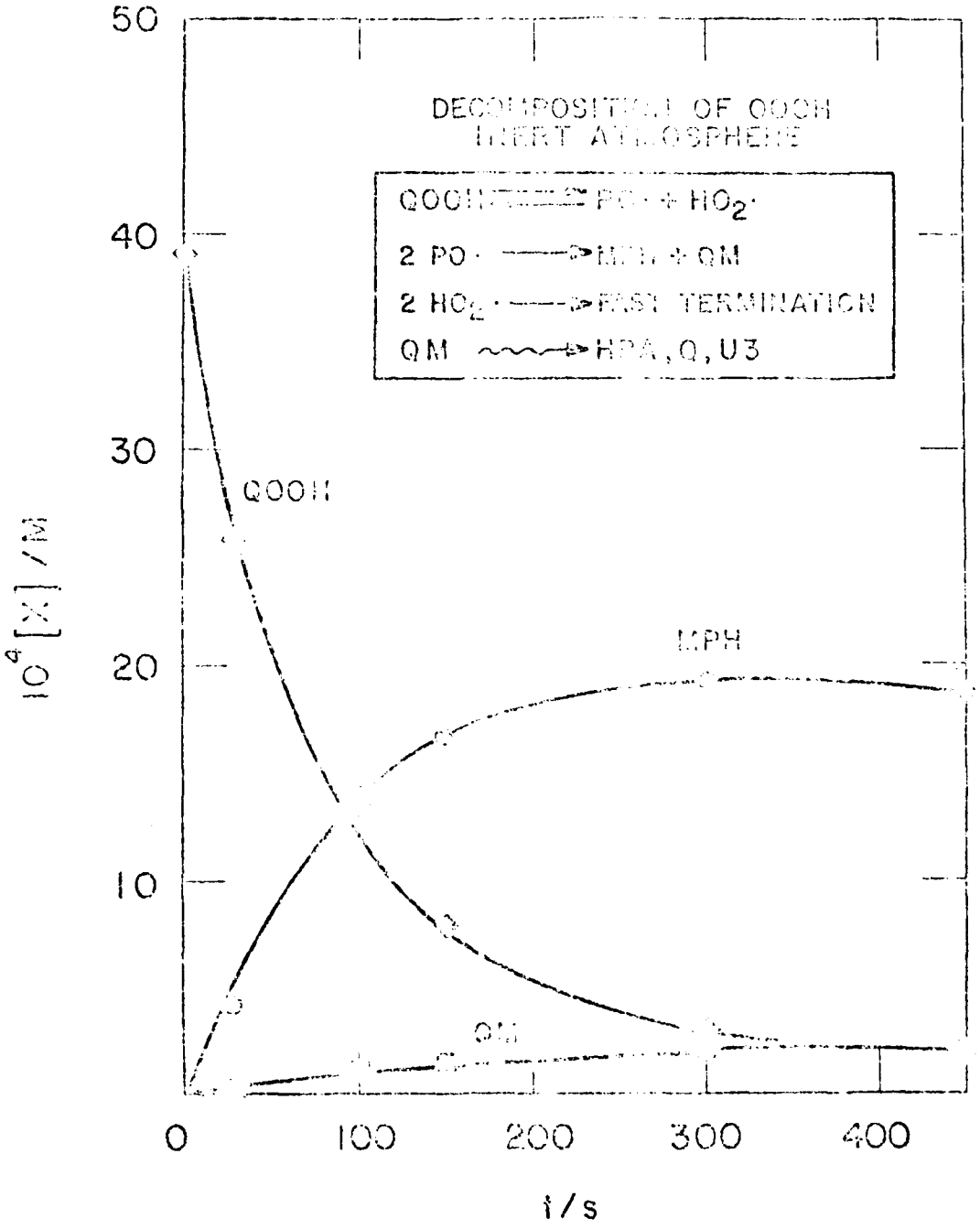

Figure 7 Thermal decomposition of QOOH under an inert atmosphere (Ref. 16).

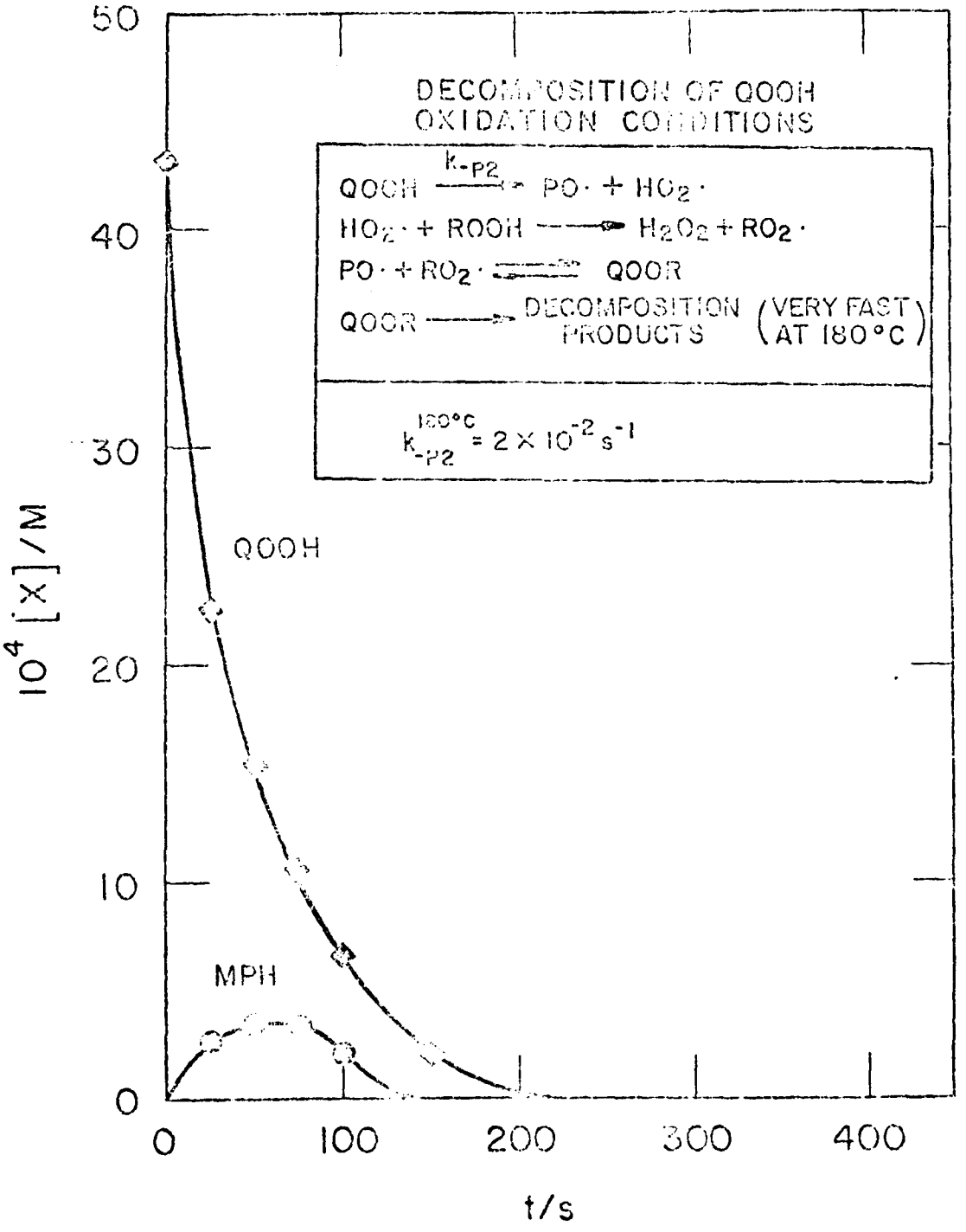

Figure 8 Decomposition of QOOH under oxidizing conditions (Run 166).

alone. When the added peroxy radical was other than hexadecylperoxy we were able to measure not only its decay but also the formation of the corresponding hexadecylperoxy compounds (Figure 9). Addition of t-butyl OOH increased the rate of ROH consumption due to an increase in radical formation from reaction P4. The dashed line in Figure 9 represents the ROH reaction at given hydroperoxide level in the absence of added OOCR. Added t-butyl OOCR decays quite fast and hexadecyl OOH is formed and further decomposed. In this case t-butyl OOCR can decompose via three pathways (Figure 10): i) back reaction -P2, ii) molecular decomposition P3, and iii) radical decomposition P4. Hydrogen abstraction by t-butylperoxy radicals from the relatively large excess of hexadecylhydroperoxides should be fast and should suppress any formation of t-butyl OOH via reaction P2. The sum of the rate constants for all t-butyl OOH decomposition processes can be obtained from the auxiliary plot of t-butyl OOH decay and is equal to 7.9×10^{-3} s^{-1} at 100°C. Kinetic treatment of the data for the tetralylperoxy compound gives a value of 6.3×10^{-3} s^{-1} for the sum of these rate constants.

In the case where the hexadecylperoxy compounds are added (Figure 11) the effects of the decomposition and formation reactions can not be separated. It is, however, anticipated that the sum of the rate constants for 1--6 hexadecyl OOH would be about the same as that for the tetralylperoxy derivative.

Kinetic analyses based on the assumption that dimerization of phenoxy radicals is not significant revealed that the rate constants for the three decomposition processes can be separately determined. The kinetic equation derived for decay of total peroxycyclohexadienones in the cases where t-butylperoxy or

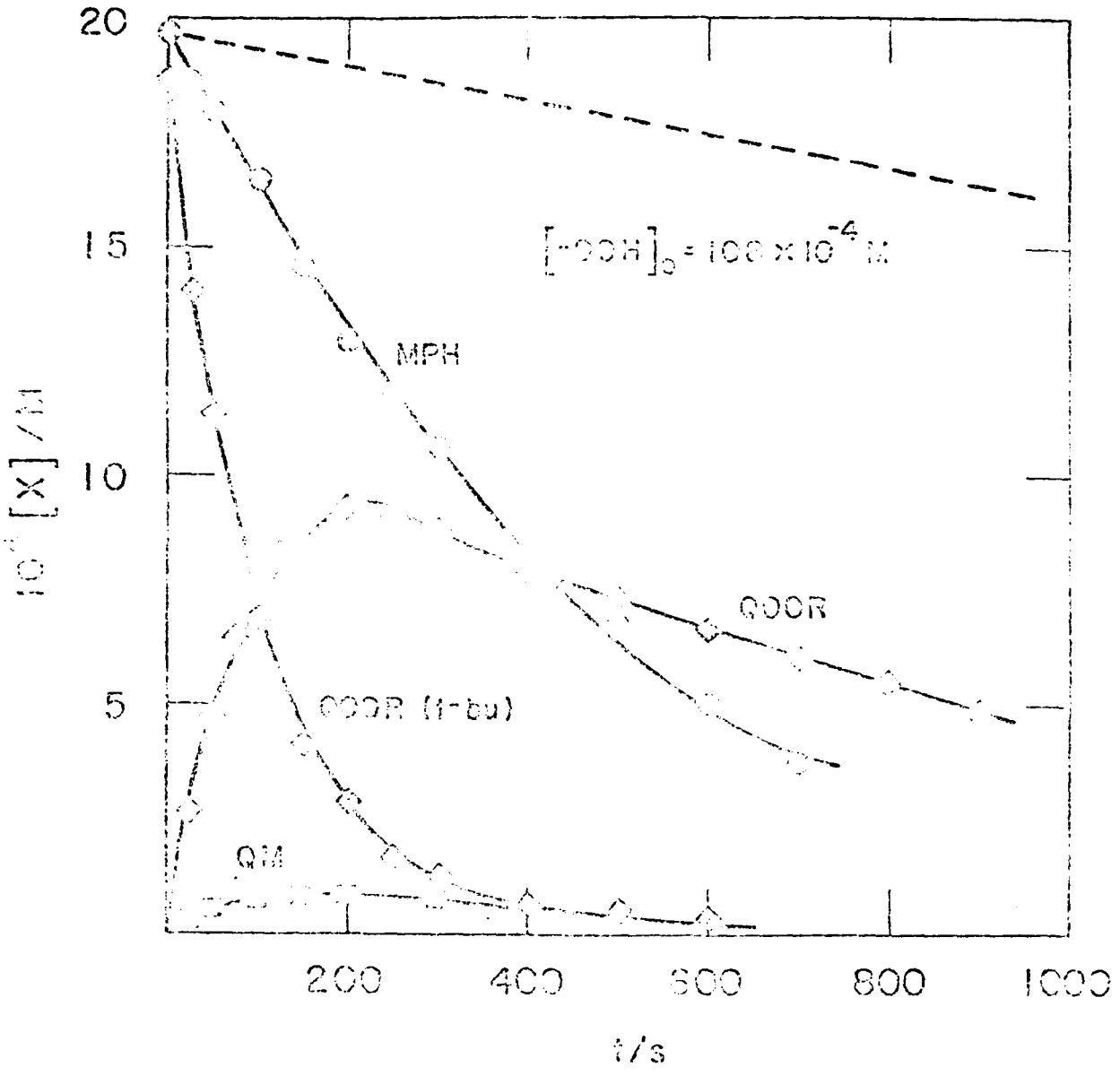

Figure 9. Addition of QOOR(t-butyl) to MPH inhibited autoxidation of precumene [illegible] (Run 128).

QOOR (t-bu)	QOOR(t-bu) $\xrightarrow{k_{-p2}}$ PO· + t-buOO· QOOR(t-bu) $\xrightarrow{k_{p2}}$ MOLECULAR PRODUCTS QOOR(t-bu) $\xrightarrow{k_{p1}}$ OO· + t-buO· t-buOO· + ROOH ⟶ t-buOOH + RO_2· $k_{-p2} + k_{p2} + k_{p1} = 7.5 \times 10^{-3}$ s^{-1}
QOOR (tetralyl)	$k_{-p2} + k_{p2} + k_{p1} = 5.3 \times 10^{-5}$ s^{-1}

Figure 10 Rate constants for QOOR(t-butyl) and QOOR(tetralyl) decomposition at 150°C.

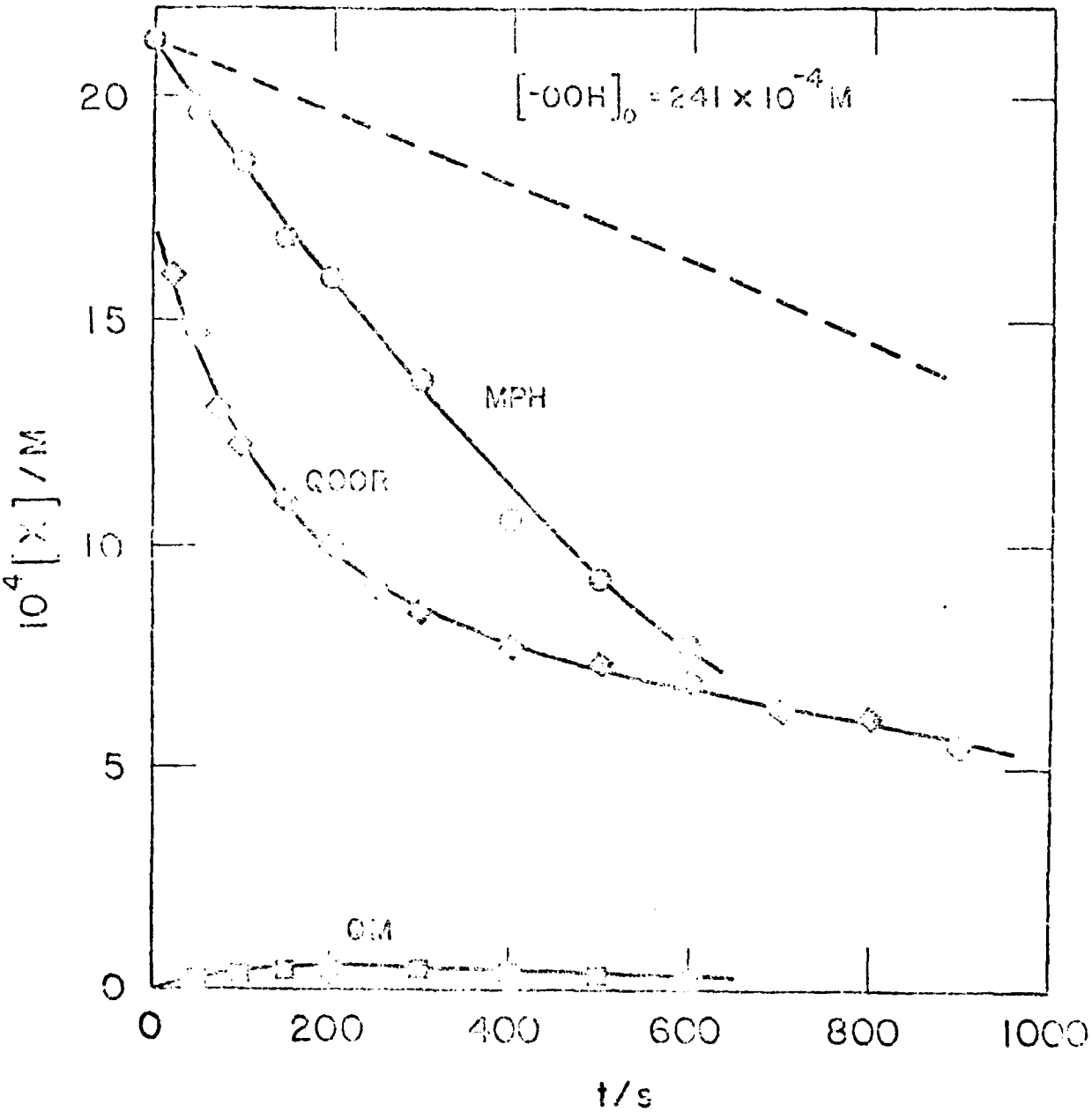

Figure 11 Addition of QOOR(1--8-$C_{16}H_{33}$) to MPH inhibited autoxidation of preoxidized n-hexadecane at 160°C (Run 133).

tetralyl peroxy compounds are added can be used for determination of k_{p3}. Plots consistent with this equation are shown in Figure 13. The linear section corresponds to that portion of the inhibition in which no added peroxy compound is left and therefore the decay represents only that of the hexadecylperoxy compounds. The slope of this line is in both cases equal to 1.35×10^{-3} s^{-1} at 150°C.

Similarly from the equation shown in Figure 13 values of $k_{p3} + k_{p4}$ for hexadecylperoxy compound can be derived. For that purpose the rates were determined graphically and yielded $k_{p3} + k_{p4}$ values of about 3-3.5 $\times 10^{-3}$ s^{-1}. Using the values derived previously then gives k_{p4} equal to about 2×10^{-3} s^{-1} and k_{p3} approximately the same. The values of k_{p3} and k_{p4} obtained here can then be utilized to estimate the amount of HPH consumed due to radical decomposition of ROOH. The shaded area in Figure 14 used earlier represents that portion. The dashed line represents HPH decay due to actual decomposition of hydroperoxides from autoxidation. The rate of initiation obtained from the slope of this line is in good agreement with that determined from termination products. The effective stoichiometric factor for HPH under these conditions is equal to approximately 1.2.

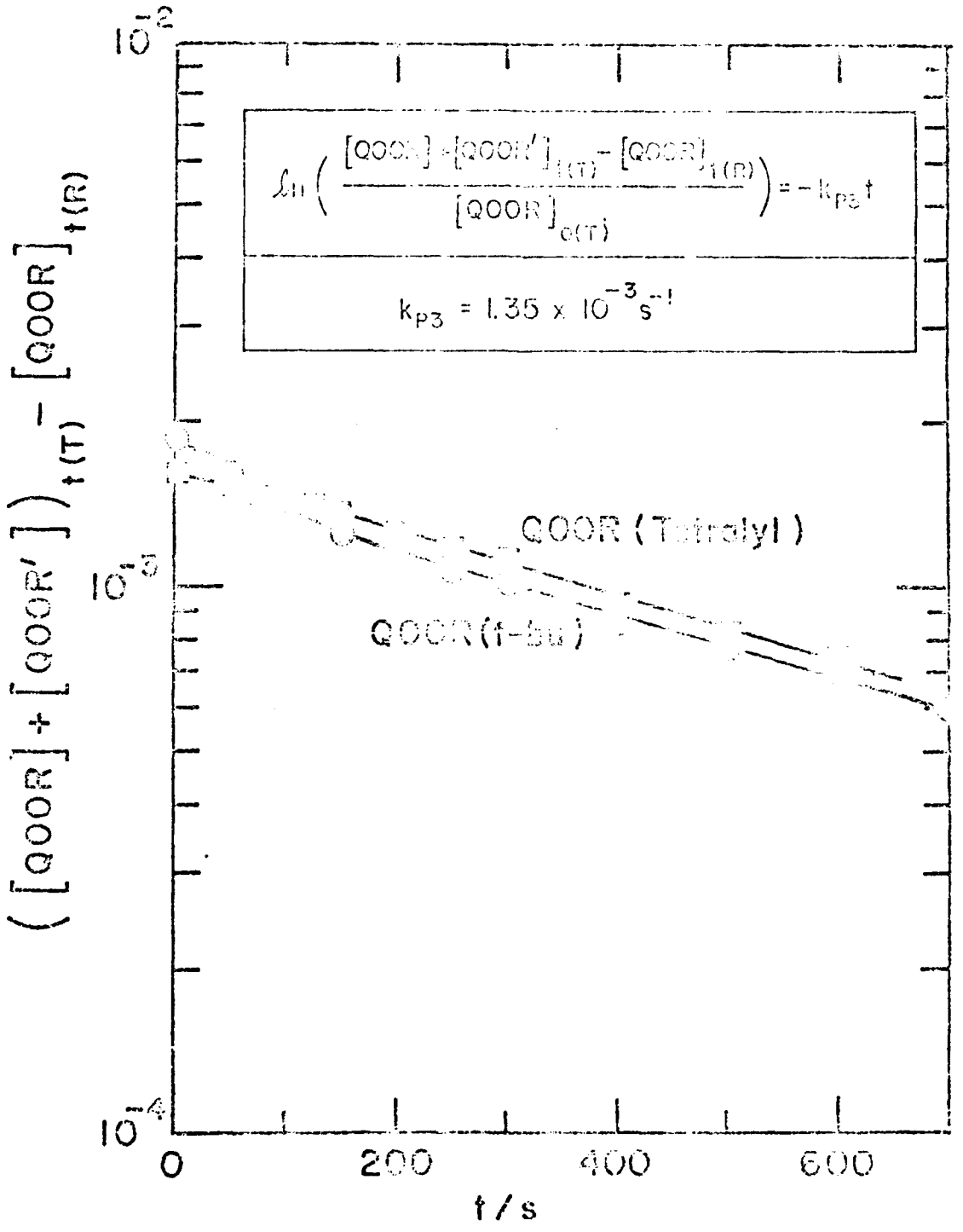

Figure 12 Plots of QOOR(t-butyl) and QOOR(tetralyl) decomposition vs. t at 160°C.

$$-\frac{d[\text{HPH}]}{dt} = \frac{d([\text{QOOR}]+[\text{QOOR}'])}{dt} = (k_{p2}+k_{p3})([\text{QOOR}]+[\text{QOOR}'])$$

$$k_{p3}+k_{p4} = 3-3.5\times10^{-3}\ s^{-1}$$

$$\Big\downarrow\ k_{p3} = 1.33\times10^{-3}\ s^{-1}$$

$$k_{p4} \simeq 2\times10^{-3}\ s^{-1}$$

$$\Big\downarrow\ k_{p2}+k_{p3}+k_{p4} \simeq 3.3\times10^{-3}\ s^{-1}$$

$$k_{-p2} \simeq 2\times10^{-3}\ s^{-1}$$

Figure 13 Rate constants for QOOR decomposition at 160°C.

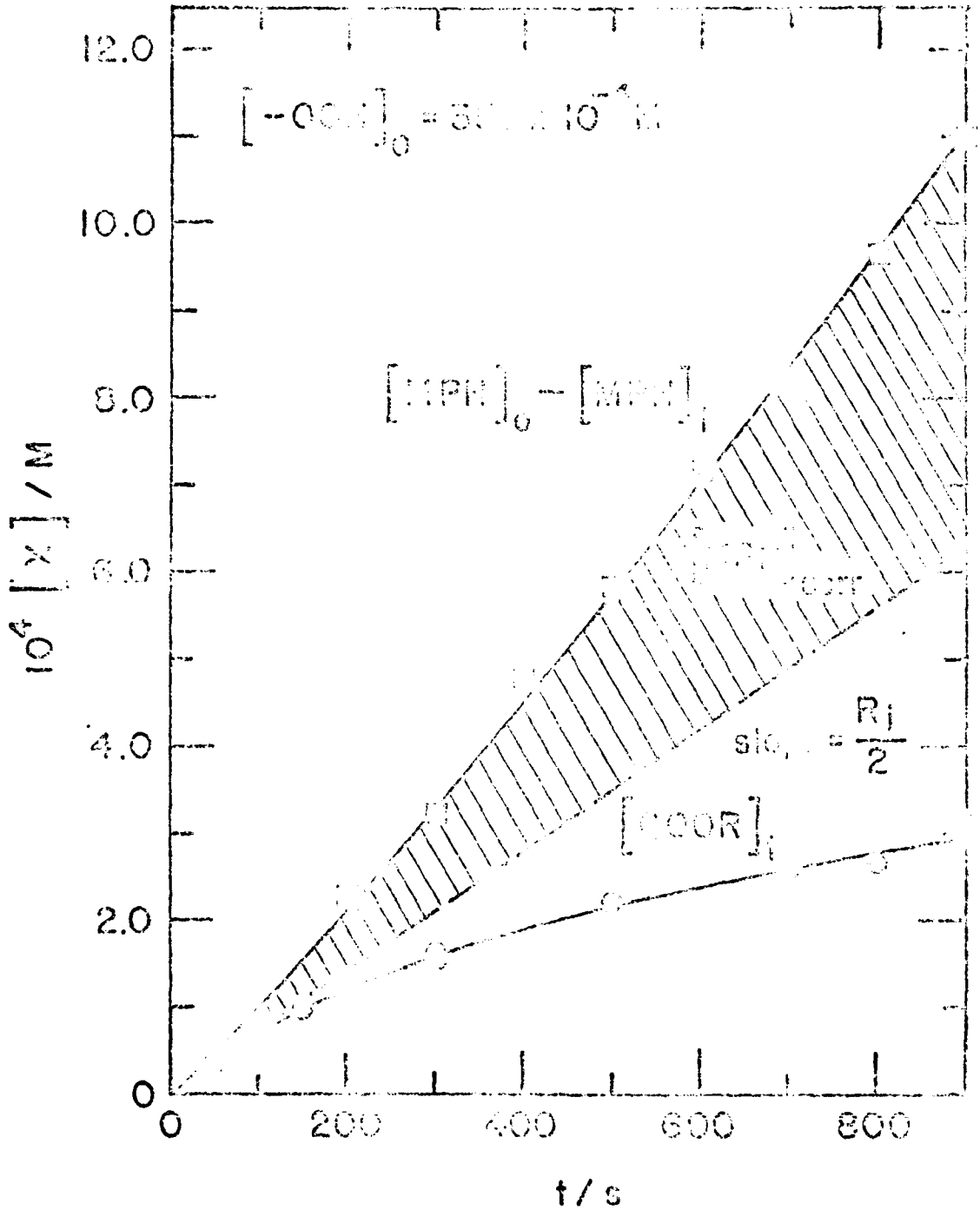

Figure 14 Consumption of HPN shown in Figure 1 corrected for HPN decay due to radical decomposition of MPH.

REFERENCES

(1) [illegible] Duben and J. Pospíšil, J. Polym. Sci. Symposium No. 44, 261 (1974).

(2) H. D. Becker, J. Org. Chem. 32, [illegible] (1967).

(3) R. H. Bauer and C. M. Cuppinger, Intersociety [illegible] 12, 1201 (1963).

PART VI

HIGH PERFORMANCE LIQUID CHROMATOGRAPHIC DETERMINATION OF HYDROPEROXIDIC PRODUCTS FORMED IN THE AUTOXIDATION OF n-HEXADECANE AT ELEVATED TEMPERATURES

R. K. Jensen, M. Zinbo, and S. Korcek

Introduction

Primary reaction products formed in the autoxidation of n-alkanes at elevated temperatures (120-180°C) include i) series of isomeric hydroperoxides, hydroperoxyketones, and dihydroperoxides, which are major products and originate from inter- and intramolecular hydrogen abstraction reactions of peroxy radicals, and ii) isomeric ketones and alcohols, which originate from termination reactions of peroxy radicals and are formed in minor amounts (1). Analysis of these primary products requires a complex sequence of analytical procedures (1,2). Due to the thermal instability of the hydroperoxidic products, these procedures involve selective reductions prior to gas chromatographic analysis of the corresponding reduction products. Also, at low conversions, enrichment of the reaction products is needed prior to analysis (1).

High performance liquid chromatography (HPLC) can be used for direct analysis of thermally unstable products without sample pretreatment. Recently, this technique has been applied to analysis of low molecular weight peroxides (3) and alkylhydroperoxides (4) using UV detection at 220-225 nm, of tert-butylhydroperoxide using amperometric detection (5), and of hydroperoxides of fatty acids (6-8) with UV detection based on the conjugated double bond absorption at 235 nm.

This paper describes procedures for direct determination of isomeric hexadecylhydroperoxides, hydroperoxyhexadecanones, and hexadecanedihydroperoxides derived from the autoxidation of n-hexadecane at 120-180°C using normal and reverse-phase HPLC with UV detection at 254 nm.

Experimental

Reagents and Standards

All of the standards used were commercial products except the 1-, 2-, and 5-hexadecylhydroperoxides which were synthesized as described previously (1). Solvents used for HPLC were distilled-in-glass grade from Burdick and Jackson Laboratories. Autoxidized n-hexadecane was prepared at conversions of 0.1-2.3 percent using a stirred-flow microreactor (1).

Apparatus

A Waters HPLC system consisting of Model 6000 solvent delivery pump, U6K septumless injector, R401 refractive index detector, and 440 UV-VIS detector was used for all of the analyses. Peak areas were determined using two Hewlett-Packard Model 3380A integrators and a cut and weigh procedure where necessary. In all HPLC analyses Waters Radial-PAK C18 or Si cartridges (5 and 10μ, 8mm x 10 cm) were used.

Methods

HPLC analyses were carried out using the following procedures: 1) isocratic normal-phase HPLC with Radial-PAK Si cartridges and a binary mobile phase consisting of methanol and hexane (0.3:99.7), Procedure 1; 2) isocratic reverse-phase HPLC with Radial-PAK C18 cartridges and a ternary mobile phase consisting of water, methylene chloride, and acetonitrile (5:10:85), Procedure 2; and 3) isocratic reverse-phase HPLC similar to Procedure 2 but with a binary mobile phase consisting of water and acetonitrile (15:85), Procedure 3.

In each of the above procedures the effluent flow was 1 mL/min and UV detection was performed at 254 nm. Sample volumes injected were 10 to 25 μL depending on the concentration of oxidation products.

The procedure for fractionation of autoxidized n-hexadecane involved placing 5 mL of autoxidized n-hexadecane on a SEP-PAK silica cartridge and eluting with two 10 mL portions of hexane (Fractions 1 and 2) followed by seven 5 mL portions of 1% methanol in hexane (Fractions 3 through 9).

Gas chromatographic (GC) analysis of triphenylphosphine reduced hydroperoxidic products from n-hexadecane autoxidation has been described previously (1). In this analysis isomeric hexadecylhydroperoxides are determined as corresponding hexadecanols, hexadecanedihydroperoxides as corresponding diols, and hydroperoxyhexadecanones as dehydration products of the corresponding hydroxyhexadecanones.

Triphenylphosphine reductions and measurement of total hydroperoxide concentrations ([-OOH]) were carried out by procedures described previously (1).

Results and Discussion

Preliminary analyses were performed using a Waters μBondapak C18 stainless steel column (3.9 mm x 30 cm). In these studies, the maximum injection volume was limited to 5 μL of oxidized n-hexadecane since with larger injection volumes severe peak broadening occurred. Thus, only samples containing higher hydroperoxide concentrations could be analyzed or preconcentration of hydroperoxides in the samples by silica column chromatography was needed. With the Radial-PAK cartridges samples of up to 25 μL could be injected without appreciable peak broadening. This larger capacity is probably due to the larger internal diameter of the cartridges and possibly the difference in packing materials.

A typical chromatogram of autoxidized n-hexadecane obtained using normal-phase HPLC, Procedure 1, is in Figure 1. Under these HPLC conditions, the isomeric hexadecylhydroperoxides as well as the series of 2-alkanones (major cleavage products) can be separated and the former can be quantitatively determined. The hydroperoxyhexadecanones and hexadecanedihydroperoxides, however, are not eluted under these conditions.

In order to elute the hydroperoxyhexadecanones and hexadecanedihydroperoxides reverse-phase HPLC, Procedure 2, was utilized. The ternary solvent system used in this procedure was selected to satisfy the diverse needs of separation of the hydroperoxy compounds and elution of unreacted n-hexadecane in a reasonable time (less than 45 minutes). Under these HPLC conditions quantitative analysis of the isomeric hexadecylhydroperoxides as well as semi-quantitative analysis of isomeric hydroperoxyhexadecanones and hexadecanedihydroperoxides can be accomplished. A typical chromatogram from this analysis is in Figure 2.

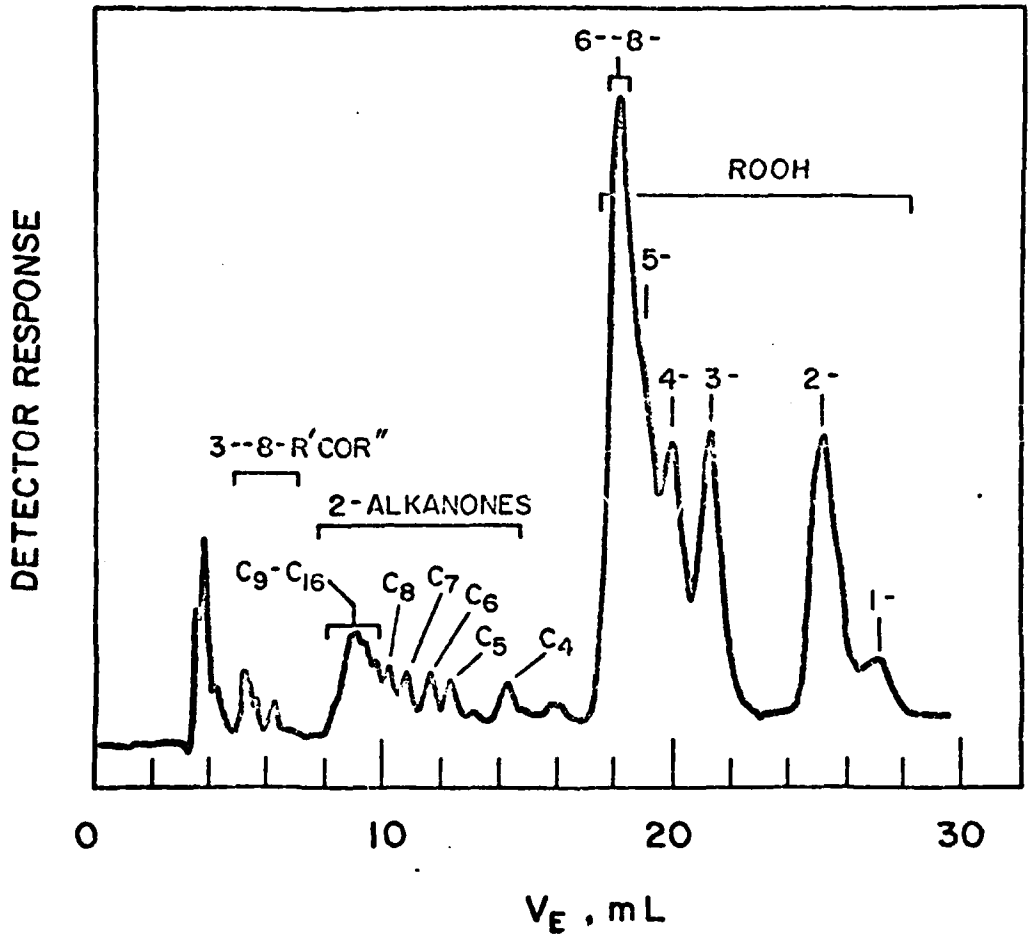

Figure 1 HPLC separation of an autoxidized n-hexadecane sample ([-OOH] = 6.31 x 10^{-2}M) obtained using HPLC Procedure 1 (ROOH - hexadecylhydroperoxides; R'COR'' - Hexadecanones).

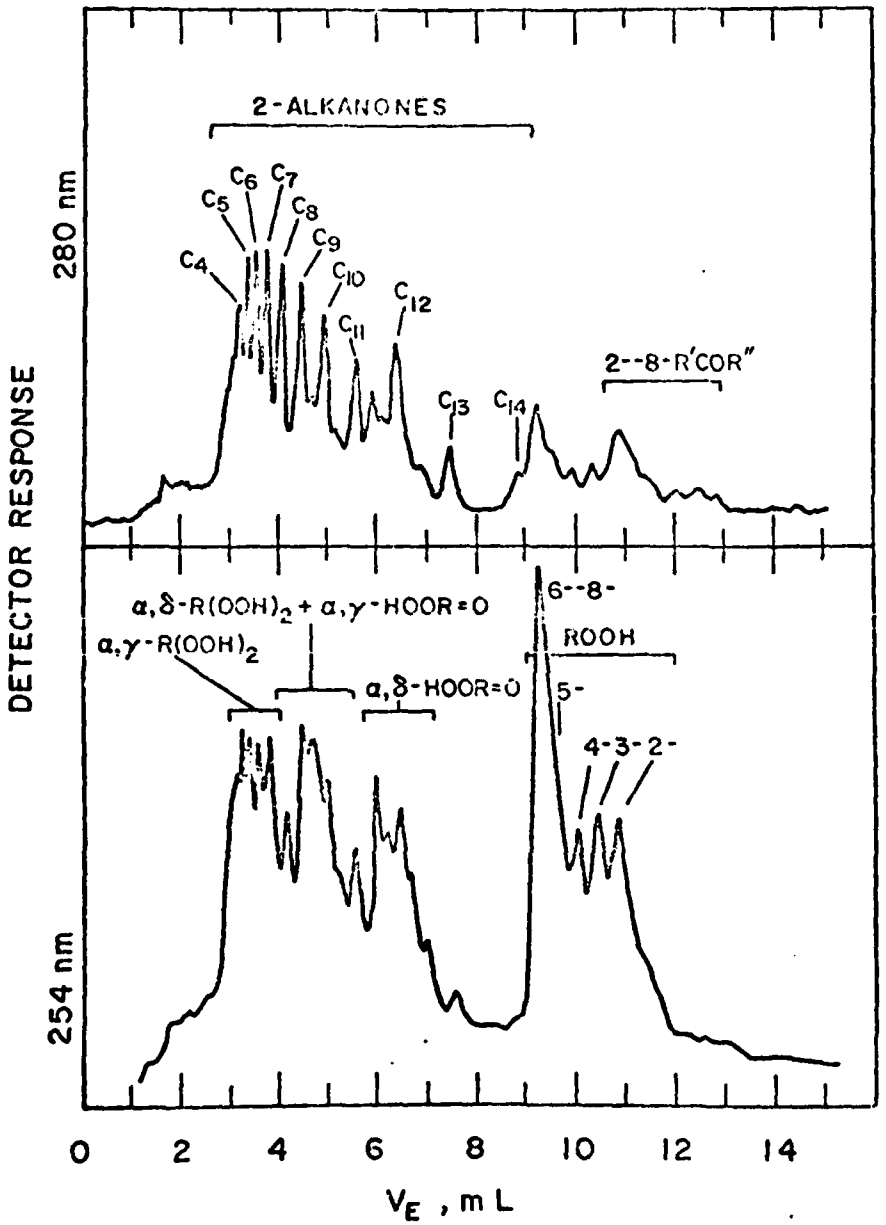

Figure 2 HPLC separation of an autoxidized n-hexadecane sample ([-OOH] = 6.31 x 10^{-2}M) obtained using HPLC Procedure 2(ROOH - hexadecylhydroperoxides; R'COR'' - hexadecanones; HOOR=O - hydroperoxyhexadecanones; $R(OOH)_2$ - hexadecanedihydroperoxides).

The assignments of peaks for 1-, 2-, and 5-hexadecylhydroperoxides and 2-alkanones in Figures 1 and 2 are based on the retention volumes of standards. Confirmation of the peak assignments for 1-, 2-, and 5-hexadecylhydroperoxides was made by mixing each standard with an oxidized n-hexadecane sample and then analyzing the mixtures by Procedures 1 and 2. Peak assignments for the other isomeric hexadecylhydroperoxides are made by analogy. Assignments of the groups of peaks for isomeric hydroperoxyhexadecanones and hexadecanedihydroperoxides in Figure 2 are based on the results of GC analyses of reduced chromatographic fractions of autoxidized n-hexadecane as described below.

The relative hexadecylhydroperoxide (ROOH) isomer distribution obtained from semi-quantitative HPLC analyses of the autoxidized n-hexadecane has been found to be similar to that obtained from GC analyses of corresponding alcohols (ROH) after reduction (Table I).

Calibration for quantitative determination of isomeric hexadecylhydroperoxides by HPLC was based on the results of GC analyses since hexadecylhydroperoxide standards were not available in sufficient purity to permit their use for this purpose. Results of this comparative calibration for determination of total hexadecylhydroperoxides are shown in Figure 3 where the sum of hydroperoxide peak areas divided by injection volume, A_{HPLC}, of an autoxidized sample are plotted versus the known total concentration of hydroperoxides, [ROOH], determined by the GC method (1). Regression analysis of this data gives a linear relationship with a coefficient of correlation of 0.998.

Analytical standards for determination of isomeric hydroperoxyhexadecanones and hexadecanedihydroperoxides are not available. In order to identify the peaks corresponding to these compounds a series of samples containing different

TABLE I. Isomer Distribution of Hexadecylhydroperoxides by GC and HPLC.

ISOMER	% of ROH by GC	% of ROOH by HPLC
1-	4.4	4.1
2-	19.7	18.5
3-	75.9	17.0
4-		12.9 } 77.5
5--8-		47.6

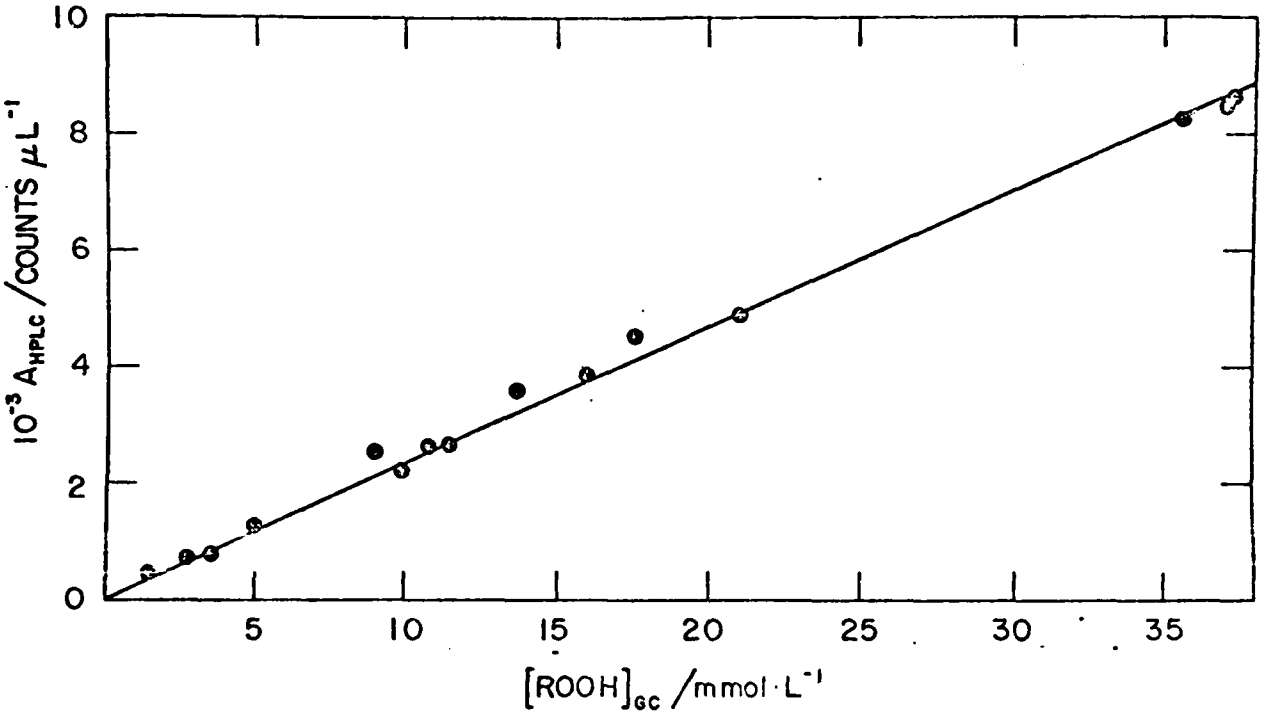

Figure 3 Calibration plot for isomeric hexadecylhydroperoxides (ROOH): relative integrated HPLC (Procedure 2) peak area per µL of sample volume, A_{HPLC}, versus $[ROOH]_{GC}$ determined by GC.

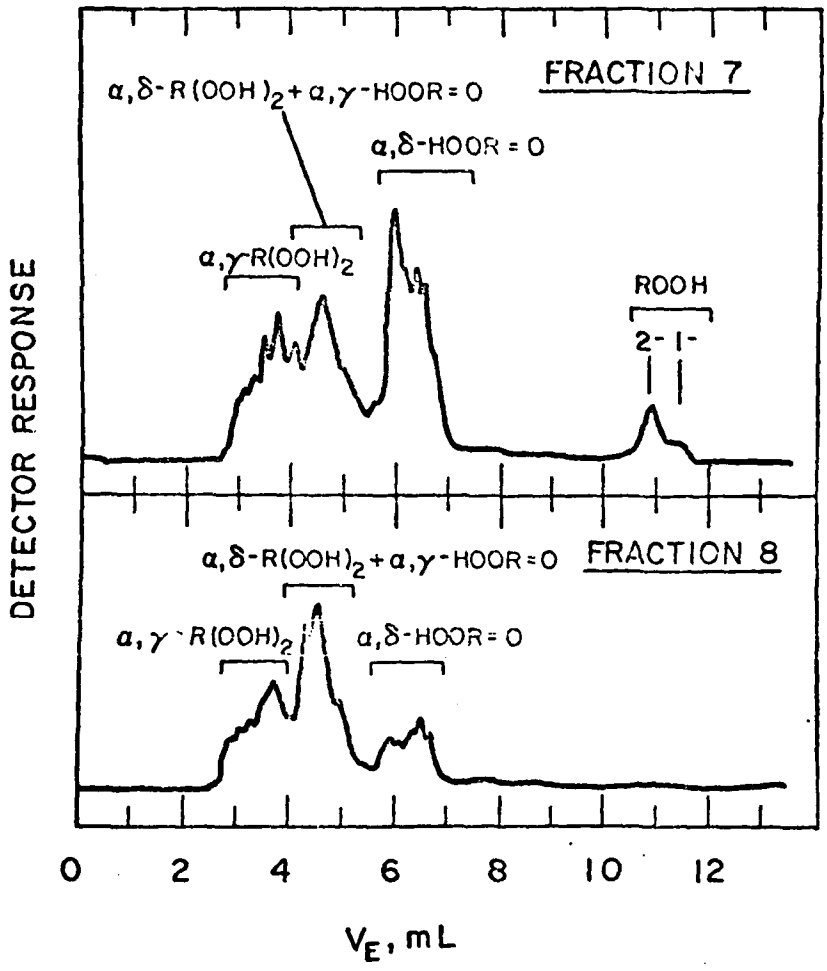

Figure 4 HPLC separation of chromatographic fractions 7 and 8 using Procedure 2(ROOH - hexadecylhydroperoxides; HOOR=O - hydroperoxyhexadecanones; $R(OOH)_2$ - hexadecanedihydroperoxides).

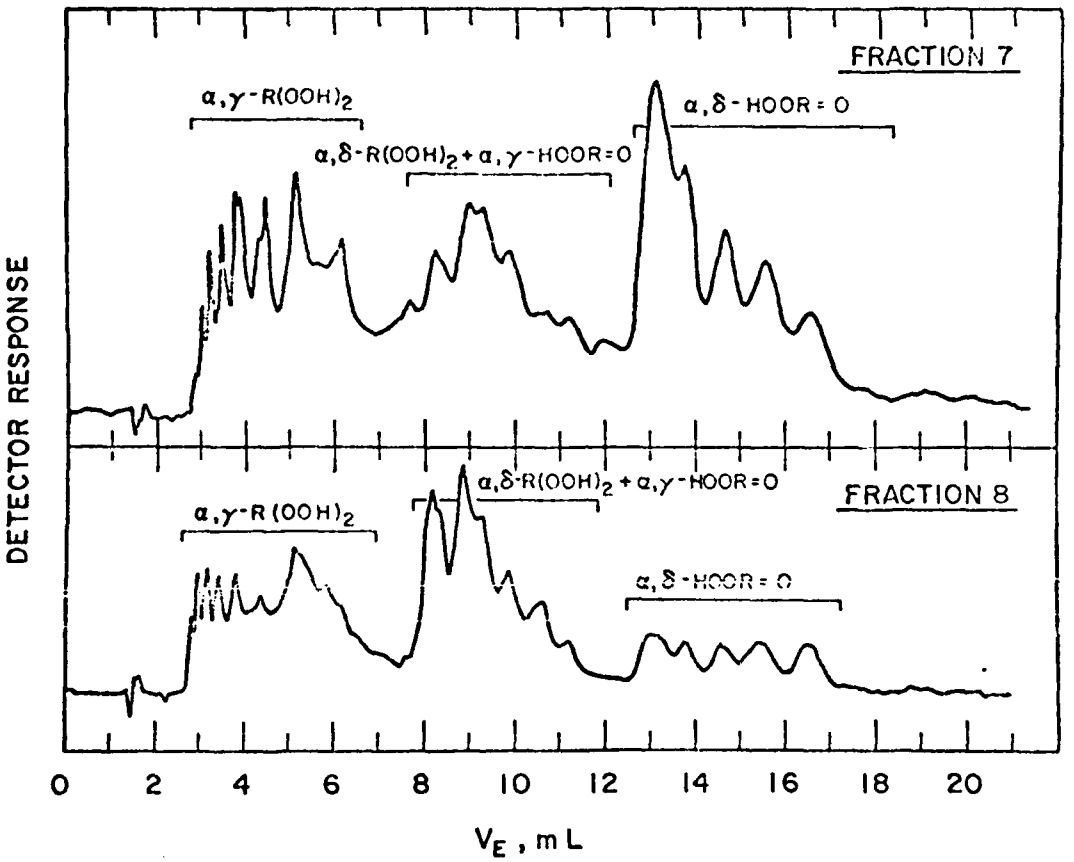

Figure 5 HPLC separation of chromatographic fractions 7 and 8 using Procedure 3 (HOOR=O - hydroperoxyhexadecanones; $R(OOH)_2$ - hexadecanedihydroperoxides).

relative amounts of isomeric hydroperoxyhexadecanones and hexadecanedihydroperoxides were prepared by fractionation of autoxidized n-hexadecane using a silica SEP-PAK cartridge. These samples were analyzed by HPLC Procedure 3 and after triphenylphosphine reduction also by GC. Peak positions for the groups of α, γ- and α, δ-substituted hydroperoxyhexadecanones and hexadecanedihydroperoxides were assigned based on a comparison of the HPLC and GC analyses of these samples. The HPLC traces of two of these samples (Fractions 7 and 8) are shown in Figures 4 and 5. Positive identification of individual isomers and quantitative calibration in the absence of standards is not possible at the present time.

Conclusions

HPLC procedures have been developed for direct analysis of isomeric hydroperoxidic products formed in the autoxidation of n-hexadecane at elevated temperatures. Procedures 1 and 2 allow quantitative determination of individual and total isomeric hexadecylhydroperoxides and Procedures 2 and 3 allow semi-quantiative estimation of isomeric hydroperoxyhexadecanones and hexadecanedihydroperoxides. Although Procedure 2 does not provide separations equal to either Procedures 1 or 3 it allows detection and reasonable separations of all three of the above types of compounds in 15 minutes.

References

1. R. K. Jensen, S. Korcek, L. R. Mahoney, and M. Zinbo. Liquid-Phase Autoxidation of Organic Compounds at Elevated Temperatures. 1. The Stirred Flow Reactor Technique and Analysis of Primary products from n-Hexadecane Autoxidation at 120-180°C. J. Am. Chem. Soc. 101: 7574-7584 (1979).

2. B. D. Boss, R. N. Hazlett, and R. L. Shepard. Analysis of n-Paraffin Oxidation Products in the Presence of Hydroperoxides. Anal. Chem. 45: 2388-2392 (1973).

3. L. A. Cornish, R. Ferrie, J. E. Paterson. High Pressure Liquid Chromatography of Some Organic Peroxides. J. Chromatogr. Sci. 19: 85-87 (1981).

4 W. J. M. VanTilborg. Qualitative and Quantitative Determination of Hydroperoxides by High Performance Liquid Chromatography. J. Chromatogr. 115: 616-620 (1975).

5. M. O. Funk, M. B. Keller, and B. Levison. Determination of Peroxides by High Performance Liquid Chromatography with Amperometric Detection. Anal. Chem. 52: 771-773 (1980).

6. N. A. Porter, J. Logan, and V. Kontoyiannidou. Preparation and Purification of Arachidonic Acid Hydroperoxides of Biological Importance. J. Org. Chem. 44: 3177-3181 (1979).

7. D. K. Park, J. Terao, and S. Matsushita. High Performance Liquid Chromatography of Hydroperoxides formed by Autoxidation of Vegetable Oils. Agric. Biol. Chem. 45: 2443-2448 (1981).

8. W. E. Neff, E. N. Frankel, and D. Weisleder. High-Pressure Liquid Chromatography of Autoxidized Lipids. II. Hydroperoxycyclic Peroxides and Other Secondary Products from Methyl Linolenate. Lipids 16: 439-448 (1981).

PART VII

THE EFFECTS OF AUTOXIDATION ON WEAR IN A SYSTEM LUBRICATED WITH n-HEXADECANE

P. A. Willermet, S. K. Kandah, and R. K. Jensen

INTRODUCTION

In our earlier studies of effects of oxidation products on wear[1] carried out with oxidized PETH and with PETH containing model oxidation products (alkanoic acids, dibasic acids, diacid monoesters, and t-butyl hydroperoxide), it was concluded that the wear rates are independent of the concentration of hydroperoxides at concentrations above ca. 100 x 10^{-4} M and that they are greatly accelerated by dibasic acids and dibasic acid esters. Based on our investigations of the kinetics and mechanisms of autoxidation of n-hexadecane, in this substrate dibasic acids and diacid monoesters are not formed and major oxidation products include monohydroperoxides, dihydroperoxides, hydroperoxyketones, and alkanoic acids. The relative ratios of these products were found to depend on oxidation conditions. At lower oxygen pressures the oxidation products consist mainly of monohydroperoxides and contain smaller amounts of difunctional and acid products than at high oxygen pressures.

Since autoxidation of PETH and n-hexadecane model lubricants produces such widely differing product distributions, an investigation of the effects of autoxidation on wear in a system lubricated with n-hexadecane should provide additional insight into the relationships between lubricant degradation and wear.

EXPERIMENTAL

Wear Measurements. Wear experiments were carried out under a dry air atmosphere using a Roxana Four-Ball apparatus. Initial experiments were conducted at 100°C and 10 Hz (600 rpm) to allow a more direct comparison with the

earlier PETH results.[1] However, large irregular wear scars were obtained with fresh n-hexadecane at even the lowest practical loads. Further work was accordingly conducted at 40°C.

The initial siezure load (ISL) was determined by a series of 2 minute experiments. Fresh n-hexadecane gave an ISL of 10-12 kg. The oxidized samples gave values above 30 kg.

From these results, the following conditions were selected for the first series of experiments conducted at constant load and variable test times: 40°C, 10 Hz and 4 Kg. A second series of experiments was carried out with variable loads at 40°C and 10 Hz for a constant time of 4 or 6 hours.

Hydroperoxide Determination. It was found that soluble iron in the wear test samples interfered with iodometric detemination of hydroperoxides. Attempts to remove soluble iron by extraction, and with complexing agents and ion exchange resins were either unsuccessful or resulted in the loss of hydroperoxides. Accordingly, the extent of interference was determined by preparing solutions of ferric octanoate and t-butyl hydroperoxide in a synthetic hydrocarbon solvent. Plots of titration value vs. hydroperoxide concentration were obtained for soluble iron concentrations of 0.36×10^{-4} M, 2.1×10^{-4} M and 42×10^{-4} M. These plots were checked by adding ferric octanoate to known solutions of oxidized synthetic hydrocarbon and determining the effect of the added iron on the titration value.

Hydroperoxide concentrations in wear test samples were then determined by diluting the samples to one of the soluble iron concentrations given above and

taking a correction factor from the master plot to compensate for the interference effect.

Soluble Iron Determination. Soluble iron was determined spectrophotometrically after formation of a colored complex. A solvent mixture consisting of 3 parts by volume each of n-propanol and n-butanol and 1 part $CHCl_3$ was prepared. A solution of 0.2 g 1,10-phenanthroline in 50 ml of the solvent was made. A solution of 1 g hydroquinone in 10 ml solvent was made up shortly before use. An aliquot of 0.5 ml of the lubricant sample was added to a 5 ml volumetric flask. Addition of 0.5 ml of the hydroquinone solution was followed by sufficient amount of 1,10-phenanthroline solution to make a total volume of 5 ml. After allowing at least 30 minutes for full color development, the solution was placed in a 1 cm quartz cell and the absorbance maximum at 5200 Å was determined against a blank. The absorbance at 6500 Å was taken as zero. The color remained stable for several hours. Concentrations were determined by comparing the absorbance versus concentration obtained with a set of ferric octanoate standard solutions.

Materials. Fresh n-hexadecane was purified by percolation through silica gel.

Autoxidized samples varying in the concentrations of different products were prepared by changing conditions in the stirred flow micro-reactor[2] (Table 1). Samples SFR-232, 240 and 268 were prepared at 115 kPa oxygen pressure and contain ca. 30-45 x 10^{-4} M acid products, [-COOH], and ca. 240-270 x 10^{-4} M of total hydroperoxides, $[-OOH]_R$, of which ca. 125-150 x 10^{-4} M are monohydroperoxides,

Table 1. - Analyses of n-Hexadecane Samples Autoxidized in the Stirred Flow Reactor at 180°C

SFR Conditions			Oxidation Products*				
	P_{O_2}	τ	$[-OOH]_R$	[HOOH]	[ROOH]	$2[R(OOH)_2]$ + [HOOR=O]	[-COOH]
Sample #	(kPa)	(s)	M /10^4				
SFR-232	115	114	237	13.5	125	112	31
SFR-240	115	116	265	-	150	115	44
SFR-268	115	116	270	-	130	140	-
SFR-233	9.5	197	243	5.6	178	65	17
SFR-234	9.6	154	164	4.4	115	49	10
SFR-235	9.4	304	454	9.9	373	81	30
SFR-239	9.5	304	430	-	350	80	31

- - - - -

*Concentrations given at room temperature

[ROOH], and the rest are dihydroperoxides and hydroperoxy ketones, i.e., $2[R(OOH)_2]$ + [HOOR=O]. Samples SFR-233, 234, 235, and 239 were prepared at reduced oxygen pressure of ca. 10 kPa and different residence times to match different products in SFR-232. Sample SFR-233 was prepared to match the total peroxide concentration, SFR-234 the monohydroperoxide concentration, and SFR-235 and 239 the acid concentration.

A sample of concentrated monohydroperoxides was prepared by autoxidizing n-hexadecane for 340 s at 9.3 kPa O_2. The autoxidized sample was adsorbed on a silica gel column and washed with hexane to remove most of the unreacted n-hexadecane. Monohydroperoxides were then eluted with CH_2Cl_2. The sample was characterized by HPLC[3] and found to consist essentially of monohydroperoxides.

Heptanoic acid was obtained commercially as reagent grade material.

RESULTS AND DISCUSSION

Wear with Pure and Autoxidized n-Hexadecane.

Preliminary Experiments. We have previously reported preliminary results illustrating the influence of autoxidation on wear in a system lubricated with n-hexadecane.[4] Additional experiments were conducted shortly thereafter aimed at defining the chemical bases for the observed effects. The results of more recent experiments, however, were found to differ in magnitude from the original data, apparently due to an error in measuring the applied load in the earlier work. Accordingly, we have elected to re-run the more important experi-

ments even though this will delay completion of this work. Since the earlier experimental results are self-consistent and showed the same trends as the recent work, we shall refer to them as appropriate in this report.

Effects of Load. Experiments at 4 kg load gave reproducible results for pure n-hexadecane (Fig. 1) and for SFR-239 (Fig. 2). Similar data for SFR 240/268 showed scatter (Fig. 3). By varying the test load at 4 h test time, the cause of this scatter was found to be an abrupt wear transition at 4-5 kg load (Fig. 4). At a lower load (3 kg), wear was a linear function of time for both stationary and rotating balls (Fig. 5). At a higher load (8 kg), an apparently linear wear rate region was preceded by a period of higher wear for the stationary balls. No abrupt wear transition was observed with n-hexadecane (Fig. 6). The data obtained to date with SFR-239 as a function of load are not inconsistent with a similar transition (Fig. 7). However, scatter was not evident in the wear vs time data (Fig. 2). This suggests a less abrupt change in wear rate for SFR-239 as compared to SFR 240/268.

Wear Asymmetry. In earlier work we have found that the distribution of wear between the rotating and stationary balls of the Four Ball machine is, in general, asymmetric.[5] Wear on the rotating ball may be greater or less than wear on the three stationary balls, depending in part on lubricant chemical composition. In the present study we have observed markedly asymmetric wear with pure and autoxidized n-hexadecane.

With pure n-hexadecane, most of the wear took place on the stationary balls with the wear rate being constant during the entire test time (Fig. 1). After

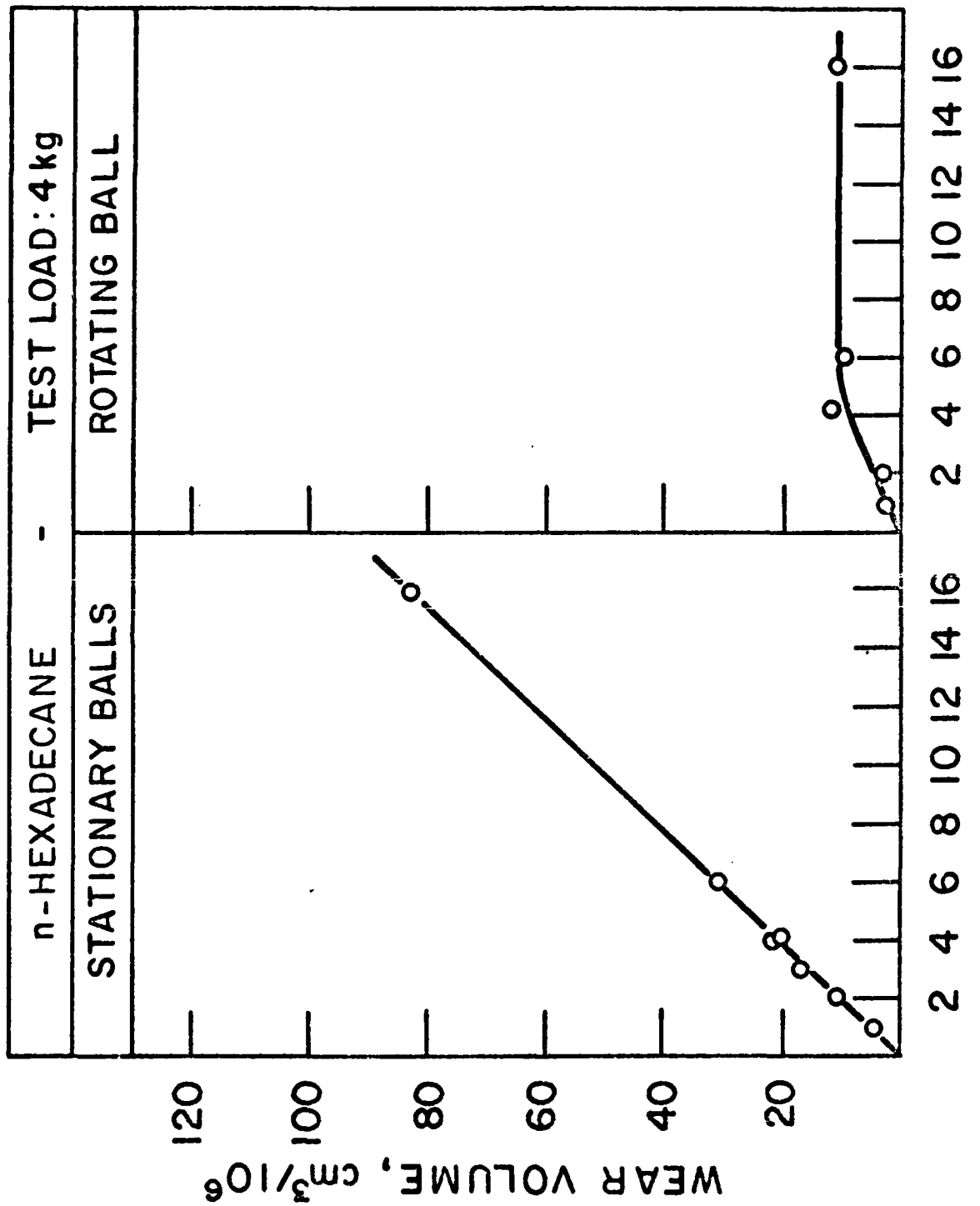

Fig. 1 - Wear volume vs test time with pure n-hexadecane.

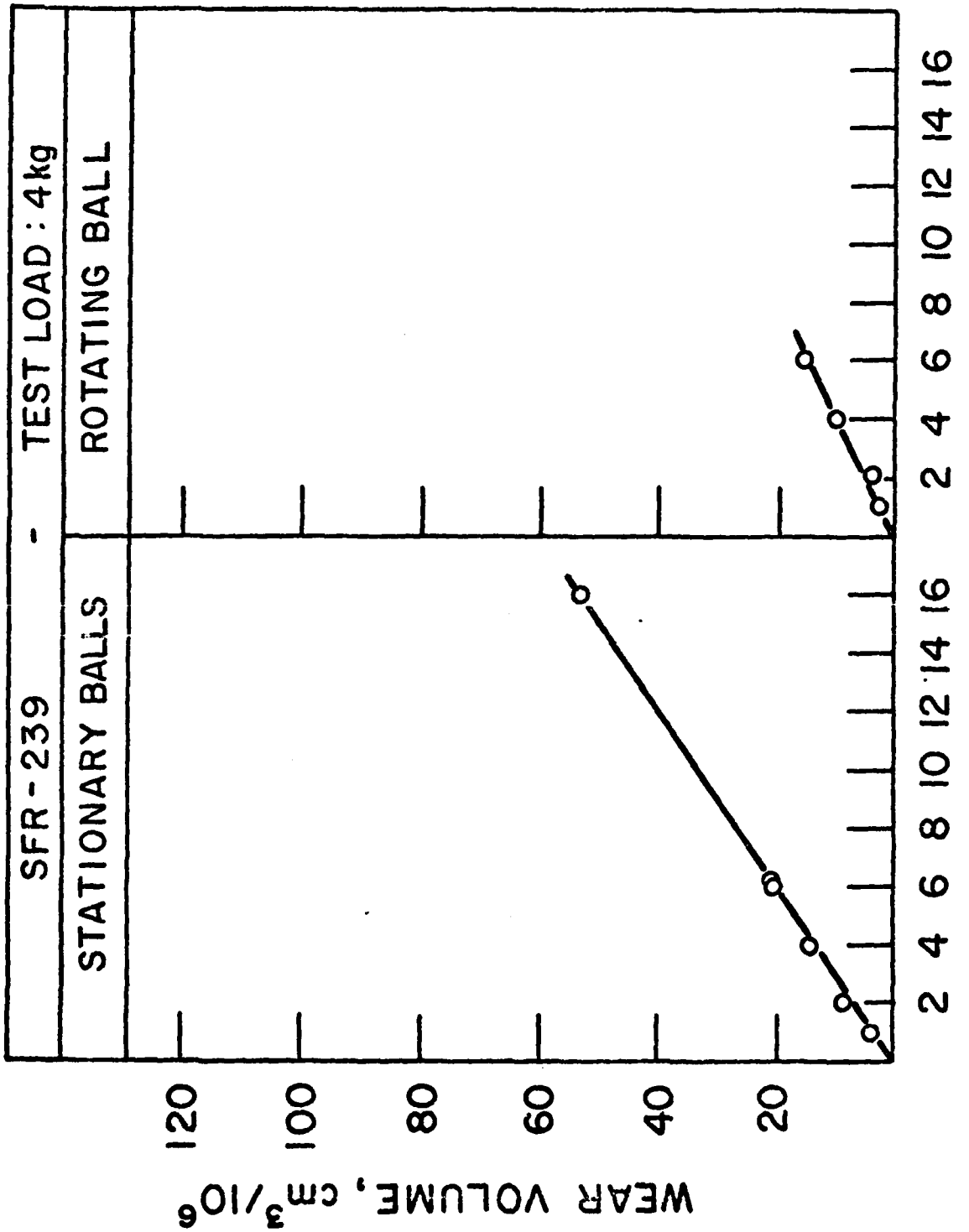

Fig. 2 - Wear volume vs test time with n-hexadecane autoxidized at low oxygen pressure (10 kPa).

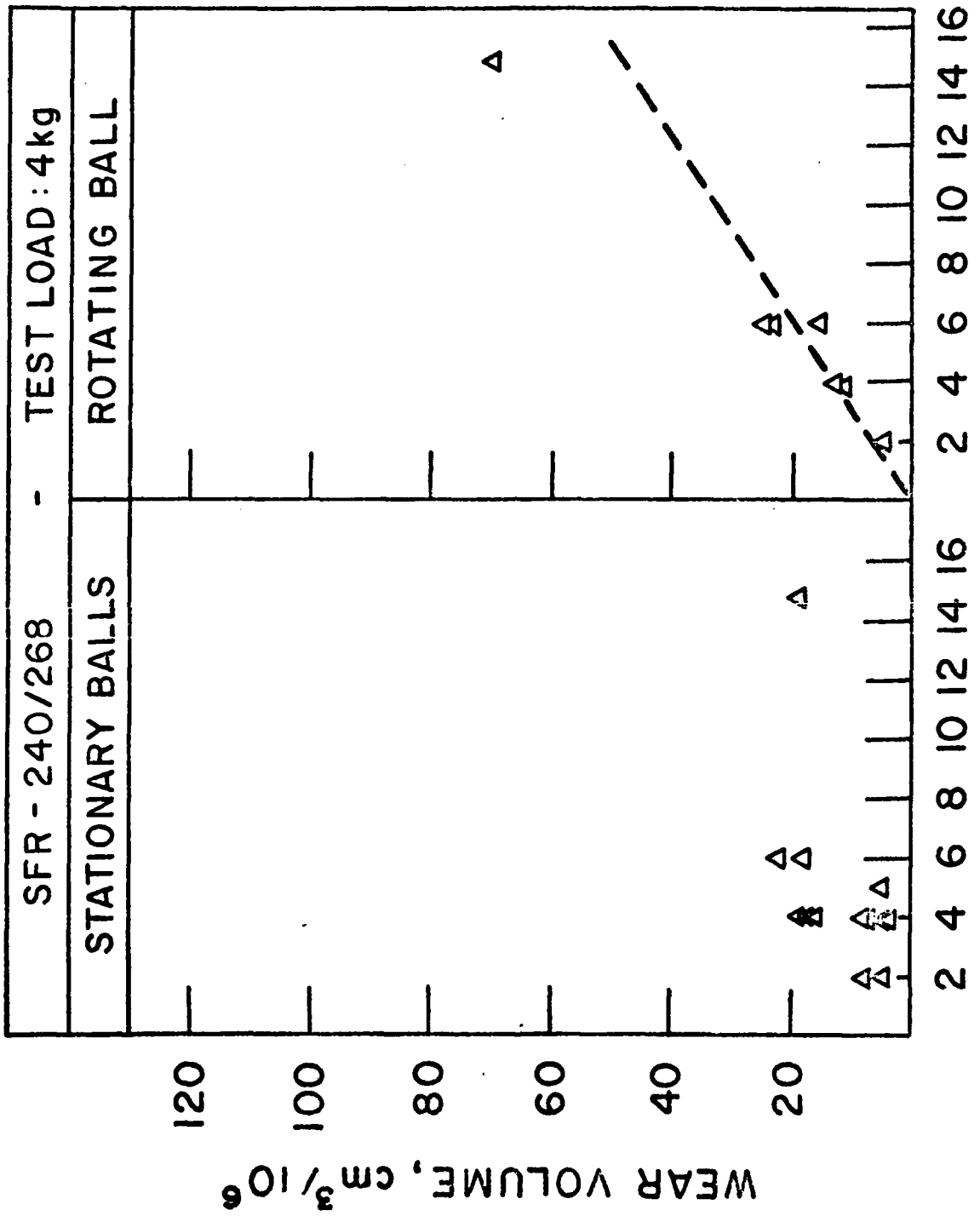

Fig. 3 - Wear volume vs. test time with n-hexadecane autoxidized at high oxygen pressure (115 kPa). Dashed line interpolated from data at 3 and 8 kg.

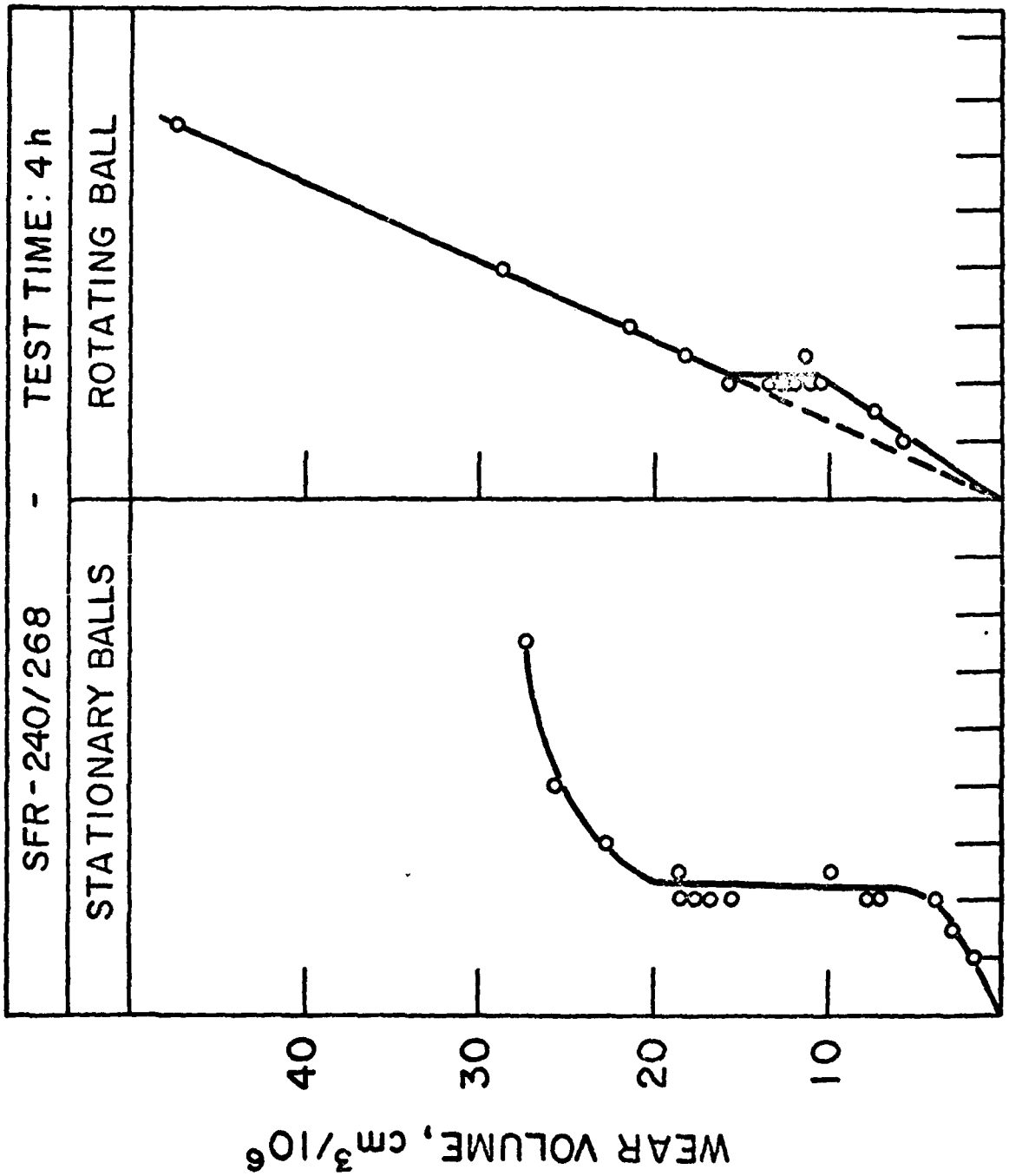

Fig. 4 - The effect of test load on wear with n-hexadecane autoxidized at high oxygen pressure (115 kPa).

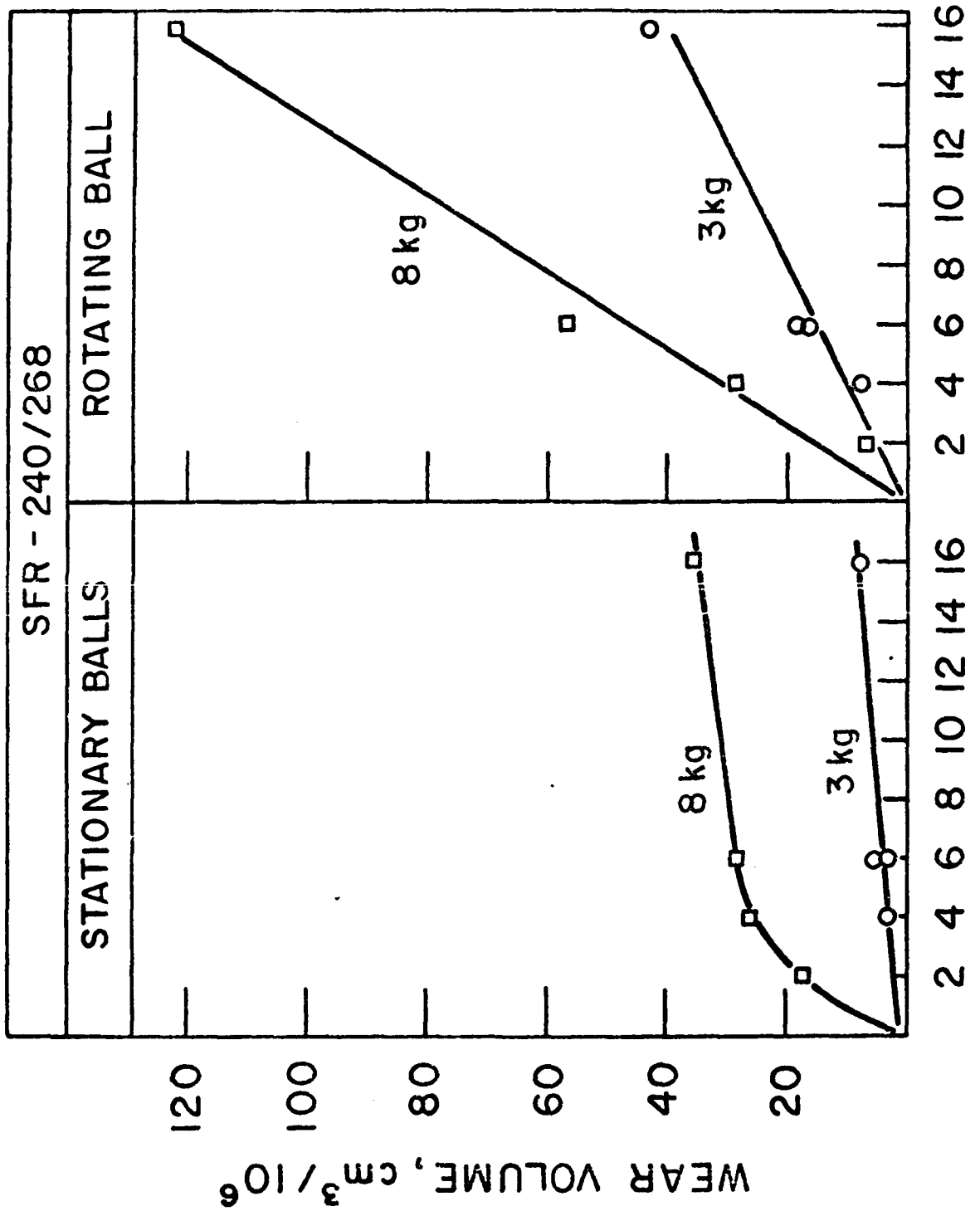

Fig. 5 - Wear volume vs test time with n-hexadecane autoxidized at high oxygen pressure (115 kPa).

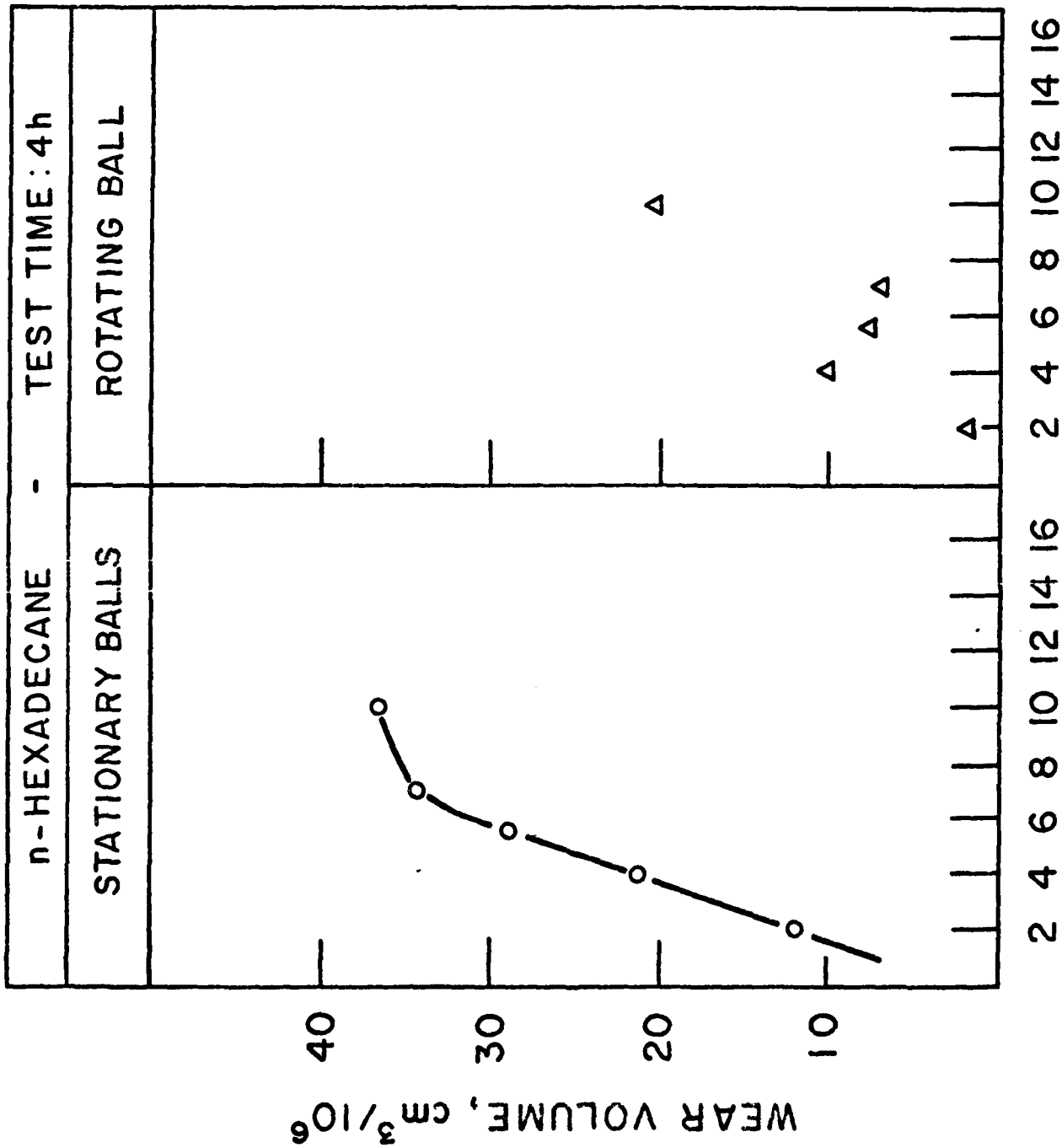

Fig. 6 - The effect of test load on wear with pure n-hexadecane.

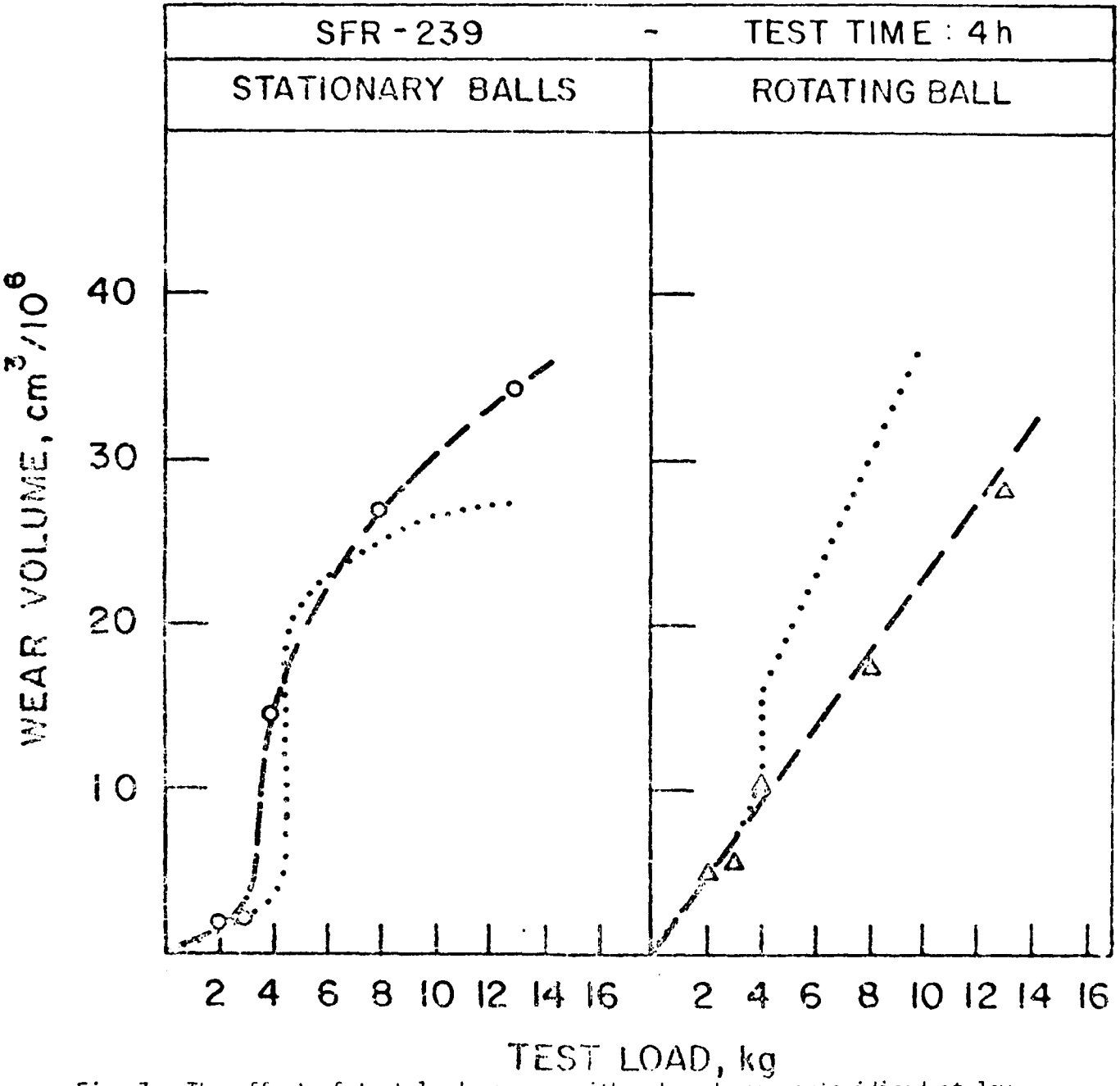

Fig. 7 - The effect of test load on wear with n-hexadecane autoxidized at low oxygen pressure (10 kPa). Dotted lines are from corresponding experiments with n-hexadecane autoxidized at high oxygen pressure (see Fig. 4).

an initial break-in period (~ 4 h) the wear rate for the rotating ball decreased to nearly zero and remained at that value even at 16 h.

This asymmetric wear feature was reversed for samples autoxidized under 115 kPa O_2 (SFR-240 and 268). At 3 kg load the wear rate for the stationary balls was much lower than that for the rotating ball (Fig. 5). At 8 kg load, similar behavior was observed after an initial period (~ 4 h) of symmetric wear.

Wear with Model Oxidation Products. Model experiments were initiated to shed light on the results obtained with the autoxidized materials. Since only preliminary results are availaable at present no firm conclusions can be drawn. The results do, however, suggest areas for further investigation.

Monohydroperoxides added to n-hexadecane in concentrations comparable to the total hydroperoxide concentrations of the autoxidized samples had little effect on wear for either the stationary or the rotating balls under the test conditions employed.

In contrast, heptanoic acid had a substantial impact on wear. In pure n-hexadecane (Fig. 8), an acid concentration of 8 x 10^{-4} M decreased stationary ball wear by a factor of 6. Wear remained at the same level up to an acid concentration of 56 x 10^{-4} M. The rotating ball was little affected. In a 400 x 10^{-4} M monohydroperoxide solution (Fig. 9), 12 x 10^{-4} M acid reduced stationary ball wear by one half. Wear remained at the same level up to 56 x 10^{-4} M acid. Rotating ball wear went through a minimum as the acid concentration was increased. At the highest level tested, rotating ball wear had increased by ca. 30%.

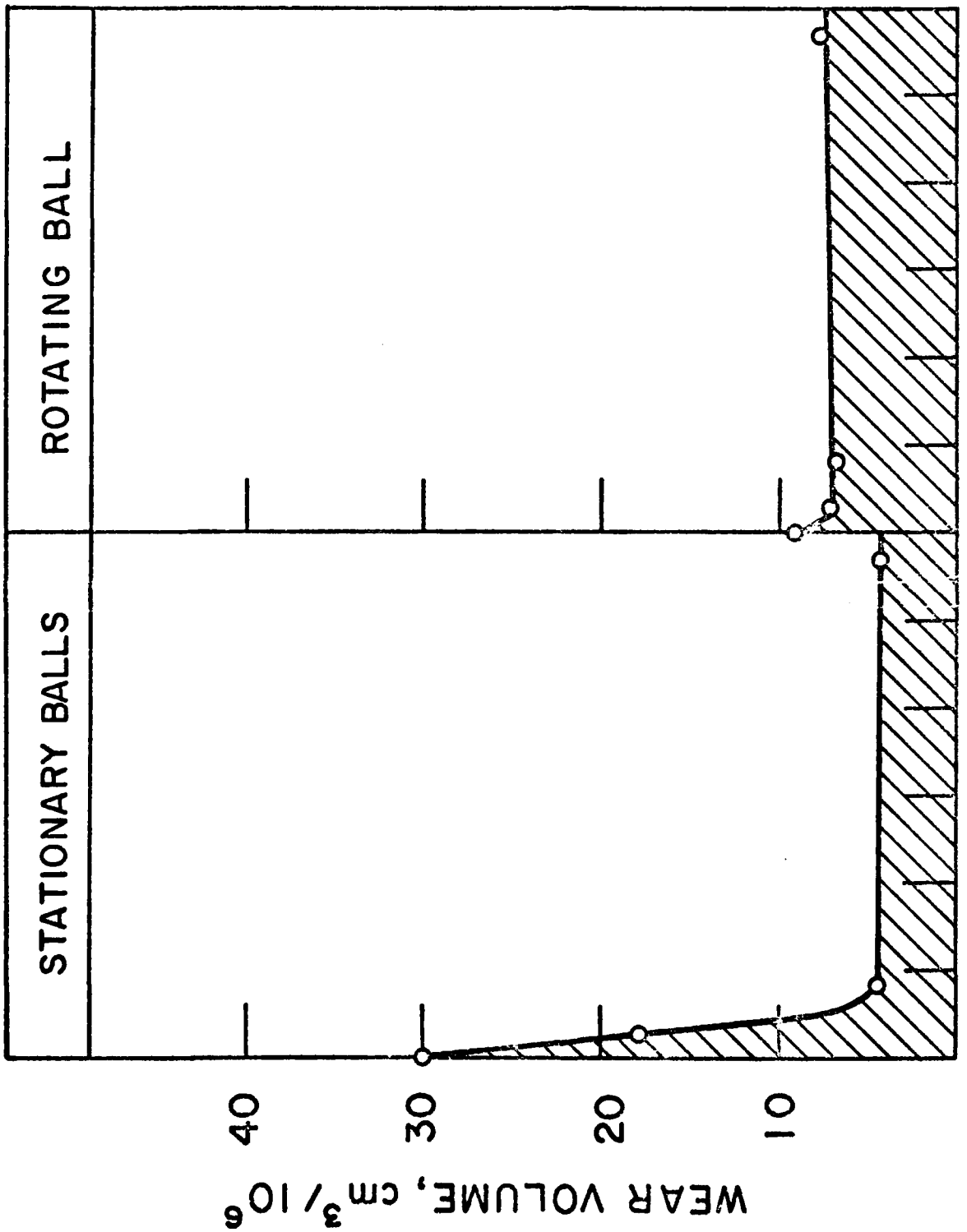

Fig. 8 - Wear vs. heptanoic acid concentration in n-hexadecane. Test conditions: 40°C, 600 rpm 4 kg, 6 h.

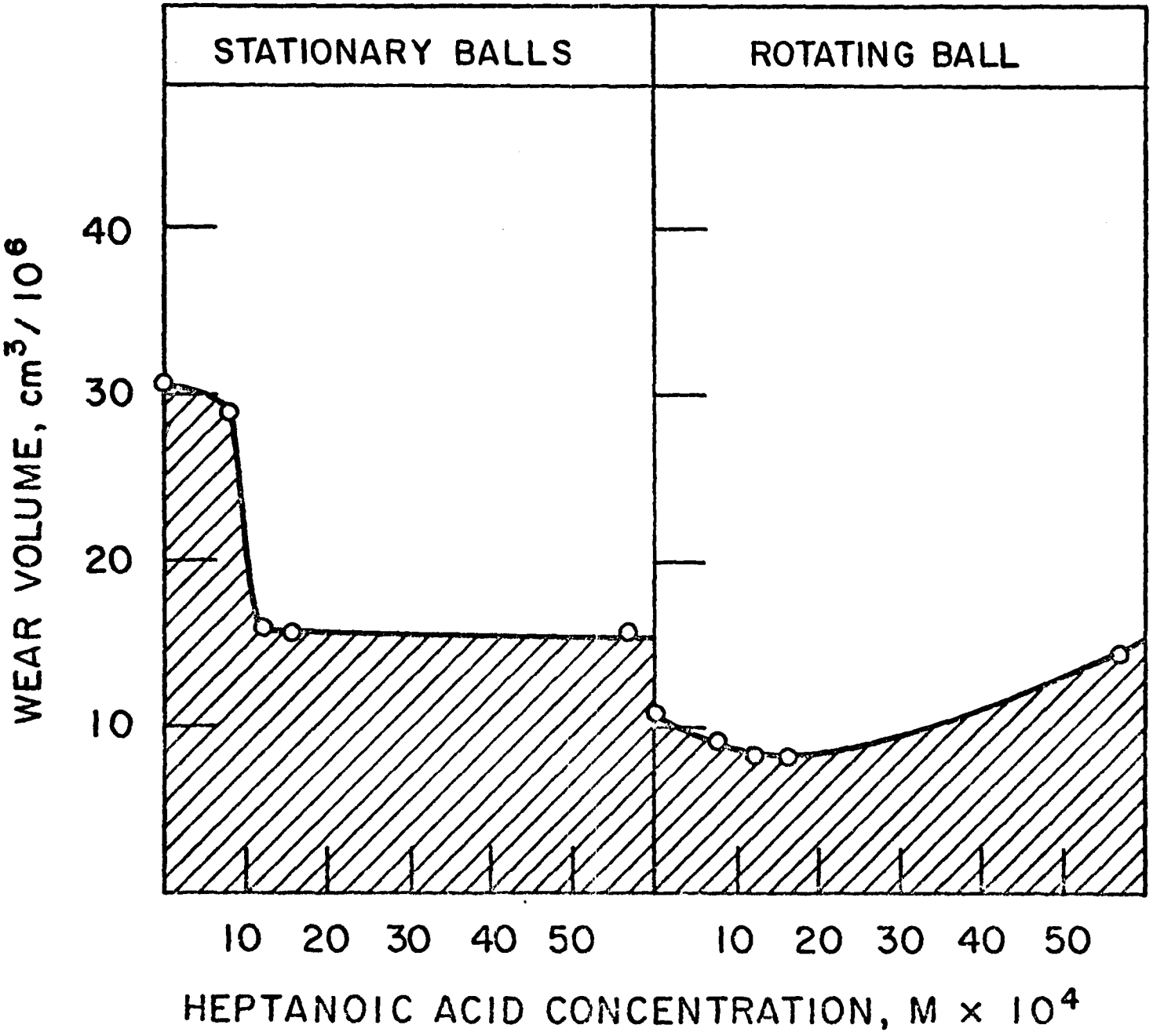

Fig. 9 - Wear vs heptanoic acid concentration in 400 x 10^{-4} M monohydroperoxides in n-hexadecane. Test conditions: 40°C, 100 rpm, 4 Kg, 6 h.

Chemical Changes During Wear

Change in Hydroperoxide Titer. SFR-239, SFR-240 and a monohydroperoxide/n-hexadecane admixture all showed significant decreases in hydroperoxide titer after the test (Fig. 10). Model system results suggest that a decrease in monohydroperoxide concentration during the course of a wear experiment might not affect the wear rate, but not enough data have been generated to firmly support that hypothesis.

Effects of Hydroperoxide Composition. Samples from the earlier series of experiments with SFR-232 through 235 were analyzed after the test more thoroughly than were samples from the more recent series of experiments (Table 2). The data show that the loss of hydroperoxide titer from difunctional products, $\Delta(2[R(OOH)_2] + [HOOR{=}O]) \approx \Delta[\text{-}OOH]_R - \Delta[ROOH]$, was proportionately larger than the loss of hydroperoxide titer from monofunctional hydroperoxides, $\Delta[ROOH]$, for SFR-232. The results for SFR-233 and 235 show the opposite and for SFR-234 the losses are about equal. These differences seem to be reflected in the wear test results. The data suggest an inverse relationship between loss of hydroperoxide titer from difunctionals and wear of the stationary balls (Fig. 11). Since α,γ difunctional intermediates are one of two major sources of acids in autoxidizing systems,[6] it is tempting to speculate that loss of difunctionals is connected with production of acids in the wear zone. The model system results suggest that this would reduce stationary ball wear.

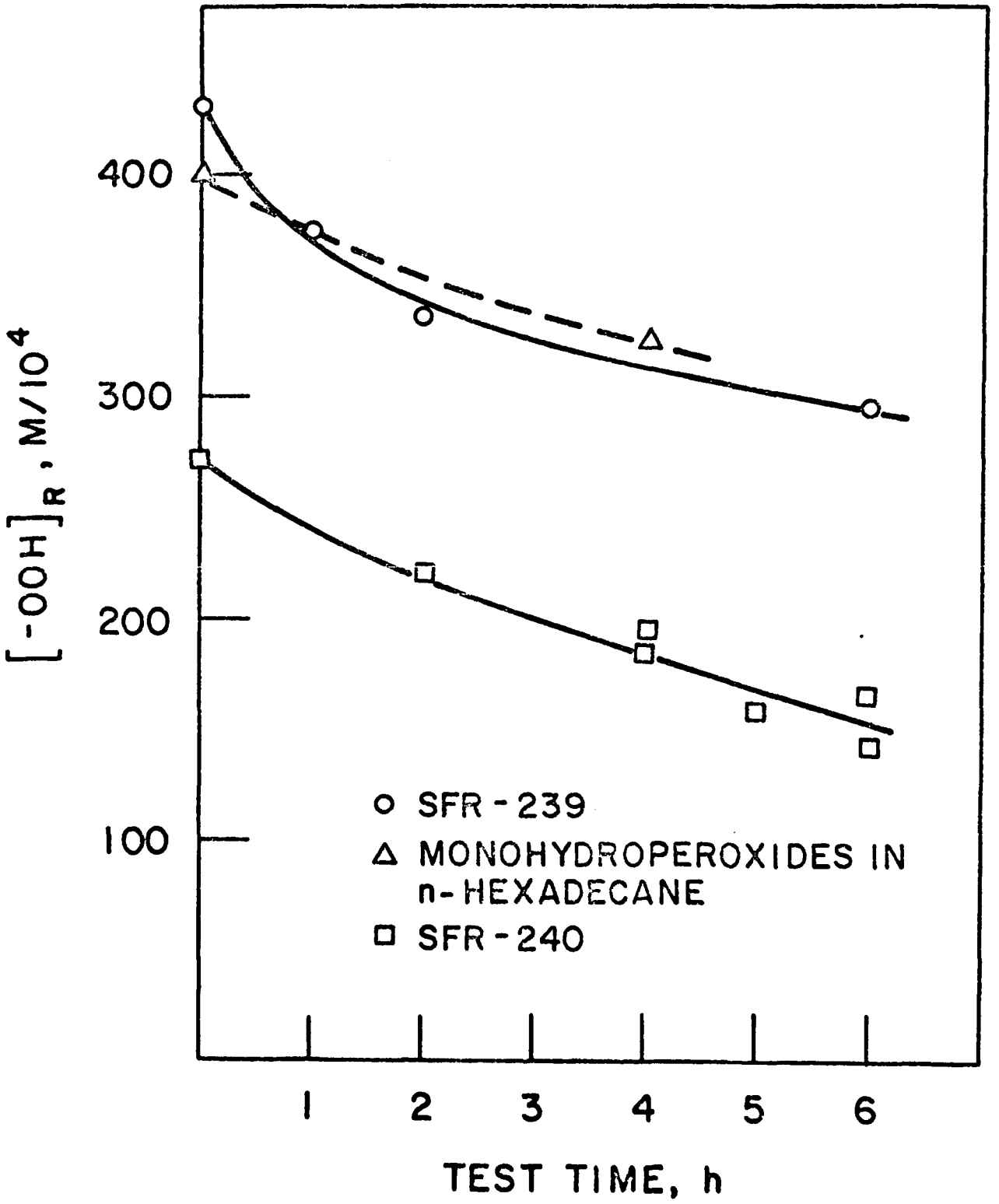

Fig. 10 - Hydroperoxide titer during wear tests. Test conditions: 4 kg load, 40°C, 10 Hz.

Table 2. Chemical Changes Resulting from Wear Tests

Sample #	Wear Test Time, h	Change in Concentration, $M/10^4$					Wear Volume, $cm^3/10^6$	
		Δ[R'COR"]	Δ[-OOH]R	Δ[ROOH]	(Δ[-OOH]-Δ[ROOH])	Δ[-COOH]	3 Stationary Balls	Rotating Ball
SFR-232	6	+10	-75	-13	-62	-11	2.7	13.8
SFR-232	17	+32	-145	-50	-95	-10	1.4	39.1
SFR-233	6	+35	-70	-60	-10	-10	13.8	11.2
SFR-234	6	+22	-72	-34	-38	-6.4	10.4	9.2
SFR-235	6	+40	-112	-76	-36	-10	11.4	11.2
n-Hexadecane	6	-	0	0	0	0	16	3

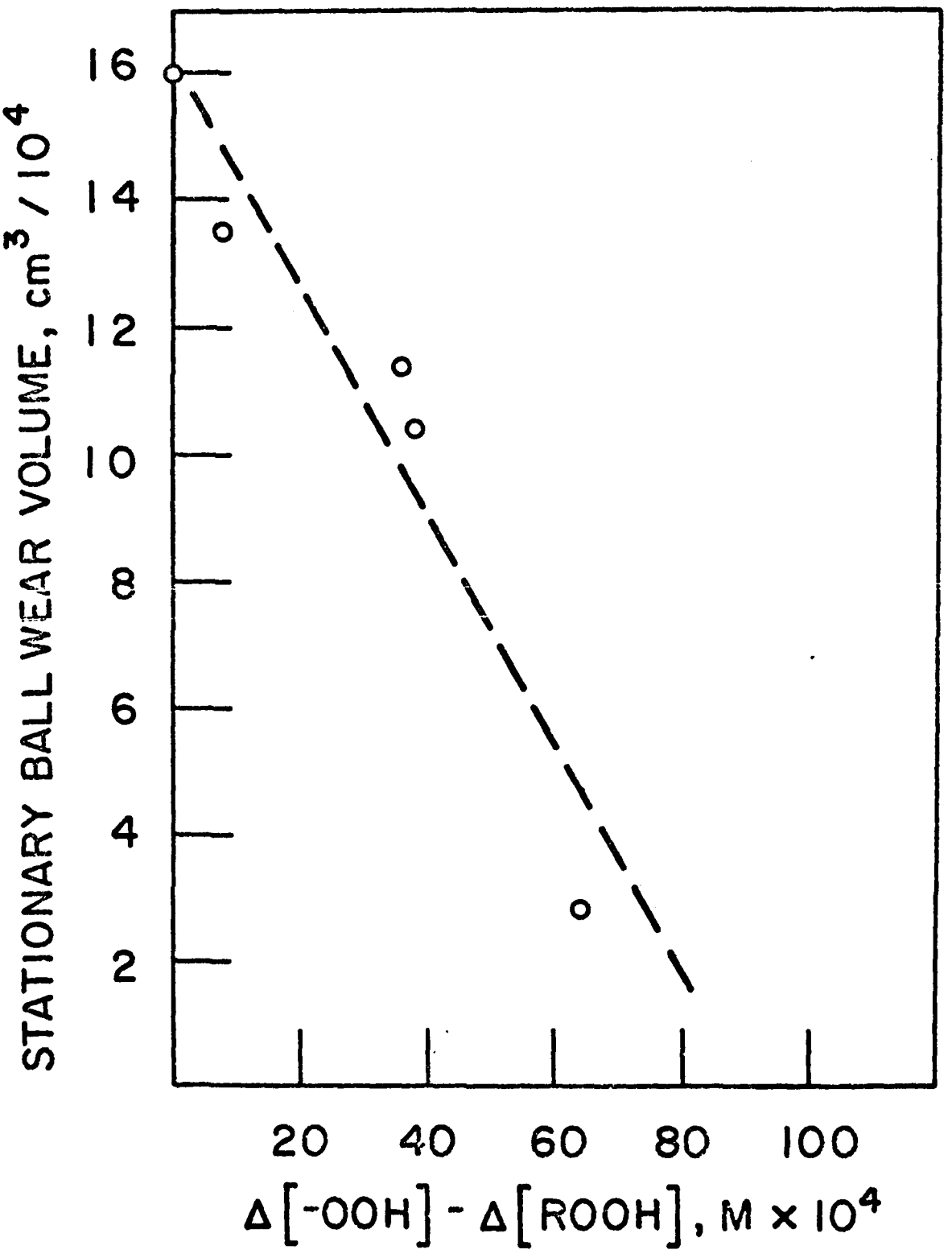

Fig. 11 - Stationary ball wear vs consumption of difunctional hydroperoxides in tests with autoxidized n-hexadecane (SFR-232-235). Test conditions: 40°C, 10 Hz, 4 kg, 6 h.

CONCLUSIONS

The experimental results presented in this report indicate that changing the chemical composition of n-hexadecane either through autoxidation or by adding model autoxidation products affects the wear of the stationary and the rotating balls in the 4-ball wear test machine differently. A composition change can simultaneously increase wear on one surface and decrease wear on the counter surface. Such effects may be ultimately explicable in terms of the different tribological environments of the counter surfaces. The different tribological environments may well affect the nature of the surface reaction layers.

It appears at present that carboxylic acids and perhaps difunctional hydroperoxides are effective in reducing stationary ball wear. Data at present indicate that the effect of monofunctional hydroperoxides is less pronounced. The effects of autoxidation on wear in systems lubricated with n-hexadecane are complex. Results obtained at this time indicate that additional studies of wear as a function of test load and time will be required to resolve the outstanding issues.

REFERENCES

(1) P. A. Willermet, L. R. Mahoney and S. K. Kandah, ASLE Trans. 24, 4, pp. 441-448 (1981).

(2) R. K. Jensen, S. Korcek, L. R. Mahoney and M. Zinbo, J. Am. Chem. Soc. 101, pp 7574-7584 (1979).

(3) R. K. Jensen, M. Zinbo and S. Korcek, J. Chromat. Sci. 21, 394 (1983).

(4) S. Korcek, L. R. Mahoney, R. K. Jensen, M. Zinbo, P. A. Willermet and S. K. Kandah, Annual Report to the Air Force Office of Scientific Research, Directorate of Chemical and Atmospheric Sciences for May 1, 1981 - April 30, 1982, under contract F49620-80-C-0061.

(5) P. A. Willermet and S. K. Kandah, ASLE Trans. 26, 2, pp 173-178 (1983).

(6) R. K. Jensen, S. Korcek, L. R. Mahoney and M. Zinbo, J. Am. Chem. Soc. 103, pp 1742-1749 (1981).

CUMULATIVE LIST OF PUBLICATIONS AND PRESENTATIONS

PUBLICATIONS

(1) L. R. Mahoney, S. Korcek, J. M. Norbeck, and R. K. Jensen, "Effects of Structure on the Thermoxidative Stability of Synthetic Ester Lubricants: Theory and Predictive Method Development," Preprints, Div. Petrol. Chem., ACS, 27, No. 2, 350 (1982).

(2) P. A. Willermet and S. K. Kandah, "Wear Asymmetry - A Comparison of the Wear Volumes of the Rotating and Stationary Balls in the Four-Ball Machine," ASLE Transactions, 26, 2, 173 (1983).

(3) R. K. Jensen, M. Zinbo, and S. Korcek, "HPLC Determination of Hydroperoxidic Products Formed in the Autoxidation of n-Hexadecane at Elevated Temperatures," J. Chromat. Sci. 21, 394 (1983).

(4) S. Korcek, R. K. Jensen, L. R. Mahoney, and M. Zinbo, "Oxidation and Inhibition of Pentaerythritol Esters," Proc. 4th Int. Colloquium on Synthetic Lubricants and Operational Fluids, Technische Akademie Esslingen, W. Germany, Jan. 1984.

(5) R. K. Jensen, S. Korcek, L. R. Mahoney, and M. Zinbo, "Effects of Oxygen Pressure on Liquid Phase Autoxidation of n-Hexadecane at 160 to 190°C," manuscript in preparation for publication in J. Am. Chem. Soc.

(6) R. K. Jensen, S. Korcek, L. R. Mahoney, and M. Zinbo, "Formation, Isomerization, and Cyclization Reactions of Hydroperoxyalkyl Radicals in n-Hexadecane Autoxidation at 160 to 190°C," manuscript in preparation for publication in J. Am. Chem. Soc.

(7) R. K. Jensen, S. Korcek, L. R. Mahoney, and M. Zinbo, "Liquid Phase Autoxidation of Organic Compounds at Elevated Temperatures. 3. Rate of Radical Formation in n-Hexadecane Autoxidation at 120 to 180°C," manuscript in preparation for publication in J. Am. Chem. Soc.

(8) R. K. Jensen, S. Korcek, L. R. Mahoney, and M. Zinbo, "Inhibition of the Autoxidation of n-Hexadecane by 2,6-di-tert-butyl-4-methylphenol at Elevated Temperatures," manuscript in preparation for publication in Oxid. Commun.

(9) R. K. Jensen, S. Korcek, L. R. Mahoney, and M. Zinbo, "Reactions of Alkylperoxycyclohexadienones during Autoxidation Inhibited by Hindered Phenols at Elevated Temperatures," manuscript in preparation for publication in Int. J. Chem. Kinet.

(10) P. A. Willermet, S. Kandah, and R. K. Jensen, "The Effects of Autoxidation on Wear in a System Lubricated with n-Hexadecane," manuscript in preparation for publication in ASLE Transactions.

PRESENTATIONS

(1) L. R. Mahoney, S. Korcek, R. K. Jensen, M. Zinbo, and E. J. Hamilton Jr., "Liquid Phase Autoxidation of Organic Compounds at Elevated Temperatures," Symposium on the Oxidation of Organic Materials, Northeast Region ACS Meeting, Potsdam, New York, June 30-July 3, 1980 (supported in part).

(2) S. Korcek, L. R. Mahoney, R. K. Jensen, and M. Zinbo, "Liquid Phase Autoxidation at Elevated Temperatures," Symposium on Radicals in Solution, National Research Council of Canada, Ottawa, July 23-24, 1980 (supported in part).

(3) P. A. Willermet, L. R. Mahoney, and S. K. Kandah, "Lubricant Degradation and Wear IV. The Effect of Oxidation on Wear Behavior of Pentaerythrityl Tetraheptanoate," ASME/ASLE Lubrication Conference, San Francisco, CA, August 18-21, 1980.

(4) S. Korcek, "Autoxidation of n-Alkanes at Elevated Temperatures," Organic Chemistry Seminar, Department of Chemistry, State University of New York at Stony Brook, April 30, 1981 (supported in part).

(5) S. Korcek, L. R. Mahoney, R. K. Jensen, and M. Zinbo, "Autoxidation of n-Alkanes - Isomerization and Cyclization Reactions of Hydroperoxyalkyl Radicals," 3rd International Symposium on Organic Free Radicals, Freiburg, West Germany, August 31-September 4, 1981.

(6) S. Korcek, "Kinetics and Mechanisms of Autoxidation of Model Lubricants at Elevated Temperatures," R. K. Jensen, "Rate of Initiation of Autoxidation at Elevated Temperatures," M. D. Johnson, "Antioxidant Reactions in Engines", and P. A. Willermet "Effects of Autoxidation on Wear Behavior. Wear Asymmetry in Four-Ball Wear Test," Air Force Wright Aeronautical Laboratories, Wright-Patterson Air Force Base, Ohio, January 12, 1982.

(7) L. R. Mahoney, S. Korcek, J. M. Norbeck, and R. K. Jensen, "Effects of Structure on the Thermoxidative Stability of Synthetic Ester Lubricants: Theory and Predictive Method Development," Symposium on Synthetic and Petroleum-Based Lubricants, Div. of Petroleum Chemistry, Inc., ACS Meeting, Las Vegas, March 28-April 2, 1982.

(8) P. A. Willermet and S. K. Kandah, "Wear Asymmetry - A Comparison of the Wear Volumes of the Rotating and Stationary Balls in the Four-Ball Machine," ASLE Annual Meeting, Cincinnati, Ohio, May 3-6, 1982.

(9) S. Korcek, R. K. Jensen, L. R. Mahoney, and M. Zinbo, "Rate of Initiation in the Autoxidation of n-Hexadecane at Elevated Temperatures," Symposium on Free Radicals at the 65th CIC Conference, Toronto, Canada, May 30-June 2, 1982 (supported in part).

(10) S. Korcek, R. K. Jensen, L. R. Mahoney, and M. Zinbo, "Liquid Phase Autoxidation of Organic Compounds at Elevated Temperatures," Symposium on

Inhibition of Liquid-Phase Autoxidation Reactions, ACS Meeting, Kansas City, September 12-17, 1982 (supported in part).

(11) R. K. Jensen, S. Korcek, L. R. Mahoney, and M. Zinbo, "Reactions of Alkylperoxycyclohexadienones during Autoxidation Inhibited by Hindered Phenols at Elevated Temperatures," Symposium on Inhibition of Liquid-Phase Autoxidation Reactions, ACS Meeting, Kansas City, September 12-17, 1982.

(12) S. Korcek, "Liquid-Phase Autoxidation Reactions at Elevated Temperatures," University of Toledo, Dept. of Chemistry, Toledo, Ohio, October 11, 1982.

(13) S. Korcek, "Theoretical and Practical Aspects of Lubricant Oxidation," ASLE-Detroit Section, Detroit, MI, February 15, 1983 (supported in part).

(14) S. Korcek, R. K. Jensen, L. R. Mahoney, and M. Zinbo, "Oxidation and Inhibition of Pentaerythritol Esters," 4th Int. Colloquium on Synthetic Lubricants and Operational Fluids, Technische Akademie Esslingen, W. Germany, Jan. 10-12, 1984.

ATTACHMENT 1

AD-A135 464 TIME-TEMPERATURE STUDIES OF HIGH TEMPERATURE DETERIORATION PHENOMENA IN L..(U) FORD MOTOR CO DEARBORN MICH RESEARCH STAFF S KORCEK ET AL. SEP 83 3/3

UNCLASSIFIED AFOSR-TR-83-0987 F49620-80-C-0061 F/G 11/8 NL

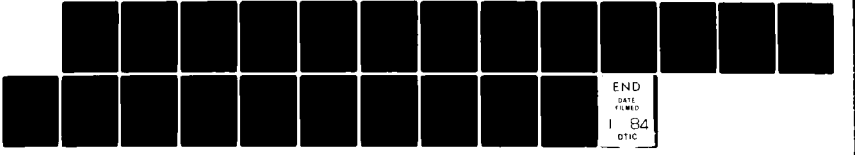

END
DATE FILMED
1 84
DTIC

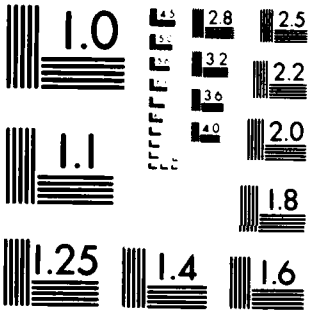

SYMPOSIUM ON SYNTHETIC AND PETROLEUM-BASED LUBRICANTS
PRESENTED BEFORE THE DIVISION OF PETROLEUM CHEMISTRY, INC.
AMERICAN CHEMICAL SOCIETY
LAS VEGAS MEETING, MARCH 29-APRIL 2, 1982

EFFECTS OF STRUCTURE ON THE THERMOXIDATIVE STABILITY OF SYNTHETIC ESTER LUBRICANTS: THEORY AND PREDICTIVE METHOD DEVELOPMENT

By

L. R. Mahoney*, S. Korcek, J. M. Norbeck and R. K. Jensen
Ford Motor Company, Research Staff, P. O. Box 2053, Dearborn, Michigan 48121

INTRODUCTION

The establishment of structure - reactivity relationships is of considerable scientific and technological importance. In this work, we describe the theoretical basis and development of the method for predicting the effects of structure changes on the thermoxidative stability of synthetic ester lubricants.

Chao and coworkers (1) have recently reported the results of a systematic study of the effects of structural changes in the alkanoyloxy group on the physical and chemical properties of synthetic polyol ester lubricants. The relative thermoxidative stabilities of the materials were determined by measurements of the lengths of inhibition periods in the presence of the same amount of an amine antioxidant, N-phenyl-α-naphthylamine (PAN). Although the inhibition periods in homologous series of esters were found to decrease monotonically with increasing number of reactive hydrogens in the alkanoyloxy group, the effects were not additive. In Figure 1 are shown the results of their measurements for the pentanoate, n-C_5-, through octanoate, n-C_8-, tetraesters of pentaerythritol versus a reactivity parameter, $\bar{f}\,N_\beta(RH)$. In this reactivity parameter, N_β is average number of hydrogen atoms in the molecule of substrate, RH, available for intermolecular abstraction reaction (cf. Figure 2). Thus, the parameter is based on the average number of reactive hydrogens available for intermolecular abstraction reaction per ester of the substrate.

Such non-additive effects on the stability of these lubricants must be in part due to the increasing importance of α,γ and α,δ intramolecular hydrogen abstraction reactions as the number of $-CH_2-$units in the alkanoyloxy group increases (2, 3). The occurrence of intramolecular reactions leads to increased rates of formation of hydroperoxide products. This results in increased autocatalytic character of the oxidation process and, thus, in a decrease of thermoxidative stability of higher members of a homologous series.

Based upon these considerations, we now develop a kinetic-mathematic model relating the length of experimental inhibition period, t_{inh}, with these structural effects and compare the predicted values of t_{inh} derived from the model with the results of Chao et al (1).

DERIVATION OF KINETIC EQUATIONS

The autoxidation of pentaerythrityl tetraheptanoate, PETH, at 180 to 220°C is described by the Reaction scheme 1-7 shown in Figure 2 (3). This reaction scheme can be generally applied to other polyol ester lubricants. Upon the addition of an efficient antioxidant, AH, Reaction 6 is replaced by the Reactions 8 and 9. By efficient antioxidant, we mean that for these species Reaction 8 is not reversible under the conditions of the inhibition period measurement. By this definition, hindered phenols and N-pheryl-α-naphthylamine, PAN, are efficient antioxidants.

$$XO_2\cdot + AH \longrightarrow XOOH + A\cdot \qquad 8)$$

$$(n-1)XO_2\cdot + A\cdot \longrightarrow \text{non radical products} \qquad 9)$$

where n is equal to the number of peroxy radicals consumed by reaction with a molecule of AH. Under these conditions,

$$(XO_2\cdot) = \frac{1}{k_8(AH)}\,\frac{-d(AH)}{dt} \qquad 1)$$

* Deceased.

and

$$2k_1(\text{-OOH}) = \frac{-n\, d(AH)}{dt} \qquad II)$$

At elevated temperatures, α, γ-hydroperoxyketone products rapidly decompose via Reaction 7; $t_{1/2(7)}$ is equal to 105 s at 210°C and 2.5 s at 232°C compared to $t_{1/2(6)}$ equal to 4330 s at 180°C and 87 s at 232°C (3). Based upon the assumption that α, γ-hydroperoxyketone species do not significantly contribute to the total hydroperoxide concentration, the rates of formation of total hydroperoxide groups are then given by,

$$\frac{d(\text{-OOH})_t}{dt} = \left\{\left[1+A+B\left[\frac{k_3}{H}\, N_3(RH)\right]+[1-A]k_8(AH)\right]\frac{1}{k_8(AH)} - \frac{n}{2}\right\}\frac{-d(AH)}{dt} \qquad III)$$

where A and B represent composite rate constants for intra and intermolecular abstraction reactions, see Appendix I. When intramolecular reactions do not occur $A = B = 0$. Noting that the time derivative may be eliminated from Equation III,

$$d(\text{-OOH})_t = G'\left[a_i, b_i, k_8/(k_3/H), N_j, (RH), n, (AH)\right]\, d(AH) \qquad IV)$$

The values of a_i, b_i and N_j are constants calculated from the structure of the reacting molecule and kinetic data (cf. Appendix I). The values of $k_8/(k_3/H)$ and n are now adjustable parameters but they may also be obtained from experimental data if available. The absolute values of k_8 are normally much less sensitive to the structure of the reacting peroxy radical than are the values of k_3/H (4).

Upon integration

$$(\text{-OOH})_t = \int_{(AH)_o}^{(AH)_t} G'\left[a_i, b_i, k_8/(k_3/H), N_j, (RH), n, (AH)\right]\, d(AH)$$

$$= G\left[a_i, b_i, k_8/(k_3/H), N_j, (RH), n, (AH)_t, (AH)_o\right] \qquad V)$$

Combining II and V

$$-\frac{n}{2k_1}\frac{d(AH)}{dt} = G\left[a_i, b_i, k_8/(k_3/H), N_j, (RH), n, (AH)_t, (AH)_o\right] \qquad VI)$$

Rearranging and integration results in

$$-\frac{2k_1}{n}(t_2-t_1) = \int_{(AH)_{t_1}}^{(AH)_{t_2}} \frac{d(AH)}{G\left[a_i, b_i, k_8/(k_3/H), N_j, (RH), n, (AH)_t, (AH)_o\right]} \qquad VII)$$

The inhibition period for a system equals

$$\frac{-n}{2k_1}$$

times the value of the integral as

$$(AH)_{t_1} \longrightarrow (AH)_o$$

and

$$(AH)_{t_2} \longrightarrow 0 .$$

Unfortunately, the integral is undefined at

$$(AH_{t_1} = (AH)_o$$

and the integral slowly diverges as

$$(AH)_{t_1} \longrightarrow (AH)_o .$$

However, the ratio of integrals for a system I where A=0, B=0 and a system II where A≠0, B≠0 can be calculated using numerical procedures described in Appendix 2. Thus, the ratio of the inhibition periods of systems I and II can be obtained from the equation,

$$\frac{n^{II}k_1^I}{n^{I}k_1^{II}}\frac{t^I_{inh}}{t^{II}_{inh}} = \frac{\int_{(AH)_t \to (AH)_o} \frac{d(AH)}{G^I[k_8'(k_3'H), N_j, (RH), n, (AH)_t, (AH)_o]}}{\int_{(AH)_t \to (AH)_o} \frac{d(AH)}{G^{II}[a_i, b_i, k_8'(k_3H), N_j, (RH), n, (AH)_t, (AH)_o]}} \qquad \text{VIII}$$

Equation VIII is utilized for the calculation of the ratios of

$$t^I_{inh}/t^{II}_{inh}$$

for a variety of polyol ester systems. The ratios are then compared with literature values. System I is a C_5 or lower member of a series since intramolecular abstractions in such structures are not possible.

n-C_5--n-C_8 ESTERS OF PENTAERYTHRITOL

In Figure 3 are plots of the inhibition periods at 232°C for the n-C_5--n-C_5 tetraesters of pentaerythritol reported by Chao et al. (1) versus corresponding values calculated from Equation VIII as a function of the values of $k_8'(k_3'H)$. The value of

$$t^I_{inh}$$

was set at 358 min. and $n=2$. The stoichiometric factor n for N-phenyl-α-naphthylamine was found to be approximately equal to 2 in styrene at 65°C (5) and also in PETH at 200°C (6). A value of $k_8'/(k_3'H)$ equal to 2.5×10^4 results in a poor correlation. The correlation improves as the value is decreased until there appears to be little effect as the value is decreased from 2.5×10^3 to 1×10^2. A value in the range of 3×10^3 would be predicted for $k_8'(k_3'H)$ from the limited kinetic data on N-phenyl-α-naphthylamine. We estimate from the temperature dependence of the autoxidation of pure PETH that $k_3'H$ will equal 23 $M^{-1}s$ at 232°C (3).

The largest differences between experimental and calculated values of t_{inh} occur for the n-C_8 ester. It is likely that, due to steric effects, there will, in fact, be a slight increase in the value of $k_3'H$ as one increases the length of the ester chain. Utilizing a value of $k_8'(k_3'H)$ equal to 1.6×10^3 for n-C_4 ester and 2.5×10^3 for n-C_5 results in a precise agreement of calculated and experimental values.

GEM-DIMETHYL SUBSTITUTED ESTERS OF PENTAERYTHRITOL

By a suitable choice of the values of $k_8'(k_3'H)$, it is possible to generate agreement between experimental and calculated values of t_{inh} for other ester systems. In Figure 4 is the result

of such an exercise for some gem-dimethyl substituted pentaerythrityl alkanoates.

In these gem-dimethyl systems, the values of k_3 H include significant contribution of primary peroxy radicals produced from reactions of initiation derived radicals, i.e.,

$$XOOH \rightarrow XO\cdot + \cdot OH$$

$$\left.\begin{matrix} XO\cdot \\ HO\cdot \end{matrix}\right\} + CH_3\text{-}\overset{|}{\underset{|}{C}}\text{-}CH_3 \longrightarrow \left.\begin{matrix} XOH \\ HOH \end{matrix}\right\} + \cdot CH_2\text{-}\overset{|}{\underset{|}{C}}\text{-}CH_3$$

$$CH_3\text{-}\overset{|}{\underset{|}{C}}\text{-}CH_2\cdot + O_2 \rightarrow CH_3\text{-}\overset{|}{\underset{|}{C}}\text{-}CH_2\text{-}OO\cdot$$

primary peroxy radical

For systems other than the 3,3-dimethyl-C_3 ester, these radical species can undergo intramolecular reactions,

$$CH_3\text{-}\overset{|}{\underset{|}{\underset{CH_2}{\underset{|}{C}}}}\text{-}CH_2\text{-}OO\cdot \longrightarrow CH_3\text{-}\overset{|}{\underset{|}{\underset{\cdot CH}{\underset{|}{C}}}}\text{-}CH_2\text{-}OOH$$

The occurrence of these reactions would lead to increased values of k_3 H and, thus, the lower values of $k_8/(k_3 \cdot H)$ necessary to obtain the fit shown in Figure 4.

In the case of 3,3-dimethyl-C_3 ester, the only reactive hydrogen is on a tertiary carbon. Due to the extreme steric effects involved in its abstraction, the value of k_3 H may be lower than that observed for a secondary C-H abstraction and lead to the higher value of k_8 (k_3 H) shown in Figure 4.

CONCLUSIONS

A method was developed for predicting the effects of structure on oxidation properties of polyol ester lubricants in the presence of an efficient antioxidant. The method requires knowledge of the stoichiometric factor for the antioxidant and the relative reactivities of lubricant-derived peroxy radicals in intra- and intermolecular hydrogen abstraction reactions from the lubricant and antioxidant. The model developed has been found to accurately describe oxidation properties (induction periods) for n-C_5 through n-C_9 pentaerythrityl tetraheptanoates containing 1 wt % N-phenyl-α-naphthylamine at 232°C and to give promising results for gem-substituted esters of pentaerythritol under the same conditions. In the latter case, however, more precise determination of ratio k_8/k_3(RH) is required to obtain complete agreement with experiment. It is concluded that a similar general approach can be used in the development of structure-reactivity relationships for the oxidation of other lubricant systems providing that the relative reactivities of peroxy radicals in hydrogen abstraction reactions and antioxidant stoichiometric factors for these systems are available.

ACKNOWLEDGMENT

This work was supported by the Air Force Office of Scientific Research under Contracts F44620-76-C-0097 and F49620-80-C-0061.

LITERATURE CITED

(1) (a) Chao, T. S., Kjonaas, M. and DeJovine, J., PREPRINTS, Div. of Petrol. Chem., ACS, 24, No. 3, 536 (1979); (b) Chao, T. S., Kjonaas, M. and Hoffman, W. D., U. S. Patent 3,441,600 (1969) and U. S. Patent 3,523,084 (1970); in "Synthetic Lubricants", M. W. Ranney, ed., Noyes Data Corporation, Park Ridge, NJ, p. 7 (1972).

(2) Jensen, R. K., Korcek, S., Mahoney, L. R. and Zinbo, M., J. Amer. Chem. Soc., 101, 7574 (1979); 103, 1742 (1981).

(3) Hamilton, E. J., Jr., Korcek, S., Mahoney, L. R. and Zinbo, M., Int. J. Chem. Kinet., 12, 577 (1980).

(4) Mahoney, L. R. and DaRooge, M. A., J. Amer. Chem. Soc., 92, 4063 (1970)

(5) Brownlie, I. T. and Ingold, K. U., Can. J. Chem., 45, 2419 (1967).

(6) Jensen, R. K. and Korcek, S., unpublished data.

(7) DCADRE Routine, IMSL Library - July, 1977, Int'l. Mathematical and Statistical Libraries, 7500 Bellaire Blvd., Houston, Texas.

(8) deBoor, C., "CADRE: An Algorithm for Numberical Quadrature", Mathematical Software, New York, Academic Press, Chapter 7 (1971).

APPENDIX 1

DERIVATION OF SINETIC EXPRESSIONS

The composite rate constants A and B in Equation III were derived from kinetic analyses of the reaction scheme (Figure 2) in which Reaction 6 was replaced by Reactions 8 and 9:

$$A = \frac{\dfrac{a_G}{1 + b_G \cdot c(AH)} + \dfrac{a_D}{1 + b_D \cdot c(AH)}}{1 + \dfrac{a_G}{1 + b_G \cdot c(AH)} + \dfrac{a_D}{1 + b_D \cdot c(AH)}} \qquad \text{AI)}$$

$$B = \frac{\dfrac{a_D\, b_D}{1 + b_D \cdot c(AH)}}{1 + \dfrac{a_G}{1 + b_G \cdot c(AH)} + \dfrac{a_D}{1 + b_D \cdot c(AH)}} \qquad \text{AII)}$$

The reaction scheme used does not include a reaction sequence starting with $HOORO_2\cdot$ and analogous to Reactions 4, 2' and 3'. Such a sequence would lead to formation of trihydroperoxide and dihydroperoxy ketone products. In the cases where these reactions could occur, i.e., in esters containing C_7 and C_8 alkanoyloxy groups, this simplification was found to introduce an error of less than 1%. Expression AII was derived assuming that all metastable α,γ-HOOR • O species produced during induction period decompose unimolecularly and do not contribute to f-OOH.

In expressions AI and AII, a_G, a_D, b_G and b_D represent ratios of rate constants for intra- and intermolecular abstraction reactions, $k_{4-\alpha,\gamma}$ $k_3(RH)$, $k_{4-\alpha,\delta}$ $k_3(RH)$, $k^{\ddagger}_{4-\alpha,\gamma}$ $k_3(RH)$ and $k^{\ddagger}_{4-\alpha,\delta}$ $k_3(RH)$, respectively, and c the ratio k_5 $k_3(RH)$. In these ratios, all rate constants may be expressed by the products of corresponding rate constants on per hydrogen atom basis and of average number of available hydrogen atoms for corresponding abstraction reactions, N_j. Thus,

$$a_i = \frac{k_{4-i}}{k_3(RH)} = \frac{k_{4-i}/H\text{-atom}}{k_3/H\text{-atom}} \cdot \frac{N_{4i}}{N_3(RH)} = [a_i/H]\,\frac{N_{4i}}{N_3(RH)} \qquad \text{AIII)}$$

$$b_i = [b_i/H]\,\frac{N_{4\cdot i}}{N_3(RH)} \qquad \text{AIV)}$$

and

$$c = \frac{k_5}{k_3/H\text{-atom}} \cdot \frac{1}{N_3(RH)} \qquad \text{AV)}$$

where i represents G or D.

The values of a_i and b_i may be calculated from Equation AIII and AIV assuming that the ratios of rate constants expressed on per hydrogen atom basis, a_i/H and b_i/H, for similar ester systems are the same. The values of a_i and b_i listed in Table A1-I were obtained using the values of ratios a_G/H, a_D/H, b_G/H and b_D/H equal to 26.3, 26.3, 1035 and 329, respectively. These values were derived from the study of PETH autoxidation at 150°C assuming that the ratios do not change with temperature significantly. The average numbers of hydrogen atoms for abstraction reactions (N_j in Table A1-I) were estimated from the structure of ester systems and availability of hydrogens assuming that the concentrations of abstracting isomeric peroxy radicals of given type are equal.

Substituting a_i, b_i and c into Equation III gives G'-function in Equation IV

$$G'[a_i, b_i, k_5/(k_3/H), N_j, (RH), n, (AH)] = \frac{n}{2} - 1 - \frac{1}{c(AH)} - \frac{\alpha + \beta c(AH) + [\gamma\, c(AH)]}{a + bc(AH) + c^2\,(AH)^2} \qquad \text{AVI)}$$

where

$$\alpha = a_G + a_D$$

$$\beta = (1 + b_D)(\alpha + b_G a_D)$$

$$\gamma = \alpha(2 + b_D) + b_G a_D$$

$$a = b - 1 + b_G a_D + b_D (a_G + b_G)$$

$$b = \alpha + b_G + b_D + 2$$

and c is defined by Equation AV.

TABLE A1-I

AVERAGE NUMBER OF AVAILABLE HYDROGEN ATOMS AND COMPOSITE RATE CONSTANTS FOR TETRAESTERS OF PENTAERYTHRITOL

Alkanoyloxy Substituent	$(RH)_{232}$ (M)	N_j					a_i		b_i	
		N_3	N_{4G}	N_{4D}	$N_4{}^*G$	$N_4{}^*D$	a_G	a_D	b_G	b_D
n-C_5	1.80	16	0	0	0	0	0	0	0	0
n-C_6	1.58	24	1.33	0	1	0	0.92	0	27.3	0
n-C_7	1.40	32	2	1	1	1	1.18	0.59	23.1	7.3
n-C_8	1.27	40	2.4	1.6	1	1	1.24	0.83	20.4	6.5
3,3-diCH_3-C_5	1.40	8	0	0	0	0	0	0	0	0
5,5-diCH_3-C_6	1.27	16	0	0	0	0	0	0	0	0
4,4-diCH_3-C_6	1.27	16	2	0	1	0	2.59	0	50.9	0
3,3-diCH_3-C_3	1.80	4[a]	0	0	0	0	0	0	0	0

Alkanoyloxy Substituent	$(RH)_{232}$ (M)	a	b	α	β	γ	δ
n-C_5		1	2	0	0	0	0
n-C_6		29.2	30.2	0.92	0.92	1.85	-0.892
n-C_7		224	34.2	1.77	127	30.0	-1.20
n-C_8		18	31.0	2.07	143	34.6	-1.29
3,3-diCH_3-C_5		1	2	0	0	0	0
5,5-diCH_3-C_6		1	2	0	0	0	0
4,4-diCH_3-C_6		54.5	55.5	2.59	2.59	5.19	-2.55
3,3-diCH_3-C_3		1	2	0	0	0	0

a. Tertiary hydrogens

Upon integration of Equation IV, we obtain G-function in Equation V.

$$G\,[a_1, b_1, k_5/(k_3{}^{1/2}H), N_j, (RH), n, (AH)_t, (AH)_o] \left[\frac{n}{2} - 1\right]\left[[(AH)_t - (AH)_o]\right] -$$

$$\frac{1}{c}\,\ell n\,\frac{(AH)_t}{(AH)_o} - \frac{1}{2c}\left[\alpha\,\ell n\,\frac{a + bc(AH)_t + c^2(AH)_t^2}{a + bc(AH)_o + c^2(AH)_o^2}\right.$$

$$\frac{\beta}{a}\,\ell n\,\frac{(AH)_t^2[a + bc(AH)_o + c^2(AH)_o^2]}{(AH)_o^2[a + bc(AH)_t + c^2(AH)_t^2]}$$

$$\left.\delta\,\ell n\,\frac{[2c(AH)_t + b - q]\;[2c(AH)_o + b + q]}{[2c(AH)_t + b + q]\;[2c(AH)_o + b - q]}\right] \qquad \text{AVII)}$$

where

$$q = \sqrt{b^2 - 4a}$$

$$\delta = \frac{2\gamma - b\left[\alpha + \frac{\beta}{a}\right]}{q}$$

The values of all composite constants used in Equation AVII for all ester systems discussed in this study are in Table A1-i.

In the absence of intramolecular abstraction reactions, the composite rate constants α, β and δ are all equal to zero. For such systems (systems I in this work) Equation AVII becomes

$$G^I\,[k_8/(k_3{}^{1/2}H), N_j, (RH), n, (AH)_t, (AH)_o] \cdot$$

$$\left[\frac{n}{2} - 1\right]\left[[(AH)_t - (AH)_o]\right] - \frac{1}{c}\,\ell n\,\frac{(AH)_t}{(AH)_o} \qquad \text{AVIII)}$$

APPENDIX 2

NUMERICAL EVALUATION OF THE RATIO OF INTEGRALS IN EQUATION VIII

The values for the ratio of integrals in Equation VIII were obtained numerically using the CADRE numerical quadrature algorithm in the IMSL library (7). The calculations were done in single precision using a DEC-10 computer system.

As mentioned above, each integral equation used to obtain an individual inhibition period Equation VII slowly diverges as $(AH)_t$ approaches $(AH)_o$, where at $(AH)_t = (AH)_o$ the integral is not defined. To avoid this singularity each integration was done from a value $(AH)_t = \xi\,(AH)_o$ for a value ξ near but not equal to 1. To show how sensitive the integrals and their ratio are to values of ξ the results of a typical calculation for two systems, I and II, are given in Table A2-I. Notice that the values of individual integrals increase as ξ approaches 1. However, the ratio of integrals, I^I/I^{II}, converges to a constant value (column 4, Table 2A-i).

The results in Table 2A-I demonstrate an interesting dichotomy. The values obtained for the individual integrals depend on what value is chosen for ξ. If one defines a critical concentration $(AH)_c = (AH)_o - \xi\,(AH)_o$, it is seen from Table A2-I that as $(AH)_c$ changes from 1×10^{-3} to 1×10^{-6} the integrals for both system increase by a factor of 3 or more. The limits of integration, as given by Equation VII, correspond to a system having an infinite inhibition time. One must introduce some value of ξ other than 1 or change the form of the kinetics to obtain a finite value for the inhibition period. Thus, one can speculate what, if any, physical significance can be placed on ξ and is it the same for all systems, as was assumed here. This should be contrasted to the fact that the ratio of integrals converges to a constant value as ξ approaches 1. This implies that Equation VIII is simply a function of I^I and I^{II} which is determined primarily by the value at $(AH)_o$. Thus, the ratio should be able to be obtained without doing the integration.

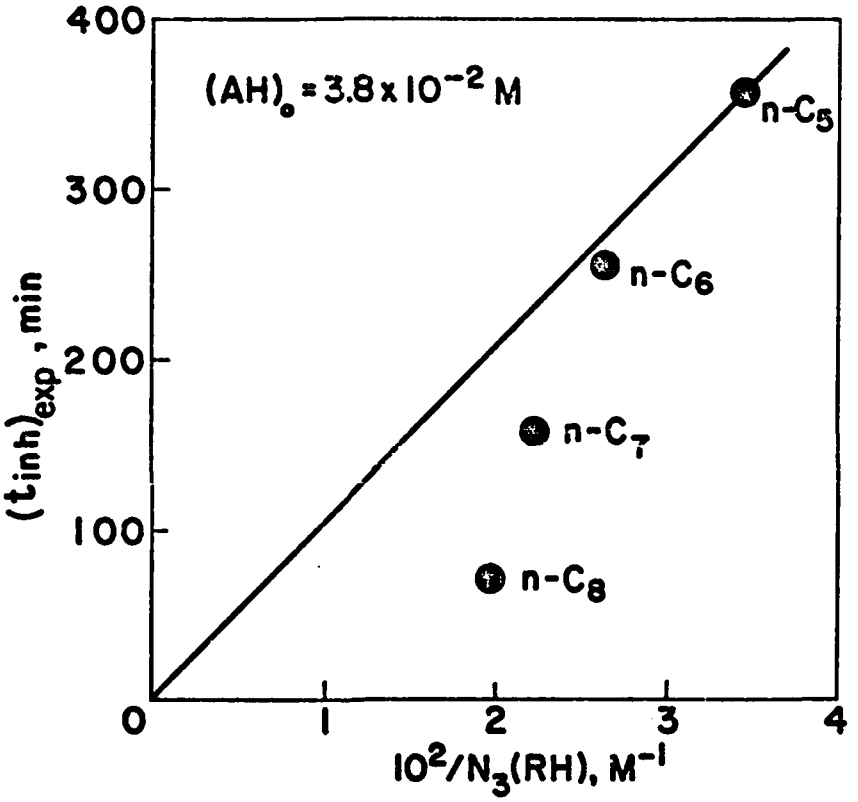

Figure 1. A plot of inhibition periods from the PAN inhibited autoxidation of straight-chain pentaerythrityl alkanoates at 232°C (1) vs. a reactivity parameter, $1/N_3(RH)$.

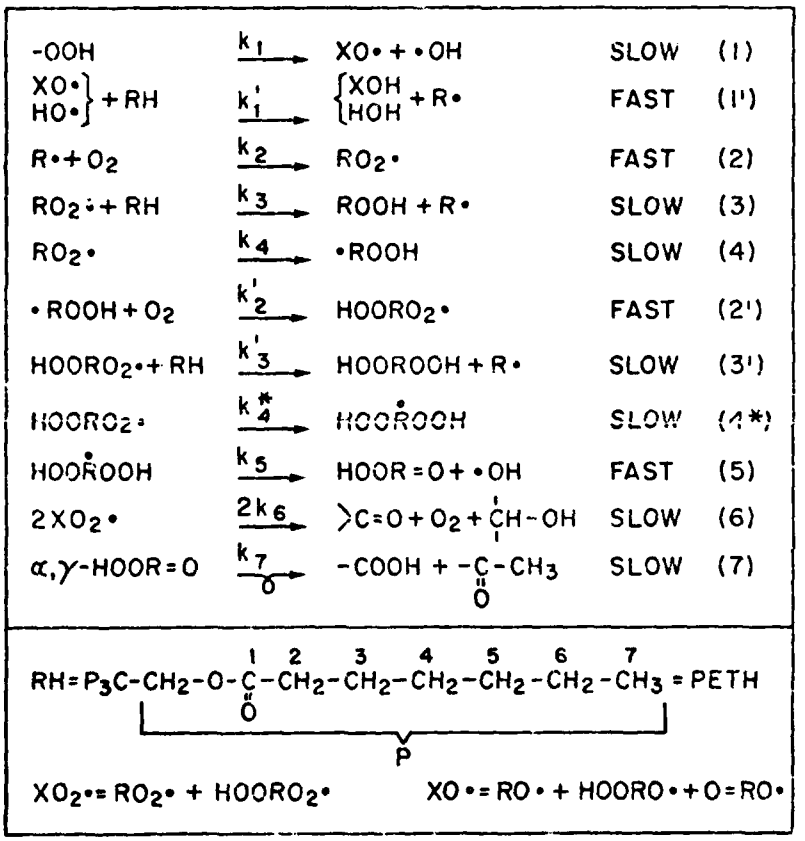
-OOH → XO• + •OH SLOW (1)
XO• / HO• + RH → XOH / HOH + R• FAST (1')
R• + O2 → RO2• FAST (2)
RO2• + RH → ROOH + R• SLOW (3)
RO2• → •ROOH SLOW (4)
•ROOH + O2 → HOORO2• FAST (2')
HOORO2• + RH → HOOROOH + R• SLOW (3')
HOORO2• → HOO•ROOH SLOW (4*)
HOO•ROOH → HOOR=O + •OH FAST (5)
2XO2• → >C=O + O2 + CH-OH SLOW (6)
α,γ-HOOR=O → -COOH + -C(=O)-CH3 SLOW (7)
RH = P3C-CH2-O-C(=O)-CH2-CH2-CH2-CH2-CH2-CH2-CH3 = PETH
P
XO2• = RO2• + HOORO2•
XO• = RO• + HOORO• + O = RO•

Fig. 1. [illegible]

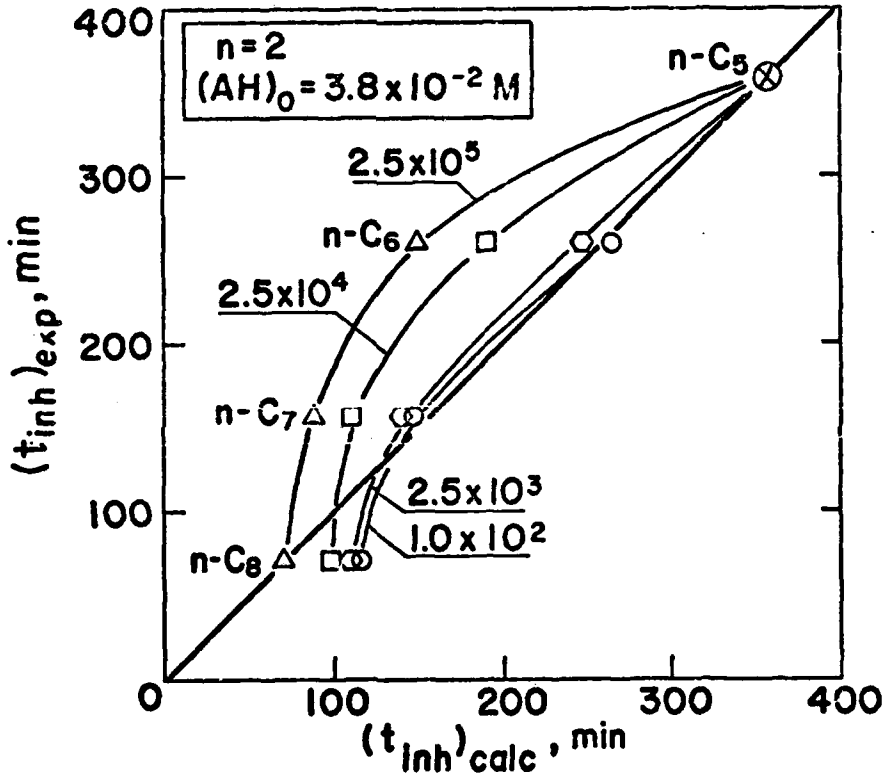

Figure 3. Plots of experimental inhibition periods from the PAN inhibited autoxidation of straight-chain pentaerythrityl alkanoates at 232°C (1) vs. corresponding values calculated from Eq. VIII as a function of $k_8/(k_3/H)$.

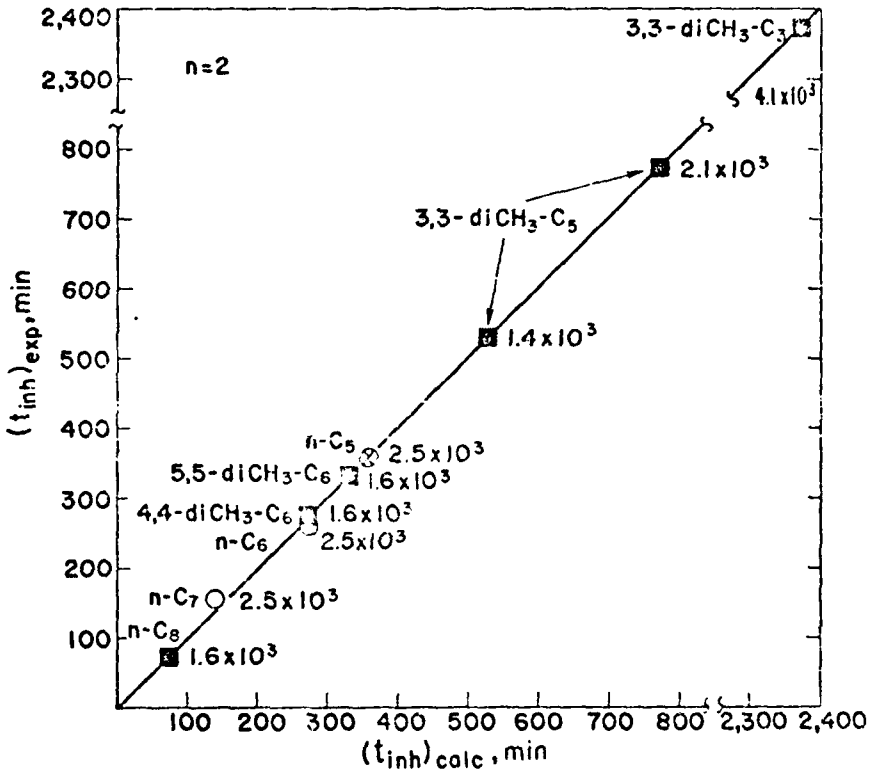
n=2
3,3-diCH3-C3
4.1x10^3
2.1x10^3
3,3-diCH3-C5
1.4x10^3
n-C5
2.5x10^3
5,5-diCH3-C6
1.6x10^3
4,4-diCH3-C6
1.6x10^3
n-C6
2.5x10^3
n-C7
2.5x10^3
n-C8
1.6x10^3
(tinh)exp, min
(tinh)calc, min
2,400
2,300
800
700
600
500
400
300
200
100
100 200 300 400 500 600 700 800 2,300 2,400

TABLE A2-I

CALCULATED VALUES OF INDIVIDUAL INTEGRALS IN EQUATION VII FOR SYSTEMS I AND II[a] AND OF RATIO OF THESE INTEGRALS IN EQUATION VIII FOR VARIOUS VALUES OF $\mathcal{E}$

$\mathcal{E}$	I^{I}	I^{II}	I^{I}/I^{II}
.50	12.4	4.13	3.00
.80	37.2	11.9	3.12
.90	58.2	18.4	3.16
.99	132	41.1	3.21
.9990	283	87.3	3.24
.99999	358	110	3.25
.999999	434	134	3.25

a. System I was n-C_5 and system II n-C_7 ester; n 2. $(AH)_0 = 3.2 \times 10^{-2}$M, $k_3'(k_3/H) = 2.5 \times 10^4$

For this paper, we have chosen to obtain the ratio numerically, using $\mathcal{E} = .9999$. However, the possibility of obtaining the same result from I^{I} and I^{II} directly is being explored.

ATTACHMENT II

VOLUME 26, 2, 173–178
ASLE TRANSACTIONS

Wear Asymmetry—A Comparison of the Wear Volumes of the Rotating and Stationary Balls in the Four-Ball Machine

P. A. WILLERMET (Member, ASLE) and S. K. KANDAH
Ford Motor Company
Dearborn, Michigan 48121

The wear behavior of two lubricant base stocks, a pentaerythrityl ester and a synthetic hydrocarbon, was investigated with the Four-Ball machine. Wear volumes of the stationary balls were evaluated from the wear scar diameter and by surface profilometry. Surface profilometry was also used to determine wear volumes for the rotating ball.

The two methods for evaluating stationary ball wear were in good agreement. Significant differences were found between wear of the rotating ball and wear of the three stationary balls. These differences were related to the lubricant and to the test conditions.

INTRODUCTION

In experiments employing the Four-Ball machine, wear is generally determined by measuring the average wear scar diameter. Similar approaches are used with other tribological devices. Two assumptions underlie this approach: (1) that the wear volume for the stationary balls is directly related to the wear scar diameter, and (2) that either the same is true for the wear volume of the rotating ball, or the wear of the rotating ball is negligible.

Feng (*1*) derived equations to relate the wear scar diameter to the wear volume and to the depth of the wear scars on the stationary balls. He found that his calculated values for the wear scar depth were in generally good agreement with measurements made by Vinogradov and Morozova (*2*). However, the accuracy of Feng's equation for wear volume does not appear to have been widely tested.

Since the asperity contact area for the rotating ball must be equal to the sum of the asperity contact areas for the stationary balls, it is reasonable to expect that the wear volume for the rotating ball would be equal to the sum of the wear volumes for the three stationary balls. However, it has been pointed out that the surfaces are, in fact, exposed to different tribological conditions (*3*). In contrast to the stationary balls, a point on the wear track of the rotating ball experiences cyclic variations in stress and temperature and is periodically exposed to the bulk lubricant. Such factors might lead to asymmetric wear of the contacting surfaces. Wear asymmetry would pose difficulties for the interpretation of wear test data and for the extrapolation of such data to practical devices.

These issues would appear to be important both for data analysis and for improved understanding of the wear process. Accordingly, we have addressed them as part of a systematic study of the wear behavior of two synthetic base stocks, a pentaerythrityl ester (PETH) and a synthetic hydrocarbon (SHC) carried out with the Four-Ball machine.

Presented at the 37th Annual Meeting
in Cincinnati, Ohio,
May 10–13, 1982

EXPERIMENTAL

Materials

The synthetic hydrocarbon (SHC) was a commercial material, predominantly a saturated trimer of decene-1. It was purified by percolation first through a bed of silica gel then through a bed of alumina. After purification, the base oil was passed through a 0.45 μM filter to eliminate particles.

Pentaerythrityl tetraheptanoate (PETH) was obtained by purification of a technical grade material as described in detail elsewhere (*4*). The material used in this study was designated PDP in Ref. (*4*).

APPARATUS AND PROCEDURES

Wear Experiments

Wear experiments were conducted using a Four-Ball apparatus (Brown, G.E. modification). The wear specimens were Hoover AISI 52100 steel balls, grade 25. Before each test, the balls, top ball chuck, and sample container were thoroughly washed with Stoddard solvent followed by reagent grade toluene, acetone, and pentane. The balls, sample container, and top ball chuck were assembled, dried at 100°C, then cooled to room temperature in a desiccator.

The spindle and drawbar were rinsed with pentane to remove any contaminants from the previous run. Syringes used for adding or withdrawing samples were cleaned and dried in the same way.

Lubricants were purged with dry air before use. At the beginning of each run, 9 ml of the lubricant were added to the sample container and the apparatus was then assembled. The liquid seal employed to maintain a controlled atmosphere was filled with the test lubricant. Load was applied and purging with dry air was begun. The sample was then brought to temperature and the test was begun. After termination of the experiment, a sample of used fluid was withdrawn and the wear scar diameter was measured in the usual manner.

Wear Measurements

The measured average wear scar diameters were converted to calculated wear volumes and depths via the equations (*1*):

$$V = 4.65 \times 10^{-2} d^4 - 3.21 \times 10^{-5} Wd$$

and

$$H = 1.97 \times 10^{-2} d^2 - 2.73 \times 10^{-5} W/d$$

where V equals wear volume in mm^3 for 3 balls, d is equal to the wear scar diameter in mm, W equals load in kg, and H equals wear scar depth in mm.

Surface profilometer measurements were carried out with a stylus instrument having a 1.3×10^{-2} mm diameter tip. The measurements were made without a skid. The balls were positioned in a holder which rotated them under the stylus at @ 2×10^{-3} m/s. The stylus load was 0.3 g. Rotating balls were positioned so that the stylus traversed the wear track at two points 180° apart. Stationary balls were carefully positioned so that the stylus tip was resting on the deepest point of the wear scar. The stylus was passed over the wear scar, then the ball was turned 90° and the process was repeated.

The profilometer output was displayed on a strip chart recorder. For the rotating balls, the vertical magnification was 1.73×10^5 and the horizontal magnification was 91.74. For the stationary balls, the vertical magnification was 1.73×10^4. Typical recorder traces are displayed in Fig. 1. The cross-sectional areas of the rotating ball scars were determined by tracing the profiles on paper of known and uniform density, then weighing the cut-out scar profiles. Multiplication by the wear halo* circumference gave the wear scar volume. In order to establish repeatability, this measurement was carried out six times for one of the smallest wear scars. The results showed a mean standard deviation of two percent for the wear volume. Although more modern equipment would be preferable in terms of experimental convenience and would be able to show small scale surface features in better detail, the repeatability of the technique was more than adequate to support the conclusions made

*The wear halo diameter is defined as the average diameter of the two circles which form the inner and outer peripheries of the scar.

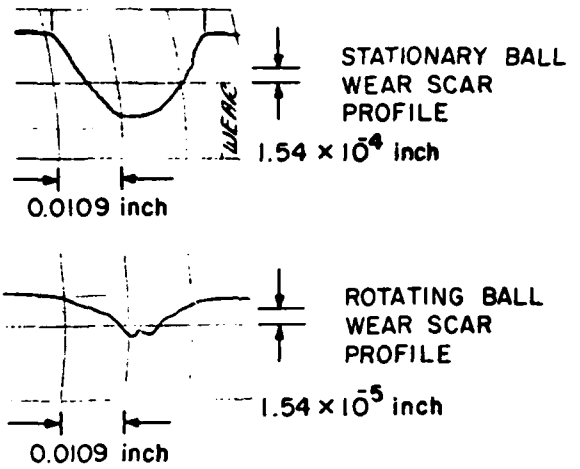

Fig. 1—Typical wear scar profile traces for a rotating and a stationary ball. Test conditions: SHC lubricant, 40-kg load, 100°C, 15 Hz (900 rpm). Sliding distance: 840 M.
Note the difference in vertical scale.

in this paper. The wear volumes of the stationary balls were determined as follows: the wear scale profiles as displayed on the strip chart were divided into @ 25 equally spaced segments along the vertical axis. The average diameter of each segment was carefully measured and the volume of the segment was calculated as a cylinder. The sum of the cylinder volumes was taken as the wear volume. Replicate measurements of the traces established that the repeatability of this procedure was better than one percent. Wear volumes were determined for the two traces made of each scar and averaged. It was generally found that the wear scar diameter as determined by profilometry was less than that measure optically, probably because the deepest point of the wear scar did not correspond to the exact center. A correction factor was applied by multiplying the volume by the square of the ratio of the optically measured wear scar diameter to the wear scar diameter as determined by profilometry.

Replicate experiments conducted with PETH and with SHC under conditions giving low wear indicated that the calculated wear volumes were reproducible within ± 5 percent. Wear data as a function of time with SHC and PETH suggest comparable reproducibility for wear volumes determined by surface profilometry. However, data for SHC at sliding speeds for which wear was a strong function of speed showed a large degree of scatter.

The dimensionless wear coefficient, K, was calculated from the equation (*5*),

$$K = VH/dL$$

where V is the wear volume, d is the sliding distance, H is the hardness (725 kg/mm2), and L is the load.

RESULTS

Calculated Wear Volumes and Surface Profilometry for the Stationary Balls

Because of the care required in properly aligning the profilometer stylus, measurements on the stationary balls

TABLE 1—WEAR DATA OBTAINED WITH PETH AND SHC. STATIONARY BALL WEAR VOLUME DETERMINED BY PROFILOMETRY. SLIDING DISTANCE = 840 M

					From Scar Diameter		From Profilometry		
Fluid	Speed, cm/s	Load, kg	Temp., °C	Wear Scar Diameter, $cm/10^2$	Wear Volume for Three Stationary Balls, $cm^3/10^6$	Scar Depth, $cm/10^4$	Wear Volume for Three Stationary Balls, $cm^3/10^6$	Scar Depth, $cm/10^4$	Rotating Ball Wear Volume, $cm^3/10^6$
PETH	3.9	40	100	6.53	7.6	15.1	7.1	14.8	18.6
	5.8			6.91	9.7	17.2	9.1	17.4	11.9
	11.7			6.46	7.3	14.7	7.5	15.6	10.8
	15.5			6.68	8.4	15.8	9.5	19.6	9.9
	23.3			6.05	5.3	12.8	6.0	15.2	16.3
	35.0			6.16	5.9	13.2	5.9	14.2	12.6
SHC	3.9			8.54	23.6	27.5	29.7	33.4	33.1
	5.8			7.69	15.3	21.8	17.1	24.3	29.1
	7.8			7.38	12.8	19.2	12.9	20.9	38.2
	15.5			7.10	11.0	16.5	13.9	23.1	8.3
	35.5			7.47	13.5	20.3	13.9	21.1	8.2

proved to be time consuming. For this reason, only a limited number of specimens were evaluated. Good agreement was found between the measured and calculated wear scar volumes and depths (Table 1).

Wear Asymmetry

A comparison of wear volume data for the rotating ball and three stationary balls, based on surface profilometer measurements, revealed differences in the wear factors for the two surfaces (Figs. 2 and 3 and Table 1). This wear asymmetry was a function of the sliding speed. Different results were obtained depending on whether PETH or SHC was employed as the lubricant. For PETH, more wear was found on the rotating ball than on the three stationary balls (Fig. 2). For SHC (Fig. 3), this relationship was reversed at sliding speeds above about 15 cm/s. At lower sliding speeds, wear was much greater, with more wear being found on the rotating ball than on the three stationary balls.

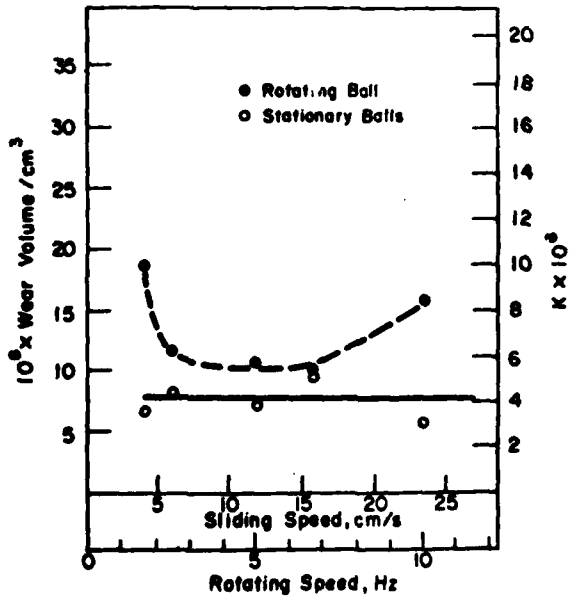

Fig. 2—Wear volume from profilometer data vs sliding speed with PETH. 40-kg load, 100°C, sliding distance: 840 M.

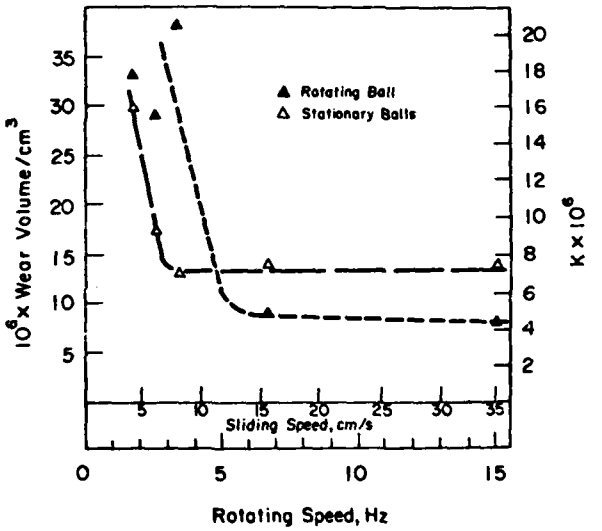

Fig. 3—Wear volume from profilometer data vs sliding speed with SHC. 40-kg load, 100 C, sliding distance: 840 M.

For experiments conducted under other test conditions, the stationary ball wear volumes were evaluated by calculation only. The results of these experiments, however, agree qualitatively with those cited above (Table 2).

DISCUSSION

The Significance of Wear Asymmetry for Wear Testing

The practice of characterizinging wear in the Four-Ball machine by measuring the wear scar diameter rests on the assumption that, for a given load, the wear volume of the stationary balls is uniquely determined by the wear scar diameter. The experimental data presented here are, indeed, consistent with that view.

However, the rotating ball wear does not appear to be uniquely related to wear of the stationary balls. Since the wear of cyclically stressed components may be of critical

TABLE 2—WEAR DATA OBTAINED WITH PETH AND SHC, STATIONARY BALL WEAR VOLUME CALCULATED ONLY. SLIDING DISTANCE = 840M

FLUID	SPEED, cm/s	LOAD, kg	TEMP., °C	WEAR SCAR DIAMETER, cm/10²	FROM SCAR DIAMETER: WEAR VOLUME FOR THREE STATIONARY BALLS, cm³/10⁶	FROM PROFILOMETRY: WEAR VOLUME FOR ROTATING BALL, cm³/10⁶
PETH	3.9	40	100	6.18	6.0	25.3
	7.8	40		6.83	9.2	14.0
SHC	23.3	40	60	6.60	8.0	12.9
	7.8		70	7.28	12.1	13.1
	11.7		80	7.12	11.0	10.6
	11.7		80	7.37	12.8	19.7
	15.5		80	7.07	10.7	26.3
	15.5		80	7.16	11.3	16.3
	23.3		80	6.83	9.2	10.6
	7.8		100	7.42	13.1	27.1
	11.7			7.38	12.8	22.5
	15.5			7.25	11.9	8.3
	23.3			7.26	12.0	10.6
	11.7		110	7.33	12.5	20.3
	23.3			7.33	12.5	11.2
	29.2			7.21	11.6	6.6
	3.9		120	7.58	14.4	14.8
	3.9		120	7.51	13.8	12.9
	3.9		120	7.54	14.1	16.8
	7.8		120	7.61	14.6	32.3
	7.8		120	8.05	18.5	15.9
	11.7		120	7.51	13.8	15.4
	15.5		120	7.10	11.0	9.1
	7.8	33	80	7.35	12.6	24.9
	15.5	33	80	6.60	8.0	10.9
	23.3	33	100	6.65	8.2	10.3

importance in practical devices, it may, therefore, be of value, depending on the end use of the data, to include evaluation of rotating ball wear along with wear scar diameter measurements.

Factors Underlying Wear Asymmetry

Two factors which might reasonably be expected to be related to wear asymmetry are fatigue wear and lubricant chemical effects. Although fatigue processes may occur, fatigue wear cannot account for all the experimental observations. In order to establish whether the phenomenon is related to lubricant chemistry, an additional series of experiments will be required.

Fatigue Wear

Fatigue wear should result in higher wear on the cyclically stressed rotating ball. This is not consistent with the experimental results for SHC at sliding speeds above 15 cm/s. By analogy with rolling contact fatigue, fatigue wear in sliding contacts would be expected to be highly dependent on the maximum Hertz stress. Wear data for PETH and for SHC as a function of test time show that the wear rates remained constant despite substantial reductions in the maximum Hertz stress (Figs. 4, 5, and 6). Fatigue wear in the very early stages of the wear tests with PETH cannot, however, be ruled out on this basis since the initial wear rate was clearly higher (Fig. 5).

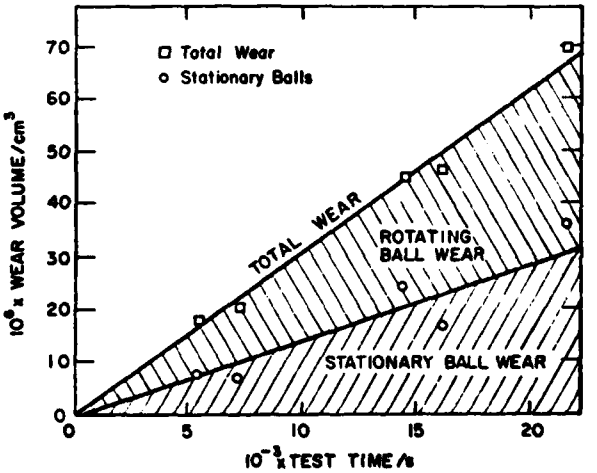

Fig. 4—Wear vs test time with SHC under conditions producing high wear. 40-kg load, 100°C, sliding speed; 1.67 Hz (3.9 cm/s). Initial maximum Hertz stress = 3400 MPa, final maximum Hertz stress = 710 MPa.

The increase in wear found for SHC at low sliding speeds suggests a transition to fatigue wear as a result of the lower strain rate. Such a transition would be expected to be re-

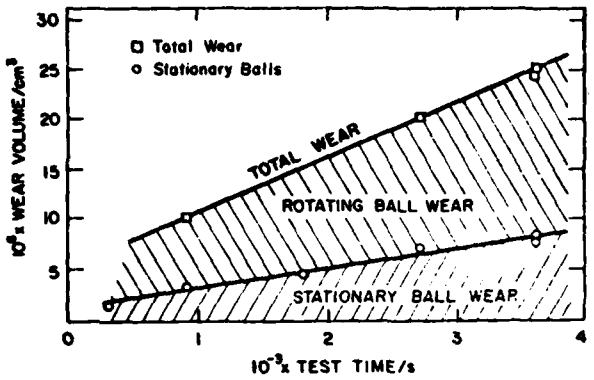

Fig. 5—Wear vs test time with PETH, 40-kg load, 100°C, sliding speed = 10 Hz (23.3 cm/s). Initial maximum Hertz stress: 3400 MPa, final maximum Hertz stress = 850 MPa.

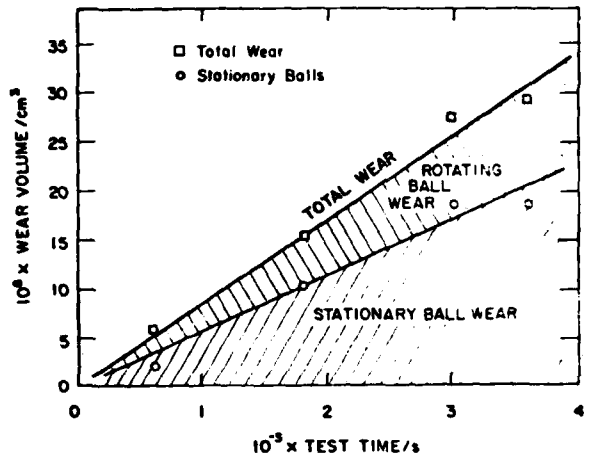

Fig. 6—Wear vs test time with SHC under conditions producing low wear. 40-kg load, 100°C sliding speed 10 Hz (23.3 cm s). Initial maximum Hertz stress = 3400 MPa, final maximum Hertz stress = 660 MPa.

flected in the surface morphology. Examination of the surface profiles produced at different sliding speeds do not support this idea (Fig. 7). In addition, no pits or spalls could be found in the wear tracks under optical microscopy at a magnification of 200× for either SHC or PETH.

Lubricant Chemistry

We have previously reported that autoxidation of PETH produces diacid monoesters which lead to increased wear (*6*). By contrast, preliminary experiments indicate that the autoxidation products of the synthetic hydrocarbon have relatively little influence on wear, and even decrease wear under some conditions.

This divergence in the effects of autoxidation on wear behavior parallels the divergence observed in wear asymmetry between PETH and SHC. This observation suggests the hypothesis that lubricant oxidation in the wear zone may be a cause of wear asymmetry. Preliminary data published in Ref. (*6*) are, indeed, consistent with the idea that lubricant oxidation products influence wear asymmetry. Factors such as differences in surface temperature and cyclic exposure of the rotating ball to the bulk lubricant together

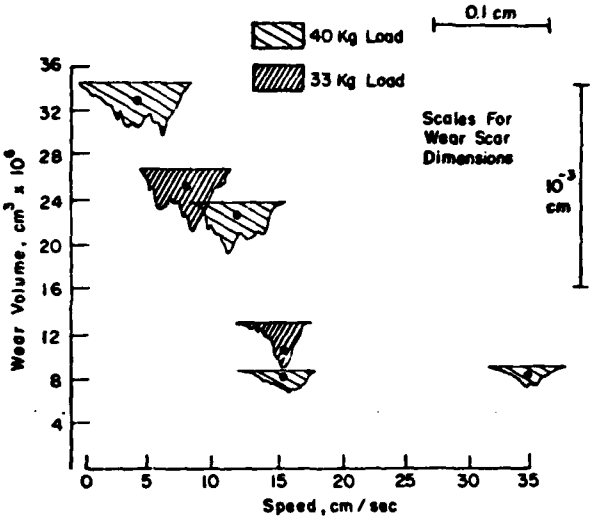

Fig. 7—Wear scar profiles for stationary balls with SHC vs sliding speed. 100° C, sliding distance = 840 M.

with the different effects of the oxidation products could, perhaps, account for the observed effects. Further work will be required to test this hypothesis.

CONCLUSIONS

A systematic comparison of wear on the stationary and rotating balls of the Four-Ball machine, using two lubricants, led to the following observations:

1. The wear volume of the rotating ball is *not*, in general, equivalent to the wear of the three stationary balls.
2. The distribution of wear between the contacting surfaces was a function of test conditions and was different for PETH and for SHC.
3. The wear asymmetry observed in these experiments appears to be related to lubricant chemistry. Further work is required to elucidate this possibility.

REFERENCES

(*1*) Feng, I-Ming, "A New Approach in Interpreting the Four-Ball Wear Results," *Wear*, **5**, pp 275–288 (1962).
(*2*) Vinogradov, G. V. and Morozova, O. E., "A Study of the Wear of Steel Under Heavy Loads with Lubricants Containing Sulfur-Based Additives," *Wear*, **3**, pp 297–308 (1960).
(*3*) Goldblatt, I. L., discussion of the paper by Willermet, P. A. Mahoney, L. R., and Bishop, C. M., "Lubricant Degradation and Wear III. Antioxidant Reactions and Wear Behavior of a Zinc Dialkyldithiophosphate in a Fully Formulated Lubricant," *ASLE Trans.*, **23**, 3, pp 225–231 (1980).
(*4*) Hamilton, E. J. Jr., Korcek, S., Mahoney, L. R., and Zinbo, M., "Kinetics and Mechanism of the Autoxidation of Pentaerythrityl Tetraheptanoate at 180–220°C," *Intl. J. of Chem. Kinetics*, **12**, pp 577–603 (1980).
(*5*) Rowe, C. N., "Lubricated Wear," *Wear Control Handbook*, ASME, United Engineering Center, N.Y., pp 143–160 (1980).
(*6*) Willermet, P. A., Mahoney, L. R. and Kandah, S. K., "Lubricant Degradation and Wear IV. The Effect of Oxidation on the Wear Behavior of Pentaerythrityl Tetraheptanoate," *ASLE Trans.*, **24**, 4, pp 441–448 (1981).

DISCUSSION

STEPHEN M. HSU (Member, ASLE)
National Bureau of Standards
Washington, DC 20234

The authors are to be commended for undertaking a careful study on the very important but often neglected aspect of wear measurement in the 4-ball machine.

The idea of better measuring wear volume or the total amount of wear has been attempted by many. E. E. Klaus at the Pennsylvania State University had conducted many such investigations on mineral oil systems, and concluded that wear scar or wear volume determined by Feng's equation generally correlated very well with the total amount of wear debris collected. In this paper, the authors used a surface profilometer to measure wear volume directly. We have been pursuing along the same line, and wish to point out that to measure the wear scar surface profile on a ½-in ball with a 0.55-mm wear scar is not an easy task. The authors mentioned that they positioned their stylus tip on the deepest point of the wear scar and then the stylus was passed over the wear scar. How did the authors determine the deepest point? And, how was the calibration conducted? Basically, by rotating the ball under the stylus, one is taking the spherical curvature out i.e., the surface of the ball would be a straight horizontal line. However, the wear volume is a concave spherical segment on a convex spherical segment. What is the effect of linearizing one on the dimension of the other? The authors found wear scar diameter determined by profilometry was less than that measured optically. Could this be the reason?

We generally agree with the authors' assessment on wear asymmetry i.e., the cause of the observed difference in wear between the rotating ball and the stationary balls probably lies in the chemistry of the fluids. What are the viscosities of the two fluids and their viscosity temperature relationship? Looking at Figs. 3 and 4, one sees the increasing influence of elastohydrodynamic component as the speed is increased, i.e., lower wear at increasing speed. We have observed this trend in many purified mineral fluids. Eventually, at high speeds, the wear increases again as illustrated by the rotating ball wear for PETH in Fig. 3.

Looking from this perspective, all four wear curves in Fig. 3 and Fig. 4 should behave alike. Figure 4 data illustrate this point. It has been suggested that this behavior could be related to the transition temperatures of the lubricating film system. Then what has been observed by the authors may be related to different surface temperatures at the rotating ball and the stationary balls surfaces. The idea of the lubricant decomposition products preferentially attacking more on one surface and not equally on the other surface remains to be proven as suggested by the authors.

Again, the authors should be commended for an interesting work on a very basic and important aspect of wear measurement.

AUTHORS' CLOSURE

We thank Stephen Hsu for a perceptive discussion of the experimental results. As he points out, these measurements are not easy to make, which, in part, explains why they are so seldom reported.

The deepest points on the wear scars of the stationary balls were determined as follows: The stylus tip was placed near the center of the scar. The minimum profile trace was found while rotating the ball through small arcs parallel and perpendicular to the stylus sliding direction. After the profiles were made, the intersection of the two marks made by the stylus was located under a microscope. By focusing on this intersection, it was determined that the deepest part of the wear scars had been located.

Wear scar profiles were independently determined optically for several stationary balls. The ball was moved across the stage of a 1500 power microscope. The vertical displacement required to focus the microscope at each of several points across the wear scar was used to generate a wear scar profile.

Since the depths of the wear scars were very much less than the ball radius, the effect of linearizing the ball surface was negligible.

As indicated in the paper, the differences between the scar diameters as determined by profilometry and those measured optically were attributable to the deepest point of the wear scars being off-center. This could be clearly seen under the microscope.

The shapes of the wear versus sliding speed curves do appear to be qualitatively similar, but displaced on the coordinate axis as indicated by the discusser. We prefer, at present, to consider this effect as being due to changes in surface reaction rates engendered by changes in surface temperature and residence time rather than attributing it to elastohydrodynamic effects.

ATTACHMENT III

Autoxidation of n-Alkanes: Isomerization and Cyclization Reactions of Hydroperoxyalkyl Radicals, by S. Korcek, L. R. Mahoney, R. K. Jensen, and M. Zinbo, presented at 3rd International Symposium on Organic Free Radicals, Freiburg, West Germany, August 31-September 4, 1981, Abstracts, No. M3.

AUTOXIDATION OF n-ALKANES

S. Korcek, L. R. Mahoney, R. K. Jensen, and M. Zinbo

Research Staff, Ford Motor Company, P.O. Box 2053, Dearborn, Michigan, 48121, U.S.A.

Kinetics and mechanism of liquid phase autoxidation of n-hexadecane have been studied at 120-180°C using the stirred flow reactor. A reaction scheme consistent with the analytical results obtained includes, in addition to prevously observed reactions, intramolecular α,γ and α,δ hydrogen abstraction reactions of peroxy radicals and an α,γ-cleavage reaction involving decomposition of di- and trifunctional α,γ-hydroperoxyketone species. The latter reaction leads to the formation of methyl ketones and carboxylic acids. From the results of studies at oxygen pressures from 5 to 110 kPa the α,γ and α,δ intramolecular reactions have been found to be reversible. Evidence for the formation of cyclic ether species at lower oxygen pressures studied was obtained. The rates of initiation for this system were measured and absolute rate constants for the above reactions have been determined.

Rate of Initiation in the Autoxidation of n-Hexadecane at Elevated Temperatures, by S. Korcek, R. K. Jensen, L. R. Mahoney, and M. Zinbo, presented at Symposium on Free Radicals at the 65th CIC Conference, Toronto, Canada, May 30-June 2, 1982, Abstracts, No. OR5-6.

OR5-6 RATE OF INITIATION IN THE AUTOXIDATION OF n-HEXADECANE AT ELEVATED TEMPERATURES. S. Korcek,* R. K. Jensen, L. R. Mahoney, and M. Zinbo. Ford Motor Company - Research, SRL - Rm. 3198. P.O. Box 2053, Dearborn, MI 48121**

Kinetic and mechanistic studies of the autoxidation of n-hexadecane at elevated temperatures, carried out in our laboratory using a stirred flow reactor technique, yielded values of the ratios of rate constants for intramolecular and intermolecular hydrogen abstraction reactions of hexadecylperoxy radicals at 120, 160, and 180°C (J. Am. Chem. Soc., 101, 7574 (1979); 103, 1742 (1981)). Absolute rate constants for these reactions, however, can only be obtained if the rate of initiation, R_i, under the conditions utilized in the above studies is known. In low temperature autoxidations R_i is maintained at known and constant rate by the addition of initiators, but at elevated temperatures R_i varies depending not only on reaction conditions but also on degree of conversion since initiation processes occur mainly due to reactions of primary oxidation products. In this work, we describe and discuss various approaches used for determination of R_i at elevated temperatures. These approaches include determinations of R_i from the rate of formation of termination products, from the length of the inhibition period caused by addition of antioxidant, and from the initial rate of antioxidant consumption.

**This work was supported in part by the Air Force Office of Scientific Research under Contract F49620-80-C-0061

Liquid Phase Autoxidation of Organic Compounds at Elevated Temperatures, by S. Korcek, R. K. Jensen, L. R. Mahoney, and M. Zinbo, presented at Symposium on Inhibition of Liquid-Phase Autoxidation Reactions, ACS Meeting, Kansas City, September 12-17, 1982, Abstracts, No. ORGN 27.

27. LIQUID PHASE AUTOXIDATION OF ORGANIC COMPOUNDS AT ELEVATED TEMPERATURES*. S. Korcek, R. K. Jensen, L. R. Mahoney, and M. Zinbo; Ford Motor Company, Research, Rm. 3198-SRL, P.O. Box 2053, Dearborn, MI 48121.

Results of kinetic and mechanistic studies of the autoxidation of n-hexadecane and pentaerythrityltetraheptanoate at 120 to 220°C will be reviewed. Kinetic information on intermolecular and α,γ and α,ε intramolecular hydrogen abstraction reactions of peroxy radicals, on the cleavage reaction of α,γ-hydroperoxyketones, and on isomerization and cyclization reactions of hydroperoxyalkyl radicals will be presented. The implications of the occurrence of these reactions with regard to the mechanisms of autoxidation of organic compounds and to the inhibition of autoxidation in the liquid phase at elevated temperatures will be discussed.

*This work was supported in part by the Air Force Office of Scientific Research under Contracts F44620-76-C-0067 and F49620-80-C-0061.

Reactions of Alkylperoxycyclohexadienones during Autoxidation Inhibited by Hindered Phenols at Elevated Temperatures, by R. K. Jensen, S. Korcek, L. R. Mahoney, and M. Zinbo, presented at Symposium on Inhibition of Liquid Phase Autoxidation Reactions ACS Meeting, Kansas City, September 12-17, 1982, Abstracts, No. ORGN 28.

28. REACTIONS OF ALKYLPEROXYCYCLOHEXADIENONES DURING AUTOXIDATION INHIBITED BY HINDERED PHENOLS AT ELEVATED TEMPERATURES.* R. K. Jensen, S. Korcek, L. R. Mahoney, and M. Zinbo, Ford Motor Company, SRL - Rm. 3198, P.O. Box 2053, Dearborn, MI 48121.

The alkylperoxycyclohexadienone products of the interaction of hindered phenols with peroxy radicals are unstable at elevated temperatures and undergo both non-radical and radical decomposition reactions. The latter reaction contributes to initiation and governs the efficiency of the phenol as an antioxidant. In order to assess this contribution in the inhibition of n-hexadecane autoxidation by 2,6-di-tert-butyl-4-methylphenol, we have investigated the decomposition reactions of a series of 4-alkylperoxy-4-methyl-2,6-di-tert-butylcyclohexadienones (QOOP; R = (CH_3)$_3$C-, tetralyl-, 1-,2-, and 5-$C_{16}H_{33}$-) in the presence of the parent phenol at 160 and 180°C. Kinetic analyses of the results yielded values of rate constants for both decomposition reactions which allow the determination of rate of initiation in autoxidizing n-hexadecane at elevated temperatures using the inhibitor method.

*This work was supported by the Air Force Office of Scientific Research Under Contract F49620-80-C-0061.